Dissertation
submitted to the
Combined Faculties for the Natural Sciences and for Mathematics
of the Ruperto-Carola University of Heidelberg, Germany
for the degree of
Doctor of Natural Sciences

presented by
Master of Philosophy Nga Yu Ho
born in: Hong Kong
Oral examination: 14th October, 2011

Characterisation of methyl mercury toxicity and identification of methyl mercury-sensitive biomarkers in zebrafish (*Danio rerio*) embryos

Referees: Prof. Dr. Uwe Strähle
Prof. Dr. Thomas Braunbeck

This dissertation is dedicated to my parents.

Abstract

Methyl mercury (MeHg) is known to be a teratogen and neurotoxicant. Human contact with it is unavoidable due to its widespread prevalence in the environment. There is a need for model organisms and biosensors for better monitoring its presence in the environment and investigating the underlying mechanisms of its toxicity.

In this study, zebrafish was chosen as the model organism due to its ecotoxicological, developmental and genetics advantages. A global view of gene expression changes in zebrafish embryos with acute sub-lethal MeHg exposure was generated. In response to MeHg, a total of 464 MeHg-up-regulated and 379 MeHg-down-regulated genes were obtained from the microarray analysis (p-value < 0.05 and M-value > 1.3 or < -1-3, in which M-value refers to the $\log_2$ ratio of the fold change). The up-regulated genes were associated with functions of oxidative stress, cell redox homeostasis, apoptosis, inflammatory response, blood circulation, hormone stimulus and so forth; while the down-regulated ones were involved in oxidation reduction, RNA splicing, RNA elongation, fatty acid metabolism, DNA repair and so forth. Eighty-eight candidate genes were selected from the microarray for whole-mount *in situ* hybridisation analysis (ISH). The ISH result showed a 68% positive correlation with the microarray result. Ectopic expressions of the genes were noted in various organs including the brain, eyes, olfactory bulb, branchial arches, heart, liver, intestine or gut, pronephos, somites, lateral lines, pectoral fins, caudal fin fold, trunk and tail blood vessels, dermal epithelium, and yolk syncytial layer. The expression levels of 12 genes at 30 μg/l and 60 μg/l MeHg were further quantified by real-time PCR. Eleven out of twelen were significantly regulated at 60 μg/l MeHg. *arfl, c4-2, c6, cbx7l, prdx1* and *zgc:101661* showed significant changes even at 30 μg/l MeHg. The sensitive expression changes of these 6 genes suggested that they may serve as marker genes for detecting the presence of MeHg in the environment.

The effects of MeHg on the nervous system and the caudal fin fold were further investigated. Although no obvious change in some of the marker genes of CNS or the neurotransmitter system examined was detected, through the toxicogenomic screen, 24 genes showing changes in the expression levels or patterns in the brain in response to MeHg exposure were identified. Besides, MeHg treatment caused a decrease in the

number of neuromast hair cells in the lateral line. The expressions of 12 genes were shown to be regulated by MeHg in the lateral line.

MeHg could induce a loss of the gap in the melanophore stripe, disruption of caudal fin growth zone and disruption of caudal fin fold tissue. The disruption of melanophore stripe by MeHg was restricted to a time window of exposure from 12 to 48 hpf. MeHg caused a specific loss of the GFP expression in the caudal fin growth zone of the transgenic line *Tg(-2.4shha-ABC:GFP)sb15*, and such an effect was induced in a significant number of embryos even in MeHg concentration as low as 6 μg/l. Although there was a slight increase in the number of apoptotic cells in the caudal fin region, no rescue of the caudal fin tissue destruction was observed when induction of apoptosis was inhibited, excluding the possibility that apoptosis is the major cause of caudal fin fold tissue disruption. Through the toxicogenomic screen, 22 genes were shown to be ectopically expressed in the caudal fin fold of MeHg-treated embryos. Among these genes, the involvement of *mmp9* and *mmp13a* in the caudal fin fold malformation was further investigated. Pharmacological inhibition of *mmp9* and *mmp13a* could rescue partially the caudal fin phenotype induced by MeHg, suggesting a role for these two extracellular matrix remodelling proteins in causing the caudal fin tissue disruption.

Zusammenfassung

Methylquecksilber (MeHg) ist ein bekanntes Teratogen und eine neurotoxisch wirkende Chemikalie. Der Kontakt des Menschen mit Methylquecksilber ist auf Grund der weiten Verbreitung in der Umwelt nicht zu vermeiden. Es gibt damit den Bedarf an Modelorganismen und Biosensoren für ein besseres Monitoring in der Umwelt und zum Erforschen der zugrunde liegenden Wirkungsmechanismen.

Der Zebrabärbling wurde in dieser Studie aufgrund seiner ökotoxikologischen, entwicklungsbiologischen und genetischen Eigenschaften als Modelorganismus herangezogen. Ein umfassender Blick auf Änderungen in der Genexpression nach akuter sublethaler Exposition gegenüber MeHg wurde ermöglichst. Als Antwort auf die MeHg-Exposition wurden in einer Mikroarrayanalyse 464 aufregulierte und 379 herunterregulierte Gene identifiziert ($p<0.05$ und $M>1.3$ or $M<-1.3$; unter dem M-Wert versteht man das $\log_2$ des Fold-Change). Die aufregulierten Gene sind assoziiert mit Funktionen des oxidativen Stress, Redoxgleichgewicht in der Zelle, Apoptose, Entzündungsprozesse, Blutkreislauf, Hormonstimuli und so weiter, wohingegen die herunterregulierten Gene in Prozesse wie Oxidationsreduktion, RNS-Splicing, RNS-Elongation, Fettsäurenmetabolismus, DNS-Reparatur und so weiter involviert sind. Basierend auf den Ergebnissen des Mikroarrays wurden 88 Gene für *in situ* Hybridisierung (ISH) an ganzen Embryonen ausgewählt. Die ISH ergaben zu 69.3% eine positive Übereinstimmung mit den Ergebnissen des Mikroarrays. Ektopische Genexpression wurde an verschiedenen Organen festgestellt: Gehirn, Augen, Riechkolben, Kiemenbögen, Herz, Leber, Darm oder Magen, Pronephros, Somiten, Lateralline, Brustflossen, Schwanzflossenfalte, Rumpf- und Schwanzblutgefäßen, Hautepithelium, syncytiale Dotterschicht. Wir quantifizierten ebenfalls das Expressionslevel von 12 Genen mit Hilfe von real-time PCR nach Expositionen gegenüber 30 µg MeHg/L und 60 µg MeHg/L. Elf von zwölf untersuchten Genen wurden bei einer Konzentration von 60 µg MeHg/L als signifikant reguliert nachgewiesen. *arfl, c4-2, c6, cbx7l, prdx1, txnl* und *zgc:101661*, waren auch bei 30µg MeHg/L signifikant reguliert. Die sensitive Änderung der Expression dieser sechs Gene lässt auf deren Eignung als Biomarker für die Detektion von MeHg in der Umwelt schließen.

Die Effekte von MeHg auf das Nervensystem und die Schwanzflossenfalte wurden in der vorliegenden Studie weitergehend untersucht. Mit Hilfe der toxikogenomischen Untersuchung konnten, obwohl keine eindeutige Regulation bestimmter Markergene des Zentralnervensystems bzw. des Neurotransmittersystems festgestellt wurde, 24 Gene identifiziert werden, die in Antwort auf die Exposition gegenüber MeHg signifikant im Gehirn reguliert wurden. Desweiteren verursacht die Behandlung mit MeHg einen Verlust in der Zahl von Neuromasthaarzellen der Seitenlinie. Die Expression von elf Genen in der Seitenlinie war nach MeHg-Exposition verändert. Änderungen bezüglich der Verbindung der Neuronen zu der neuromuskulären Verbindung wurden ebenfalls untersucht und zeigten keinen Defekt in der Verteilung der Motorneuronen oder in deren Verbindung nach Behandlung mit MeHg.

MeHg konnte den Verlust der Lücke in dem Melanophorenstrich, die Störung der Wachstumszone der Schwanzflosse, sowie die Störung des Gewebes der Schwanzflossenfalte induzieren. Die Störung des Melanophorenstrichs durch MeHg war auf ein Expositionszeitfenster von 12 bis 48 Stunden nach Befruchtung (hpf) beschränkt. MeHg konnte ebenfalls einen spezifischen Verlust der GFP-Expression in der Schwanzflossenwachstumszone des transgenen Linie *Tg(-2.4shha-ABC:GFP)sb15* verursachen, der auch noch bei einer MeHg Konzentration von 6 µg/l in einer signifikanten Anzahl an Embryonen auftrat. Auch wenn ein geringer Anstieg in der Zahl apoptotischer Zellen in der Schwanzflossenregion zu beobachten war, so konnte die Zerstörung des Schwanzflossengewebes auch bei Inhibition des Apoptose nicht verhindert werden. Dies schließt die Möglichkeit der Apoptose als Hauptursache des für die Störung des Schwanzflossengewebes aus. Mit Hilfe des toxikogenomischen Screens konnten 22 Gene identifiziert werden, die ektopisch in der Schwanzflossenfalte von MeHg-exponierten Embryos exprimiert werden. Unter diesen Genen befanden sich *mmp9* and *mmp13a*, die ektopisch und spezifisch in MeHg-exponierten Embryos exprimiert werden. Die pharmakologische Inhibition von *mmp9* and *mmp13a* konnte den durch MeHg induzierten Phänotypen teilweise verhindern. Dies legt eine Rolle von *mmp9* and *mmp13a* - beide Gene sind in der Regulation der extrazelluläen Matrix beteiligt - im Zusammenhang mit der Störung des Schwanzflossengewebes nahe.

Acknowledgement

I would like take this chance to express my thanks to my supervisor Uwe Strähle for providing me the opportunity to join his group. I am grateful to his supports, discussions, advices and broad knowledge of science.

I would also like to thank my second supervisor Thomas Braunbeck for his helpful comments, discussions and advices.

Many thanks are bestowed to Lixin Yang for all of his guidance, helps, supports, discussions and suggestions.

Thanks to Sepand Rastegar for taking care of everyone in the group. Thanks to Maryam Rastegar for the help with the microscopes. Thanks to Jessica Legradi for the help with microarray analyses. Thanks to Sepand Rastegar, Olivier Armant, Isabelle Baader, Martin März, Rebecca Schmidt and other members of our lab's transcription factor team for the provision of the transcription factor ISH probes. Thanks to Masanari Takamiya for all the helps and advices. Thanks to Jens Otte for helping the abstract translation. Thanks to Urmas Roostalu for letting me invite my examiners first and his humour. Thanks to Nadine Borel and her fish team for the husbandary of our beloved zebrafish.

Again, many thanks are given to my group mates, office mates and floor mates for the pleasant working environment, their helps and the fun.

Thanks to the rest of people in the ITG.

Last but not least, I would like to give my special thanks to my family, my boyfriend Pietro, siù lam sik tou, my former supervisor Shuk Han Cheng and all my friends in Hong Kong and Karlsruhe for their very grateful love and support in life.

Big thanks to all of you!!!

Table of contents

Introduction 1
1.1 Toxicogenomics 1
1.2 Toxicity of methyl mercury 1
1.2.1 Sources of environmental mercury 1
1.2.2 Human contact with Hg and its derivatives and their depositions in the body 2
1.2.3 Occurrence and symptoms of MeHg poisonings 4
1.2.4 Large-scale studies of the neurotoxicity of MeHg to children 6
1.2.5 Neurotoxicity of MeHg to animal models 7
1.2.6 Mechanisms of MeHg toxicity 8
1.2.7 Hg and MeHg biosensors 10
1.2.8 Toxicity of MeHg or Hg to zebrafish 10
1.3 Advantages of using zebrafish embryo as an animal model 11
1.4 Hypotheses and aims 12
2 Materials and methods 14
2.1 Fish strains and fish maintenance 14
2.2 Chemical treatment 14
2.3 RNA extraction 14
2.4 DNA Microarray 15
2.4.1 Microarray experiment 15
2.4.2 Microarray data analysis 16
2.5 Whole-mount in situ hybridisation 18
2.6 Immunohistochemistry 25
2.7 α-Bungarotoxin staining 25
2.8 Morpholino knock-down 25
2.9 Real-time polymerase chain reaction 25
2.10 Acridine orange hydrochloride staining 27
2.11 Mmp activity assay 27
2.12 Mmp inhibitor treatment 27
2.13 Histological section 28
2.14 Birefringence analysis 28
2.15 Function analysis of MeHg-regulated genes 28

2.16 Imaging 28
2.17 Statistics analysis 28
3 Results 29
3.1 Dose-dependent effect of MeHg on zebrafish embryos 29
3.2 Toxicogenomic screen of MeHg-responsive genes 32
3.2.1 Microarray analysis of MeHg-regulated genes 32
3.2.2 *In situ* hybridisation analysis of MeHg-regulated genes 38
3.2.3 Quantitative analyses of MeHg-regulated genes by real-time PCR 50
3.2.4 Summary 51
3.3 Zebrafish nervous system 53
3.3.1 Study on zebrafish brain after MeHg exposure 53
3.3.1.1 No obvious change in the expression pattern of genes expressed in the brain after sub-lethal concentration of MeHg treatment 54
3.3.1.2 Genes showing ectopic expression in the brain of MeHg-treated embryos 57
3.3.2 Study on the lateral line system in MeHg-treated embryo 66
3.3.2.1 Decreased number of neuromast hair cells in the PLL 67
3.3.2.2 Genes induced in the lateral line of MeHg-treated embryos 68
3.3.3 No observable defects in the myofibril or motor neuron structures 71
3.3.4 Summary 73
3.4 Study on the melanophore stripes and caudal fin fold in the tail in MeHg-exposed embryos 75
3.4.1 Disruption of the melanophore stripes and caudal fin fold in embryos exposed to MeHg 76
3.4.2 Loss of GFP expression in the caudal fin primordium in the *Tg(-2.4shha-ABC:GFP)sb15* transgenic line after MeHg treatment 77
3.4.3 Reduction of caudal fin GFP expression at MeHg concentration as low as 6 μg/l 79
3.4.4 Critical period of MeHg exposure lying between 12 hpf and 48 hpf 80
3.4.5 Slight increase in the number of apoptotic cells in the caudal fin fold and no rescue of caudal fin fold abnormality by inhibition of apoptosis 81
3.4.6 Involvement of *mmp9* and *mmp13a* in the induction of caudal fin malformation in MeHg-treated embryos 84

3.4.6.1 Specific ectopic *mmp9* and *mmp13a* expression in the caudal fin of embryos exposed to MeHg 84
3.4.6.2 No ectopic expression of myeloid genes in the caudal fin fold of MeHg-treated embryos 85
3.4.6.3 Increased Mmp activity in MeHg-treated embryos 86
3.4.6.4 Partial rescue of the MeHg-induced caudal fin phenotype by inhibition of Mmp activity 87
3.4.7 Induction of the gene expression in the caudal fin fold 89
3.4.8 Summary 91
3.5 Study of *complement component 7-1* (*c7-1*) 92
3.5.1 Ectopic expression of *c7-1* in the retina of MeHg-treated embryos 92
3.5.2 No ectopic expression of other membrane attack complex complement components genes in the retina after MeHg treatment 93
3.5.3 Expression of *c7-1* in scattered cells in the hindbrain, midline, trunk and tail during embryonic development 95
3.5.4 No ectopic expression of myelin marker genes in the retina after MeHg exposure 96
3.5.5 Functional study of *c7-1* 97
3.5.6 Summary 99
4 Discussion 100
4.1 Malformations in fish caused by MeHg exposure 100
4.2 Toxicogenomic screen of MeHg-responsive genes 100
4.3 The effects of MeHg on the nervous system of zebrafish embryos 105
4.4 The effects of MeHg on trunk pigmentation 107
4.5 Study on the effects of MeHg on the caudal fin fold 108
4.6 Ectopic expression of *c7-1* in the eye after MeHg exposure 110
5 Conclusion 112
References 113
Appendix 138
Publications related to the dissertation 168
Declarations 169

List of figures

Fig. 2.1 Schematic representation of the procedure of DNA microarray. 16
Fig. 2.2 A plot of the CV against the M-values from one microarray data set. 18
Fig. 3.1 Mortality of zebrafish embryos exposed to different concentrations of MeHg. 29
Fig. 3.2 Malformations in zebrafish embryos exposed to MeHg. 31
Fig. 3.3 Gene ontology enrichment analysis of MeHg-regulated genes. 37
Fig. 3.4 Changes in gene expression patterns in after MeHg exposure. 49
Fig. 3.5 Changes in gene expression levels measured by quantitative real-time PCR in response to MeHg. 51
Fig. 3.6 Sculpturing of the brain rudiment during the segmentation period. 54
Fig. 3.7 Expression patterns of genes or proteins expressed in the central nervous system or neurotransmitter system of zebrafish embryos after MeHg exposure. 57
Fig. 3.8 Changes in gene expression in the zebrafish brain after MeHg treatment. 66
Fig. 3.9 Pattern and structure of the zebrafish lateral line at the end of embryogenesis. 67
Fig. 3.10 Decreased number of neuromast hair cells in the lateral line in embryos exposed to MeHg. 68
Fig. 3.11 Changes in the gene expression levels in the lateral line after MeHg exposure. 71
Fig. 3.12 No observable change in myofibers structure or motor neuron distribution and connection in embryos exposed to MeHg. 73
Fig. 3.13 Zebrafish tail development. 76
Fig. 3.14 MeHg-specific disruptions of the caudal fin fold tissue and the melanophore gap. 77
Fig. 3.15 Induction of caudal fin fold defects and caudal fin primordium disruption in embryos exposed to MeHg. 78
Fig. 3.16 Reduction or loss of GFP expression at the caudal fin primordium of MeHg-exposed embryos. 80
Fig. 3.17 Disruption of melanophore gap in embryos exposed to MeHg for all the time windows within 12 and 48 hpf. 81
Fig. 3.18 Slight increase in the number of apoptotic cells in the caudal fin fold. 82
Fig. 3.19 No rescue of MeHg-induced caudal fin fold disruption in *p53* morphants. 83

Fig. 3.20 Specific inductions of *mmp9* and *mmp13a* in the caudal fins of embryos exposed to MeHg. 85
Fig. 3.21 No ectopic expression of myeloid genes at the caudal fin fold of MeHg-treated embryos. 86
Fig. 3.22 Up-regulation of Mmp activity in embryos exposed to MeHg. 87
Fig. 3.23 Partial rescue of the MeHg-induced caudal fin phenotype by inhibition of Mmp activity. 88
Fig. 3.24 Genes showing ectopic expression in the caudal fin fold after MeHg exposure. 90
Fig. 3.25 Ectopic expression of *complement component 7-1* in the retina of MeHg-exposed embryos. 92
Fig. 3.26 No ectopic expression of other membrane attack complex complement components in the retina of embryos exposed to MeHg. 94
Fig. 3.27 Expression patterns of *c7-1* during development. 95
Fig. 3.28 No ectopic expression of *mpz* and *plp1b* in the eyes of embryos exposed to MeHg. 97
Fig. 3.29 Effective blocking of *c7-1* by morpholino MO-c7-1 98
Fig. 3.30 No observable morphological difference in *c7-1* morphants. 99
Fig. A1 Schematic drawing of zebrafish embryos at selected stages between 4 and 72 hpf. 139

List of tables

Tab. 2.1 Information of RNA probes for *in situ* hybridisation. 19
Tab. 2.2 Primers for real-time PCR. 26
Tab. 3.1 Result of whole-mount *in situ* hybridisation analysis of MeHg-regulated genes in 72 hpf-old zebrafish embryos. 40
Tab. A1 Stages of zebrafish embryonic development. 138
Tab. A2 MeHg-up-regulated genes determined by DNA-microarray with $M > 1.30$ and $p < 0.05$. 140
Tab. A3 MeHg-down-regulated genes determined by DNA-microarray with $M < -1.30$ and $p < 0.05$. 151
Tab. A4 Gene ontology of MeHg-responsive genes selected for *in situ* hybridisation analysis. 162

Definitions of acronyms and symbols used in the dissertation

Acronym or symbol	Definition
AAP	American Academy of Pediatrics
ANOVA	Analysis of variance
As	Arsenic
As_2O_3	Arsenic (III) oxide
ATP	Adenosine triphosphate
^oC	Degree Celsius
C7D	Complement C7 deficiency
Ca	Calcium
CCD	Charge-coupled device
Cd	Cadmium
$CdCl_2$	Cadmium chloride
cDNA	Complementary deoxyribonucleic acid
cm	Centimeter
cRNA	Complementary ribonucleic acid
CV	Coefficient of variation
Cy	Cyanine
DNA	Deoxyribonucleic acid
dpf	Days post-fertilisation
EtHg	Ethyl mercury
FAO	Food and Agriculture Organization
g	Gram
GFP	Green fluorescent protein
GPR	GenePix Result
GTP	Guanosine triphosphate
Hg	Mercury
$HgCl_2$	Mercury chloride
hpf	Hours post fertilisation
IHC	Immunohistochemistry
I.M.A.G.E.	Integrated Molecular Analysis of Genomes and their Expression
IR	Interquartile range
ISH	*In situ* hybridisation
LC10	Lethal concentration 10% (concentration which will cause 10% lethality)
LL	Lateral line
LOWESS	Locally weighted scatterplot smoothing
MD	Minamata disease
MeHg	Methyl mercury
MeHgCl	Methyl mercury chloride
M-value	Log_2 of fold change
mg	Microgram
mg/l	Microgram per litter
ml	Milliliter

Acronym or symbol	Definition
mRNA	Messenger Ribonucleic acid
NAS	National Academy of Sciences
Oligo(dT)	Oligodeoxythymidylic acid
Pb	Lead
$PbCl_2$	Lead (II) chloride
PMT	Photomultiplicator
PTWI	Provisional tolerable weekly intake
RfD	Reference dose
SCDS	Seychelles Child Development Study
RNA	Ribonucleic acid
SD	Standard deviation
SEM	Standard error of the mean
SNR	Signal-to-noise ratio
U.S. EPA	U.S. Environmental Protection Agency
U.S. FDA	U.S. Food and Drug Administration
U.S. PHS	U.S. Public Health Service
µg	Microgram
µg/g	Microgram per gram
µg/l	Microgram per liter
µg/kg	Microgram per kilogram
µg/ml	Microgram per milliliter
µl/ml	Microliter per milliliter
UTP	Uridine-5'-triphosphate
WHO	World Health Organization
Zn	Zinc

Introduction

1.1 Toxicogenomics

Toxicogenomics is a scientific field that studies the interaction between the genomes of cells and/or organisms and toxic substances (Gomase and Tagore, 2008; Hamadeh *et al*., 2002). When cells and organisms are exposed to toxicants or stresses, alteration of the gene expression patterns of the cells and organisms will be triggered as a mean to cope with the unfavourable environment. Such an alteration can be monitored by the DNA microarray technology, which enables the detection of the activity of thousands of genes simultaneously (de Longueville *et al.*, 2004, Nuwaysir *et al.*, 1999). Since the introduction of toxicogenomics in the area of toxicological research in the late 1990's, the principles and technologies relevant to toxicogenomics have been widely adopted in both the academic and industrial fields (Nuwaysir *et al.*, 1999). Toxicogenomics allows a more comprehensive insight on how cells and organisms adapt to the changes in the external environment at the molecular level than traditional toxicological studies. This advancement of molecular technique provides a powerful tool for classifying chemicals, predicting potential toxicity, exploring mechanisms of toxicity and identifying potential biomarkers of toxic substances (Afshari *et al.*, 2010; Gatzidou *et al*., 2007; Hamadeh *et al*., 2002, Pennie *et al*., 2001; Pennie and Kimber, 2002; Tennant, 2002; Tugwood *et al.*, 2003; Suter *et al*., 2002; Yang *et al*., 2007). Knowing the mechanisms of toxicity allows us to identify ways to reduce or prevent the toxic effects by pinpointing biochemical and molecular functions that have been perturbed by toxic substances while the development of biomarkers helps to monitoring environmental toxicants and screening of drugs.

1.2 Toxicity of methyl mercury

1.2.1 Sources of environmental mercury

Mercury (Hg) presents naturally in the Earth's crust and it is estimated that 25,000 to 150,000 tons per year are emitted into the environment through normal geological

processes like soil erosions and volcano eruptions (USEPA, 1995). An additional 20,000 tons are produced anthropogenically each year by industrial activities such as electric utilities, waste incineration, residential, commercial, and industrial coal burning, mining, chlor-alkali facilities and mobile sources (Sams, 2004; Seigneur *et al*. 2004; USEPA, 1995).

1.2.2 Human contact with Hg and its derivatives and their depositions in the body

Due to the widespread prevalence of Hg and its derivatives in the environment, the contact of human with these toxic chemicals is unavoidable. The consumption of methyl mercury (MeHg)-contaminated seafood, the use of Hg-containing dental amalgam for tooth fillings and the uptake of ethylmercury (EtHg) in the form of thimerosal added as an antiseptic in vaccines are the three most common ways that poses the risk of Hg poisoning nowadays (Clarkson, 2002).

The accumulation of MeHg in seafood is of particular concern since MeHg is present in virtually all edible marine and freshwater organisms. Analytical studies which measured MeHg in surface water, groundwater and ocean water in Europe and the United States indicated that Hg concentrations in the water bodies were highly variable (USEPA, 1997). Total Hg levels in the water body were generally under 20ng/l (NJDEPE, 1993). However, in areas where were heavily polluted by anthropogenic mercury sources could have MeHg level more than 2,000 ng/l (Dooley, 1992). Once entering the aquatic environments, Hg will be modified biologically and chemically into organic Hg including MeHg (Celo *et al*., 2006; King *et al*., 2000). The concentration of MeHg increases by bio-accumulation in fish via the food chain. As MeHg has a long half-life in biological tissues, this facilitates the bio-accumulation and bio-magnification of MeHg by transferring MeHg from one to another tropic level (Clarkson, 1993; Madenjia *et al.*, 2008). The concentrations of MeHg in long-lived piscivorous fishes and marine mammals, which located at the high tropic levels of the food chain, have been estimated to be up to million-folds of the surrounding environment (USEPA, 2001). Although most fish were reported to have MeHg content of less than the U.S. Environmental Protection Agency (U.S.

EPA) advisory guideline of 0.3 μg/g in their muscle, large piscivorous fish could accumulate up to more than 1 μg/g (Chalmers *et al.*, 2011; Greigl and Krzynowek, 1979; Hellou *et al.*, 1992). Upon consumption of MeHg containing food, about 95% of MeHg in the diet will be absorbed by the gastrointestinal tract and distributes to all the tissues and organs through the bloodstream in about 30 hours (Clarkson, 2002). MeHg can pass through the blood-brain barrier and accumulates in the brain, and be readily transferred to the fetus through the placenta during pregnancy and distribute throughout fetal tissues including the brain (Ask *et al.*, 2002; Cernichiari *et al*., 1995). MeHg levels in the cord blood are proportional but slightly higher than those in the maternal blood (Vahter *et al.*, 2000). While the brain to blood ratio in adult is of approximately similar range, this ratio is about 5 to 7 times higher in the fetus in human and other primates (Cernichiari *et al*., 1995; Grandjean *et al*., 1997). The growing scalp hair also show high levels of MeHg accumulation and the concentrations are proportional to simultaneous concentrations in blood and target organs including the brain (Al-Shahristani *et al.*, 1976; Berglund *et al.*, 2005; Cernichiari *et al*., 1995). Thus, scalp hair and blood samples are frequently used as indicators of adult and fetal brain MeHg levels in MeHg exposure studies (Bencko 1995; Crump *et al.*, 1998; Grandjean *et al*., 1997; Myers *et al.*, 2003). MeHg has a biological half-life of 35 to 100 days (Al-Shahristani *et al.*, 1976; Smith and Farris, 1996). It has been suggested that MeHg would be converted to Hg by intestinal microorganisms and eliminated from the body through fecal excretion in the form of Hg (Kozak and Forsberg, 1979; Smith and Farris, 1996).

Dental amalgam has been used for the restoration of carious lesions or structural defects in teeth for over 150 years. It is a metallic material comprises several metals, including Hg, silver, tin and copper, with Hg being the principal component and constituting about 50% of the amalgam by weight (Marshall and Marshall, 1992; Ray 1993). Hg vapour levels of 0.1 to 10 μg were calculated to be released per day from each amalgam filling into the oral cavity. About 80% of the inhaled Hg vapour was estimated to be absorbed by the respiratory system (Ekstrand *et al.*, 1998; Olsson and Bergman, 1992). The total Hg levels in plasma and urine was shown to be highly positively correlated with the number of dental amalgam fillings (Berglund *et al.*, 2005). Animal model studies indicated that Hg accumulates in the retina, cerebral cortex, cerebellum and kidney (Warfvinge, 2000; Warfvinge and Bruun, 2000;

Warfvinge *et al.*,1994). Studies measuring the concentrations of Hg in urine and faeces showed that Hg has a biological half-life of 21 to 121 days in the human body (Björkman *et al.*, 1997; Sandborgh-Englund, 1998; Ekstrand *et al.*, 1998). However, some other studies indicated that the deposition and toxicity of Hg could last many years (Hargreaves et *al.* 1988; Kobal *et al.*, 2004; Letz *et al.*, 2000; Opitz *et al.*, 1996).

Thimerosal is an Hg-containing compound comprising 49.6% of Hg by weight and will be converted to EtHg and thiosalicylate through metabolisation or degradation (Geier *et al.*, 2007; Tan and Parkin, 2000). It is widely used as an antimicrobial preservative in a number of biological and drug products, including many topical medications and vaccines, in the U.S. since the 1930s (Geier *et al.*, 2007). In the U.S., a normal dose of a pediatric vaccine contains around 17.5 to 25 μg Hg per 0.5 ml dose (USFDA). It was reported that infants who were immunised according to the recommended schedule might have cumulative Hg level up to 187.5 μg during the first 6 months of life, exceeding the U.S. EPA limits for Hg exposure, which was calculated based on the MeHg data (Ball *et al.*, 2001). Due to the limited data on thimerosal or EtHg metabolism in the body, the estimation of health risks possessed by thimerosal was mainly based on the assumption that the toxicity of EtHg is similar to that of MeHg (Magos *et al.*, 1985). It has been hypothesised that thimerosal exposure is associated with autism or other developmental disorders. However, the evidences supporting such an association are controversial (reviewed in Schultz 2010). Nonetheless, as a precautionary measure, the U.S. Public Health Service (U.S. PHS) and the American Academy of Pediatrics (AAP) published a joint statement in 1999 recommending that thimerosal-containing vaccines should be removed as soon as possible (CDC, 1999).

1.2.3 Occurrence and symptoms of MeHg poisonings

Hg compounds have long been known to be highly toxic, but they, particularly MeHg, started to receive special attention after several serious Hg poisonings in the last century (Bakir *et al.*, 1973; Elhassani, 1982; Harada, 1995). The first outbreak occurred in the Minamata city in Japan in the year 1953 and was caused by the consumption of seafood that had been contaminated by MeHg due to the

inappropriate discharge of sewage into the sea from an acetaldehyde plant in which inorganic Hg compounds were used as catalyst (Harada, 1995). It led to devastating consequences to the fishermen, their families, seafood consumers, fish, birds and cats in the polluted area, and resulted in 2,264 officially recognised victims (Ekino *et al*., 2007). Several outbreaks also occurred later in Iraq due to the ingestion of wheat and/or barley seeds treated with organomercurial fungicides (Greenwood, 1985). This resulted in 100 cases with 14 deaths in the year 1956, an estimate of 1000 cases in the year 1960 and 6530 cases with 459 deaths in the year 1972 (Bakir *et al.*, 1973; Jalili and Abbasi, 1961). Follow-up studies of the poisonings, termed Minamata disease (MD) named after the city, showed that in human, acute MeHg poisoning could result in blurred vision, hearing impairment, olfactory and gustatory disturbances, ataxic gait, clumsiness of the hands, dysarthria, and somatosensory and psychiatric disorders (Ekino *et al*., 2007; Eto *et al.*, 2010; Harada, 1995). Children with maternal exposure to MeHg showed impairments in chewing, swallowing, speech, gait, and other coordination and involuntary movement due to extensive damage of the brain, particularly the cerebral and cerebellar cortices. Infection, cancer, cerebrovascular disorder, cardiac failure and hepatic disorder were also observed in MD patients (Harada, 1995). Investigation on patients with chronic MeHg exposure, the residences living in the vicinity of Minamata city, indicated that chronic MeHg poisoning could lead to somatosensory disturbances, sensory ataxia and pseudoathetoid movements, disorders of visual and hearing discrimination (Ekino *et al*., 2007). Autopsy examinations of the brains showed that depopulation of neurons in calcarine, temporal, pre- and post-central cortices and diffuse degeneration of the deep white matter were commonly observed in chronic MD patients (Eto, 1997; Eto *et al.*, 2010). Although depositions of Hg were also detected in liver and kidney, no functional disorder was clinically recognised (Eto, 1997). Epidemiologic studies have also showed that there was an increase risk of cardiovascular diseases and hypertension in people with high body Hg levels (Bautista *et al.*, 2009; Salonen *et al.*, 1995; Yoshizawa *et al.*, 2002).

1.2.4 Large-scale studies of the neurotoxicity of MeHg to children

The developing brain of fetus is much more susceptible to toxic chemicals than the adult brain (Rice and Barone, 2000). In order to gain a better insight on the toxicity of MeHg to children's brain development, large-scale, chronic low-level dietary exposure studies were conducted on human in the Faroe Islands (Grandjean *et al*., 1997), New Zealand (Crump *et al*., 1998) and the Republic of Seychelles (Myers *et al.*, 2003), where the residents had high fish consumption. In the Faroe study, the Hg concentrations in the cord blood and the maternal hair of a cohort of 917 new born infants and in the hair of the children at the age of 12 months and 7 years were measured (cord blood: mean = 22.9 μg/l, interquartile range (IR) = 11-41.3; maternal hair: mean = 4.27 μg/g, IR = 2.6-7.7; 12-month-old: mean = 1.12 μg/g, IR = 0.69-1.88; 7-year-old: mean = 2.99 μg/g, IR = 1.7-6.1), and detailed neurobehavioral examinations were performed on the children at the age of approximately 7 (Grandjean *et al*., 1997). Although the clinical examination and neurophysiological testing did not show any clear-cut relationship between MeHg exposure and abnormalities, Hg-related neuropsychological dysfunctions were pronounced in the domains of language, attention and memory, and also to a lesser extent in visuospatial and motor functions. In the New Zealand study, prenatal exposure to MeHg in a cohort of 237 children was determined by measuring the mother's hair Hg concentration during pregnancy (mean = 20 μg/g), and a range of scholastic and psychological tests were administrated to the children at the age of 6 to 7 years (Kjellstrom *et al.*, 1986, 1989). Statistical analysis revealed that the scores on six tests were significantly associated with the mothers' hair Hg level (Crump *et al*., 1998). In the Seychelles Child Development Study (SCDS), the effects of prenatal exposure to MeHg were examined in 779 mother-infant pairs by measuring the MeHg concentrations of the mothers' hair during pregnancy (mean 6.89 = μg/g, standard deviation (SD) = 4.52) and correlating them with the performance of the developmental tests examined on the children periodically from the age of 6.5 months to 10.5 years (Myers *et al.*, 2003), while the effects of postnatal MeHg exposure were determined by measuring the hair Hg levels of 537 to 739 children (66-month-old: mean = 6.5 μg/g, SD = 3.3; 107-month-old: mean = 6.1 μg/g, SD = 3.6) and examining the children's intelligence quotient (IQ) at the age of 66 and 107 months

(Myers *et al.*, 2009). A follow-up study examining the school achievements of 215 children or teenagers in the SCDS main cohort at the age of 9 (prenatal MeHg: mean = 6.77 μg/g, SD = 4.21; 9-year-old: mean = 6.09 μg/g, SD = 17) and 17 (prenatal MeHg: mean = 6.95 μg/g, SD = 4.67; 17-year-old: mean = 8.00 μg/g, SD = 4.68) was also performed (Davidson *et al.*, 2010). All the SCDS results indicated that there was no consistent pattern of associations to support a causal relationship between MeHg exposure from fish consumption and children's brain development since children's brain development might benefit from the nutrients obtained from fish consumption despite the concomitant MeHg intake.

Based on these three studies with special reference to the Faroe Island one, the U.S. Environmental Protection Agency (U.S. EPA) and the National Academy of Sciences (NAS) recommended a Hg reference dose (it is an estimate of a level of exposure to the human population without causing any adverse effect on health when the exposure is encountered on a daily basis for a whole lifetime) of no more than 0.1 μg/kg body weight per day (NAS, 2000; Rice *et al.*, 2003; USEPA, 2001). Similarly, the Food and Agriculture Organization of the United Nations (FAO) and the World Health Organization (WHO) recommended 1.6 μg/kg body weight per week (that is 0.23 μg/kg body weight per day) as the provisional tolerable weekly intake (PTWI) (FAO/WHO, 2010).

1.2.5 Neurotoxicity of MeHg to animal models

In order to gain more insight into the toxicity of MeHg, studies using animal models have been widely employed. Studies performed on mammalian models have showed that prenatal and postnatal exposure to MeHg could result in neurobehaviorial, neurodevelopmental and neuropathological defects (Castoldi *et al*., 2008; Johansson *et al.*, 2007). Monkeys exposed to MeHg prenatally exhibited visual and auditory impairment (Burbacher *et al.*, 2005; Rice, 1998), decrease in social play behavior and increase in non-social passive behavior (Burbacher *et al.*, 1990) and subtle change in fixed interval/fixed ratio performance (Gilbert *et al.*, 1996). Rodents treated with MeHg prenatally and postnatally also showed various neurobehavioral defects such as decreased learning and memory performances (Baraldi *et al.*, 2002), hearing

impairment (Beyrouty *et al.*, 2006), lowered locomotion activity (Elsner *et al.*, 1998), and reduced swimming activity (Elsner *et al.*, 1998). Rodents exposed to MeHg during development exhibited a range of neuroanatomical defects including cerebellar dysplasia (Sakamoto *et al.*, 2002), neural degeneration and inhibition of spontaneous neuronal differentiation in the brainstem, cerebral cortex, cingulate cortex, striatum, thalamus, hippocampus, or amygdala (Kakita *et al.*, 2000a,b; Sakamoto *et al.*, 2004), reduced thickness of the molecular and granular layers of the cerebellum (Markowski *et al.*, 1998; Sager *et al.*, 1984), change in distribution, structure or number of Purkinje cells and granule neurons in the cerebellar cortex (Chiang *et al.*, 1977 a, b; Sager *et al.*, 1984), disruption of myelin sheath (Chiang *et al.*, 1977b; Wakabayashi *et al.*, 1995), and mitotic arrest of cells in the cerebellum (Rodier *et al.*, 1984; Sager *et al.*, 1984). Alterations in the neuroendocrine and neurochemical systems, such as monoaminergic (Beyrouty *et al.*, 2006; Cagiano *et al.*, 1990), glutamatergic (Cagiano *et al.*, 1990; Carratu *et al.*, 2006) and cholinergic (Zanoli *et al.*, 1994) neurotransmitter systems, and in the electrophysiological systems, like membrane potential, amplitude of spikes and degree of excitability (Vilagi *et al.*, 2000), have been also observed in rodents treated with MeHg during development. Besides neurological disorders, MeHg has also been reported to cause cardiovascular disease, affect reproduction, suppress immune functions and induce autoimmunity in multiple species (Silbergeld *et al.*, 2005).

1.2.6 Mechanisms of MeHg toxicity

MeHg exposure has been shown to result in various cellular changes such as lipid peroxidation, DNA damage, membrane structure alteration, mitochondrial dysfunction, cell cycle alteration, apoptosis and necrosis (Clarkson and Magos, 2006). The interactions with sulfhydryl groups, the induction of oxidative stress and the disruption of calcium (Ca) ion homeostasis have been reported to be the three major and critical mechanisms. With its property of being a sulfhydryl-reactive metal, MeHg has a high affinity for free thiol (sulfhydryl) groups (Vallee and Ulmer, 1972). Thiol-containing amino acid cysteine and thus, virtually all proteins, especially cysteine-rich glutathione (GSH) and metallothionein (MT), are potential targets of MeHg (Kidd 1997; Quig, 1998; Vallee and Ulmer, 1972). MeHg decrease body's

antioxidative capacity as it leads to the depletion of GSH antioxidant and the decrease in activities of other antioxidants molecules including superoxide dismutase (SOD), catalase (CAT) and glutathione peroxidase (GPx) (Stohs and Bagchi, 1995). The pro-oxidant property of MeHg is, at the same time, further exacerbated by the increase in the production of reactive oxygen species (ROS) as shown by biochemical studies (Ali *et al.*, 1992; Sarafian, 1999; Shanker *et al.*, 2004). A cell culture study demonstrated that MeHg affected the redox-sensitive mitogen-activated protein (MAP) kinase/AP-1 and NF-kB pathways, which are implicated in cell cycle progression, cell proliferation and apoptosis (Korashy and El-Kadi, 2008). The formation of ROS and the induction of oxidative stress are believed to contribute to the neuropathogenesis of MeHg as co-treatment of brain cell cultures with MeHg antioxidants could attenuate the production of ROS and neurotoxicity (Park *et al.*, 1996; Shanker and Aschner, 2003; Shanker *et al.*, 2005). Metallothionein (MT) is an intracellular metal-chelating protein, which binds to both physiological and xenobiotic heavy metals, (Stillmann, 1995) and plays a neuroprotective role against Hg exposure (Yoshida *et al.*, 2005, 2006). MT has been shown to be induced by Hg directly and indirectly through the displacement of Zinc (Zn) ion (Aschner *et al.*, 2006; Coyler *et al.*, 2002). Under normal physiological condition, MT serves as a storage depot for Zn (Henkel and Krebs, 2004). When Hg is present, Hg will displace Zn to from a complex with MT due to the higher affinity of MT to Hg than Zn (Stillman, 1995, Stillmann *et al.*, 2000). The increased intracellular Zn ion concentration induces the expression of MT, and thus, in return, increases the binding capacity for Hg and Zn (Davis and Cousins, 2000). MeHg is also known to disrupt intracellular Ca ion homeostasis. Such a disruption was suggested to be caused by blocking the function of Ca ion channels (Atchison, 2003; Shafer *et al.*, 1990). The blocking is irreversible and it remains even after MeHg was washed out of the bathing solution (Sirois and Atchison, 2001). The interfering with Ca ion channels attenuates or blocks completely cell current and affects skeletal and cardiac muscle contractility as well as neurotransmitter release (Follonier Castella *et al.*, 2010; Ho, 2010; Lee and Michalak, 2010). Massive increases in intracellular calcium can be detrimental for the cell and will cause cell death (Brnjic *et al.*, 2010; Harr and Distelhorst, 2010; Szydlowska and Tymianski, 2010).

1.2.7 Hg and MeHg biosensors

In order to monitor the presence of bioavailable MeHg in the environment through a rapid, non-invasive and non-labour intensive way, biosensors have been developed. Zebrafish containing a luciferase-green fluorescent protein (LUC-GFP) fusion protein under the regulation of the antioxidant response element (ARE) has been generated (Kusik *et al.*, 2008). The ARE promoter would drive the expressions of the reporter genes in response to oxidative stress. Increase in luciferase activity was observed in embryos exposed to 40 μg/l MeHg, although the GFP expression could not be detected. Systems involving lower class organisms of *C.elegans* and *E.coli* transfected with plasmid containing a cysteine located in close proximity of GFP showed specific induction of fluorescence signal in the presence of ionic Hg with a lower detection limit of 400 ng/l (Chapleau *et al.*, 2008; Chapleau and Sagermann, 2009). A luminescence-based MeHg-specific system using *E.coli* transfected with a plasmid carrying the luciferase gene *luxAB* under the control of the Hg inducible regulatory part of *mer*-operon has also been developed recently (Nagata *et al.*, 2010). It exhibited a detection limit of 2 ng/l MeHg.

1.2.8 Toxicity of MeHg or Hg to zebrafish

Zebrafish have been previously shown to be highly sensitive to MeHg. Exposure of zebrafish embryos to 20 and 30 μg/l MeHg led to impairment of caudal fin fold tissue and posterior tail flexure (Samson and Shenker, 2000). Doses between 10 and 20 μg/l MeHg induced faint heartbeats, severely enlarged body cavities and upward flexures of the spinal cord, body cavity and head edema, reduced swimming activity, impaired prey capture performance and delayed mortality syndrome and behavioural deficits (Samson *et al.*, 2001). Concentration of 32 μg/l Hg could inhibit hatching completely (Dave and Xiu, 1991). Embryos exposed to 10, 50 and 80 μg/l Hg showed decreased cell proliferation rate in the neural tube (Hassan *et al.*, 2011). Global transcriptome studies on zebrafish embryos showed that acute exposure to 60 μg/l MeHg induced genes involved in acute inflammatory response, detection of stimulus, amino acid derivative metabolism and transmembrane receptor protein tyrosine kinase signalling pathway and insulin receptor signalling pathway (Yang *et al.*, 2007). Similar genomic study in adult zebrafish indicated that sub-lethal acute or chronic exposure to MeHg

or Hg also caused genes expression changes in a variety of biological and molecular functions, such as gene expression change in oxidative stress, immune defence, DNA damage, apoptosis, lipid peroxidation, glycolysis/gluconeogenesis and so forth, in individual organs (Cambier *et al.*, 2010; Klaper *et al.*, 2008; Richter *et al.*, 2011; Ung *et al.*, 2011). A research on the localisation of MeHg in adult zebrafish after trophic and chronic MeHg exposure revealed that the brain accumulated highest level of MeHg among the three organs examined (Gonzalez *et al.*, 2005). Another study concerning the visual system showed that MeHg could pass through the blood-retina barrier and accumulated in various regions of the retina, especially in the photoreceptor layer and in the inner and outer nuclear layers in adult zebrafish (Mela *et al.*, 2010). It has also been shown in whole zebrafish embryos and larvae by X-ray fluorescent imaging that the lens epithelium had the highest level of MeHg deposition, with lower levels in the brain, optic nerve and other organs, after acute exposure to MeHg (Korbas *et al.*, 2008). MeHg continued to accumulate in the lens even after the removal of MeHg from the solution (Korbas *et al.*, 2010).

1.3 Advantages of using zebrafish embryo as an animal model

Zebrafish was introduced as a model organism for research study for more than three decades (Laale, 1977). It has a small size of 4 to 5 cm in length which allows low housing space and maintenance cost. The short generation time, rapid embryonic development and large number of offspring enable the generation of vast amount of data within short period of time. The transparent body of the embryo and the development outside the body of the mother provide a vertebrate model whose development is easy to observe and is not complicated by the physiology of the mother as in mammals while it possesses a body plan in which the basic structure does not differ much from mouse or human (Kimmel *et al*. 1995). Animal embryos are not regarded as animals according to the legislation of the Council of European Communities (Commission of the European Communities, 1986). Thus, zebrafish embryo serves as non-animal model while, in contrast to cell lines, it offers the advantages of a multi-cellular, complex, *in vivo* system for experimental studies.

Zebrafish may not only be an ecotoxicological relevant model, but may also be useful in elucidating underlying mechanisms through which chemicals, drugs or toxicants exerts its toxicity through the application of genomic and molecular techniques available (Hill *et al*., 2005; Yang *et al.*, 2009). The zebrafish genome sequencing has almost complete by now (http://www.sanger.ac.uk/Projects/D_rerio/). It contains comprehensive information on the genes and regulatory sequences, facilitating the mining of genetic information. A wide range of molecular tools and techniques has been developed in zebrafish to allow monitoring and manipulating of gene functions. Gene mutations can be generated by the use of the alkylating agent ethylnitroso urea (ENU), retroviral insertion and zinc finger nuclease. Morpholino antisense oligonucleotide, which can block the translation of mRNA transiently, is widely employed for studying gene functions during early development. The use of loss-of-function method in gene function studies is complemented by the gain-of-function approach such as injection or transfection of synthetic mRNAs. The generation of transgenic lines, which drive expression of fluorescent reporter genes in the cell of interest, helps to mark specific tissues or physiological changes.

1.4 Hypotheses and aims

It is known that the developing brain is much more susceptible to neurotoxicants than the adult brain, while there is a lack of data and enormous backlog of chemicals that require testing and some of these chemicals may poses effects on the developing brain like what MeHg does (Claudio *et al.*, 2000; Grandjean and Landrigan, 2006; Rodier, 1995). Therefore, there is a need of having model organisms for better monitoring and evaluating the effects of environmental pollutants and neurotoxicants. As MeHg is known to be a teratogen and neurotoxicant, the underlying hypothesis of this study is that zebrafish embryos exposed to sub-lethal concentration of MeHg will result in developmental defects and neural developmental defects, and the toxic effects of MeHg are associated with the modulation of expression of specific genes in the embryos.

One of the aims of this study is to establish biomarkers which could be used to develop *in vivo* biosensors to monitor waterborne MeHg or other toxicants that

showed similar toxicological profile as MeHg. Since morphological and behavioural endpoints are frequently not very informative with respect to the underlying mechanisms of the toxic effect, another aim of this study is to screen genes which are differentially expressed in MeHg-treated embryos to provide information for dissecting the underlying mechanisms through those MeHg exerts its toxicity.

In this study, a MeHg toxicity test was first performed to determine a suitable concentration of MeHg for further sub-lethal dosage study. As toxicogenomics has been shown to be a comprehensive and sensitive tool for examining the responses of genes toward changing environments in the molecular level, a toxicogenomic-based gene screening has been adopted in this study for identifying candidate genes which are regulated by MeHg. Herein, I reported the results of the toxicogenomic-based gene screen of MeHg-responsive genes in zebrafish embryos in response to acture MeHg exposure. Based on the phenotype observed and the current knowledge on MeHg toxicity, I further focused the study on 2 biological structures: the nervous system and the caudal fin. I also reported the study of one of the candidate genes *complement component c7-1* which was expressed specifically in the retina after MeHg treatment.

2 Materials and methods

2.1 Fish strains and fish maintenance

All adult zebrafish were maintained in aerated fish water at 28.5°C, subjected to a photoperiod of 10 hours light and 14 hours dark, and fed with dry flake food and brine shrimp as described (Westerfield, 2000). The *Tg(-2.4shha-ABC:GFP)sb15* transgenic line contains the 2.4 kb *shha* promoter upstream of and the elements ar-A, ar-B, ar-C of the *shha* introns 1 and 2 downstream of the *gfp* coding sequence (Ertzer *et al.*, 2007; Hadzhiev *et al.*, 2007; Müller *et al.*, 1999; 2000). The *Tg(-1.7CaTuba1:GFP)mi2* line contains the 1.7 kb goldfish (*Carassius auratus*) *α1-tubulin* promoter fragment and the first intron upstream of the *gfp* coding sequence (Goldman *et al.*, 2001; Gulati-Leekha and Goldman, 2006)

2.2 Chemical treatment

Methyl mercury chloride (MeHgCl), lead (II) chloride ($PbCl_2$), arsenic (III) oxide (As_2O_3) and cadmium chloride ($CdCl_2$) were purchased from Sigma-Aldrich (Missouri, USA). Working solutions of 6 to 120 µg/l MeHg, 20 mg/l of $PbCl_2$, 79 mg/l of As_2O_3 and 15 mg/l of $CdCl_2$ were prepared by diluting the chemicals from stock solution of 100 mg/l MeHg, 5 g/l of $PbCl_2$, 10 g/l of As_2O_3 and 4 g/l of $CdCl_2$, respectively, with embryo medium (60 µg/ml of Instant Ocean, Red Sea, Houston, USA) (Westerfield, 2000). Embryos were exposed to the chemicals from 4 to 72 hpf unless otherwise stated (descriptions and schematic diagrams of zebrafish embryos at selected stages are shown in the appendix Tab. A1 and Fig. A1, respectively). As reported by Yang *et al.* (2007), toxicant concentrations were chosen so that more than 60% of the treated embryos showed malformations but with minimal lethality.

2.3 RNA extraction

Total RNA was extracted from independent groups of 6, 30, 60 µg/l MeHg-treated and control embryos according to the RNeasy Mini Kit (Qiagen, Netherlands) protocol. One µg of total RNA was used in each sample for performing reverse

transcription following standard procedures (Sambrook *et al.*, 1989). M-MLV Reverse Transcriptase (Promega, USA) and oligo(dT) primer (Promega, USA) were used for reverse transcription.

2.4 DNA Microarray

2.4.1 Microarray experiment

Two-colour DNA microarrays using the zebrafish gene expression microarray chip 4x44K (Agilent Technologies, USA) were performed according to Agilent Low RNA Input Linear Amplification Kit protocol (Agilent Technologies, USA; Fig. 2.1). In brief, total RNA was extracted from control and MeHg-treated samples as described in section 2.3. Three independent biological repeats were performed for both control and MeHg-treated samples. Two microgram of total RNA from each sample was reverse transcripted into cDNA. cRNA was trancripted from the cDNA and labelled with Cyanine3 (Cy3) –CTP and Cy5-CTP fluorescent dyes (PerkinElmer/NEN Life Science, USA). The cRNA samples were purified with the RNeasy Mini Kit (Qiagen, Netherlands) and fragmented. Microarray chips were handled according to the user guide available with the Agilent Microarray hybridisation Chamber Kit (Agilent Technologies, U.S.A). cRNA was carefully loaded to the chips. Dye swap was performed for each set of biological repeat to avoid bias of the signal given by any of the dye. Cover slips were placed gently on top of the chips and the chips were incubated at 65^{o}C for 17 hours with rotation. After hybridisation, the probes were washed away from the chips. The fluorescent signals of the chips were detected by GenePix 4000B dual-channel microarray scanner (Molecular Device, USA) using the GenePix Pro 6.01 software (Molecular Device, USA). Signals for both Cy3 (532 nm) and Cy5 (635 nm) were scanned in parallel and the gain of the scanner photomultiplicator (PMT) was tuned so that the overall signal ratio of the two colours would be equal to 1. The captured images were stored as 16-bit TIFF files. Files in GenePix Result (GPR) format that contained a data part, including raw signal and background values, several statistical parameters including mean, standard deviation and the annotation provided by the microarray supplier, and a header with general scanning and image analysis information, such as colour channel used, laser settings,

date and time of scanning, feature type and grid-file used were generated using GenePix Pro 6.01 for data analysis.

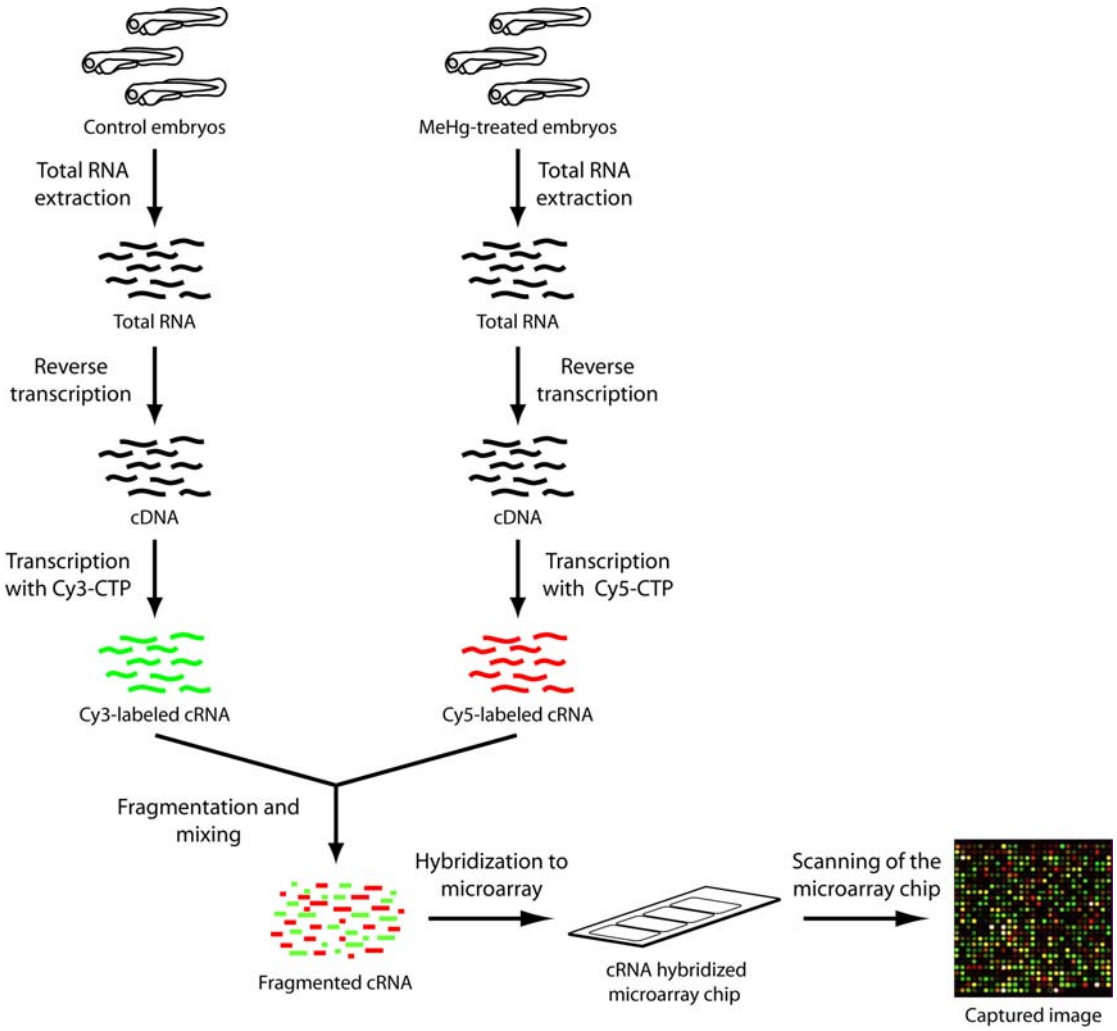

Fig. 2.1 Schematic representation of the procedure of DNA microarray.

2.4.2 Microarray data analysis

To maximise the true positive rate and minimise the false positive rate and to sort out the most robustly differently expressed genes from the raw microarray, a number of mathematical and computing steps (Russell *et al.*, 2009) were performed using the software MATLAB (version R2010a; the Math Works, USA) or MATLAB toolbox Gait-CAD (Mikut *et al*, 2008), which is a graphical user interface allowing easy analysis of different datasets via MATLAB. An add-on consisting of different filtering functions, normalisation methods and statistical tests were implemented in MATLAB for microarray analysis (Legradi, 2011).

The data analysis was performed as described below:

1) The raw data was uploaded into Gait-cad.
2) Log_2 transformations were performed on the data set to obtain a more symmetric distribution for better comparison. The log_2 transformed values were termed M-values.
3) Quality values for low-signal or flagged spots were calculated. The determination of the threshold value for low signal filtering was based on the analysis of the background signal of all the microarrays from one experiment. As the values of almost all the background (region without any spots) were below 200, the lowest signal limit was set to 200. Spots with low signals in both colour channels were marked as bad quality. Spots were flagged when the signals were generated due to artifacts like dusts or scratches or when the data values were missing due to empty spots. As these flagged spots could lead to problems in downstream data analysis, and might interfere with statistical tests or affect the stability of gene cluster, they were also penalised.
4) Locally weighted scatterplot smoothing (LOWESS) normalisation and centering normalisation was performed to correct for intensity dependent dye bias and array differences.
5) Quality plots showing the data distribution of each microarray were examined for quality control. The spike controls were also analysed.
6) All the data sets of the experiment, including all the biological repeats and the dye swaps, were fused together to make one data set.
7) The average values of the data from dye swaps were calculated and were used for quality measurement.
8) T-test was performed with the p-values and other parameters calculated from the averaged dye swap values.
9) As there were about 44,000 data points in each microarray, a t-test with a p-value of less than 0.05 (that is $p < 0.05$) would result in about 2,200 false-positive results. To decrease the false-positive rate, adjustment of the data set was required. Taken the advantage that false positives usually have rather small M-values, and based on a plot of the coefficient of variation (CV) against the M-values of the whole data set (Fig. 2.2), M-value of 1.3 was chosen as the cut-off value.

10) The data was then exported as a tab delimited text file.

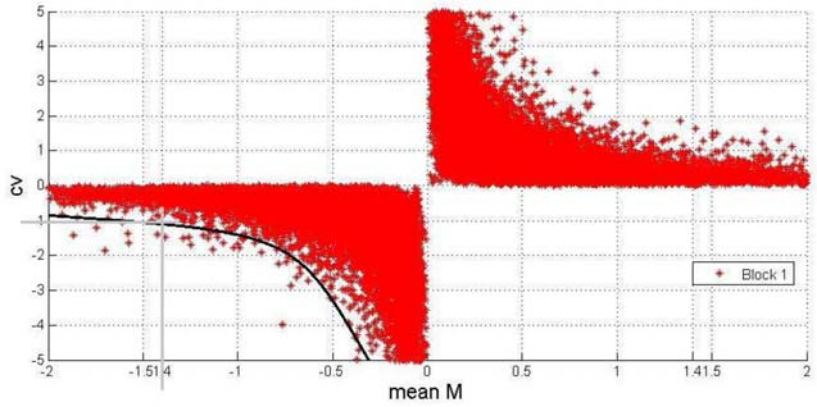

Fig. 2.2 A plot of the CV against the M-values from one microarray data set.
Each red dot represents one data point from the microarray. The black line indicates the maximal variance for a particular M-value. This figure is provided by J. Legradi.

2.5 Whole-mount *in situ* hybridisation

Whole-mount *in situ* hybridisation (ISH) was carried out as described (Westerfield, 2000). Antisense RNA probes of *ache* from Dr. Cousin (Bertrand *et al.*, 2001), *cb1* (Lam *et al.*, 2006), *crestin* from Prof. Halpern (Rubinstein *et al.*, 2000), *mmp9* (Yang, 2007), *mmp13a* (Yang, 2007), *nurr1* from Prof. Laudet (Escriva *et al.*¸1997), *pax6a* from Prof. Fjose (Krauss *et al.*¸1991), *serta* from Dr. Shirabe (Wang *et al.*, 2006), *shha* from Prof. Ingham (Krauss *et al.*, 1993) and *txnl* (Yang, 2007) were kindly provided. All other RNA probes used in this thesis were obtained by cloning from cDNA extracted from 72 hpf embryos, I.M.A.G.E. clones (Source BioScience imaGenes, Germany) or cDNA library screen according to the standard protocol (Sambrook *et al.*¸1989), and the information on the generation of these probes is listed in Tab. 2.1.

Tab. 2.1 Information of RNA probes for *in situ* hybridisation.

Gene	Primers/ probe sequence* (5' → 3')	Vector	Restriction enzyme	Transcriptase
adam8a	F: GTGTGACTGCGGAACTGTTG; R: ATGGCAGAAGGTGGTACAGG	pGEM-T Easy	SacII	Sp6
agt	F: CCGGATCCGGTGGTGCAAATCAAAGAACTGCTCCTCAGTG; R: CAGAGATGCATAATACGACTCACTATAGGGAGAGACAAACCACAACTAGAATG	pME18S-FL3	NiI	T7
AI397362	F: GATTGAAGATGAGCTACCATGC; R: GAGCTGACAGCGAGACAGAG	pGEM-T Easy	SalI	T7
AI544649	F: GGGTCACATTCTTCACAGGTAGT; R: GCTGATTGGCTGACTATCGAA	pGEM-T Easy	SacII	Sp6
AI793818	F: GAGCTGGAGCACCAGGAGAT; R: GAAGCACATCCTGTCAATCACC	pGEM-T Easy	Sac II	Sp6
apoeb	F: TCTGGCAGTATGTGTCTGAACTC; R: AATAGCCTCCAAGACAGACAAG	pGEM-T Easy	SalI	T7
arfl	F: CCGGATCCGGTGGTGCAAATCAAAGAACTGCTCCTCAGTG; R: CAGAGATGCATAATACGACTCACTATAGGGAGAGACAAACCACAACTAGAATG	pME18S-FL3	NiI	T7
atf3	NiI	FLC III	CeuI	T7
AI793818	F: GCCGGAAGGAGCTCTCTGTA; R: GAAGCACATCCTGTCAATCACC	pGEM-T Easy	SacII	Sp6
AW115990	F: CCGGATCCGGTGGTGCAAATCAAAGAACTGCTCCTCAGTG; R: CAGAGATGCATAATACGACTCACTATAGGGAGAGACAAACCACAACTAGAATG	pME18S-FL3	NiI	T7
BE016163	F: GCTGAGCACTGTATTTAAAGAACCA; R: GCTGAATGTATTTGTGACCCATAGC	pGEM-T Easy	SacII	Sp6
BG727211	F: GGTGGATGACACTACATGTAACACC; R: GTGAACATGATCCTCAATACACAGG	pGEM-T Easy	SacII	Sp6
BG891932	F: GGCATACGGTGAAACATTTG; R: GATTGACCAGTGGTTGAATGG	pGEM-T Easy	SacII	Sp6
BI474700	F: CCGGATCCGGTGGTGCAAATCAAAGAACTGCTCCTCAGTG; R: CAGAGATGCATAATACGACTCACTATAGGGAGAGACAAACCACAACTAGAATG	pME18S-FL3	NiI	T7
BI883993	F: CAAGATTCGTTATCCTCTGGTG; R: GTAGTCAATTCATCAACACCTGGA	pGEM-T Easy	SacII	Sp6
BI892110	F: GATTCCCCTGCCTAGCTATTATAAG; R: GCCCGCATTCTCTCCACCAATATAT	pGEM-T Easy	SacII	Sp6
BI983579	NiI	pBluescript SK-	EcoRI	T7

Gene	Primers/ probe sequence* (5' → 3')	Vector	Restriction enzyme	Transcriptase
BM036361	Nil	pBluescript SK-	EcoRI	T7
BM101698	F: CCGGATCCGGTGGTGCAAATCAAAGAACTGCTCCTCAGTG; R: CAGAGATGCATAATACGACTCACTATAGGGAGAGACAAACCACAACTAGAATG	pME18S-FL3	Nil	T7
c3a	F: GGAAGGTCGTCACACGATTC; R: GCCGAGTAAGGCATCTTGAG	pGEM-T Easy	SacII	Sp6
c4-2l	Nil	pBluescript SK-	EcoRI	T7
c5-1	F: ATCTGCACGAACCGTCACTC; R: TAGAGTCTGCCACCAGCTCAG	pGEM-T Easy	SacII	Sp6
c6	F: GGTCTGTGTTGAGGCCATCT; R: GCACTTCATTGCAGCCATA	pGEM-T Easy	SacII	Sp6
c7-1	F: GACCGTATGGAGACTGGTCA; R: GCCTCACATTCTGACATCATCT	pGEM-T Easy	SacII	Sp6
c7-2	F: GAACCTGTGCATTGCTTGTG; R: TGACAGGCGGAGTCTTCAG	pGEM-T Easy	SacI	T7
c8a	F: ACCGTGTCAATCATGCACAG; R: GCACTGGAACGCCATTATTC	pGEM-T Easy	SacII	Sp6
c8b	F: TCTGCGCTGTAATGGAGATG; R: TGAGCTCCAGCACATGCTAC	pGEM-T Easy	SalI	T7
c8g	F: TTGCTGTGATGATTCGCTTC; R: TCGTTGTGTTGTGTAACTCTGAAC	pGEM-T Easy	SacII	Sp6
c9	F: ACGATCCACCACCAGTTGAC; R: CAGCACTGCCAGCATTACC	pGEM-T Easy	SacII	Sp6
cartll	F: GGCTGCAGAAATGGACTTTG; R: AAGAGCAGCAAGGAACTAAACG	pGEM-T Easy	SacII	Sp6
cbx7l	F: CCAGTCCAAGAATCCGTCTG; R: GTAATGGCGACTGCTGGAAG	pGEM-T Easy	SacII	Sp6
cebpg	Nil	FLC III	CeuI	T7
cfb	Nil	pSPORT1	EcoRI	Sp6
copeb	Nil	pBlueScript SK	XhoI	T3
cxc46l	F: CCGGATCCGGTGGTGCAAATCAAAGAACTGCTCCTCAGTG; R: CAGAGATGCATAATACGACTCACTATAGGGAGAGACAAACCACAACTAGAATG	pME18S-FL3	Nil	T7

Gene	Primers/ probe sequence* (5' → 3')	Vector	Restriction enzyme	Transcriptase
cyldl	F: GGAGGTAGCATCAGGAGCAG; R: GAGATTCCATCCTGCCTCAT	pGEM-T Easy	SacII	Sp6
drl	F: GCATGGAGGGAAACAAGAAA; R: CTTCCCATTCTGGGGAAACT	pGEM-T Easy	SacII	Sp6
elf3	F: GAGCGAATCTGAACGTCACC; R: GCCGGAAGGAGCTCTCTGTA	pGEM-T Easy	SacII	SP6
fn1b	F: ACCTGCCTTAAGTGGACGTG; R: CAGAGTGGCAGTTGTGGATG	pGEM-T Easy	SacI	T7
fos	Nil	FLC III	CeuI	T7
foxb1.2	Nil	pBlueScript SK	XhoI	T3
gclm	F: CCGGATCCGGTGGTGCAAATCAAAGAACTGCTCCTCAGTG; R: CAGAGATGCATAATACGACTCACTATAGGGAGAGACAAACCACAACTAGAATG	pME18S-FL3	Nil	T7
gldc	F: CCGGATCCGGTGGTGCAAATCAAAGAACTGCTCCTCAGTG; R: CAGAGATGCATAATACGACTCACTATAGGGAGAGACAAACCACAACTAGAATG	pME18S-FL3	Nil	T7
gpx1a	F: GGCAGGAACCATGAAGAAGT; R: GACTGCACAGTCGGTCTATATCA	pGEM-T Easy	SalI	T7
gpx4a	F: GACTATGTCTGCACAGCTAGAGG; R: GCATGTCTCTTCATCTGTCCTCTC	pGEM-T Easy	SacII	SP6
hhex	Nil	pBlueScript SK	XhoI	T3
homez	Nil	FLC III	CeuI	T7
irf9	F: CCGTCTGCGTTCATGGATAG; R: TTGCAATGGACTCTCTGAAGG	pGEM-T Easy	SalI	T7
junb	F: TCGGAGCATCACAGAGGAG; R: ACAGGATCTGCTCTTCCAGTG	pGEM-T Easy	SalI	T7
klf10l	GGATCAAGATGTCTCAACAAGTTTC	pBlueScript SK	XhoI	T3
klf11b	Nil	pBlueScript SK	XhoI	T3
lamp1l	GGATCAAGATGTCTCAACAAGTTTC	pBlueScript SK	XhoI	T3
lcp1	F: GCCAAGGTGGTTCATGACTT; R: CCAGTCGATGTCCTGGTTTT	pGEM-T Easy	SacI	T7

Gene	Primers/ probe sequence* (5' → 3')	Vector	Restriction enzyme	Transcriptase
mafba	Nil	pBlueScript SK	XhoI	T3
maff	Nil	pBlueScript SK	XhoI	T3
mmp9	F:CAGCAACACTGCTTGCACTT; R:AGGAAACCCATCATGACCAA	pCS2+	BamHI	T7
mmp13a	F:GGCACGAGAAACATGAAGACC; R:CACACACAAATGATTTTCAAGGA	pCS2+	EcoRI	T7
mmp14a	F: AGCTACGCTCTCGGCAATG; R: TAGTCCTGTGCCAAGCTCCT	pGEM-T Easy	SacI	T7
mpx	F: CTGCCCATGGTTAGACTGGT; R: AAGACGTTCGCAATGGTAGG	pGEM-T Easy	SacII	SP6
mpz	F: GTTGGCAGCGAAACTCAAAC; R: GGCAGAATGGAGACAGAGGT	pGEM-T Easy	SacI	T7
noxo1	F: CCGGATCCGGTGGTGCAAATCAAAGAACTGCTCCTCAGTG; R: CAGAGATGCATAATACGACTCACTATAGGGAGAGACAAACCACAACTAGAATG	pME18S-FL3	NiI	T7
opn1lw1	F: GGCCAGTGACAGCAGATAAT; R: GGCAGGCATCTACCAATCA	pGEM-T Easy	SalI	T7
opn1mw1	F: GGACAGAAGGGAGCAACTTCTA; R: GGAGTAGATATTGTGCATAGATCCAG	pGEM-T Easy	SacII	SP6
opn1sw1	F: GTTGACTCCACCAGGACACA; R: GAGCAGACAGTGAACGATTCC	pGEM-T Easy	SacII	SP6
pax2a	Nil	FLC III	CeuI	T7
pax6a	Nil	pBlueScript SK	XhoI	T3
pck1	GGATCAAGATGTCTCAACAAGTTTC	pBlueScript SK	XhoI	T3
pfkfb4l	F: GGAGGTGAAGATTGAGGAACC; R: GCTTCGAAGGCATTAACATTG	pGEM-T Easy	PstI	T7
plac8l1l	F: GCAGTGACCTACTTGTCTGTGCTCT; R: GGTCTGGAACTGTAATTATGTCTCT	pGEM-T Easy	SacI	T7
plp1b	F: CGTCCAGGACTTCACTGTCA; R: GAGCACCATCATTGATCAGG	pGEM-T Easy	SpeI	T7
prdm1a	Nil	FLC III	CeuI	T7

Gene	Primers/ probe sequence* (5' → 3')	Vector	Restriction enzyme	Transcriptase
prdx1	F: GTATCGCGAGACTTGAGCAC; R: GCATTAATTCACATCACTTCTGTC	pGEM-T Easy	SalI	T7
rrad	F: GCGAGGATATTCGGTGGAG; R: CTTGGCTGAGTTACGAACCTG	pGEM-T Easy	SalI	T7
rx1	Nil	pBlueScript SK	XhoI	T3
s100z	F: AACTACTCCGGCAGTGAAGG; R: CACAGCAAGAACCTCACAGG	pGEM-T Easy	SacII	Sp6
sar2	Nil	pBluescript SK-	EcoRI	T7
sepw1	F: GAGGCACAGCACAACCAAT; R: GTTGTGCGTTGTAGCAAAGG	pGEM-T Easy	SacII	Sp6
sgk1	F: CCGGATCCGGTGGTGCAAATCAAAGAACTGCTCCTCAGTG; R: CAGAGATGCATAATACGACTCACTATAGGGAGAGACAAACCACAACTAGAATG	pME18S-FL3	NiI	T7
si:ch1073-126c3.2	Nil	pSPORT1	EcoRI	Sp6
si:ch211-106h4.4	F: GGAGAGATGGAGTGGACCAA; R: GGTGGAGAAGTGGGATCTGA	pGEM-T Easy	SacII	Sp6
six3a	Nil	FLC III	CeuI	T7
six3b	Nil	pBlueScript SK	XhoI	T3
slc16a9a	F: GAGAATGGCTGCTGTGAAGA; R: GTCCAGTCGAAGAACCAACC	pGEM-T Easy	SalI	T7
slc16a9b	GGATCAAGATGTCTCAACAAGTTTC	pBlueScript SK	XhoI	T3
socs3a	F: GGTAACGCATAGTAGGCTTGACAG; R: GCTTGCACTGCGGTCATC	pGEM-T Easy	ApaI	Sp6
socs3b	F: GCCGAGACTCGACACTCTGTAT; R: GTGTGTTCAGTCTTGCTATGTTGT	pGEM-T Easy	ApaI	Sp6
sox7	Nil	FLC III	CeuI	T7
sp9	Nil	pBlueScript SK	XhoI	T3
sqrdl	F: ATTTAGGTGACACTATAGGAATTACAACAGTACTGCGATGAG; R: CCTGATTCTGTGGATAACCGTATTACCGCCTTACGC	pDNR-LIB	XhoI	T7

Gene	Primers/ probe sequence* (5' → 3')	Vector	Restriction enzyme	Transcriptase
sqstm1	GGATCAAGATGTCTCAACAAGTTTC	pBlueScript SK	XhoI	T3
tp53	Nil	pBlueScript SK	XhoI	T3
txnl4a	F: GAGGGCGATGTAGATATCAGTTAGTA; R: GCTAAACAAGACCATTAAACTGTCC	pGEM-T Easy	SacII	Sp6
ucp1	GGATCAAGATGTCTCAACAAGTTTC	pBlueScript SK	XhoI	T3
ugt5a2	F: CCGGATCCGGTGGTGCAAATCAAAGAACTGCTCCTCAGTG; R: CAGAGATGCATAATACGACTCACTATAGGGAGAGACAAACCACAACTAGAATG	pME18S-FL3	Nil	T7
uox	Nil	pExpress-1	EcoRI	T7
zgc:56382	F: CCGGATCCGGTGGTGCAAATCAAAGAACTGCTCCTCAGTG; R: CAGAGATGCATAATACGACTCACTATAGGGAGAGACAAACCACAACTAGAATG	pME18S-FL3	Nil	T7
zgc:92254	Nil	pSPORT1	EcoRI	Sp6
zgc:101661	F: CCGGATCCGGTGGTGCAAATCAAAGAACTGCTCCTCAGTG; R: CAGAGATGCATAATACGACTCACTATAGGGAGAGACAAACCACAACTAGAATG	pME18S-FL3	Nil	T7
zgc:162126	F: GTCTGTCAGCTCCAGAACGA; R: GGATCTGCTCGCATAACTCC	pGEM-T Easy	SacII	Sp6

* F, forward primer; R, reverse primer

2.6 Immunohistochemistry

Immunohistochemistry (IHC) using primary antibodies of rabbit anti-activated Caspase-3 (casp3; 1:500 dilution; R & D systems, USA), mouse anti-acetylated tubulin (1:1000 dilution; Sigma-Aldrich, USA), anti-slow myosin F59 (1:10 dilution; Developmental Studies Hybridoma Bank, USA), mouse anti-tyrosine hydroxylase (TH; 1:200 dilution; Chemicon, USA), and secondary antibodies of Alexa fluor 488 (1:500 dilution; Molecular Probes, Invitrogen, USA) and Alexa flour 546 (1:500 dilution; Molecular Probes, Invitrogen, USA) were carried out as described (Westerfield, 2000).

2.7 α-Bungarotoxin staining

α-Bungarotoxin (α-BTX) staining using Alexa Flour 647 conjugated α-BTX (1:1500 dilution; Molecular Probes, Invitrogen, USA) was performed as described (Downes and Granato, 2004).

2.8 Morpholino knock-down

p53 morpholino oligos (5'-GACCTCCTCTCCACTAAACTACGAT-3') (Robu *et al.*, 2007) and c7-1 morpholino oligos (5'-GCACATCTGAAAAACACCAGTGTTA-3') were synthesised by Gene Tools, LLC (Oregon, USA). Stock solutions of 1 mM were prepared by dissolving the oligos in water and stored at 4 or -20^{o}C. Working solutions of 0.5 mM were prepared from the stock and phenol red was added to a final concentration of 0.1%. The morpholino oligos were microinjected into the yolk of embryos at zero to two cell stages with a microinjector (Eppendorf, USA) according to published protocol (Ekker and Larson, 2001).

2.9 Real-time polymerase chain reaction

Real-time polymerase chain reaction (PCR) of selected genes were carried out according to the supplier's instructions (Applied Biosystems) using the fluorescent dye SYBR Green (Qiagen, Netherlands) and the comparative Ct method. Gene-

specific primer sets flanking intron(s) to avoid errors due to genomic DNA contamination were designed for all the genes using the software ProbeFinder provided by Roche Applied Science (Germany; https://www.roche-applied-science.com/sis/rtpcr/upl/index.jsp?id=UP030000). Sequences of the primers used were listed in Tab. 2.2. Amplification and fluorescence signal detection were performed by the StepOnePus Real-Time PCR System (Applied Biosystem, USA) and the StepOne software v2.1 (Applied Biosystem, USA). Melting curve analyses were performed at the end of the PCR reactions to ensure there was no primer dimer formation. All signals were normalised against the reference control *elongation factor 1α (ef1a)*. At least three independent biological repeats were performed for each gene. Raw data were processed and analysed by the Microsoft Excel software (Microsoft Corporation, USA). The transcript levels were calculated using the $2^{-\Delta\Delta Ct}$ method.

Tab. 2.2 Primers for real-time PCR.

Gene	**Primers* (5' → 3')**
agt	F: TGCTAGTTCAGTGCATTTCAAAG; R: CTGGAGTTCTTTTGAGTCCAGAA
arfl	F: TCAGAACACCAAGGGTCTGAT; R: GCGTCTCTCATCTCGTCCTC
atf3	F: CAGAGGAGAACGACCGAAG; R: GCTCTGCATTGATGGACTCA
c4	F: GGCCTGGCCTTCATCTCT; R: CCAGACTCACAGCTGAAACCTT
c6	F: AAAAGCTGTTCGTGAAAGTGC; R: GAAGGCCTGTTGGAAATTGA
c7-1	F: CATGTCCTTGGAGAGCAACC; R: CTCCAGGCAGACCAGCAG
cbx7l	F: TGTTTGCGGTGGAGTCAATA; R: TGCCACTTTAAAAGATATTCCACA
ef1a	F: CTTCTCAGGCTGACTGTGC; R: CCGCTAGCATTACCCTCC
homez	F: CAACCCTGAGAGAAATTCAAGC; R: GAAGGTTCCATCTTGCCTTTT
irf9	F: TTGGAGGGAGATAACATCTCTGA; R: TGAAGGCCTTGACCTCTTCT
opn1mw1	F: TTTCTTTACCTATGGCAGTCTGG; R: GGACTCAGATTCCTGCTGTTG
prdx1	F: TCATTGGTGCTTCTGTCGAT; R: CTTGTTTCCGGGGTGTTTT
sgk1	F: CCTGCTGCAAAAAGACAGAAC; R: GAACATGTGGTTCTTGATTTCAGT
zgc:101661	F: TCCAGACCTGCATCAGTCAA; R: CCTGGCACTGGTACAGCAT

* F, forward primer; R, reverse primer

2.10 Acridine orange hydrochloride staining

For detection of apoptotic cells, embryos were incubated in 0.5 µl/ml of acridine orange hydrochloride (AO; Sigma-Aldrich, USA) for 1 hour as described (Ton *et al*., 2006).

2.11 Mmp activity assay

Mmp activity assay using fluorescein conjugated collagen type IV substrate (Molcular Probes, Invitrogen, USA) was performed as describe with slight modifications (Crawford and Pilgrim, 2005). Lysates were obtained from 100 embryos in each treatment group and suspended in 1 ml cold lysis buffer. Negative control containing 10 µl of the collagen substrate together with 190 µl lysis buffer was included in each measurement. All samples were loaded to the chambers of 96-well plates. FITC fluorescence was measured every 15 minutes for 3 hours at 28^{o}C using Lambda Fluoro 320 plus microplate reader (Bio-Tek Instruments, USA) and KC4 software (Bio-Tek Instruments, USA). The averages of the relative fluorescent unit after background fluorescence subtraction and error bars indicating the SEM are presented.

2.12 Mmp inhibitor treatment

Zebrafish embryos were treated with 0.1 mM GM 6001 (general Mmp inhibitor, Calbiochem, USA), 1% DMSO, 100 µg/l MeHg or 0.1 mM MMP-9/MMP-13 Inhibitor II (Mmp9 and Mmp13 specific inhibitor, Calbiochem, USA), 1% DMSO, 100 µg/l MeHg in embryo medium. Controls were exposed to 100 µg/l MeHg, 1% DMSO in embryo medium without the Mmp inhibitors or to embryo medium with 1% DMSO. All the treatments were conducted from 4 to 72 hpf. At 72 hpf, MeHg and the Mmp inhibitors were removed by washing the embryos with embryo medium 3 times, 5 minutes each. Photos of the tail region of the embryos were captured and the area of the fin fold was calculated by the software ImageJ (Abramoff *et al.*, 2004).

2.13 Histological section

Plastic sections were performed according to the standard protocol (Westerfield, 2000). Samples were sectioned using a microtome (RM2065, Leica, Germany).

2.14 Birefringence analysis

Birefringence was analysed as described previously (Behra *et al.*, 2002).

2.15 Function analysis of MeHg-regulated genes

The zebrafish regulated genes obtained from microarry were first assigned to the closet human homologues using the website BioMart (http://www.biomart.org/) (Durinck *et al.*, 2005). The gene ontology (GO) analyses were then carried out with the website Gene Set Analysis Toolkit V2 (http://bioinfo.vanderbilt.edu/wg_gsat/) (Zhang *et al.*, 2005; Duncan *et al.*, 2010). Lists of the human homologues were uploaded on the website and blasted against the human genome. Hypergeometric test, Benjamini & Hochberg (1995) multiple test adjustment (MTC), and a significance level of 0.01 were used for the analysis. Three genes were selected as the minimum number for a category to be determined as enriched.

2.16 Imaging

Images of embryos or sections were captured by CCD cameras (Diagnostic instruments, Inc.) connected to a stereomicroscope (MZ16F, Leica, Germany) or a compound microscope (DM5000B, Leica, Germany).

2.17 Statistics analysis

One-way ANOVA followed by Bonferroni's or Dunnett's multiple comparison tests were used for the statistics analysis of calculating the significance of various treatment group using the GraphPad Prism 4 (v4.0) software (GraphPad Software, USA).

3 Results

3.1 Dose-dependent effect of MeHg on zebrafish embryos

In order to determine which concentration of MeHg should be used in the study, a dose-response of toxicity to zebrafish embryos was first performed. The mortality of embryos exposed to different concentrations of MeHg was scored. According to the lethal endpoints of the fish egg test (FET), a 72-hour post fertilisation (hpf)-old embryo was scored as dead when there was it appeared as coagulation, tail not detached, no somite formation and no heart-beat (Braunbeck *et al.*, 2005). A dose-dependent effect was observed in zebrafish embryos exposed to 30 to 120 µg/l MeHg from 4-72 hpf (Fig. 3.1). Lethality of 5% was observed in the control group. At 60 µg/l, 10% lethality (LC10) was induced and malformation were noted. The mortality rate increased with increasing MeHg concentration.

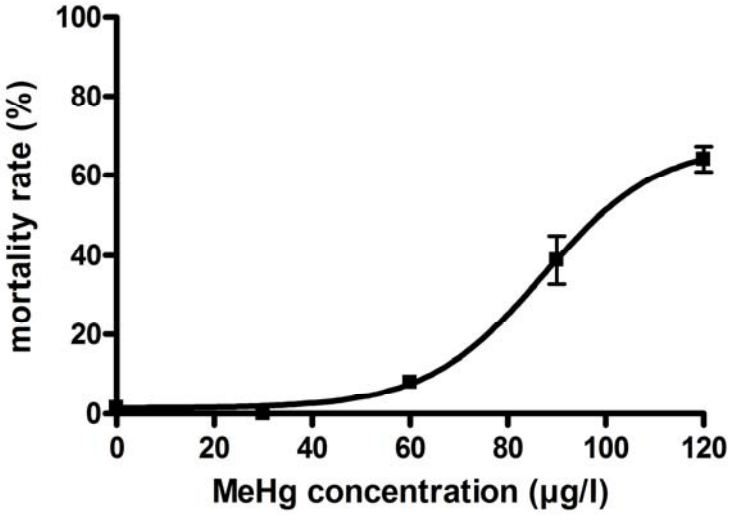

Fig. 3.1 Mortality of zebrafish embryos exposed to different concentrations of MeHg.
Zebrafish embryos were exposure to 30, 60, 90 and 120 µg/l MeHg from 4 to 72 hpf and the mortality rates were scored at 72 hpf. The mean ± standard error of the mean (SEM) are reported. n = 7, 20 embryos each. Increased mortality rate of zebrafish embryos with increasing concentrations of MeHg examined was observed.

Various types of malformations at different frequencies were noted in zebrafish embryos exposed to 30 to 120 μg/l MeHg from 4 to 72 hpf (Fig. 3.2). Caudal fin fold tissue abnormality in which the caudal fin fold showed disorganised tissue structure and smaller size instead of being clear, thin and fan-shaped was detected. Very interestingly, I also observed the disruption of trunk pigmentation with a smaller gap size of the melanophore stripe in the tail. This melanophore stripe gap marks the growth zone of the tail. Some of the embryos also exhibited posterior tail flexure with flexed spinal cord and notochord at the posterior part of the tail instead of ones that remained straight to the posterior-most tip of the tail. The caudal fin abnormality of caudal fin fold tissue disruption, loss of melanophore stripe gap, and/or posterior flexure was detected in 59.5% of the embryos treated with 30 μg/l MeHg and the occurrence of this phenotype was even up to 87% or more in embryos exposed to higher MeHg concentrations. Besides the tail malformation, pericardial edema, smaller head and eye, stunted body and trunk flexure were also detected in embryos exposed to MeHg concentrations of 60 μg/l or higher. Based on the result of the toxicity test, MeHg concentration of 60 μg/l, which caused 10% lethality and induced morphologically observable phenotypes, was chosen for the study.

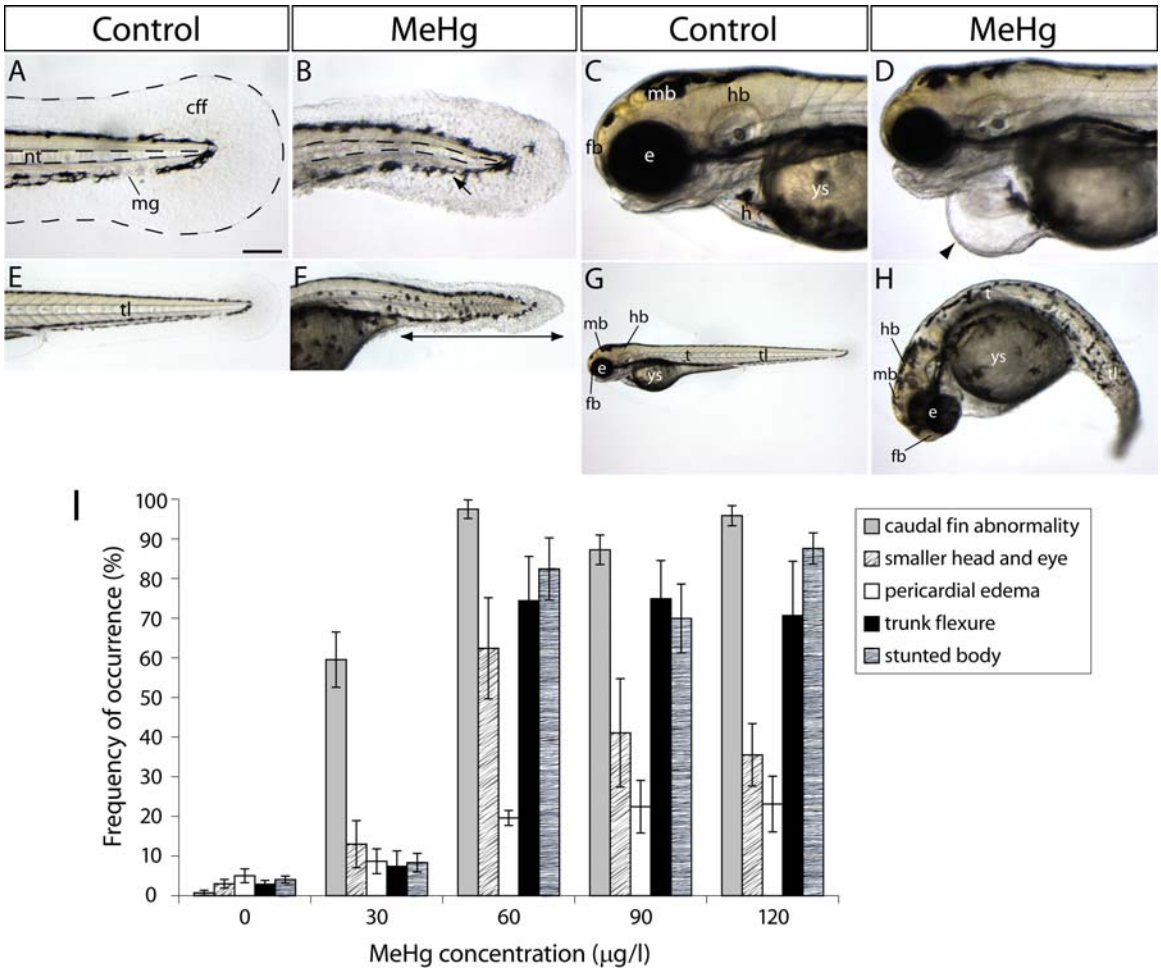

Fig. 3.2 Malformations in zebrafish embryos exposed to MeHg.

All the embryos shown in the thesis were positioned in a way that the lateral views are anterior to the left and dorsal to the top, and the dorsal views are anterior to the left. Lateral views of control (A, C, E, G) and MeHg-treated embryos (B, D, F, H) at 72 hpf. (A, B) Caudal fin fold abnormality, posterior tail flexure and disruption of trunk melanophore were observed in embryos exposed to MeHg. The dotted lines in (A) outline the notochord and the caudal fin fold. Other phenotypes including pericardial edema, (C, D, arrowhead), smaller head and eye (C, D), stunted body (E, F, double-headed arrow) and trunk flexure (G, H) were also detected. (I) The frequency of occurrence of caudal fin abnormality, pericardial edema, trunk flexure and stunted body exposed to 30, 60, 90 and 120 µg/l MeHg from 4 to 72 hpf was scored. The mean ± SEM are presented. n = 7, 20 embryos in each exposure with dead embryos excluded from the scoring. Abbreviations, cff, caudal fin fold; e, eye: fb, forebrain; h, heart; hb, hindbrain; mb, midbrain; mg, gap of the melanophore stripe; nt, notochord; t, trunk; tl, tail; ys, yolk sac. Scale bar, A-D, 90 µm; E, F, H, 215 µm; G, 425 µm.

3.2 Toxicogenomic screen of MeHg-responsive genes

3.2.1 Microarray analysis of MeHg-regulated genes

In order to examine the underlining mechanisms through which MeHg exerts its effects and to identify genes which can serve as sensitive biosensors for monitoring environmental MeHg, a toxicogenomic screen of genes has been performed in this study. In addition to the information reported by Yang (2007), another microarray analysis, which had much larger gene coverage, was conducted for obtaining a more comprehersive view of MeHg-regulated genes. The microarray analysis indicated that a total of 464 genes were up-regulated with M-values ($\log_2$ of the fold change) greater than or equal to 1.3 ($p < 0.05$) and 379 genes were down-regulated with M-values less than or equal to -1.3 ($p < 0.05$). The M-values of these MeHg-responsive genes are listed in the appendix Tab. A2 and Tab. A3.

Gene ontology (GO) enrichment analysis was performed on these differentially expressed genes to examine the alteration of the putative biological processes and molecular functions in response to MeHg. The result of the functional analysis indicated that MeHg caused dysregulation of various biological processes and molecular functions (Fig. 3.3). The most significantly up-regulated biological functions were those related to cell death, apoptosis, response to wound, inflammatory response and response to oxidative stress (adjusted $p < 0.001$) (Fig. 3.3 A). Other biological processes including calcium-independent cell-cell-adhesion, extracellular matrix organisation, blood circulation, response to hormone stimulus, response to oxidative stress, response to ROS, and regulation of homeostatic process, cell redox homeostasis, prostaglandin (a group of lipid derived from fatty acid) metabolism, aromatic compound catabolic, were also significantly regulated (adjusted $p < 0.01$). MeHg also caused the up-regulation of genes associated with DNA or protein binding and with catalytic activities (Fig. 3.3 A'). It affected transcription factor activity, endopeptidase activity, aryldialkylphosphatase, MAP kinase phosphatase activity and arylesterase activity (adjusted $p < 0.01$). On the other hand, for genes which were down-regulated by MeHg, they were implicated in biological processes of oxidation reduction, RNA splicing, RNA elongation, fatty acid metabolism and DNA repair

(adjusted $p < 0.01$) (Fig.3.3 B). MeHg also led to down-regulation of genes which were involved in binding and catalytic activity (Fig. 3.3 B'). These included the translation factor activity, nucleic acid binding, coenzyme binding, oxidoreductase activity, protein kinase activity and isomerase activity (adjusted $p < 0.01$).

A

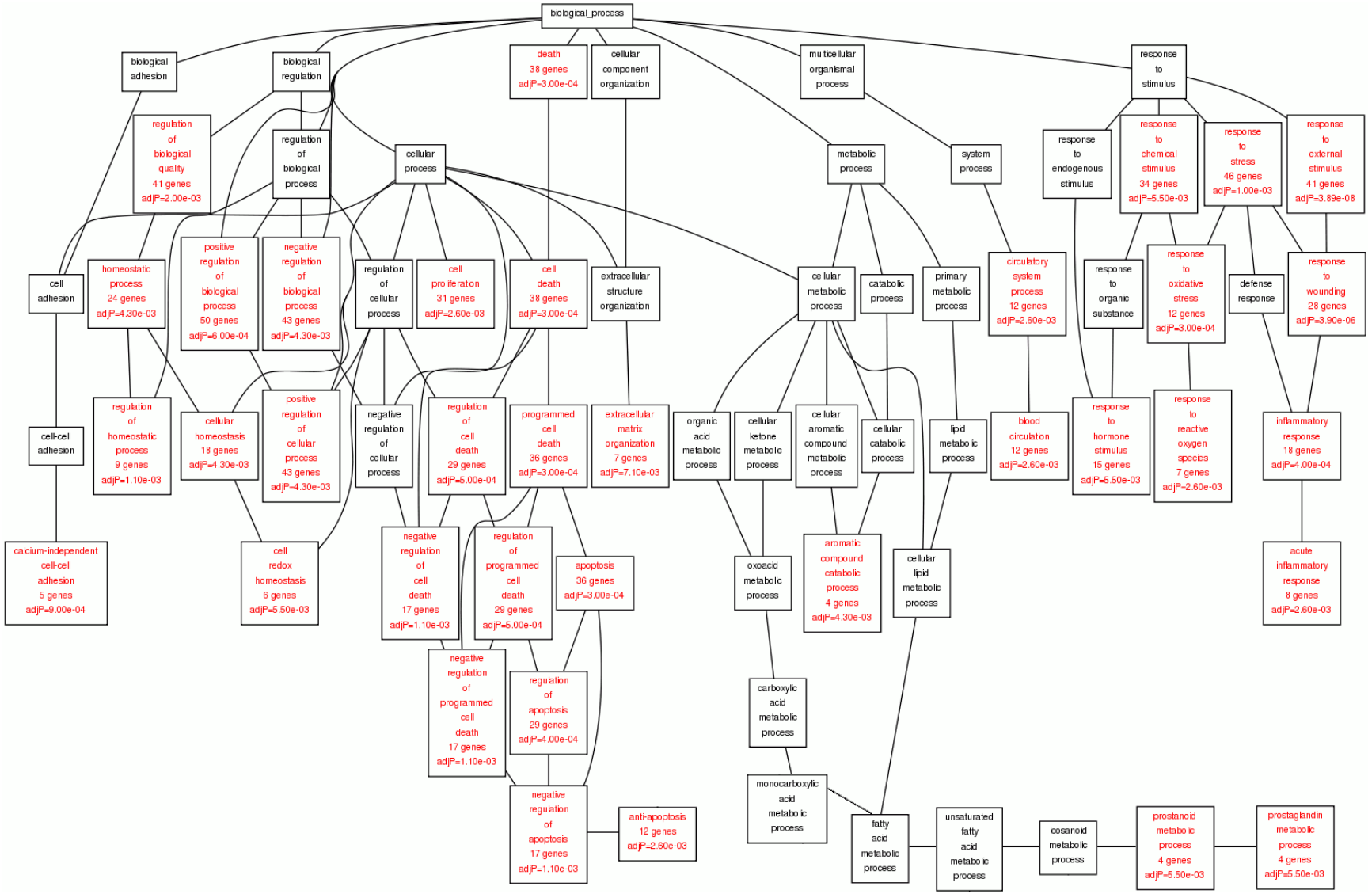

(Fig. 3.3 Continued)

A’

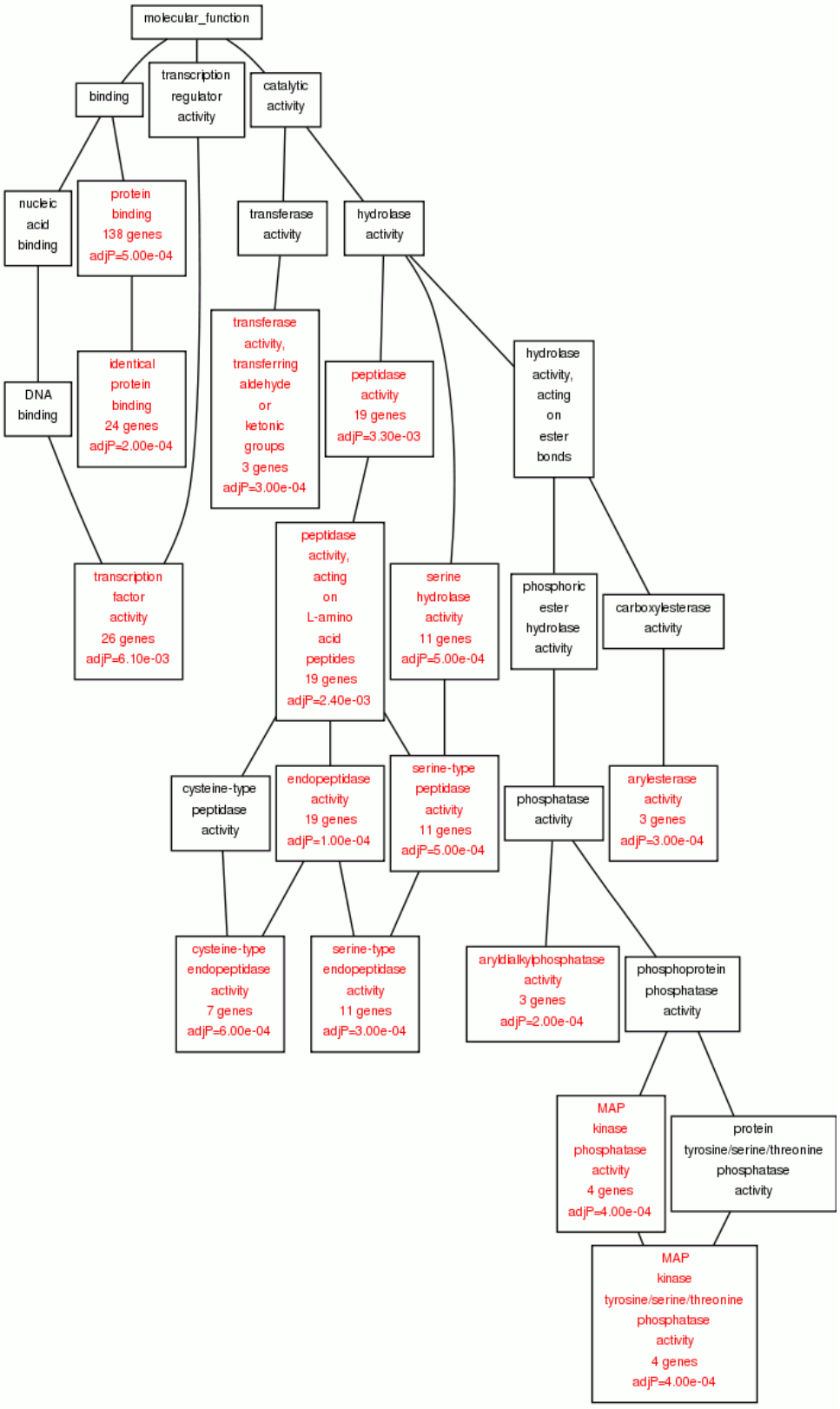

(Fig. 3.3 Continued)

B

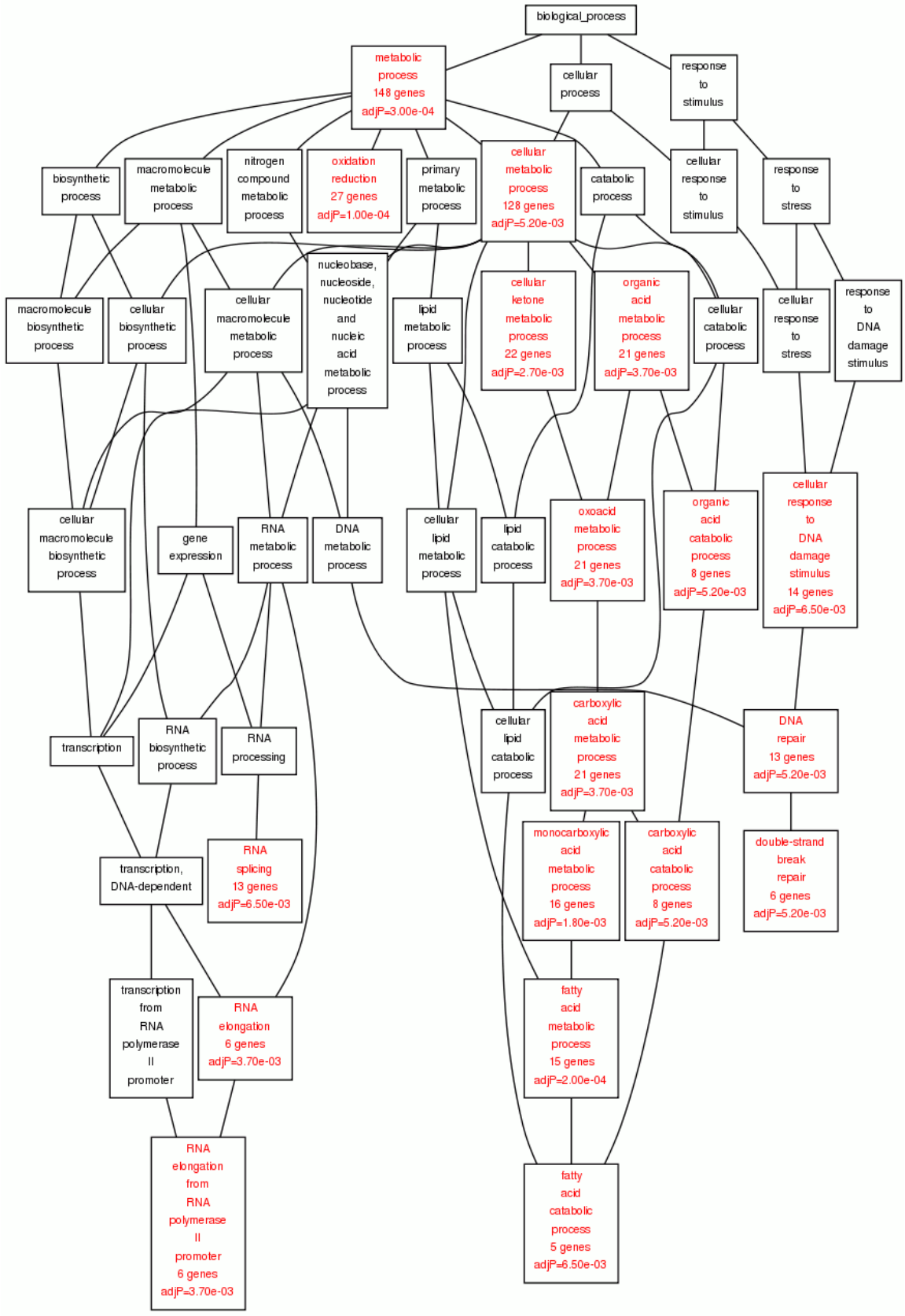

(Fig. 3.3 Continued)

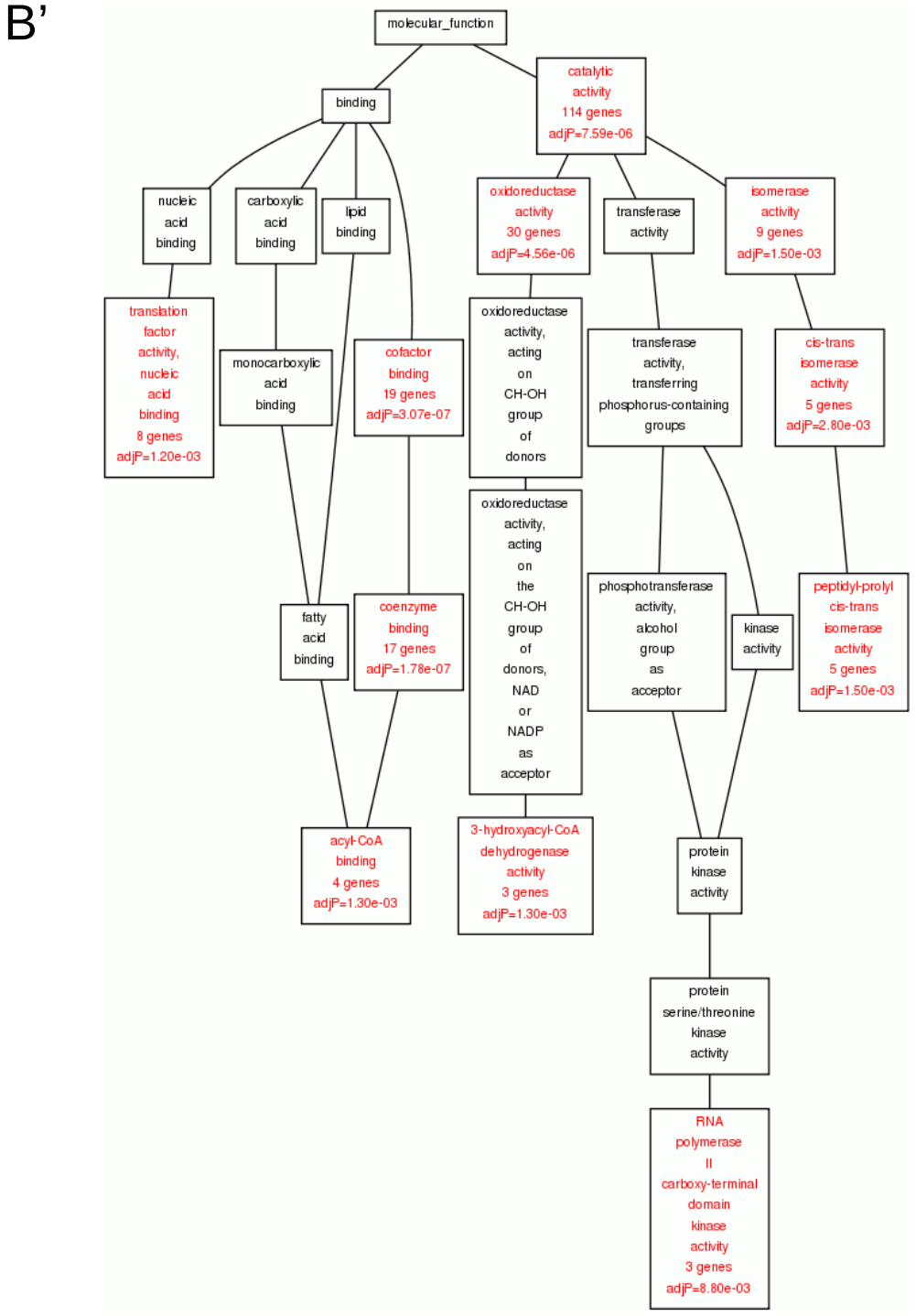

Fig. 3.3 Gene ontology enrichment analysis of MeHg-regulated genes.

Gene ontology (GO) enrichment analysis of MeHg-up-regulated (A, A') and down-regulated (B, B') genes. (A, B) Biological processes; (A', B') molecular functions. GO categories that adjusted $p < 0.01$ are coloured red. Those in black are the parents of the red GO categories. The number of genes which fell into each of the red GO categories and the adjusted p-value are indicated.

3.2.2 *In situ* hybridisation analysis of MeHg-regulated genes

According to the microarray data performed in this study and that obtained by Yang (2007), candidate genes were further analysed by whole-mount ISH to examine any change in the expression patterns of the genes. For better selection of candidate genes for ISH analysis, the gene identity and gene ontology of the EST clones used in microarray analysis was determined by blasting the EST sequences against RefSeq RNA database or UniGene database in NCBI (Cates, 2006), the ZFIN database (ZFIN Staff, 2002) and the ensemble database (Flicek *et al.*, 2005). Through the blast search, I was able to find out the gene identity of about three-forth of the EST clones. However, for the remaining one-forth of the EST clones, either no information on the gene identity was available or even no matches of the clones to other sequences in the database were obtained, and I wrote the gene name of these clones as "to be determined (TBD)" in Tab. 3.1 and appendix Tab. A4. Based on the result of the database search, I chose genes which were highly regulated by MeHg for the establishment of sensitive biomarkers for monitoring the environmental MeHg and genes which were transcription factors for examining the underlying mechanisms through which MeHg induced its toxicity. Eighty-eight MeHg-responsive genes which are involved in different molecular functions and biological processes including regulation of transcription, antioxidant defence, immune response, enzymatic activity and transmembrane transport were chosen. Details of the gene ontology of these genes are listed in the appendix Tab. A4. Some of the genes with unknown function or without known gene identity were also chosen for the discovery of the possible important functions of these unknown genes.

The result of the screen is summarised in Tab. 1. The expression patterns in different organs including brain, eyes, olfactory bulb, branchial arches, heart, liver, intestine or gut, pronephos, somites, lateral lines, pectoral fins, caudal fin fold, blood vessels, dermal epithelium, yolk syncytial layer (YSL), and others, were classified. The column labelled 'overall' indicated the overall change in the expression level in the whole embryos. Among the 88 MeHg-regulated genes analysed by ISH, 60 genes were confirmed to be positively correlated with the microarray result. However, I was not able to determine the overall change in the expression levels of three of the genes,

elf3, *noxo1* and *slc16a9a*, by ISH (indicated as 'TBD' in the 'overall' column of Tab. 3.1) due to the fact that the expression of these genes were highly up-regulated in certain parts of the body, but were also strongly down-regulated in other parts of the body.

The changes in the expression patterns some of the genes regulated by MeHg exposure are shown in Fig. 3.4 as a demonstration of the anatomical structures indicated in Tab. 1. For example, in response to MeHg, *prdx1* was highly up-regulated in the lateral line and liver, and slightly up-regulated in the hypothalamus of the brain (Fig. 3.4 A, A'); increased expression of *pck1* was observed in the YSL of the yolk and the yolk sac extension (YSE) (Fig. 3.4 B, B'); *fn1b* showed a strong up-regulation in the dermal epithelium throughout the whole embryo (Fig. 3.4 C, C'); *mmp13a* was up-regulated in blood cells scattered all over the body, the posterior blood island (PBI), where blood cells are produced, the edges of the pectoral fins and the caudal fin fold (Fig. 3.4 D, D'); the expression of *noxo1* was increased in the lateral line, pectoral fin and dermal epithelium (arrow in Fig. 3.4 E'), but decreased in the branchial arches of the jaw (Fig. 3.4 E, E'); *elf3* also showed a decrease in expression in the branchial arches, but an increase in the pronephos (embryonic kidney) was noted (Fig. 3.4 F, F'); the expression of *opn1mw1* in the eyes decreased and was restricted to the anterior part of the eyes (Fig. 3.4 G, G'). *BI474700* exhibited a ubiquitous increase in expression and was up-regulated in various organs including the brain, eye, liver and gut (Fig. 3.4 H, H'); *BM101698* was up-regulated in both the olfactory bulb and the outer region of the pectoral fins (Fig. 3.4 I, I'); increased expression of *c6* was observed in the adenohypophysis (anterior pituitary) (Fig. 3.4 J, J'); *c4-2* was up-regulated in the trunk blood vessels, showing expression in the dorsal aorta (DA), dorsal anastomotic vessel (DLAV), posterior caudal vein (PCV) and inter-segmental vessels (ISV) (Fig. 3.4 K, K'); *sqstm1* showed an up-regulation in the pigment cells and the caudal fin fold (Fig. 3.4 L, L'); the expression of *cartI* was increased in the notochord and the somites (Fig. 3.4 M, M'); *txnl* was up-regulated in the lateral line, the caudal fin fold and the proctodeum, which is the posterior ectodermal part of the alimentary canal (Fig. 3.4 N, N').

Tab. 3.1 Result of whole-mount *in situ* hybridisation analysis of MeHg-regulated genes in 72 hpf-old zebrafish embryos.

GenBank accession number	Gene name (gene symbol)	Anatomical structures																	
		Brain	Eyes	Olfactory bulb	Branchial arches	Heart	Liver	Intestine, gut	Pronephos	Somites	Lateral lines	Pectoral fins	Caudal fin fold	Notochord	Blood vessels	Pigment cells	Dermal epithelium	YSL	Others	Overall
NM_200637	*a disintegrin and metalloproteinase domain 8a (adam8a)*																			NC
NM_200964	*activating transcription factor 3 (atf3)*	+	+							+									+ (proctodeum)	+
AI477644	*ADP-ribosylation factor-like (arfl); Zgc:112199*	+																	+ (scattered cells over the body)	+
BG727310	*angiotensinogen (agt)*	+	+				+		+									+		+
NM_131098	*apolipoprotein eb (apoeb)*											+	+				+			+
NM_131886	*CCAAT/enhancer binding protein (C/EBP), gamma (cebpg)*	+																		+
NM_001017853	*chromobox protein homolog 7-like (cbx7l); zgc:110152*	+	+								-				+					+
DN857240	*cocaine and amphetamine regulated transcript protein type I-like (cartll)*	+												+						+
AF047413	*complement component 3a (c3a); si:dkey-76b14.4*						+											+		+
BI672168	*complement component 4-2 (c4-2)*						+								+			+		+
BI474371	*complement component 6 (c6)*					+		+				+						+	+ (oesophagus)	+
BC100054	*complement component 7-1 (c7-1)*		+																	+

GenBank accession number	Gene name (gene symbol)	Anatomical structures																		
		Brain	Eyes	Olfactory bulb	Branchial arches	Heart	Liver	Intestine, gut	Pronephos	Somites	Lateral lines	Pectoral fins	Caudal fin fold	Notochord	Blood vessels	Pigment cells	Dermal epithelium	YSL	Others	Overall
AW019018	*complement factor b (cfb)*						+											+		+
NM_201461	*core promoter element binding protein (copeb)*					+							+							+
BI845861	*CXC chemokine 46-like (cxc46l)*		+								+	+	+		+					+
BE016427	*ubiquitin carboxyl-terminal hydrolase CYLD-like (cyldl)*																			NC
AI385059	*E74-like factor 3 (elf3)*			+	-			+	+		+								+ (proctodeum)	TBD
NM_001013261	*fibronectin 1b (fn1b)*																+			+
NM_131285	*forkhead box B1.2 (foxb1.2)*																			NC
BG304082	*glutamate-cysteine ligase modifier subunit (gclm)*	+	+				+	+			+	+					+			+
AW232474	*glutathione peroxidase 1a (gpx1a)*						-	-	-		-									-
BI896246	*glutathione peroxidase 4a (gpx4a)*						-	-												-
BM777961	*glycine dehydrogenase (decarboxylating) (gldc)*																			NC
NM_130934	*hematopoietically expressed homeobox (hhex)*					+	+													+
NM_001007120	*homeodomain leucine zipper gene (homez)*	+										+	+		+		+			+
NM_205710	*interferon regulatory factor (irf9)*	+				+														+

GenBank accession number	Gene name (gene symbol)	Anatomical structures																		
		Brain	Eyes	Olfactory bulb	Branchial arches	Heart	Liver	Intestine, gut	Pronephos	Somites	Lateral lines	Pectoral fins	Caudal fin fold	Notochord	Blood vessels	Pigment cells	Dermal epithelium	YSL	Others	Overall
NM_213556	*Jun B proto-oncogene (junb)*											+	+				+			+
AI641738	*kruppel-like factor 10-like (klf10l)*																			NC
NM_001077604	*kruppel-like factor 11b (klf11b)*																			NC
AI793516	*lysosomal-associated membrane glycoprotein 1-like (lamp1l); zgc:64072*	+	+								+							+		+
AW174507	*matrix metalloproteinase 9 (mmp9)*										+	+	+				+		+ (blood cells)	+
AW305943	*matrix metalloproteinase 13a (mmp13a)*											+	+						+ (blood cells and PBI)	+
NM_194416	*matrix metalloproteinase 14a (mmp14a)*												+							+
BI878214	*NADPH oxidase organizer 1 (noxo1)*				-						+	+	+				+			TBD
AF109371	*opsin 1 (cone pigments), long-wave-sensitive, 1 (opn1lw1)*	-	-																	-
AF109369	*opsin 1 (cone pigments), medium-wave-sensitive, 1 (opn1mw1)*		-																	-
AF109373	*opsin 1 (cone pigments), short-wave-sensitive 1 (opn1sw1)*		-																	-
NM_131184	*paired box gene 2a (pax2a)*																			NC
NM_131304	*paired box gene 6a (pax6a)*																			NC

GenBank accession number	Gene name (gene symbol)	Anatomical structures																		
		Brain	Eyes	Olfactory bulb	Branchial arches	Heart	Liver	Intestine, gut	Pronephos	Somites	Lateral lines	Pectoral fins	Caudal fin fold	Notochord	Blood vessels	Pigment cells	Dermal epithelium	YSL	Others	Overall
BI980610	*peroxiredoxin1 (prdx1); zgc:110343*	+					+	+			+									+
BG727092	*phosphoenolpyruvate carboxykinase 1 (pck1)*						+											+		+
BI888564	*6-phosphofructo-2-kinase/fructose-2,6-biphosphatase 4-like (pfkfb4l)*	+	+																	+
BE557057	*PLAC8-like protein 1-like (plac8l1l)*																			NC
NM_199515	*PR domain containing 1a, with ZNF domain (prdm1a)*		+									+	+							+
BI889255	*protein phosphatase 1 regulatory subunit 15A (ppp1r15a)*	+	+							+										+
NM_199798	*Ras-related associated with diabetes (rrad)*					+				+		+								+
NM_131225	*retinal homeobox gene 1 (rx1)*																			NC
BC095285	*S100 calcium binding protein Z (s100z)*																			NC
BM102635	*SAR1a gene homolog 2 (S. cerevisiae) (sara2)*	+																		+
AW128247	*selenoprotein W, 1 (sepw1)*																			NC
AW343560	*sequestosome 1 (sqstm1)*			+		+					+	+	+			+	+	+		+
BI673466	*serum/glucocorticoid regulated kinase 1 (sgk1)*								+			+	+		+			+		+

GenBank accession number	Gene name (gene symbol)	Anatomical structures																		
		Brain	Eyes	Olfactory bulb	Branchial arches	Heart	Liver	Intestine, gut	Pronephos	Somites	Lateral lines	Pectoral fins	Caudal fin fold	Notochord	Blood vessels	Pigment cells	Dermal epithelium	YSL	Others	Overall
BG302634	*si:ch211-106h4.4*																			NC
AI974163	*si:ch1073-126c3.2*																			NC
NM_131362	*sine oculis homeobox homolog 3a (six3a)*	+	+																	+
NM_131363	*sine oculis homeobox homolog 3b (six3b)*																			NC
AW421040	*solute carrier family 16 (monocarboxylic acid transporters), member 9a (slc16a9a)*	-	-			-						+			+					TBD
BE016639	*solute carrier family 16 (monocarboxylic acid transporters), member 9b (slc16a9b)*																			NC
NM_212960	*sp9 transcription factor (sp9)*												+							+
NM_001080750	*SRY-box containing gene 7 (sox7)*																			NC
BI882244	*Sulfide quinone reductase-like (sqrdl)*																			NC
BI878700	*suppressor of cytokine signaling 3a (socs3a)*																			NC
BG727181	*suppressor of cytokine signaling 3b (socs3b)*																+			+
BI864190	*thioredoxin-like (txnl); zgc:92903*			+							+	+	+				+		+ (proctodeum)	+

GenBank accession number	Gene name (gene symbol)	Anatomical structures																		
		Brain	Eyes	Olfactory bulb	Branchial arches	Heart	Liver	Intestine, gut	Pronephos	Somites	Lateral lines	Pectoral fins	Caudal fin fold	Notochord	Blood vessels	Pigment cells	Dermal epithelium	YSL	Others	Overall
BI886657	*thioredoxin-like 4A (txnl4a)*																			NC
NM_131327	*tumor protein p53 (p53)*												+							+
AW127886	*UDP glucuronosyltransferase 5 family, polypeptide A2 (ugt5a2)*	+																		+
AW420321	*uncoupling protein 1 (ucp1)*					+				+			+							+
AW019321	*urate oxidase (uox)*																			NC
NM_205569	*v-fos FBJ murine osteosarcoma viral oncogene homolog (fos)*	+		+						+								+		+
NM_131015	*v-maf musculoaponeurotic fibrosarcoma oncogene family, protein B (avian) (mafba)*																			NC
NM_200336	*v-maf musculoaponeurotic fibrosarcoma oncogene homolog f (avian) (maff)*										+									+
BM101640	*zgc:56382*			+								+	+				+			+
AW019036	*zgc:92254*																			NC
AI657551	*zgc:101661*	+	+				+									+		+		+
AI397362	*AI397362*			+	+								+		+		+			+
AI544649	*AI544649*																			NC

GenBank accession number	Gene name (gene symbol)	Anatomical structures																		
		Brain	Eyes	Olfactory bulb	Branchial arches	Heart	Liver	Intestine, gut	Pronephos	Somites	Lateral lines	Pectoral fins	Caudal fin fold	Notochord	Blood vessels	Pigment cells	Dermal epithelium	YSL	Others	Overall
AI793818	*AI793818*				+												+			+
AW115990	*AW115990*	+	+				+					+	+				+			+
BE016163	*BE016163*	+																		+
BG727211	*BG727211*																			NC
BG891932	*BG891932*																			NC
BI474700	*BI474700*	+	+	+	+	+	+	+		+		+								+
BI883993	*BI883993*																			NC
BI892110	*BI892110*																			NC
BI983579	*BI983579*		+				+								+		+	+		+
BM036361	*BM036361*	+	+																	+
BM101698	*BM101698*			+								+	+				+			+

+, increase in expression; -, decrease in expression; NC, no change; TBD, to be determined

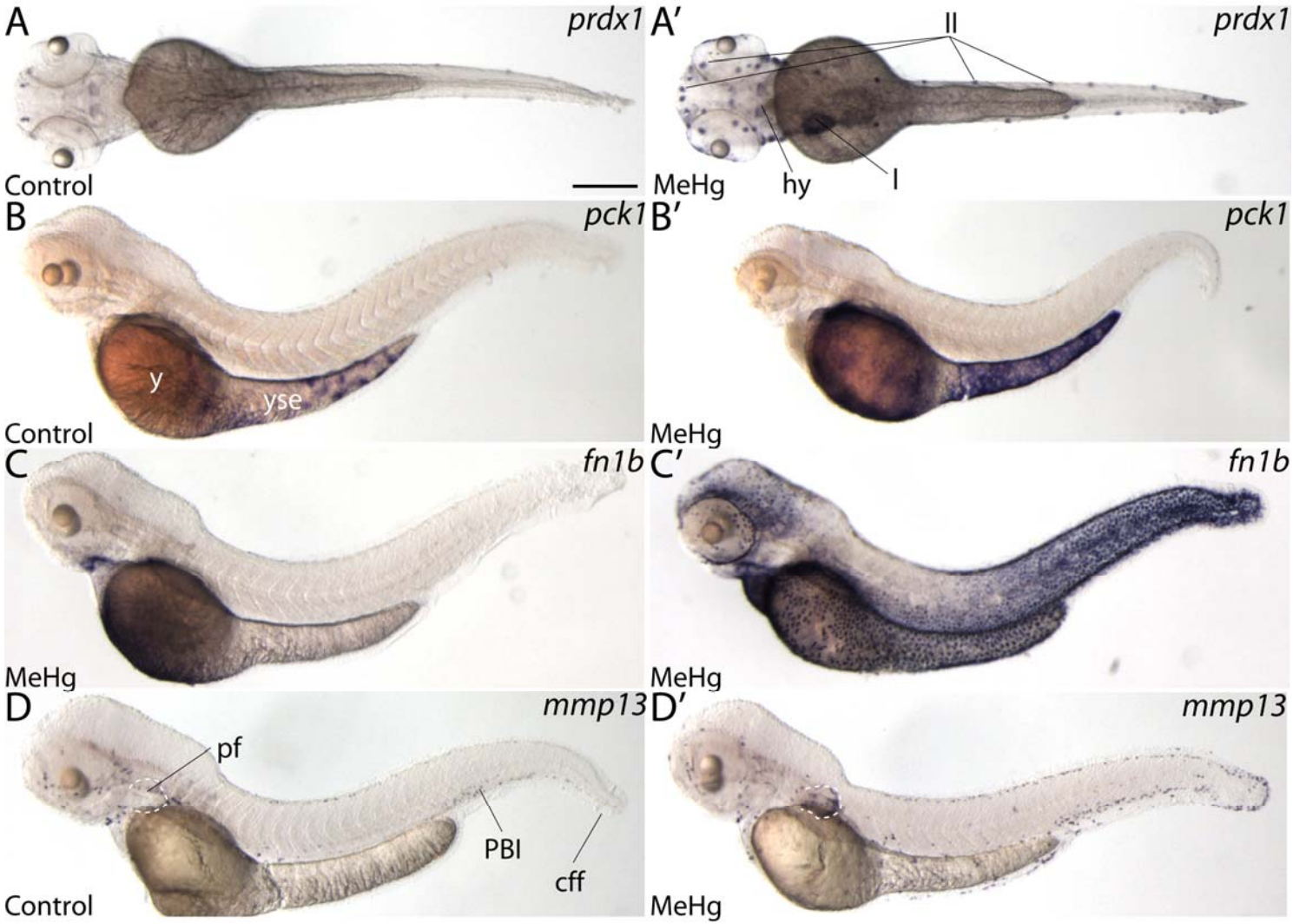

(Fig. 3.4 Continued)

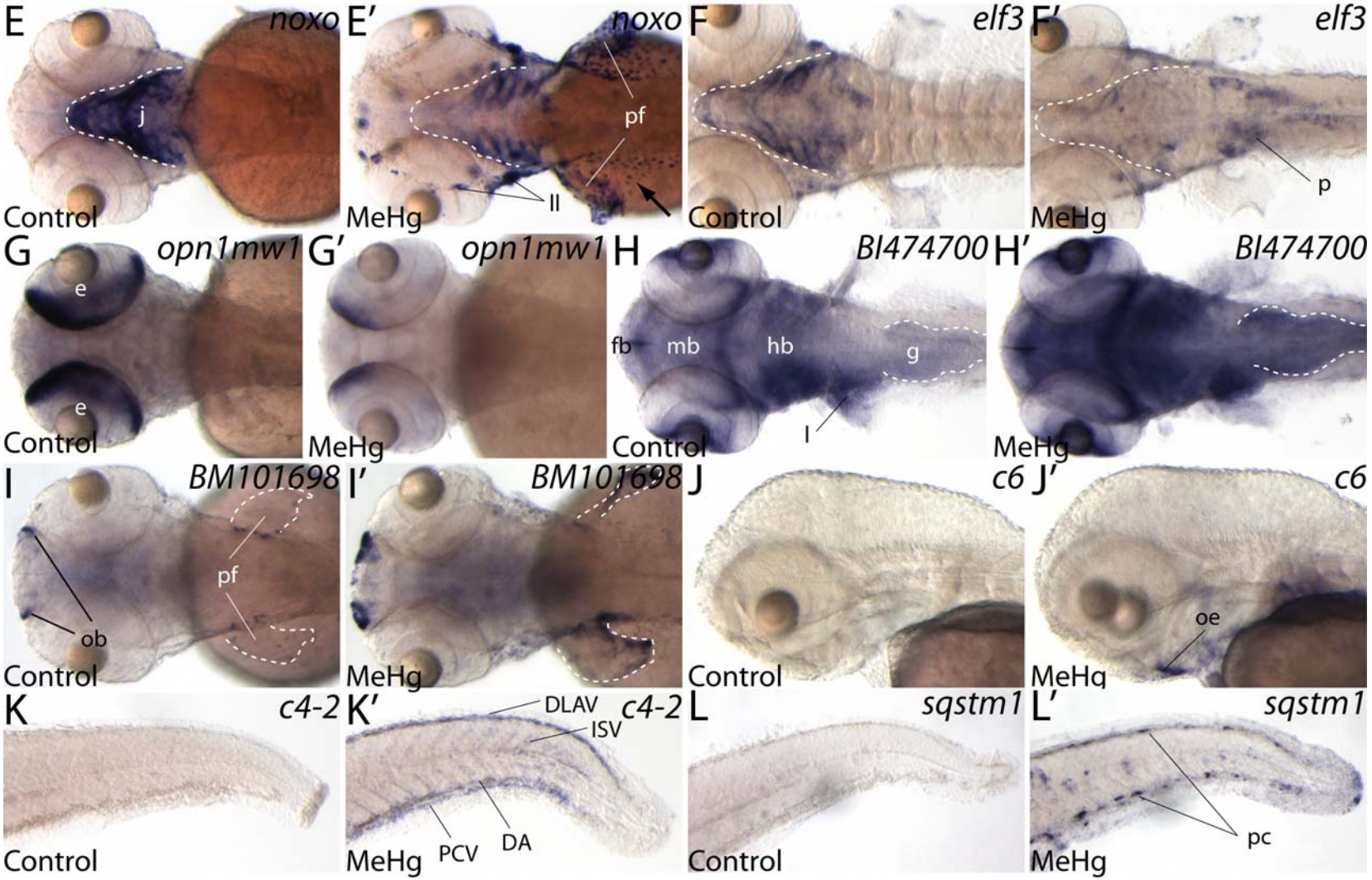

(Fig. 3.4 Continued)

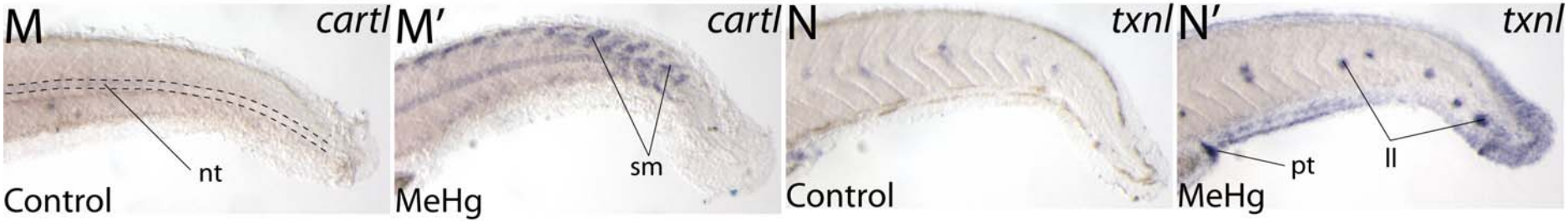

Fig. 3.4 Changes in gene expression patterns in after MeHg exposure.

Dorsal (A, A', E, E' – I-I') and lateral (B, B' – D, D', J, J' – N, N') views of 72-hpf-old control (A, B, C, D, E, F, G, H, I, J, K, L, M, N) and MeHg-treated (A', B', C', D', E', F', G', H', I', J', K', L', M', N') embryos. The whole embryo (A, A' – D, D'), and the anterior part (E, E' – J, J'), the trunk (I, I') and posterior part (K, K' – N, N') of the embryos are shown. The embryos were staining with *in situ* hybridisation using probes complementary to *prdx1* (A, A'), *pck1* (B, B'), *fn1b* (C, C'), *mmp13a* (D, D'), *noxo1* (E, E'), *elf3* (F, F'), *opn1mw1* (G, G'), *BI144700* (H, H'), *BM101698* (I, I'), *c6* (J, J'), *c4-2* (K, K'), *sqstm1* (L, L'), *cartl* (M, M'), *txnl* (N, N'). The dotted lines in D, D', I, I' quote the pectoral fins; the dotted lines in E, E', F, F' mark the outer region of the jaws; the dotted lines in H, H' outline the gut; the dotted lines in M mark the notochord. Abbreviations, DA, dorsal aorta; DLAV, dorsal anastomotic vessel; cff, caudal fin fold; e, eye, fb, forebrain; g, gut; hb, hindbrain; hy, hypothalamus; ISV, inter-segmental vessel; j, jaw; l, liver; ll, lateral line; mb, midbrain; nt, notochord; ob, olfactory bulb; oe, oesophagus; p, pronephos; PBI, posterior blood island; pc, pigment cell; PCV, posterior caudal vein; pf, pectoral fin; pt, proctodeum; sm, somite; y, yolk; yse, yolk sac extension. Scale bar, A, A' – D, D', 200 μm; F, F', J, J' – N, N', 100 μm; E, E', G, G' – I, I', 80 μm.

3.2.3 Quantitative analyses of MeHg-regulated genes by real-time PCR

To further quantify the expression levels and to determine if these changes could be induced by lower levels of MeHg, real-time PCR was performed. Zebrafish embryos were exposed to 30 and 60 μg/l MeHg and the samples were then subjected to real-time PCR analyses. Genes *arfl, atf3, c4-2, c6, cbx7l, homez, irf9, prdx1, ppp1r15a, txnl, zgc:101661* and *opn1mw1* that showed obvious changes in the expressions in both microarray and ISH were investigated. As indicated by real-time PCR, the expression levels of all the genes examined, except *homez*, were significantly regulated by 60 μg/l-MeHg exposure (Fig. 3.5). *arfl, c4-2, c6, cbx7l, prdx1* and *txnl* have M-values of more than 2 (that is more than 4-fold induction), *atf3, irf9, ppp1r15a* and *zgc:101667* exhibited M-values of more than 1 (that is more than 2-fold induction), and *opn1mw1* showed a negative M-value of more than 2 (that is more than 4-fold repression) after exposing to 60 μg/l MeHg. *arfl, c4-2, c6, cbx7l, prdx1, txnl* and *zgc:101661* even showed significant changes of more than 1 (that is more than 2-fold induction) at lower MeHg concentration of 30 μg/l. The sensitive changes in the expression levels of *arfl, c4-2, c6, cbx7l, prdx1, txnl* and *zgc:101661* suggested that they may serve as marker genes for detecting the presence of MeHg in the environment.

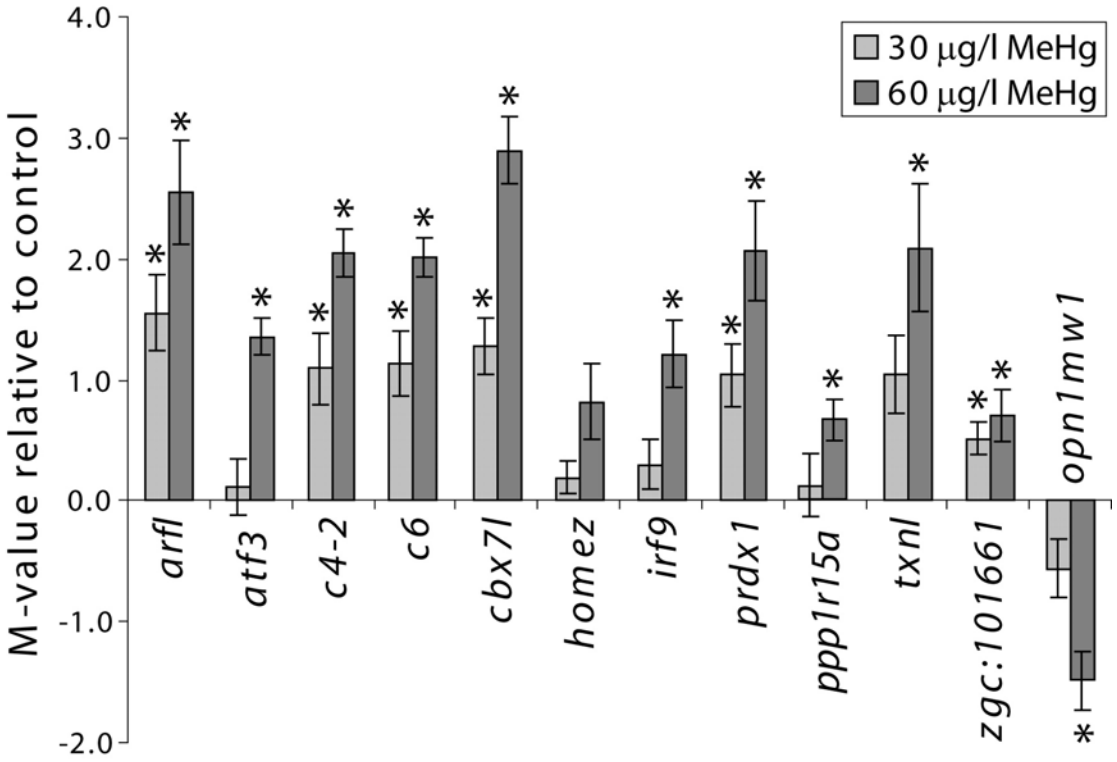

Fig. 3.5 Changes in gene expression levels measured by quantitative real-time PCR in response to MeHg.

The changes in the expression levels of *arfl*, *atf3*, *c4-2*, *c6*, *cbx7l*, *homez*, *irf9*, *prdx1*, *ppp1r15a*, *txnl*, *zgc:101661*and *opn1mwl* were determined by real-time PCR of control and MeHg-treated samples. Graphs of MeHg concentration against the M-value ($\log_2$ of the fold change) relative to controls are plotted. The mean ± SEM are presented. T-test and Dunnett adjustment, $p < 0.05$ (*).

3.2.4 Summary

A toxicogenomic-based screen on MeHg-regulated genes was performed. A total of 464 MeHg-up-regulated and 379 MeHg-down-regulated genes were obtained from the microarray analysis. The microarray result was verified and the changes in the expression patterns of 88 candidate genes after MeHg exposure were examined by whole-mount ISH. The result of the ISH indicated that 60 out of the 88 genes were positively correlated with the microarray result. Ectopic expressions of the genes were noted in various organs including the brain, eyes, olfactory bulb, branchial arches, heart, liver, intestine or gut, pronephos, somites, lateral lines, pectoral fins, caudal fin fold, blood vessels, dermal epithelium, and YSL. The expression levels of 12 genes including *arfl, atf3, c4-2, c6, cbx7l, homez, irf9, prdx1, txnl, zgc:101661, ppp1r15a* and *opn1mw1*, in embryos exposed to 30 and 60 μg/l MeHg were further quantified

by real-time PCR. Eleven genes were shown to be significantly regulated at 60 μg/l MeHg. The expression levels of *arfl, c4-2, c6, cbx7l, prdx1* and *zgc:101661* were significantly regulated even at 30 μg/l MeHg. The sensitive expression changes of these 6 genes suggested that they may serve as marker genes for detecting the presence of MeHg in the environment.

3.3 Zebrafish nervous system

3.3.1 Study on zebrafish brain after MeHg exposure

Under normal development, the cellular fate of different regions of the blastoderm has been established by the onset of gastrulation (at 6 hpf when the embryo was maintained at temperature of 28.5^{o}C) (Driever *et al.*, 1995; Kimmel *et al.*, 1995; Solnica-Krezel, 2005). The positions of the precursors for different tissues and organs including the brain, spinal cord, notochord, epidermis, heart, somite, blood, pronephros and perichordal plate have been specified. At 18 hpf, the first half of segmentation, the morphological segmentation of the brain is visible and about ten distinctive swellings, the neuromeres which mark the telencephalon, diencephalon**,** mesencephalon and seven hindbrain rhombomeres, are formed along the brain rudiment (Kimmel *et al.*, 1995; Lowery and Sive, 2004; Fig. 3.6). At 24 hpf, more prominently sculptured regions of the brain can be seen. Anatomical brain structures of cerebellum, epiphysis, floor plate and rudiment of hypothalamus are formed, and partitioning of the midbrain into the dorsal tectum and the ventral tegmentum is visible.

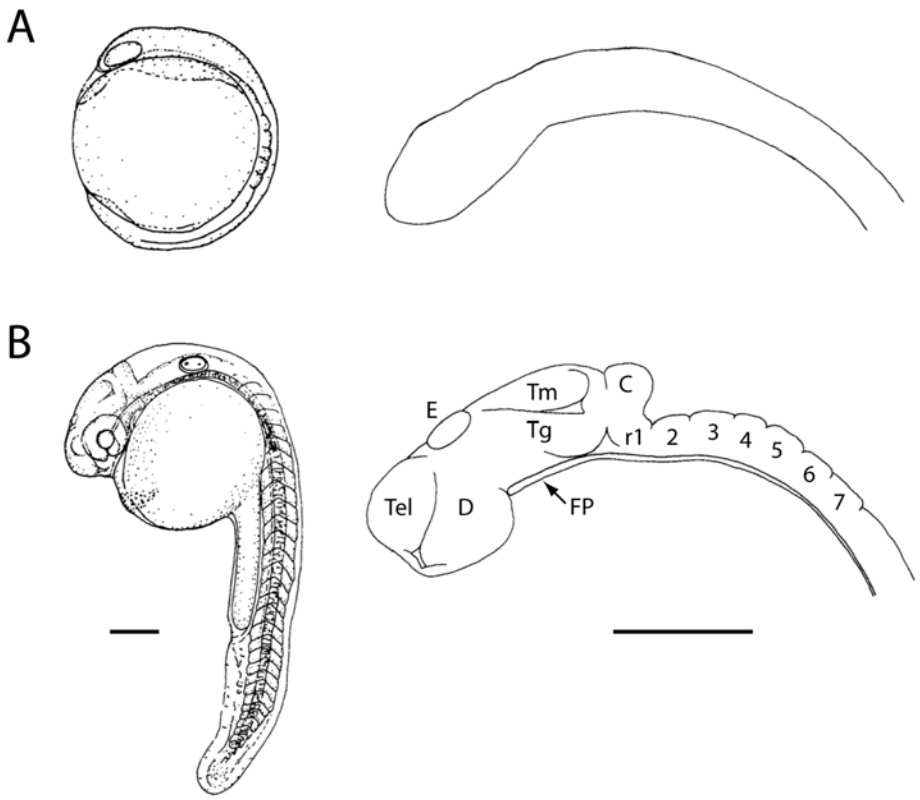

Fig. 3.6 Sculpturing of the brain rudiment during the segmentation period.
(A) At 12 hpf, no morphological subdivisions of the brain region are visible. (B) By 24 hpf, prominently sculptured regions of the forebrain composed of diencephalon (D) and telencephalon (Tel), the midbrain including tectum (Tm), tegmentum (Tg) and epiphysis (E), the hindbrain consisting of cerebellum (C) and rhombomeres (r1-7), and the floor plate (FP) are visible. Scale bars: 200 μm. This figure is modified from Kimmel *et al.* (1995).

3.3.1.1 No obvious change in the expression pattern of genes expressed in the brain after sub-lethal concentration of MeHg treatment

As MeHg is known to cause neural developmental defects in mammals and decreased swimming activity was noted in zebrafish embryos (Samson *et al.*, 2001), I hypothesised that low dosage of MeHg exposure would cause neurotoxic effects like retardation of neurological development or interference of neurochemical processes at later stage of development instead of affecting the general structure of the brain. To determine any abnormal change in the expression patterns of genes in the central nervous system (CNS) or in the neurotransmitter system, whole mount ISH and IHC

were performed to study the expression of *acetylcholinesterase* (*ache*; Bertrand *et al.*, 2001), which is a member of acetylcholinic neurotransmitter system and responsible for degrading acetylcholine, *paired box gene 6a* (*pax6a*), which is a homeodomain transcription factor and is very important for the development of eye and other sensory organs, *cannabinoid receptor 1* (*cb1*; Lam *et al.*, 2006), which is a G protein-coupled receptor of the inhibitory Gamma-aminobutyric acid (GABA) neurotransmitter system, *serotonin transporter a* (*sert*a; Wang *et al.*, 2006), which is an monoamine transporters that transports the neurotransmitter serotonin from synaptic spaces into presynaptic neurons, *nuclear receptor-related factor 1* (*nurr1*; Escriva *et al.*, 1997), which is an orphan nuclear receptor and involved in the maintenance of the dopaminergic neurotransmitter system, *sonic hedgehog* a (*shha*; Krauss *et al.*, 1993), which plays key roles in the development of organs including the brain, *crestin* (Luo *et al.*, 2001), which marks the neural crest cells and tyrosine hydroxylase (TH), which is responsible for catalysing the conversion of the amino acid L-tyrosine to dihydroxyphenylalanine, a precursor of dopamine. However, no obvious change in the expression patterns was observed in any of the genes or proteins examined (Fig. 3.7).

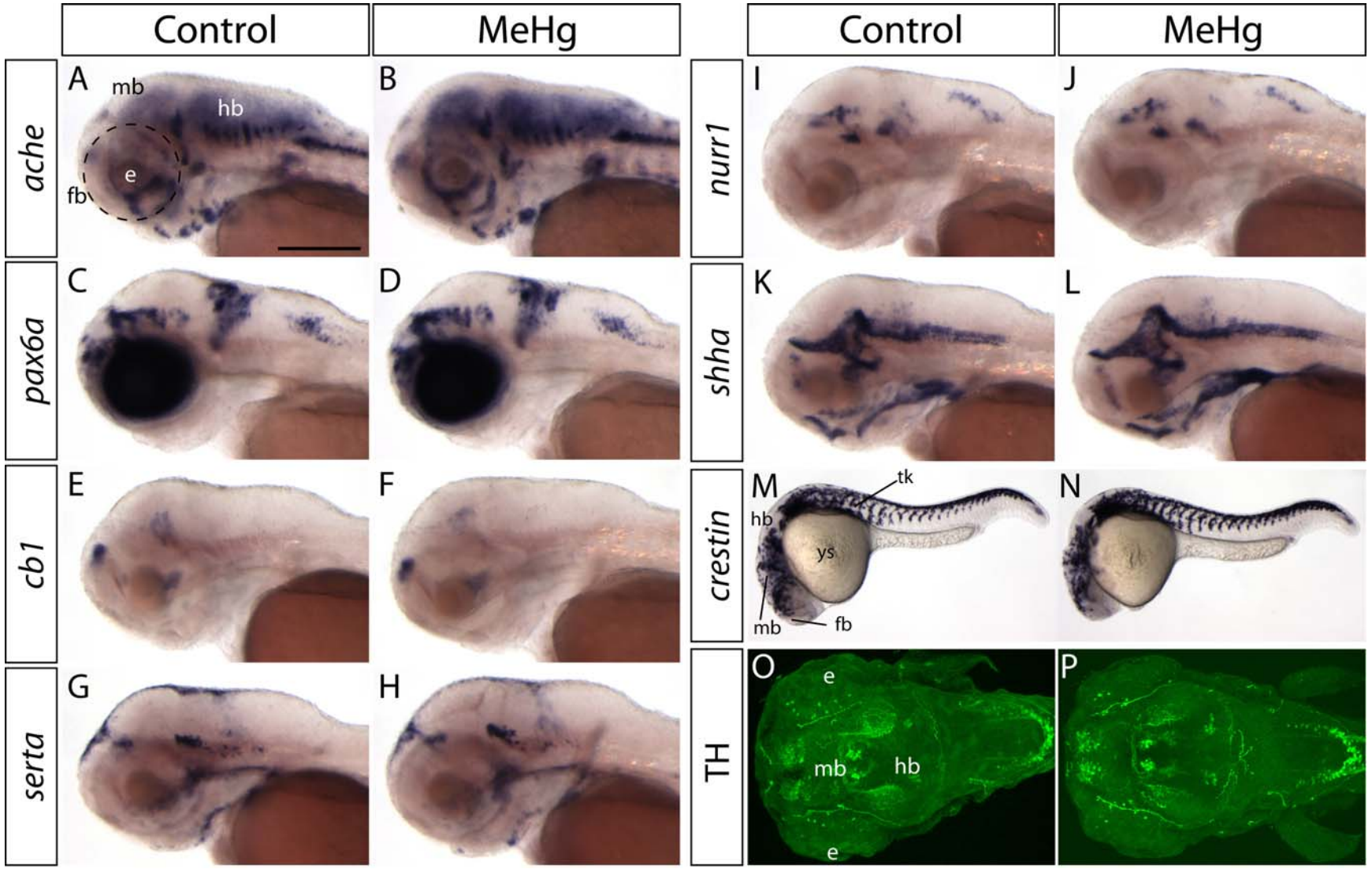
Control
MeHg
Control
MeHg
ache
A
mb
hb
e
fb
B
nurr1
I
J
pax6a
C
D
shha
K
L
cb1
E
F
crestin
M
tk
hb
ys
mb
fb
N
serta
G
H
TH
O
e
mb
hb
e
P

Fig. 3.7 Expression patterns of genes or proteins expressed in the central nervous system or neurotransmitter system of zebrafish embryos after MeHg exposure.
In situ hybridisation (regions which expressed the genes were stained in deep purple) (A-N) and immunohistochemistry (regions which the proteins were present were fluorescent green) (O,P) stainings were performed on control (A, C, E, G, I, K, M, O) and MeHg-treated (B, D, F, H, J, L, N, P) embryos at 72 hpf (A-L, O, P) and 24 hpf (M, N). Lateral views of the head region (A-L) and whole embryos (M, N) and dorsal views, anterior to the left and right side up, of the head region of the embryos (O, P) are shown. (A, B) *ache*; (C, D) *pax6a*; (E, F) *cb1*; (G, H) *serta*; (I, J) *nurr1*; (K, L) *shha*; (M, N) *crestin*; (O, P) TH. No obvious change in the expression pattern of the genes or proteins examined was observed. Abbreviations, e, eye; fb, forebrain; hb, hindbrain; mb, midbrain; tk, trunk; ys, yolk sac. Scale bar, A-L, O, P, 200 μm; M,N, 650 μm.

3.3.1.2 Genes showing ectopic expression in the brain of MeHg-treated embryos

To order to identify genes which show changes in the brain in response to MeHg exposure and may play a role in causing the decreased swimming activity in zebrafish embryos, the toxicogenomic screen is performed in parallel to the study of the marker genes of the CNS or the neurotransmitter system. Through the toxicogenomic screen, I identified 24 genes which were specially regulated in the brain under MeHg exposure. These genes are involved in diverse biological processes and molecular functions.

In response to MeHg exposure, the expression of *ADP-ribosylation factor-like (arfl)* was up-regulated in scattered cells in the brain (Fig. 3.8 A, A') and such an expression was also observed in other parts of the body (supplementary disc). *arf* are members of the Arf family of the Ras superfamily of GTPase enzymes which can bind and hydrolyse GTP (Gillingham and Munro *et al.*, 2007; Wennerberg *et al.*, 2005). They are involved in the regulation of membrane traffic and organisation of the cytoskeleton (Donaldson and Honda, 2005; D'Souza-Schorey and Chavrier, 2008).

activating transcription factor 3 (atf3) was induced in patches of cells in the brain in MeHg-treated embryos (Fig. 3.8 B, B'). It is a transcription factor of the ATF/cyclic AMP response element-binding (ATF/CREB) family (Liang *et al.*, 1996). It is an adaptive-response gene which can be induced by various stress signals and has been

implicated in immune responses and oncogenesis (Hai *et al.*, 2010; Thompson *et al.*, 2009).

The expression of *angiotensinogen (agt)* was slightly increased in the boundaries between forebrain and midbrain and between midbrain and hindbrain and in the outer region of the tectum in embryos exposed to MeHg (Fig. 3.8 C, C'). *agt* is a part of the renin-angiotensin system that plays an important role in the regulation of blood pressure and water balance. In both human and rat brains, *Agt* was shown to be expressed by astrocytes (Intebi *et al.*, 1990; Stornetta *et al.*, 1988; Wosik *et al.*, 2007). In the human brain, *AGT* was required for blood-brain barrier maintenance (Wosik *et al.*, 2007).

The expression of *CCAAT/enhancer binding protein (C/EBP), gamma (cebpg)* was up-regulated in the outer region of the tectum after MeHg treatment (Fig. 3.8 D, D'). *cebpg* is a transcription factor of the C/EBP family which regulates viral and cellular CCAAT/enhancer element-mediated transcription. A pervious study showed that the levels of expressions of *cebpg* correlated with those of antioxidant and DNA repair genes in normal bronchial epithelial cells (Mullins *et al.*, 2005).

chromobox protein homolog 7-like (cbx7l) was induced in patches of cells in the brain in MeHg-treated embryos ((Fig. 3.8 E, E', arrows). It belongs to the polycomb group proteins which repress transcription epigenetically through the remodelling of chromatin and are involved in the control of cell cycle and oncogenesis (Morey and Helin, 2010; Schwartz, Pirrotta, 2008). Studies using human cancer cell lines showed that *CBX7* was highly expressed in cells of urothelial carcinomas (Hinz *et al.*, 2008), prostate cancer (Bernard *et al.*, 2005), follicular lymphomas (Scott *et al.*, 2007) and gastric cancer (Zhang *et al.*, 2010), but down-regulated in those of thyroid carcinoma (Pallante *et al.*, 2008) and pancreatic cancer (Karamitopoulou *et al.*, 2010).

The expression of *cocaine and amphetamine regulated transcript protein type I-like (cartIl)* in small groups of cells located in the brain was slightly increased after MeHg exposure (Fig. 3.8 F, F', arrows). *Cart* has been shown to be involved in multiple physiological functions, including feeding, endocrine regulation, and mediation of the stress response (Kuhar *et al.*, 2000). In human and rat, *Cart* was more widely

expressed and the expression was noted in neurons in the hypothalamus (Elias *et al.*, 2001).

The expression of *v-fos FBJ murine osteosarcoma viral oncogene homolog (fos)* was strongly induced in the dorsal part of the brain after MeHg exposure (Fig. 3.8 G, G'). *Fos* is a transcription factor with a leucine-zipper DNA binding domain. It is important in normal and pathological conditions, and its deregulation has been shown to be linked with a variety of pathological conditions including oncogenesis, hypoxia, and neurological, immunological and skeletal defects (Herdegen and Waetzig, 2001; Milde-Langosch, 2005; Prabhakar and Kumar, 2004; Saitoh *et al.*, 1993; Wagner and Eferl, 2005). In rodents, medium- or long-term dietary intake of Hg-contaminated rice were also shown to increase *Fos* expression levels in the brain (Cheng *et al.*, 2005; 2009).

glutamate-cysteine ligase modifier subunit (gclm) showed a general up-regulation in the brain in MeHg-treated embryos (Fig. 3.8 H, H'). It encodes a part of the enzyme glutamate cysteine ligase which is critical for the synthesis of the GSH antioxidant (Lu, 2009). Increased *Gclm* expression levels were observed in conditions of oxidative stress caused by various substances (Lavoie *et al.*, 2009; Thompson *et al.*, 2009; Woo *et la.*, 2008). In human patients, polymorphism of *GCLM* has been reported to be associated with coronary endothelial vasomotor dysfunction and myocardial infarction (Koide *et al.*, 2003; Nakamura *et al.*, 2003).

homeodomain leucine zipper gene (homez) was strongly up-regulated in the brain, especially in the dorsal hindbrain region after MeHg treatment (Fig. 3.8 I, I'). It is a transcription factor containing leucine-zipper like motifs (Bayarsaihan *et al.*, 2003). In mouse, it showed restricted expressions in the brain, the optic vesicle and the otic placode during later stages of embryonic development (Bayarsaihan *et al.*, 2003).

interferon regulatory factor (irf9) showed a ubiquitous up-regulation in the brain in MeHg-treated embryos (Fig. 3.8 J, J'). *Irf* are transcription factors that involve in the protective defences of the immune system through the regulation of the transcription of interferons which can activate immune cells, increase the recognition of infection or tumor cells by up-regulating antigen presentation to T lymphocytes, and increase

the ability of uninfected host cells to resist new infection by virus (Gastl and Huber, 1988; Pestka *et al.*, 1987; Taniguchi *et al.*, 2001).

The expression of *lysosomal-associated membrane glycoprotein 1-like (lamp1l)* was up-regulated in the brain, especially in the epithelium lining the brain ventricle (Fig. 3.8 K, K'). Lamp1 together with Lamp2 account for about 50% of all the proteins of the lysosome membranes (Hunziker *et al.*, 1996). In mouse embryonic fibroblasts, lacking both *Lamp1* and *Lamp2* resulted in an accumulation of autophagic vacuoles and disturbed cholesterol metabolism (Eskelinen *et al.*, 2004).

opn1lw1 showed a general decrease in expression levels in the epiphysis in addition to in the eye after MeHg exposure (Fig. 3.8 L, L'). *opn1lw1* encodes a long-wavelength sensitive cone opsin having maximum light absorption at the red light region. Opsins are light-responsive membrane-bound G protein-coupled receptors of the retinylidene protein family (chromophore, vitamin A derivatives) found in photoreceptor cells (Nickle and Robinson, 2007).

6-phosphofructo-2-kinase/fructose-2,6-biphosphatase 4-like (pfkfb4l) showed an increase in expression in the whole brain after MeHg treatment (Fig. 3.8 M, M'). *pfkfb4* is a member of the Pfkfb enzymes which induce glycolysis through activating 6-phosphofructo-1-kinase and blocking gluconeogenesis by inhibiting fructose-1,6-bisphosphatase (Pilkis *et al.*, 1995). The expressions of *PFKFBs* have been shown to be induced in cancer cells and by hypoxia (Minchenko *et al.*, 2005a, 2005b, 2005c).

ppp1r15a was up-regulated in the tegmentum and rhombomeres after MeHg exposure (Fig. 3.8 N, N'). *Ppp1r15a* encodes the growth arrest and DNA damage 34 (GADD34) protein which dephosphorylates the alpha subunit of translation initiation factor 2 (eIF2α), promoting the recovery of protein synthesis in the unfolded protein response (a response to the accumulation of unfolded or misfolded proteins in the lumen of endoplasmic reticulum) (Novoa *et al.*, 2001). *Ppp1r15a* mutant cells exhibit impaired recovery of protein synthesis while *Ppp1r15a* knockout mice are phenotypically indistinguishable from wild type (Kojima *et al.*, 2003; Novoa *et al.*, 2003).

The expression of *peroxiredoxin1 (prdx1)* was slightly up-regulated in the hypothalamus after MeHg exposure (Fig. 3.8 O, O'). *Prdx1* is a member of the antioxidant thioredoxin-dependent peroxidase family (Immenschuh and Baumgart-Vogt, 2005; Rhee *et al*., 2005). It protects cellular components by removing the low levels of ROS produced as a result of normal cellular metabolism and is a stress-inducible antioxidant (Ishii and Yanagawa, 1997; Rhee *et al*., 2005). *Prdx1* is also known as *natural killer enhancing factor A (NkefA)* and in human cell lines, it has been shown to be implicated in enhancing natural killer cell activity and antivirual activity (Geiben-Lynn*, et al.*, 2003; Shau *et al.*, 1993).

SAR1a gene homolog (sara2) showed mild up-regulation in the brain in embryos exposed to MeHg (Fig. 3.8 P, P'). *sara2* is a zebrafish homologue of the yeast *S. cerevisiae SAR1*, which is also a small GTPase of the Arf family as *arfl* (Gillingham and Munro *et al.*, 2007). It is found in COPII vesicles (a type of vesicle which transports proteins from the rough endoplasmic reticulum (ER) to the Golgi apparatus) (Bi *et al.*, 2002) and it regulates the membrane constriction, assembly and fission of the vesicles and the transport of ER (Bielli *et al.*, 2005; Long *et al.*, 2010).

The expression of *sine oculis homeobox homolog 3a (six3a)* in the forebrain was up-regulated after MeHg exposure (Fig. 3.8 Q, Q'). *six3a* is a member of the Six gene family which was first identified in *Drosophila* for compound-eye formation (Kawakami *et al.*, 2000). In zebrafish, *six3a* plays important roles in both eye and rostal forebrain developments (Kobayashi *et al.*, 1998; Seo *et al.*, 1998).

solute carrier family 16 (monocarboxylic acid transporters), member 9a (slc16a9a) showed a general decrease in the expression in the whole brain after MeHg treatment (Fig. 3.8 R, R'). *slc16a9a* is a member of *Slc16* gene family (Meredith and Christian, 2008). Some members of this family catalyse the transport of monocarboxylates such as lactate, pyruvate and ketone or bodies aromatic amino acids (Halestrap and Meredith, 2004; Meredith and Christian, 2008). However, the substrate(s) of *slc16a9a* is still unknown.

UDP glucuronosyltransferase 5 family, polypeptide A2 (ugt5a2) was up-regulated in the dorsal region of the brain of MeHg-treated embryos (Fig. 3.8 S, S'). *ugt5a2*

belongs to the *UDP-Glucuronosyltransferase* (*Ugt*) superfamily. Members of this superfamily encode enzymes responsible for the glucuronidation of the xenobiotics, producing the more water soluble glucuronic acid-bound xenobiotics, and thus, aid the excretion of the xenobiotics from the body (King *et al.*, 2000; Miners *et al.*, 2002). The *Ugt5* family exist only in teleosts and amphibians, but not in reptiles, birds or mammals (Huang and Wu, 2010).

Eight other genes with unknown identity including *zgc:101661, AW115990, BE016163, BI474700* and *BM036361* were also ectopically expressed in the brain after MeHg exposure (Fig. 3.8 T, T' – X, X'). The changes in the expression patterns of these 24 genes in the brain might suggest the induction of the behavioural changes reported by Samson *et al.* (2001) after MeHg exposure.

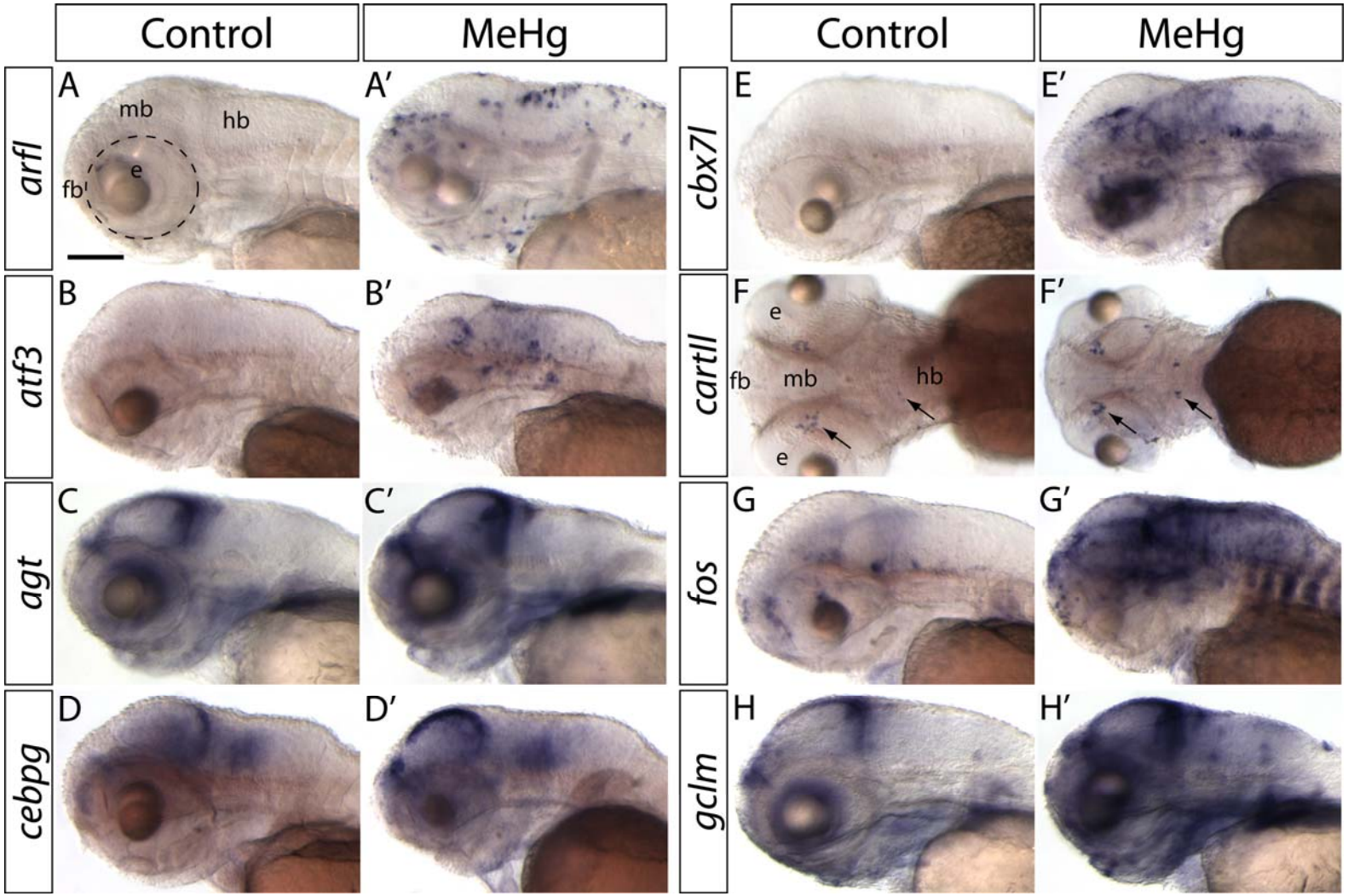

(Fig. 3.8 Continued)

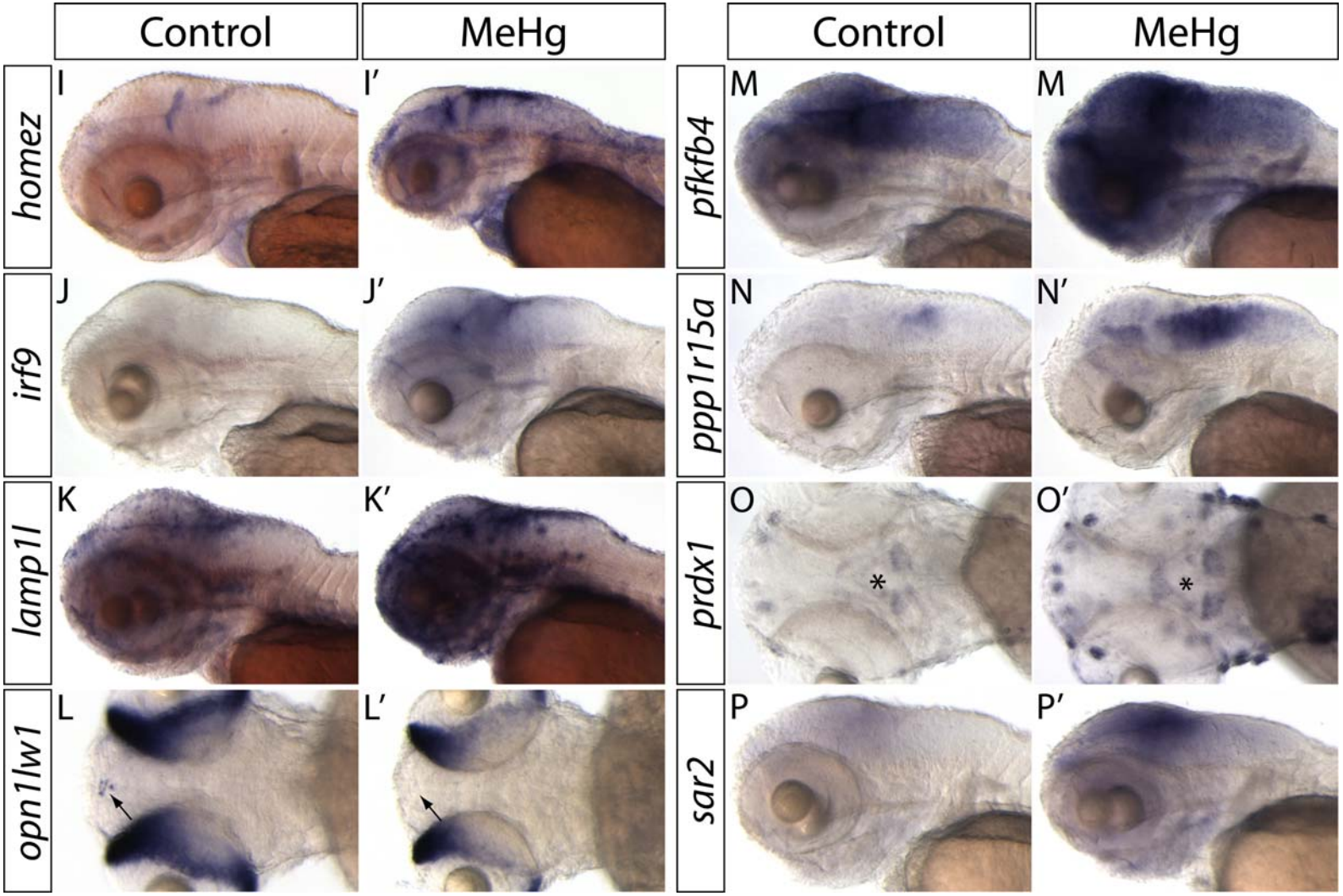

(Fig. 3.8 Continued)

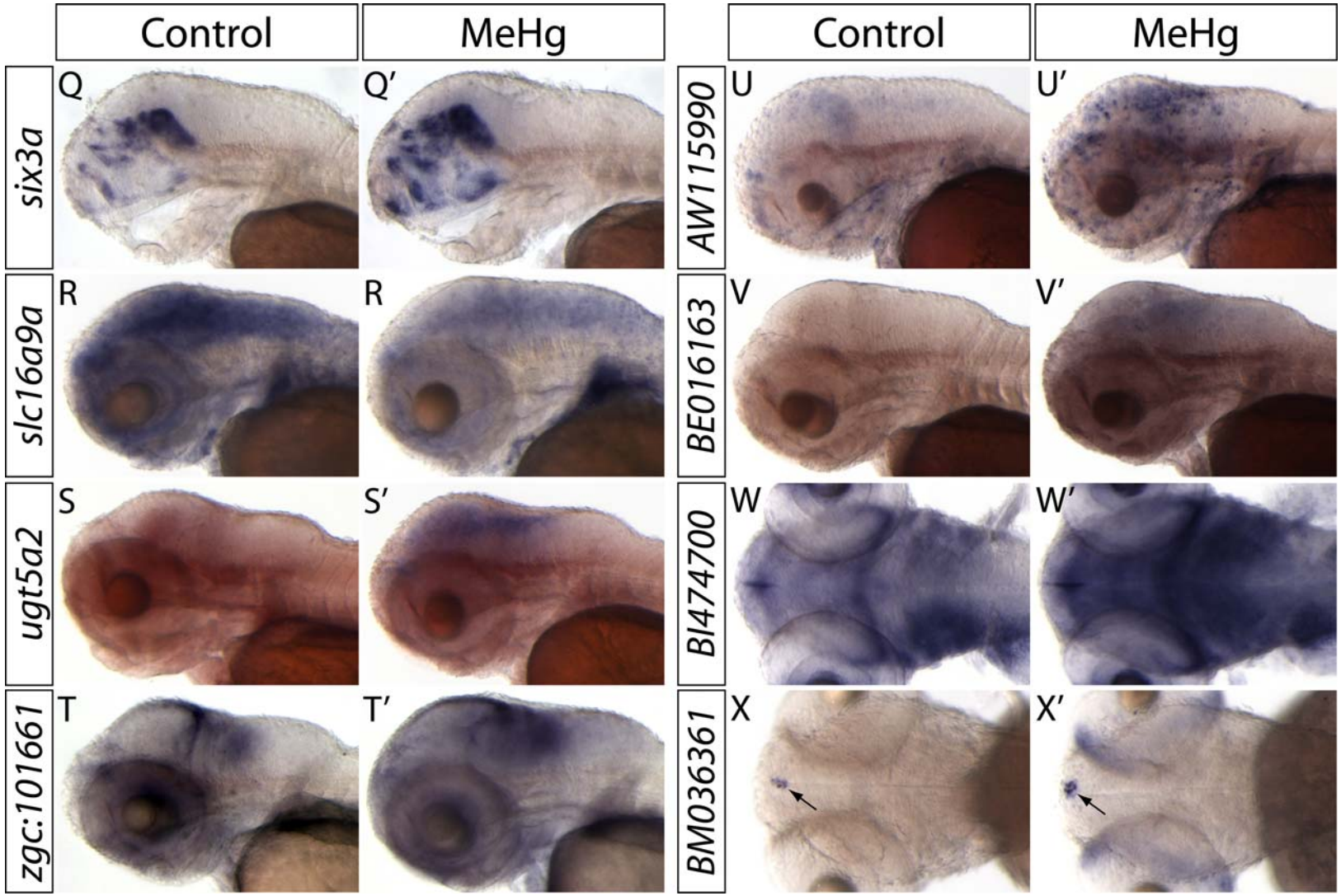
Control
MeHg
Control
MeHg
six3a
Q
Q′
AW115990
U
U′
slc16a9a
R
R
BE016163
V
V′
ugt5a2
S
S′
BI474700
W
W′
zgc:101661
T
T′
BM036361
X
X′

Fig. 3.8 Changes in gene expression in the zebrafish brain after MeHg treatment.
Lateral (A, A'- E, E', G, G'- K, K', M, M' – N, N', P, P'- V, V') and dorsal (F, F', L L', O, O', W, W', X, X') views of 72-hpf-old control (A, B, C, D, E, F, G, H, I, J, K, L, M, N, O, P, Q, R, S, T, U, V, W, X) and MeHg-treated (A', B', C', D', E', F', G', H', I', J', K', L', M', N', O', P', Q', R', S', T', U', V', W', X') embryos performed with *in situ* hybridisation are shown. The dotted line in A indicates the position of the eye; the arrows in L, L', X, X' mark the epiphysis. Up-regulations of *arfl* (A, A'), *atf3* (B, B'), *agt* (C, C'), *cebpg* (D, D'), *cbx7l* (E, E'), *cartIl* (F, F', the patches of cells with increased expression are indicated by the arrows), *fos* (G, G'), *gclm* (H, H'), *homez* (I, I'), *irf9* (J, J'), *lamp1l* (K, K'), *pfkfb4l* (M, M'), *ppp1r15a* (N, N'), *prdx1* (O, O', the asterisks indicate the hypothalamus), *sara2* (P, P'), *six3a* (Q, Q', eyes removed for better observation of the expression pattern in the brain), *utg5a2* (S, S'), *zgc:101661* (T, T'), *AW115990* (U, U'), *BE016163* (V, V'), *BI474700* (W, W') and *BM036361* (X, X'), and down-regulations of *opn1lw1* (L, L') and *slc16a9a* (R, R') were observed in the brain of embryos exposed to MeHg. Abbreviations, e, eye; fb, forebrain; hb, hindbrain; mb, midbrain. Scale bar, A, A'- E, E', G, G'- K, K', M, M' – N, N', P, P'- V, V', 100 μm, F, F', L L', O, O', W, W', X, X', 80 μm.

3.3.2 Study on the lateral line system in MeHg-treated embryo

Lateral line is a sensory organ of the peripheral nervous system in fish and is responsible for sensing the local disturbances of the water flow and detecting the orientation of the animal in the surrounding water current. It is essential for detecting prey, escaping from predators, and performing social interactions. In zebrafish, the lateral line runs lengthwise on each side of the body, from the vicinity of the operculum to the base of the tail (Metcalfe *et al*., 1985). It comprises a stereotyped array of sensory structures called neuromasts, each of which is composed of mechanoreceptive hair cells, support cells and mantel cells and is innervated (Ghysen and Dambly-Chaudière, 2004; Fig. 3.9 A). The neuromasts located on the head are termed anterior lateral line system (ALL), whose ganglion is located between the ear and the eye, while those present on the trunk and tail are referred to posterior lateral line system (PLL) whose ganglion is just posterior to the ear (Dambly-Chaudière *et al*., 2003; Metcalfe *et al.*, 1985; Raible and Kurse, 2000). The PLL is formed by a migrating primordium. During embryonic development, the migrating primordium moves in an anterior-to-posterior manner along the horizontal myoseptum all the way to the tip of the tail and deposits clusters of cells at regular intervals, each of which

will later differentiate into individual neuromast (Dambly-Chaudière *et al*., 2003; Fig. 3.9 B).

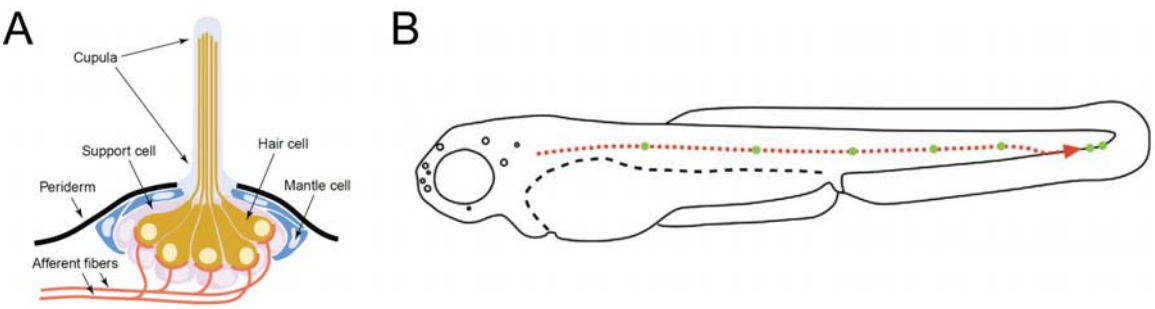

Fig. 3.9 Pattern and structure of the zebrafish lateral line at the end of embryogenesis.
(A) Scheme of a neuromast, showing the organisation of hair cells, the surrounding support cells and mental cells and afferent fibers. (B) Schematic diagram of the lateral line of a zebrafish embryo at 48 hpf. The red dotted arrow indicates the direction of neuromast formation in posterial lateral line (PLL) during development and the green dots represent the positions of the PLL neuromasts. The round dots and small circles in the head region mark the positions of the anterior lateral line (ALL) neuromasts. This figure is reproduced after Ghysen and Dambly-Chaudière (2004).

3.3.2.1 Decreased number of neuromast hair cells in the PLL

The neuromasts are in direct contact with the environment and it has been reported that waterborne contaminants, such as copper, aminoglycoside and neomycin, could lead to disruption of the neuromasts and death of hair cells (Froehlicher *et al.*, 2009; Harris *et al.*, 2007; Hernández *et al.*, 2006; Owens, *et al.*, 2007). This led to the speculation that exposure to MeHg would also result in disruption of the neuromasts of the lateral line system in the zebrafish embryo. I examined this by employing the transgenic line *Tg(-1.7CaTuba1:GFP)mi2*, which GFP in the hair cells (Gulati-Leekha and Goldman, 2006). The transgenic embryos were exposed to 60 µg/l MeHg from 4 to 80 hpf and the number of hair cells in the transgenic lines was scored at 80 hpf at which the embryonic pattern of PLL is completed (Gompel *et al.*, 2001; Ledent, 2002). Compared to the control, there is a significant decrease in the number of hair cells in embryos exposed to MeHg while no change in the location of the neuromasts was observed in MeHg-treated embryos (Fig. 3.10).

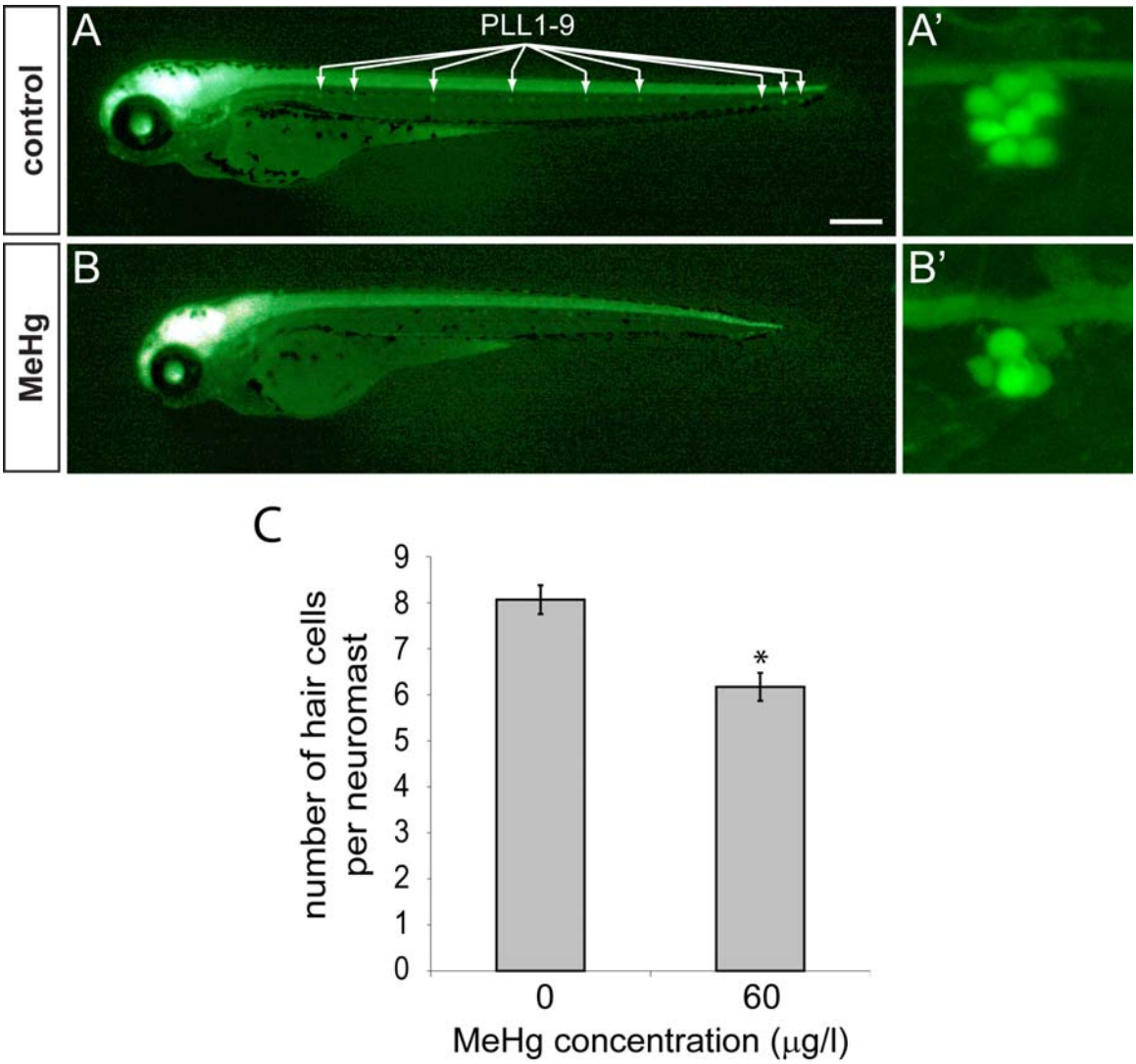

Fig. 3.10 Decreased number of neuromast hair cells in the lateral line in embryos exposed to MeHg. Lateral views of control (A, A') and MeHg-treated (B, B') *Tg(-1.7CaTuba1:GFP)mi2* transgenic embryos at 80 hpf. GFP is expressed in the hair cells of the neuromasts. The 9 neuromasts in the trunk, posterior lateral line (PLL) 1 (the anterior-most) to PLL 9 (the posterior-most) are indicated by the arrows in (A). (A', B') Magnified images of neuromasts. (C) The number of hair cells in the neuromasts PLL 4 to PLL 6 was scored. The mean ± SEM are reported (control, n = 15; MeHg-treated, n = 16). The number of hair cells in MeHg-treated embryos is significantly lower than that of the control. T-test, $p < 0.001$ (*). Scale bar, A, B, 200 µm; A', B', 15 µm.

3.3.2.2 Genes induced in the lateral line of MeHg-treated embryos

In the toxicogenomic screen, changes in the expression levels of 12 genes were observed in the neuromasts of the MeHg-treated embryos. *peroxiredoxin1 (prdx1), CXC chemokine 46-like (cxc46l), E74-like factor 3 (elf3), v-fos FBJ murine osteosarcoma viral oncogene homolog (fos), glutamate-cysteine ligase modifier*

subunit (gclm), lysosomal-associated membrane glycoprotein 1-like (lamp1l), NADPH oxidase organizer 1 (noxo1), , sequestosome 1 (sqstm1), v-maf musculoaponeurotic fibrosarcoma oncogene homolog f (avian) (maff) and *thioredoxin-like (txnl)* showed up-regulations in the lateral line while the expression of *chromobox protein homolog 7-like (cbx7l)* and *glutathione peroxidase 1a (gpx1a)* in the lateral line was down-regulated (Fig. 3.11). These genes showed mild to strong changes in the expressions in response to MeHg. From the magnified images of the neuromasts, it was noticed that these genes were ectopically expressed in different parts of the neuromasts (Fig. 3.11 inserts). However, further investigations are required to identify in which cell types these genes are expressed in the neuromast. The specific changes of these 12 genes in the neuromasts may suggest their correlation with the decrease in neuromast hair cell number in MeHg-exposed embryos.

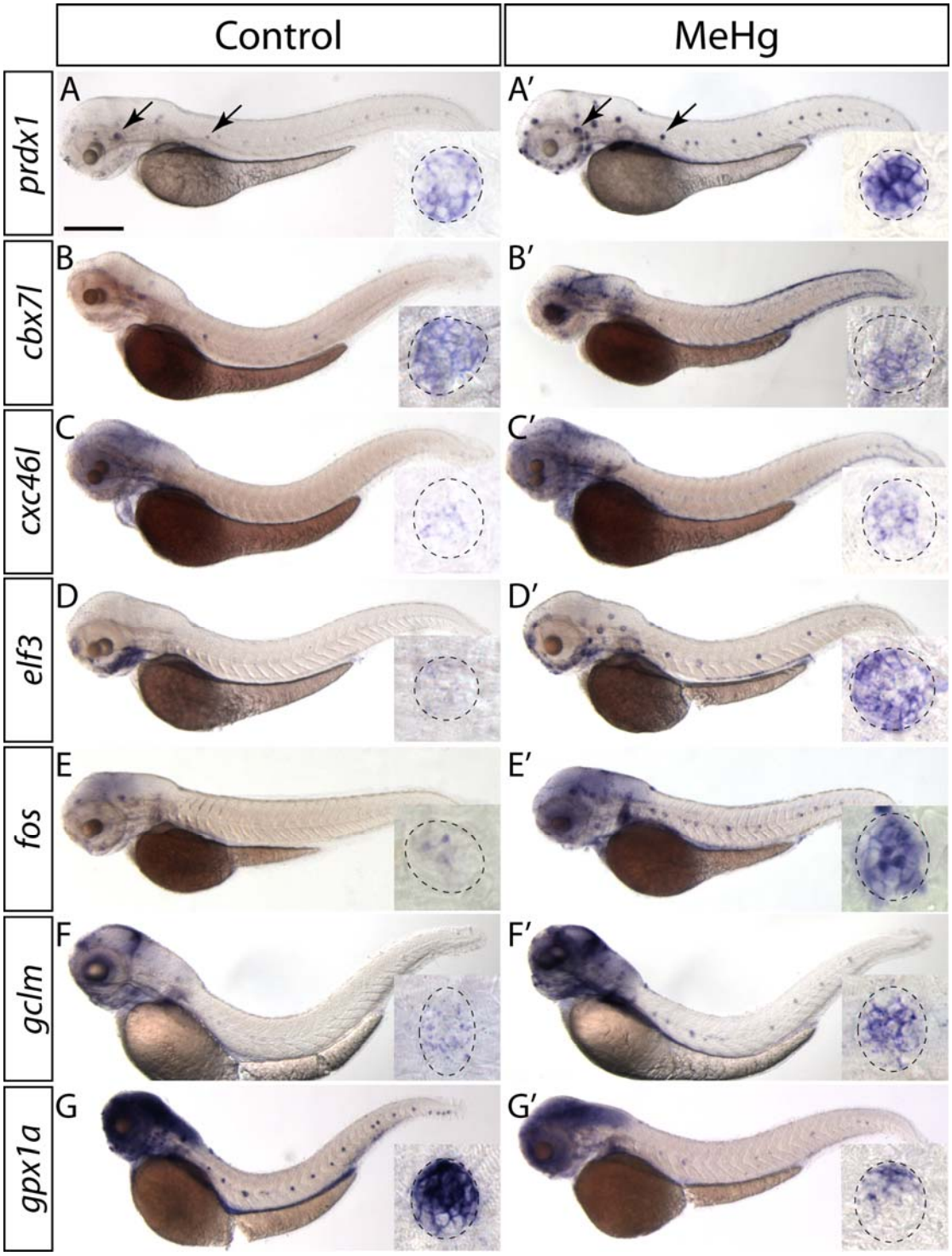

(Fig. 3.11 continuted)

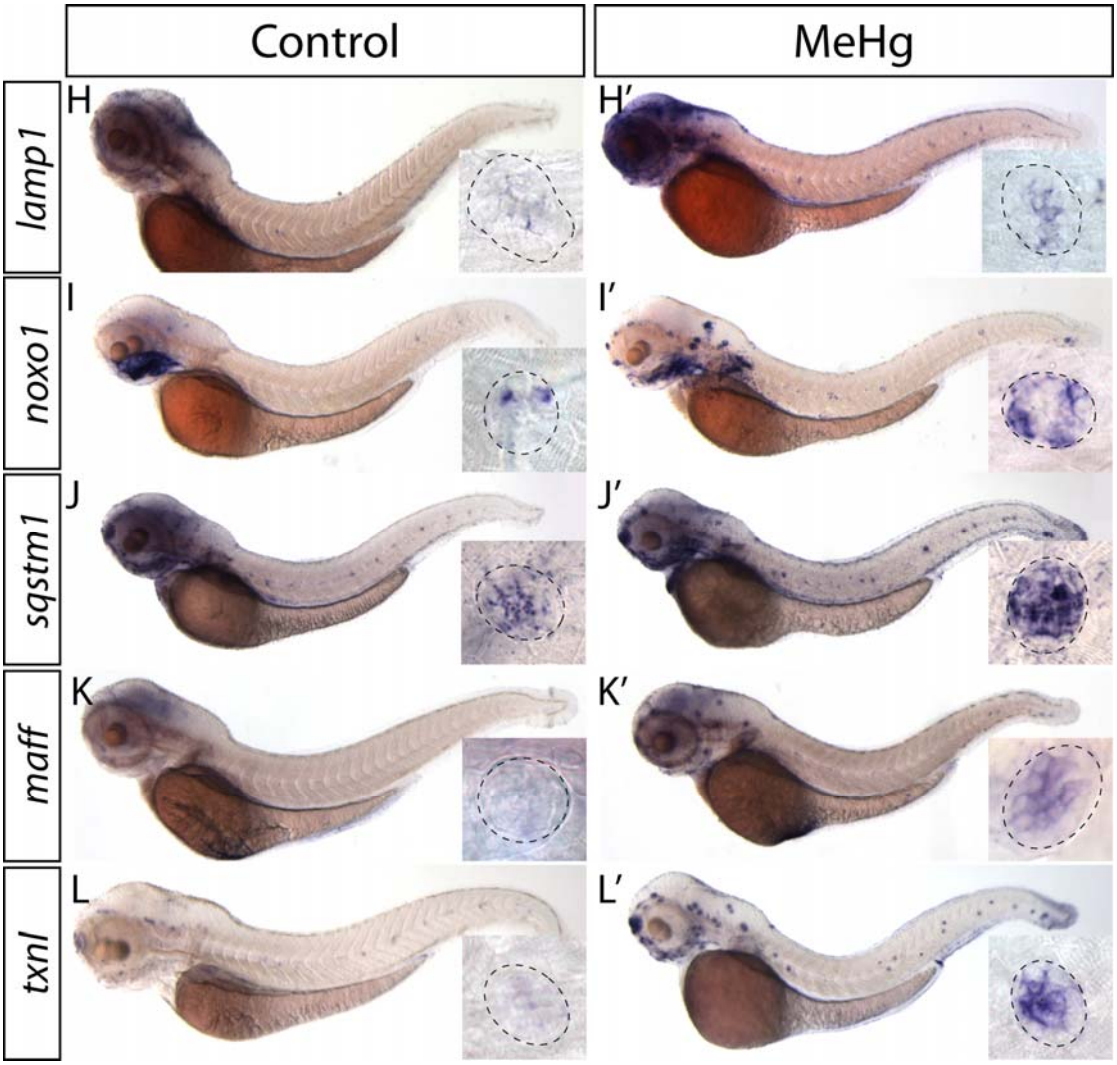

Fig. 3.11 Changes in the gene expression levels in the lateral line after MeHg exposure.
Lateral views of control (A, B, C, D, E, F, G, H, I, J, K, L) and MeHg-exposed (A', B', C', D', E', F', G', H', I', J', K', L') 72-hpf-old embryos subjected to *in situ* hybridisation. The arrows in A and A' indicate the neuromasts. The inserts are higher magnification of the posterior lateral line (A, A' – I, I', K, K', L, L') or anterior lateral line (J, J') neuromast and the dotted lines outlines the neuromasts. Increased expressions of *prdx1* (A, A'), *cxc46l* (C, C'), *elf3* (D, D'), *fos* (E, E'), *gclm* (F, F'), *lamp1l* (H, H'), *noxo1* (I, I'), *sqstm1*(J, J'), *maff* (K, K') and *txnl* (L, L') and decreased expression of *cbx7l* (B, B') and *gpx1a* (G, G') were detected in the lateral lines of embryos treated with MeHg. Scale bar, A, A' – K, K', 200 μm, inserts, 20 μm.

3.3.3 No observable defects in the myofibril or motor neuron structures

As MeHg-treated embryos exhibited a decrease in spontaneous swimming activity (Samson *et al*., 2001) and this promoted us to examine if any defect in the arrangement or the integrity of myofibers would be the cause of the problems. I

addressed this question by comparing the birefringence of embryos under polarised light (Behra *et al*., 2006; Fig. 3.12 A, B). Both control and MeHg-treated embryos showed similar brightness of the birefringence, indicating that there was no obvious different in the axial musculature. This result was confirmed by the slow muscle myosin staining using the anti-slow myosin F59 antibody (Crow and Stockdale, 1986) that the arrangement and integrity of the slow muscle myosins looked similar to those of the control ones.

As defects in the axial musculature do not seem to be the cause of the impaired motility, I next asked if the motor neurons were properly formed. I examined populations of interneurons and sensory neurons, and the connections of the neurons to the neuromuscular junction by co-staining the embryos with anti-acetylated tubulin antibody (Behra *et al*., 2002; Piperno and Fuller, 1985), and with α-bungarotoxin, a toxin which specifically binds to nicotinic acetylcholine receptor (Downes and Granato, 2004; Panzer *et al.*, 2005; Fig. 3.12 C-F). The co-staining revealed that there was no obvious difference in the interneuron and sensory neuron distribution or the connection between the neurons and the neuromuscular junctions. So, it is concluded that the decreased spontaneous swimming activity was neither due to structural defects in myofibers nor motor neuron distribution and connection.

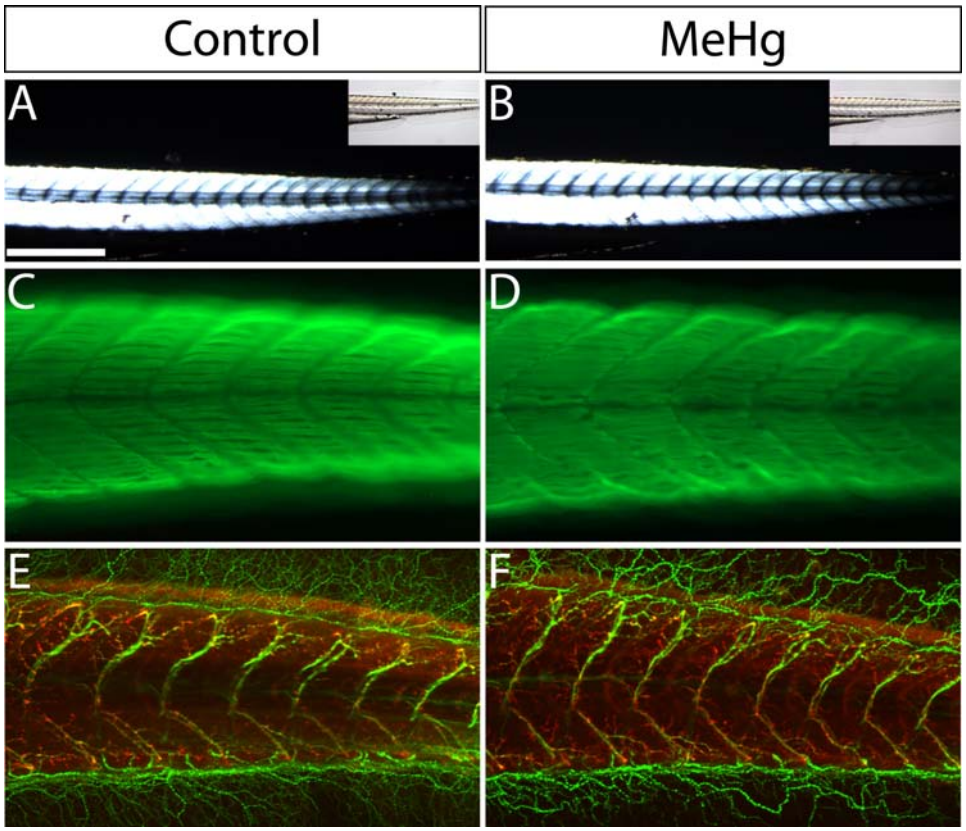

Fig. 3.12 No observable change in myofibers structure or motor neuron distribution and connection in embryos exposed to MeHg.

Lateral views of the trunks and tails of 72 hpf control (A, C, E) and MeHg-treated (B, D, F) embryos are shown. (A, B) Birefringence images. The inserts in A, B are the bright field images. (C, D) slow muscle myosin stained with the antibody F59. (E, F) Staining with antibody against acetylated-tubulin (green) and with α-bungarotoxin (red). Scale bar, A, B, 250 μm, C-F, 75 μm.

3.3.4 Summary

The effects of MeHg on the nervous system, including the brain, the lateral line and the neuromuscular junction connection, of zebrafish embryos were investigated in this study. Although no obvious changes in some of the marker genes of CNS or the neurotransmitter system examined were detected, through the toxicogenomic based approach, 24 genes which showed changes in the expression levels or patterns in the brain in response to MeHg exposure were identified. MeHg treatment also caused a decrease in the number of neuromast hair cells in the lateral line. The expressions of 12 genes were shown to be regulated by MeHg in the lateral line. The changes in the connections of the neurons to the neuromuscular junction were also examined. No

defects in the motor neuron distribution or connection in the embryos after MeHg treatment were detected.

3.4 Study on the melanophore stripes and caudal fin fold in the tail in MeHg-exposed embryos

In zebrafish, tail morphogenesis occurs rapidly and the tail can be well-recognised by the end of the first day of development (Dane and Tucker, 1985; Kimmel *et al.*, 1995; Fig. 3.13). The tail bud becomes visible at 10.3 hpf and derives from a distinct swelling at the posterior end of the embryonic axis the so-called tail bud. Most of the cells of the tail bud will contribute progeny to the tail. Tail morphogenesis continues to occur and the tail bud becomes more prominent as the embryo develops. At 16.5 hpf, the tail bud begins to protrude from the body of the embryo. As the tail extends, the overall body length of the embryo increases. At 24 hpf, the tail bud becomes very small. Cells flanking the sides of the tail bud become flattened and this leads to the formation of the caudal fin fold around the tail bud. At 30 hpf, fast tail morphogenesis has finished and the embryo begins to have a slower rate of body lengthening. Melanophores, which are melanin-containing cells and possess a dark brown or black colour, start to form three lengthwise stripes on the trunk and tail with one located dorsally, one ventrally and one laterally. At 36 hpf, arrays of extracellular matrix fibers called actinotrichia are present in the subepidermal space of the caudal fin fold. Melanophores in the dorsal stripe exist sparsely from the diencephalon region of the head to the tip of the tail, and those in the ventral strip locate dispersedly to about halfway to the tip of the tail. At 42 hpf, the caudal fin fold is prominent. The dorsal melanophore stripe becomes very well filled out and the ventral stripe now also contains melanophores up to the end of the tail. However, gaps exist in the ventral stripe at the tail region and one of these occurs at the posterior end where the caudal fin primordium locates (Hadzhiev *et al*., 2007; Iovine, 2007). At 72 hpf, the caudal fin fold is even more prominent and adopts a fan shape. Both the dorsal and ventral stripes become very well-defined and densely populated with melanophores. However, a small gap in the ventral stripe of the caudal fin primordium persists with absence of melanophores.

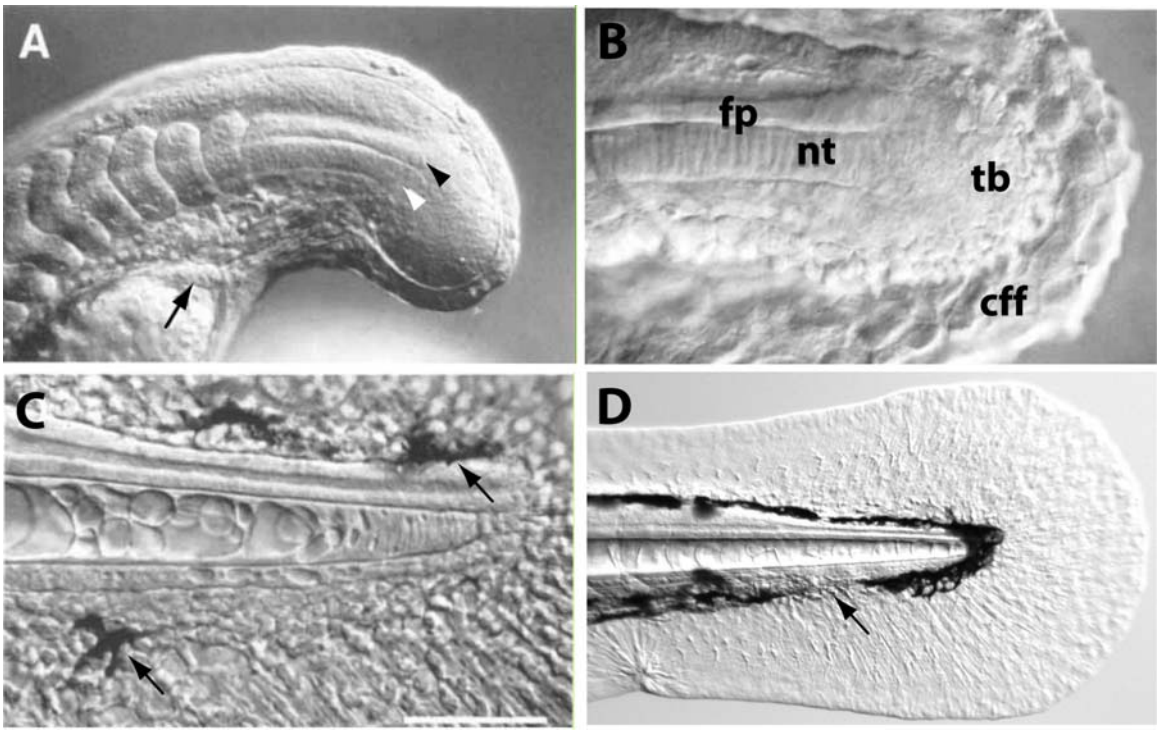

Fig. 3.13 Zebrafish tail development.

Lateral views of the tail part of zebrafish at 19.5 hpf (A), 24 hpf (B), 42 hpf (C) and 72 hpf (D). (A) The primordium of the notochord (white arrowhead) and the spinal cord (black arrowhead), develop from the tail bud mesenchyme. The arrow indicates the pronephric duct. (B) At 24 hpf, the tail bud (tb) becomes very small and is surrounded by the caudal fin fold (cff). The notochord primordium (nt) and the spinal cord floor plate (fp) become more distinct. (C) At 42 hpf, the tail bud disappears. The spinal cord and notochord narrow to a blind-ended tube with a simple cuboidal lining. The caudal fin fold becomes more prominent and surrounds the entire structure. The melanophores (arrows) are differentiating. (D) At 72 hpf, the caudal fin fold shows a clear, thin and fan-shaped appearance. The melanophores have differentiated and migrated to form two well-defined stripes with one above and one below the tail at the boundary to the fin fold in the developing zebrafish embryo. The ventral stripe is characterised by a gap (arrow) in the row of pigment cells slightly anterior to the tip of the tail and this gap marks the caudal fin primordium. Scale bar, A-C, 50 μm; D, 125 μm. (A-C) Reproduced after Kimmel *et al.* (1995).

3.4.1 Disruption of the melanophore stripes and caudal fin fold in embryos exposed to MeHg

Disruption of trunk pigmentation with a smaller gap size of the melanophore stripe was observed in MeHg-exposed embryos. In order to examine if these malformations are specific to MeHg or can be induced by other heavy metals, I exposed embryos to sub-lethal concentrations of lead chloride ($PbCl_2$), arsenic oxide (As_2O_3) and

cadmium chloride ($CdCl_2$), which triggered related toxicogenomic responses (Yang *et al.*, 2007). Interestingly, only embryos exposed to MeHg, but not other heavy metals examined, showed the malformations in the tail (Fig. 3.14). Thus, I concluded that the tail malformations are specific to MeHg.

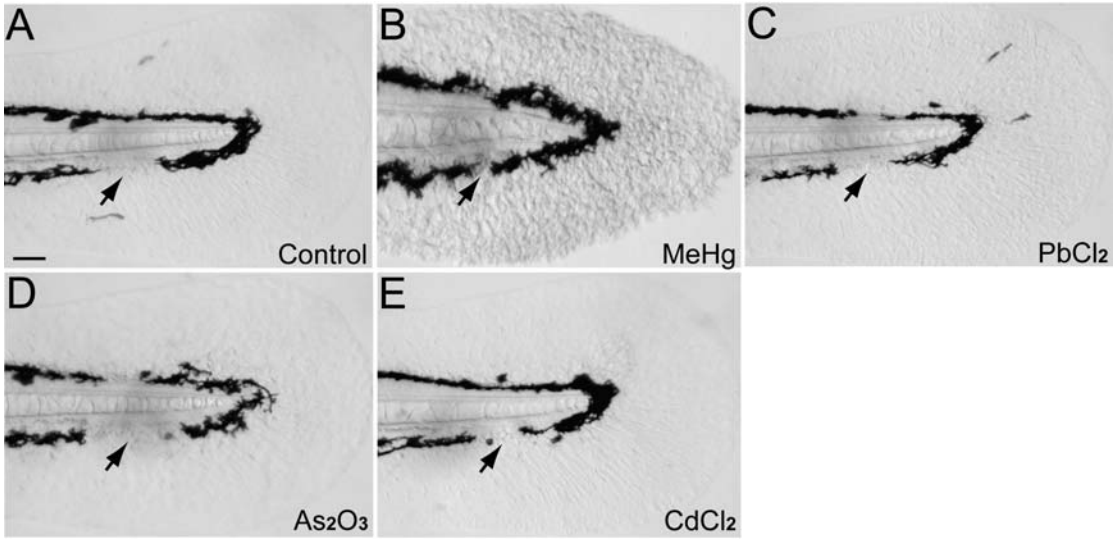

Fig. 3.14 MeHg-specific disruptions of the caudal fin fold tissue and the melanophore gap.
Lateral views, anterior to the left and dorsal side up, of the posterior part of the tails of embryos at 72 hpf. The dotted lines outline the outer region of the caudal fin folds and the arrows indicated the position of the melanophore gap. Embryos were exposed to MeHg (B), lead chloride ($PbCl_2$) (C), arsenic oxide (As_2O_3) (D) and cadmium chloride ($CdCl_2$) (E) or embryo culture only as control (A). Tail malformations of disruption of the caudal fin fold tissue and melanophore gap were only observed in embryos exposed to MeHg (B), but not to the 3 other heavy metals examined (C-E). Scale bar, 50 μm. This figure is provided by L. Yang.

3.4.2 Loss of GFP expression in the caudal fin primordium in the *Tg(-2.4shha-ABC:GFP)sb15* transgenic line after MeHg treatment

Strikingly, the phenotypes induced by MeHg exposure were very similar to those resulted from the loss of *sonic hedgehog* (*shh*) expression in zebrafish embryos, including the disruption of the melanophore gap (Hadzhiev *et al.*, 2007). It has been shown that the caudal fin primordium, which is a region located at the posterior region of the developing fin bud and serves as a signaling center to instruct the developing fin bud to migrate and generate appropriate structures along the anterior-posterior axis,

is located at the melanophore gap (Hadzhiev *et al*., 2007; Iovine, 2007). GFP from the transgene *Tg(-2.4shha-ABC:GFP)sb15* is specifically expressed in this primordium (Hadzhiev *et al.*, 2007).

I was tempted to speculate that MeHg affects the development of the caudal fin primordium through interacting with the *shh* signaling pathway. I wanted to know if exposure to MeHg would diminish the GFP expression in the caudal fin primordium. Transgenic embryos were exposed to 60 µg/l MeHg from 4 to 72 hpf. A high proportion of embryos (86%, n = 5, 20 embryos each) showed a complete loss of expression of GFP in the caudal fin primordium (Fig. 3.15). This correlated with loss or reduction of the gap in pigmentation. Transgene expression in the floor plate or in the pectoral fins was not affected by the MeHg treatment, indicating that MeHg specifically impaired GFP expression in the caudal fin primordium.

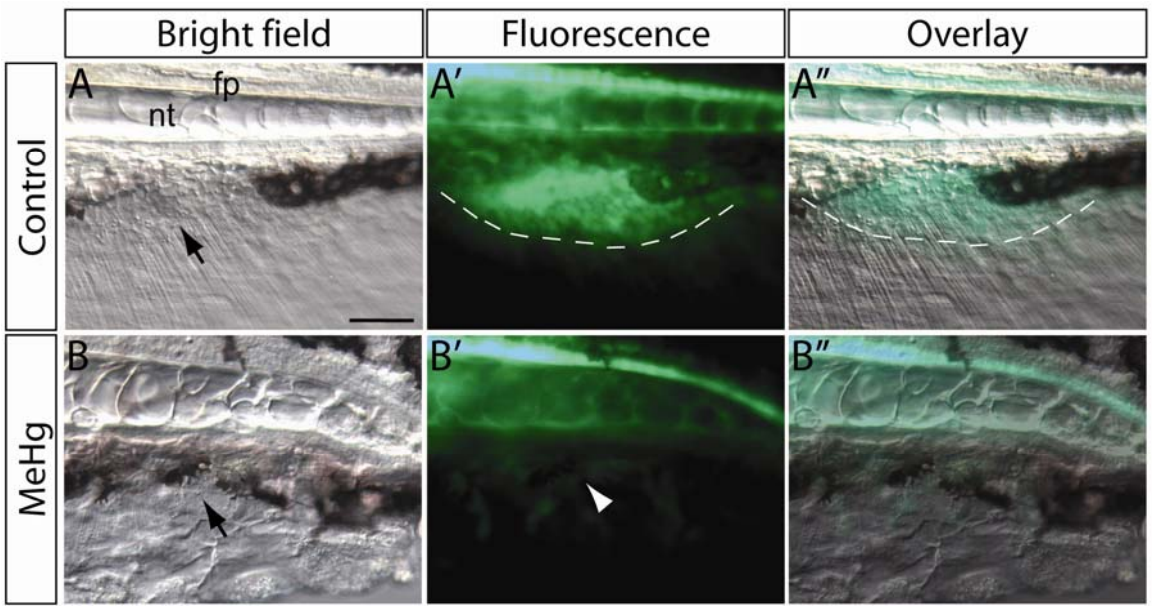

Fig. 3.15 Induction of caudal fin fold defects and caudal fin primordium disruption in embryos exposed to MeHg.

The lateral views of the pigment gap of control (A-A'') or MeHg-treated embryos (B-B'') at 72 hpf are shown. (A, B) Bright field images; (A', B') fluorescence images; (A", B") overlay images. The caudal fin primordium (outlined by dashed lines) is marked by GFP expression in the *Tg(-2.4shha-ABC:GFP)sb15* transgenic line in control embryos (A-A''). The GFP expression in the primordium is reduced or absent in embryos exposed to MeHg (B-B'', arrowheads). Abbreviations, nt, notochord; fp, floor plate. Scale bar, 50 µm.

3.4.3 Reduction of caudal fin GFP expression at MeHg concentration as low as 6 µg/l

I wanted to know the lowest effective concentration at which MeHg could induce the loss of GFP expression in the caudal fin primordium. I exposed zebrafish embryos to MeHg concentrations of 6, 30 and 60 µg/l from 4 to 72 hpf. According to the degree of loss in the GFP domain, I classified the reduction into two categories, type I and type II. For the type I class, the GFP domain was reduced (Fig. 3.16) while for the type II class, no GFP expression could be observed at all. There was already a significant increase in the number of embryos with reduced GFP expression (type I plus type II) at 6 µg/l MeHg. The percentage of embryos showing the severer type II phenotype increased with the concentrations of MeHg. At 60 µg/l, almost all of the treated embryos fell into the type II class.

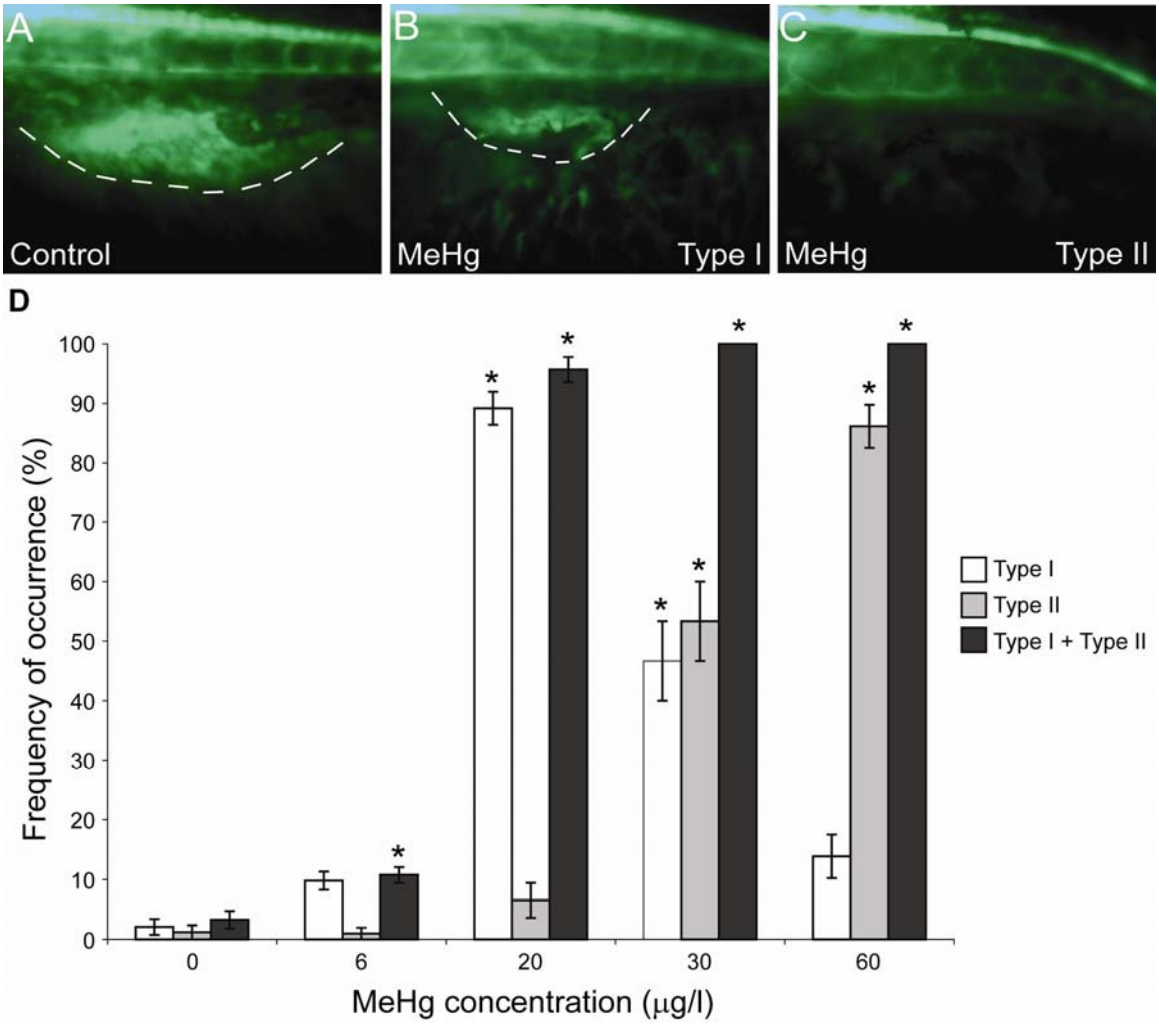

Fig. 3.16 Reduction or loss of GFP expression at the caudal fin primordium of MeHg-exposed embryos.

Lateral views of the primordium of the caudal fin of 72 hpf embryos are shown. (A) Control; (B, C) MeHg-treated embryos. Depending on the degree of reduction or loss of GFP expression at the primordium, embryos were classified either as type I when they displayed a smaller GFP expression domain (B) in comparison to control (A) or as type II when the GFP expression was completely absent (C). (D) Graph showing the frequency of occurrence of type I (white bar) and type II (gray bar) or type I plus type II (black bar) reduction or loss of GFP expression at the caudal fin primordium. Embryos were exposed to 0, 6, 20, 30 and 60 µg/l MeHg. MeHg concentration of 6 µg/l could already lead to a significant increase in the number of embryos with reduced GFP expression. At 60 µg/l, almost all of the treated embryos fell into the type II reduction. Mean ± SEM are reported. N = 6, 20 embryos each. Type I: ANOVA, $F = 94.51$ and Dunnett, $p < 0.01$ (*); type II: ANOVA, $F = 108.1$ and Dunnett, $p < 0.01$ (*); type + type II: ANOVA, $F = 1601$ and Dunnett, $p < 0.01$(*).

3.4.4 Critical period of MeHg exposure lying between 12 hpf and 48 hpf

In order to address the critical period of MeHg exposure, zebrafish embryos were exposed to 60 µg/l MeHg at different time windows for 6 or 12 hours during embryonic development from 4 to 72 hpf, and the occurrence of the phenotype was assessed at 6 dpf at which the melanophore stripe in the tail region is well-defined (Kelsh *et al*., 1996). No significant change in number of larvae having a smaller gap of the melanophore stripe in the tail was observed when treated before 12 hpf while significant increases were observed in all the time windows afterwards (Fig. 3.17). However, no obvious difference was noted among the time windows in between 12 to 48 hpf. Comparison of the frequency distribution of pigmentation disruption also indicated that the longer the duration of exposure the more the embryos were affected as, in general, embryos exposed to MeHg for 12 hours resulted in higher frequency of occurrence of the phenotype than those for 6 hours. Hence, I concluded that the critical period of MeHg exposure started from 12 hpf and the longer the duration of exposure the stronger the phenotype.

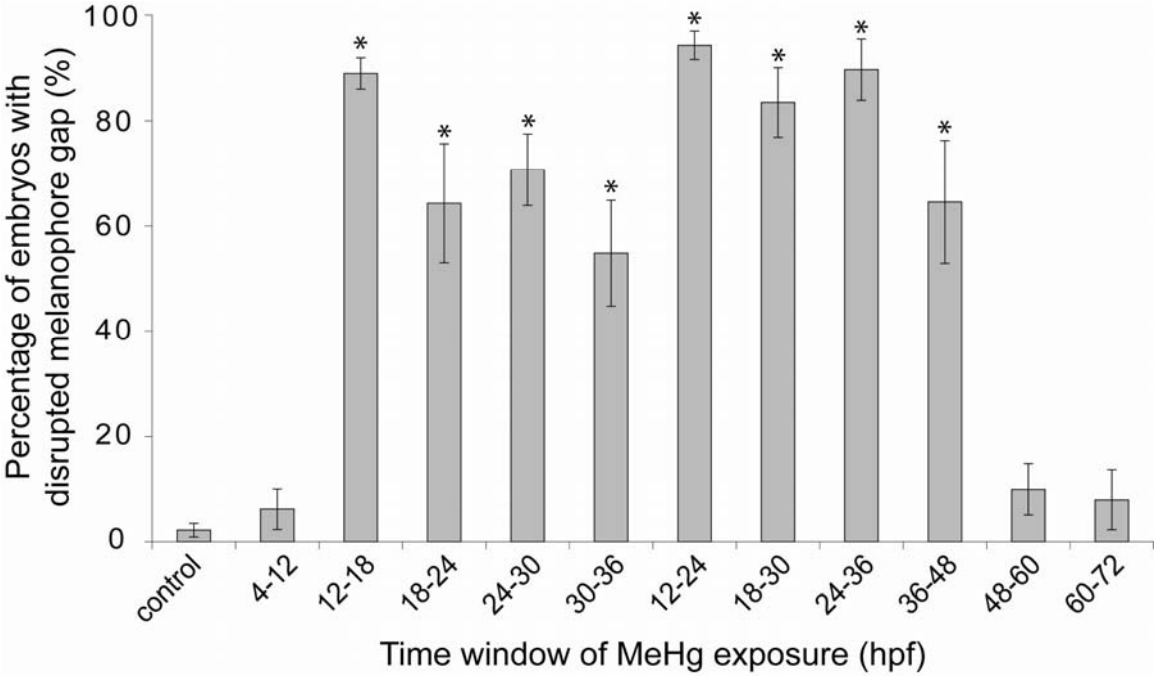

Fig. 3.17 Disruption of melanophore gap in embryos exposed to MeHg for all the time windows within 12 and 48 hpf.

Embryos were treated with MeHg for 6- or 12-hour-periods between 4 and 72 hpf (n = 5, 20 embryos each). The percentage of occurrence of disrupted melanophore gap in the tail region of embryos exposed to different time windows of MeHg is presented. The mean ± SEM are reported. Significant differences were noted in all the time windows within 12 and 48 hpf, but not in those before 12 or after 48 hpf. ANOVA, $F = 30.11$; Dunnett adjustment, $p < 0.01$ (*).

3.4.5 Slight increase in the number of apoptotic cells in the caudal fin fold and no rescue of caudal fin fold abnormality by inhibition of apoptosis

No information on the mode of action how MeHg causes this phenotype is available. As the size of the caudal fin fold of MeHg-treated embryos was smaller than that of the control, I speculated that MeHg-induced cell apoptosis might be the cause of the caudal fin fold abnormality. The ISH analysis indicated that there was a slight up-regulation of *tumor protein p53* (*p53*), which is one of the key mediators of apoptosis, in the caudal fin fold (Fig. 3.18 A, B). To verify any increase in apoptosis, MeHg embryos were stained with acridine orange (AO) which detects DNA denaturation (Fig. 3.18 C-C", D-D"). There was a very slight increase in the number of AO-positive cells in the tip of the caudal fin fold in MeHg-treated embryos. To confirm the result of AO staining, apoptosis was examined by determining activation of

Caspase-3 (Casp3), which is important for the initiation of apoptosis (Nicholson, 1995, Nicholson, 1997). Similarly, the number of Casp3-activated cells increased slightly in the caudal fin fold of embryos exposed to MeHg (Fig. 3.18 E-E", F-F").

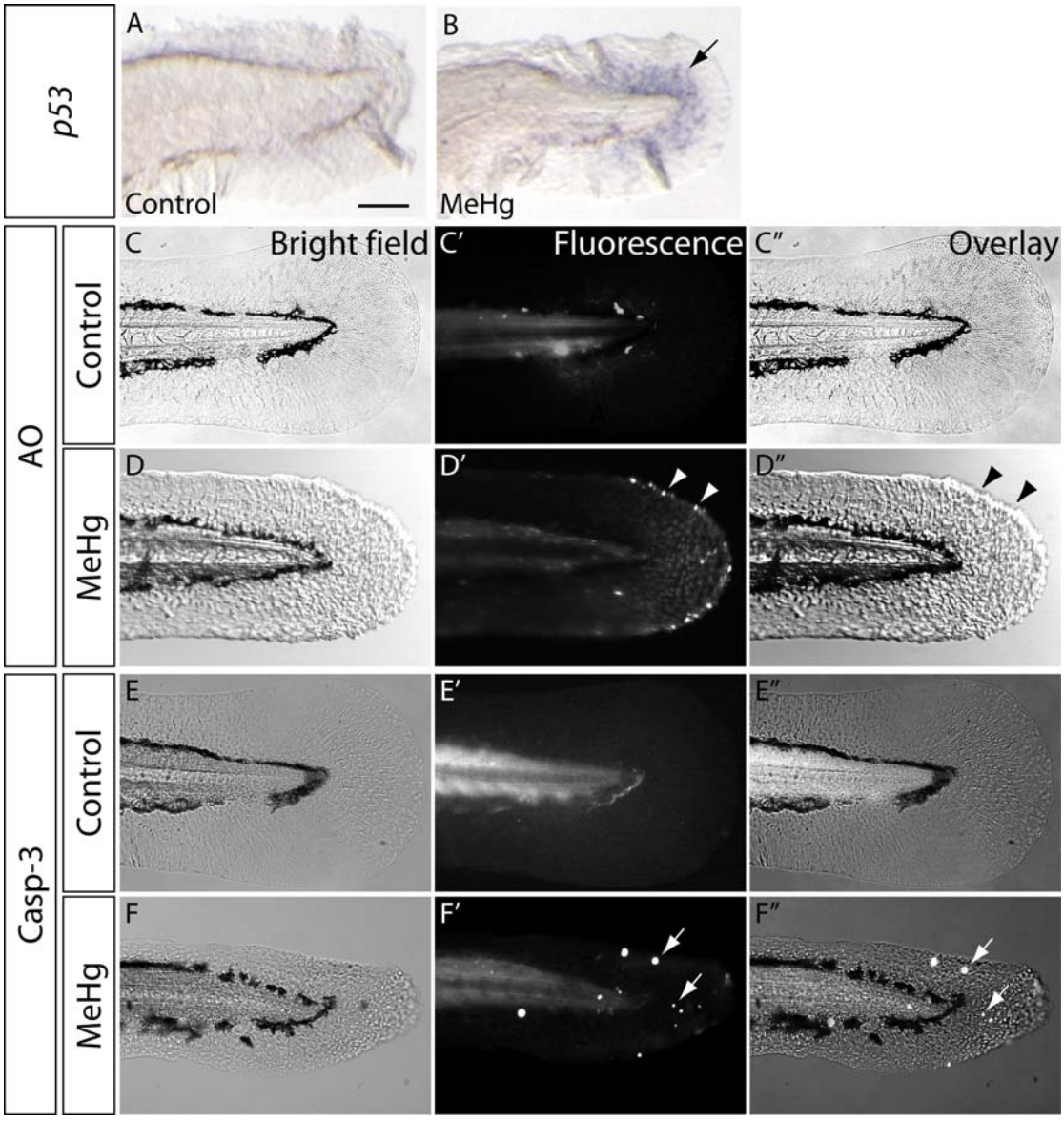

Fig. 3.18 Slight increase in the number of apoptotic cells in the caudal fin fold.

The caudal fin folds of 72-hpf-old control (A, C-C", E-E") and MeHg-treated (B, D-D", F-F") zebrafish embryos stained with *in situ* hybridisation using probe complementary to *p53* (A, B), acridine orange (AO) (C-C", C-C") and immunohistochemistry using antibody against Casp3 (E-E", F-F") are shown. (A, B, C, D, E, F) Bright field images; (C', D', E', F') fluorescence images; (C", D", E", F") overlay images. (A, B) Moderate increase in the mRNA expression level of *p53* (B, black arrow) was observed in the caudal fin fold of MeHg-treated embryos. Slight increases in the number of AO-positive cells (D' and D", arrowheads) and Casp3-positve cells (F' and F", white arrows) were also detected in the caudal fin folds after exposure to MeHg. Scale bar, A, B, 140 µm , C-C'' – F-F'', 75 µm.

Since a slight increase in apoptosis was observed in the MeHg-treated embryos, I examined if inhibition of apoptosis could rescue the caudal fin fold abnormality. Knockdown of *p53* by microinjection of morpholino (MO) into zebrafish embryos was performed to inhibit apoptosis (Ekker *et al.*, 2001; Robu *et al.*, 2007). The *p53* morphants (morpholino treated organisms) were then treated with MeHg and the occurrence of caudal fin fold abnormality was assessed at 72 hpf. No rescue of the caudal fin fold abnormality by knockdown of *p53* was observed in MeHg-treated embryos (Fig. 3.19).

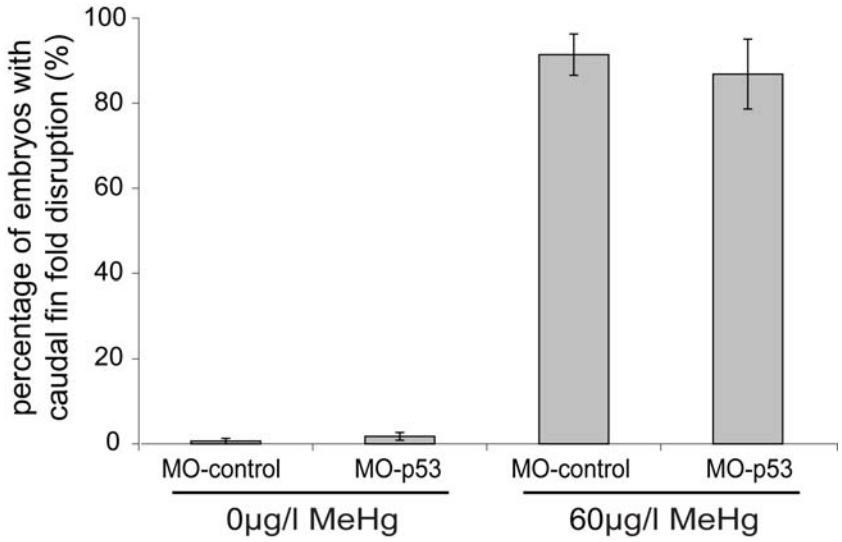

Fig. 3.19 No rescue of MeHg-induced caudal fin fold disruption in *p53* morphants.
Embryos were microinjected with *p53* morpholino (MO-p53) and then exposed to 60 µg/l MeHg. Control groups with the replacement of MO-p53 with water were set up. No significant difference between the *p53* knockdown group and the control group was detected. The mean ± SEM are reported (n = 9, 20 embryos each).

I concluded here that MeHg treatment could induce moderate increase in the expression level of *p53* and a slight increase in the number of apoptotic cells in the caudal fin fold while no rescue of the caudal fin fold abnormality was observed in embryos having inhibited *p53*-dependent apoptosis.

3.4.6 Involvement of *mmp9* and *mmp13a* in the induction of caudal fin malformation in MeHg-treated embryos

To unravel the underlying mechanism through which MeHg induces the caudal fin fold phenotype, I screened the MeHg-regulated genes to look for candidate genes which were ectopically expressed in the tail after MeHg exposure. *matrix metalloproteinase 9* (*mmp9*) and *matrix metalloproteinase 13a* (*mmp13a*) seemed to be two of the good candidates since they were strongly and restrictedly expressed in the caudal fin fold of MeHg-treated embryos (Yang, 2007; Fig. 3.20 B, G), and they were able to degrade the components of the collagenous extracellular matrix (ECM), which is one of the major components of the caudal fin fold (Dane and Trucker, 1985).

Matrix metalloproteinases (*Mmp*s) are a family of over twenty zinc-dependent endopeptidases. They play important roles in normal development and pathogenesis through the degradation of ECM components (Lemaître and D'Armiento, 2006; Page-McCaw *et al*., 2007; Stamenkovic, 2003; Vu and Werb, 2000). *mmp9*, also known as gelatinase B, is responsible for degrading gelatins and collagen type IV, and *mmp13a*, also known as collagenase-3, is responsible for cleaving collagen type I, II and III (Chakraborti *et al.*, 2003; Wyatt *et al.*, 2009).

3.4.6.1 Specific ectopic *mmp9* and *mmp13a* expression in the caudal fin of embryos exposed to MeHg

As I wanted to know if such the induction is specific to MeHg or is a more general response to heavy metals, ISH using *mmp9* and *mmp13a* probes were performed on embryos exposed to Pb, As and Cd. Interestingly, although up-regulation of *mmp13*a was observed in scattered cells in the tail of embryos treated with Pb, As and Cd, no ectopic expression of *mmp9* or *mmp13a* was induced in the caudal fin fold of these embryos (Fig. 3.20).

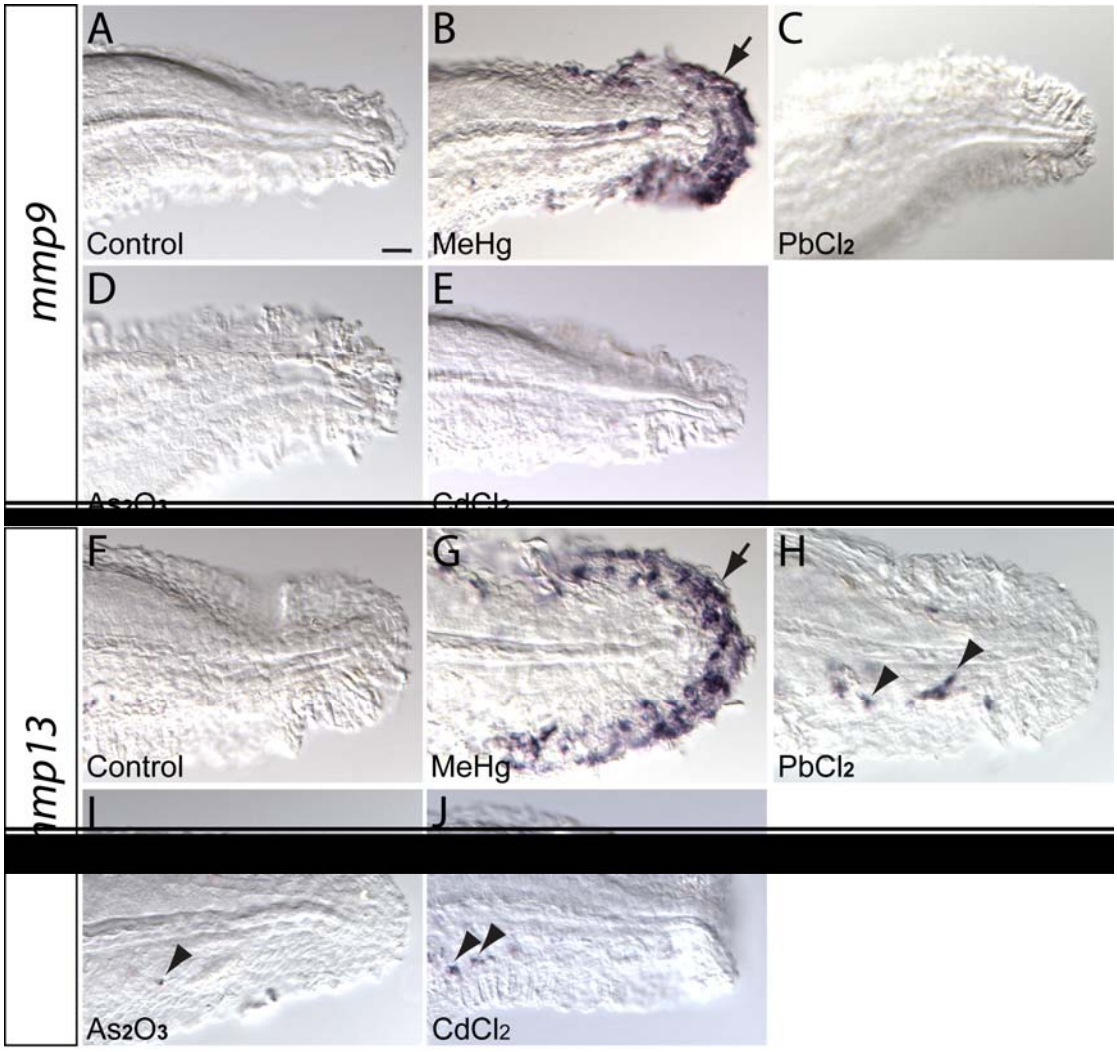

Fig. 3.20 Specific inductions of *mmp9* and *mmp13a* in the caudal fins of embryos exposed to MeHg. Later views of the tip of the tail region of embryos at 72 hpf are showed. *In situ* hybridisation was performed using RNA probes against *mmp9* (A-E) and *mmp13a* (F-J) on control (A, F), MeHg- (B, G), lead chloride ($PbCl_2$)- (C, H), arsenic oxide (As_2O_3)- (D, I) and cadmium chloride ($CdCl_2$)- (E, J) treated embryos. (B, G) Ectopic expressions of *mmp9* and *mmp13a* were induced in the caudal fin fold in embryos exposed to MeHg (arrows). (C-D) No ectopic expression of *mmp9* was induced in the caudal fin fold of embryos exposed to other heavy metals examined. (H-J) Although ectopic expression of *mmp13a* was detected in the tail of $PbCl_2$, As_2O_3 and $CdCl_2$ (arrow heads), no ectopic expression was observed in the caudal fin fold of these embryos. Scale bar, 50 μm.

3.4.6.2 No ectopic expression of myeloid genes in the caudal fin fold of MeHg-treated embryos

Both *mmp9* and *mmp13a* have been reported to be expressed in various cell types including myeloid cells during embryonic development and wound healing in zebrafish (Qian *et al.*, 2005; Yoong *et al.*, 2007; Zhang *et al.*, 2008). In order to

examine if the presence of *mmp9*- and *mmp13a*-expressing cells in the caudal fin fold in MeHg-treated was a result of an inflammatory response, I compared the expression patterns of the macrophage markers *draculin* (*drl*; NM_130977) and *lymphocyte cytosolic plastin 1* (*lcp1*; NM_131320), and the neutrophil marker *myeloid-specific peroxidase* (*mpx*; NM_212779) (Bennett *et al.*, 2001; Herbomel *et al.*, 1999) with those of *mmp9* and *mmp13a*. As shown by the result of ISH, no ectopic expression of any of these myeloid genes in the caudal fin fold was observed (Fig. 3.21), suggesting that the ectopic expression of *mmp9* and *mmp13a* in the caudal fin fold was not because of an inflammatory response.

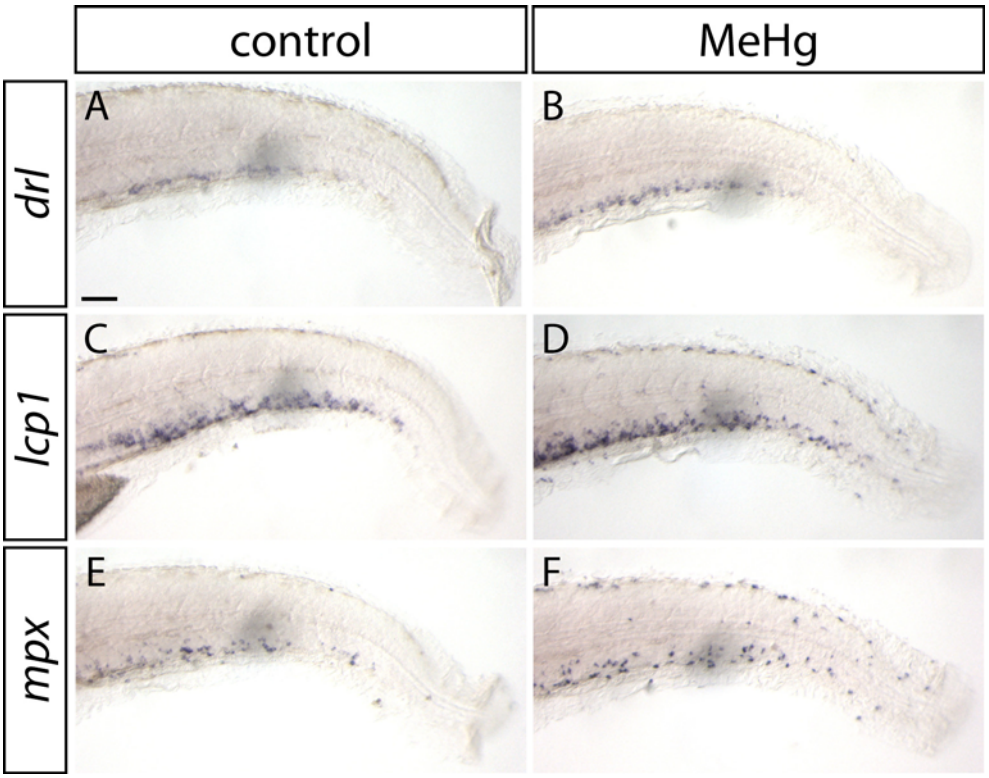

Fig. 3.21 No ectopic expression of myeloid genes at the caudal fin fold of MeHg-treated embryos. Later views of the caudal fins of 72-hpf-old embryos are shown. *In situ* hybridisation was performed using probes complementary to *drl* (A, B), *lcp1* (C, D) and *mpx* (E, F) on control (A, C, E) and MeHg-treated (B, D, F) embryos. None of the myeloid genes examined showed an ectopic expression in the caudal fin fold (arrows). Scale bar, 75 μm.

3.4.6.3 Increased Mmp activity in MeHg-treated embryos

In order to examine if an increase in *mmp9* and *mmp13a* transcript levels would result in an increase in Mmp9 and Mmp13a activity, *in vitro* Mmp activity assays, which

have been shown to be an effective mean for determining Mmp activity (collagenase activity) quantitatively (Crawford and Pilgrim, 2005), were performed. Fluorescein-conjugated collagen was used in the assay and would emit fluorescent signals upon degradation, serving indicators of collagenase activities. Protein lysates were extracted from control and MeHg-treated zebrafish embryos at 72 hpf and added to the fluorescein-conjugated collagen and incubated with the collagen substrate up to 3 hours. The result of the assays showed that a much higher level of fluorescent signals was detected in the MeHg-treated samples than in the controls, indicating that the Mmp activity was highly increased in embryos treated with MeHg (Fig. 3.22).

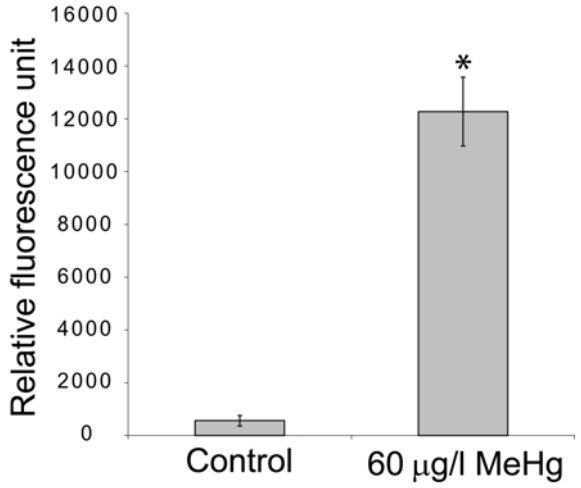

Fig. 3.22 Up-regulation of Mmp activity in embryos exposed to MeHg.
The fluorescent intensities emitted from the mixtures of fluorescein-conjugated collagen together with the protein lysate of control or MeHg-treated embryos were measured. Significant increase in fluorescent signal and thus Mmp activity was detected in protein lysates of MeHg-treated embryos. The mean ± SEM are reported. T-test, $p < 0.05$ (*).

3.4.6.4 Partial rescue of the MeHg-induced caudal fin phenotype by inhibition of Mmp activity

The specific expression of *mmp9* and *mmp13a* in the disrupted caudal fin fold in MeHg-treated embryos led to the speculation that *mmp9* and *mmp13a* are responsible for the caudal fin fold abnormality. To examine the involvement of Mmp9 and Mmp13a in the disruption of the caudal fin fold tissue with a pharmacological approach. I co-treated embryos with MeHg and GM 6001, a general Mmp inhibitor, or MMP-9/MMP-13 Inhibitor II, a Mmp9 and Mmp13 specific inhibitor (Bai *et al.*, 2005; Yoshinari *et al.*, 2009). Negative controls in which embryos were exposed to

MeHg and null controls in which embryos were incubated in embryo culture medium only were set up as well. At 72 hpf, the embryos were assessed for the phenotype. To quantify the measurement, images of the embryos were taken, and on each of the images, a vertical line was drawn through the tip of the notochord and the fin fold area posterior to the line was measured (Fig. 3.23 A-D). The result showed that inhibition of Mmp activitiy by GM 6001 and MMP-9/MMP-13 Inhibitor II could increase the fin fold area by 18 and 25%, respectively, relative to embryos treated with MeHg (Fig. 3.23 E).

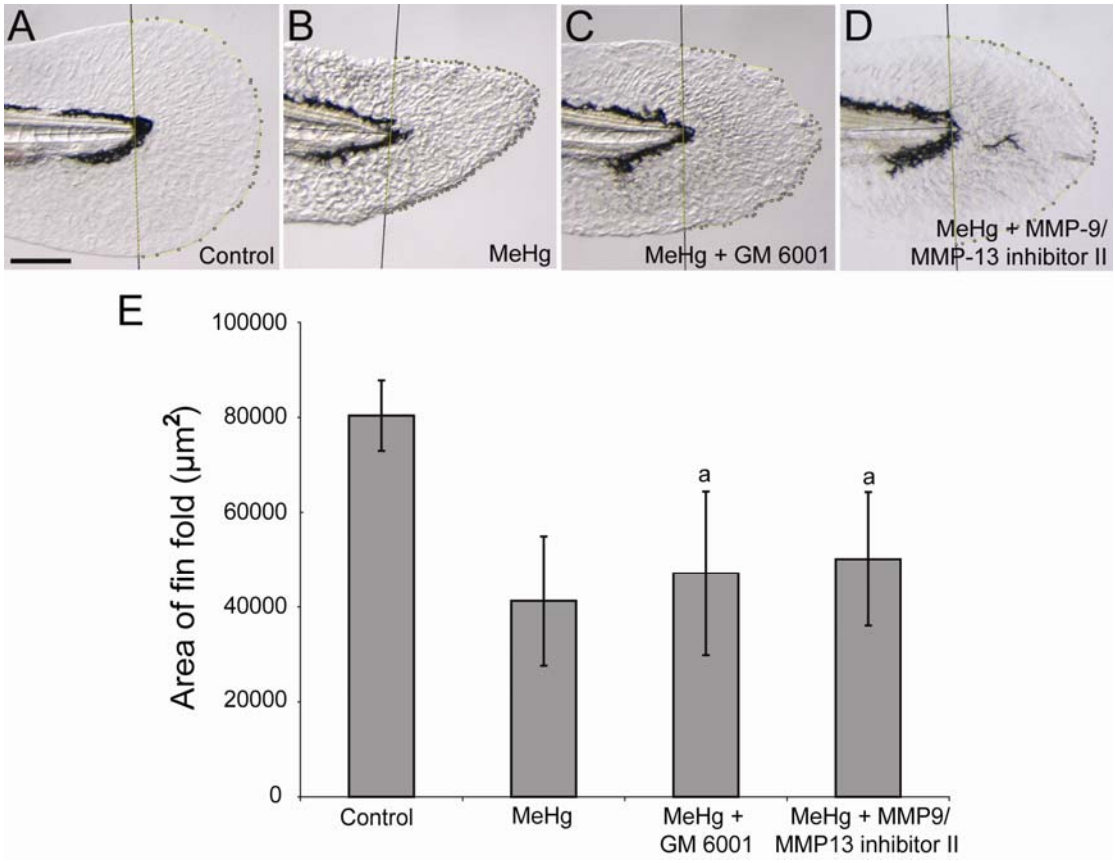

Fig. 3.23 Partial rescue of the MeHg-induced caudal fin phenotype by inhibition of Mmp activity. Lateral views of the tip of tails of control (A), MeHg-treated (B), MeHg- and GM 6001-co-treated (C), MeHg- and MMP-9/MMP-13 Inhibitor II-co-treated (D) embryos at 72 hpf. (E) Partial rescue of the MeHg-induced caudal fin phenotype by inhibition of Mmp activity was determined by quantitative measurement. The area of the caudal fin tip was quantified by drawing a vertical line through the tip of the notochord and counting the fin fold area posterior to the line. The presence of Mmp inhibitors increased the fin fold area by 18 and 25% relative to embryos treated with MeHg. The mean of the area of the fin fold from 86 to 92 measurements in four independent experiments and the SEM are presented. Bars marked with the letter ‘‘a’’ are not significantly different from each other. ANOVA, $F = 150.9$; Bonferroni, $p < 0.05$. Scale bar, 100 µm.

3.4.7 Induction of the gene expression in the caudal fin fold

Besides *mmp9* and *mmp13a*, some other genes were also shown to be up-regulated in the caudal fin fold region in this toxicogenomic screen and it included *apolipoprotein eb (apoeb), core promoter element binding protein (copeb), CXC chemokine 46-like (cxc46l), homeodomain leucine zipper gene (homez), jun B proto-oncogene (junb), matrix metalloproteinase 14a (mmp14a), NADPH oxidase organizer 1 (noxo1), PR domain containing 1a, with ZNF domain (prdm1a), sequestosome 1 (sqstm1), serum/glucocorticoid regulated kinase 1 (sgk1), suppressor of cytokine signaling 3a (socs3a), sp9 transcription factor (sp9), thioredoxin-like (txnl), uncoupling protein 1 (ucp1), zgc:56382, AI397362, AW115990* and *BM101698* (Fig. 3.24). The ectopic expression of these genes in the fin fold region suggested that these genes may also contribute to the fin fold phenotype.

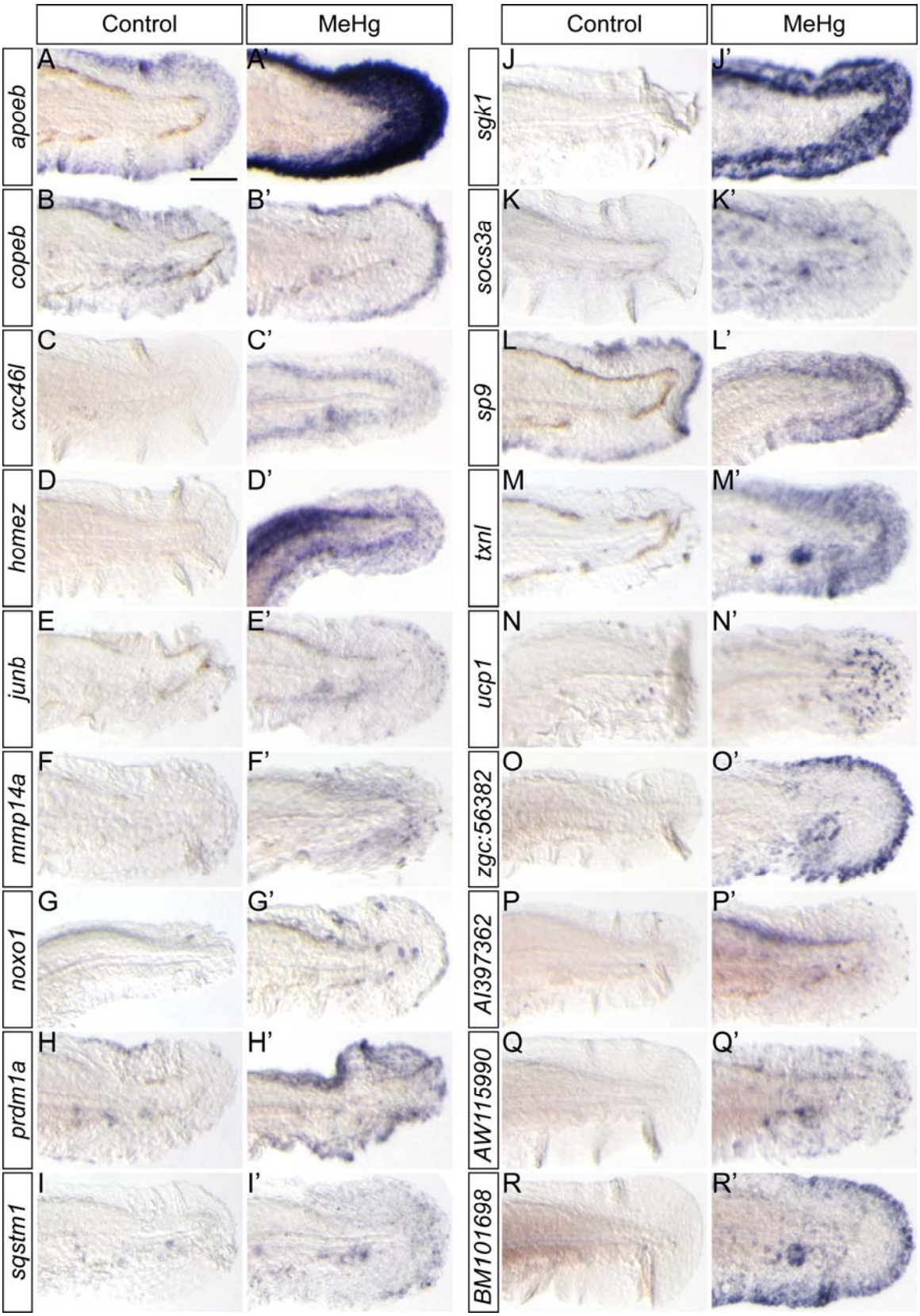

Fig. 3.24 Genes showing ectopic expression in the caudal fin fold after MeHg exposure.

Lateral views of the posterior part of the tail of 72 hpf zebrafish embryos stained by *In situ* hybridisation are shown. Eighteen genes including *apoeb* (A, A'), *copeb* (B, B'), *cxc46l* (C, C'), *homez* (D, D'), *junb* (E, E'), *mmp14a* (F, F'), *noxo1* (G, G'), *prdm1a* (H, H'), *sqtm1* (I, I'), *sgk1* (J, J'), *socs3a*

(K, K'), *sp9* (L, L'), *txnl* (M, M'), *ucp1* (N, N'), *zgc:56382* (O, O'), *AI397362* (P, P') *AW115990* (Q, Q') and *BM101698* (R, R') were observed to be ectopically expressed in the caudal fin fold of zebrafish embryos treated with MeHg. Scale bar, 50 μm.

3.4.8 Summary

MeHg could induce the loss of the gap in the melanophore stripe, disruption of the caudal fin growth zone and destruction of the caudal fin fold. The disruption of the melanophore stripe by MeHg is restricted to a time window between 12 and 48 hpf. MeHg could induce the specific loss of the GFP expression in caudal fin growth zone in the transgenic line *Tg(-2.4shha-ABC:GFP)sb15*, and such a disruption could be induced in a significant number of embryos even in a MeHg concentration as low as 6 μg/l. Although there was a slight increase in the number of apoptotic cells in the caudal fin region, no rescue of the caudal fin tissue destruction was observed when apoptosis was inhibited, excluding the possibility that apoptosis is the major cause of caudal fin fold tissue disruption. Twenty-two genes have been shown here to be expressed ectopically in the caudal fin fold of MeHg-treated embryos. Among these genes, *mmp9* and *mmp13a* were further shown to be ectopically and specifically expressed in MeHg-exposed embryos. Pharmacological inhibition of *mmp9* and *mmp13a* could rescue partially the caudal fin phenotype induced by MeHg, suggesting a role for these two ECM regulation genes in causing the caudal fin tissue disruption.

3.5 Study of *complement component 7-1 (c7-1)*

3.5.1 Ectopic expression of *c7-1* in the retina of MeHg-treated embryos

I further examineed the gene *complement component 7-1* (*c7-1*, BC100054*)* due to its specific ectopic expression induced by MeHg. After MeHg exposure, *c7-1* was found to be up-regulated in MeHg-exposed embryos by ISH. It was expressed ectopically in the retina, expecially the inner nuclear layer (INL), in 72-hpf-old zebrafish embryos after MeHg treatment (Fig. 3.25).

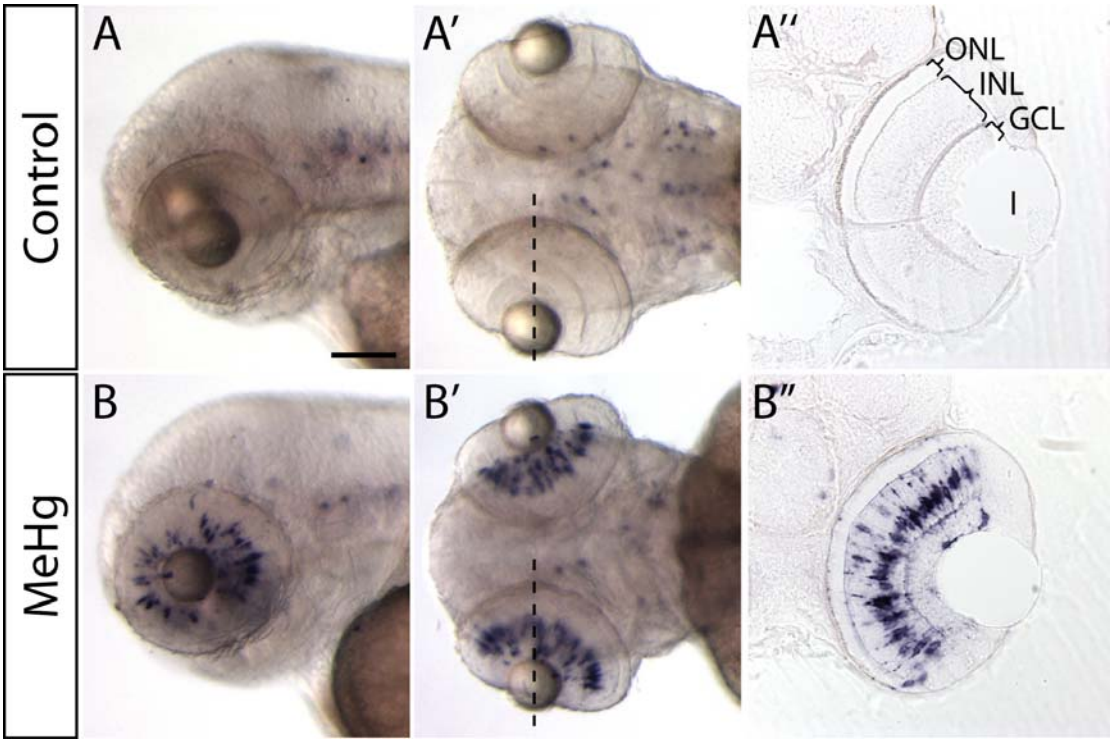

Fig. 3.25 Ectopic expression of *complement component 7-1* in the retina of MeHg-exposed embryos. Lateral views of the heads (A, B), dorsal views of the heads (A', B') and longitudinal sections of the eyes (A'', B'') of control (A-A'') and MeHg-treated (B-B'') embryos at 72 hpf are shown. The dashed lines in A' and B' indicate the position of the sections in A'' and B'', respectively. (B-B'') Ectopic expression of *complement component 7-1 (c7-1*) was detected mostly in the inner nuclear layer of the retina of the embryos exposed to MeHg. Abbreviations, GCL, ganglion cell layer; INL, inner nuclear layer; l, lens; ONL, outer nuclear layer. Scale bar, A, A', B, B', 75 μm, A'', B'', 135 μm.

3.5.2 No ectopic expression of other membrane attack complex complement components genes in the retina after MeHg treatment

C7 is a member of the complement system and it works together with other complement proteins to trigger the immune response (Kondos *et al.*, 2010). Activation of the complement system will lead to the formation of C5b by proteolytic cleavage of C5, and C5b will initiate the sequential binding of C6, C7, C8 and multiple C9 proteins, generating a trans-membrane structure called membrane attack complex (MAC). MAC will create a pore on the membrane of invading pathogens and abnormal cells, leading to subsequent lysis and death of the target cells. It can also lead to activation of various biological responses, such as secretion, adherence, aggregation, chemotaxis and cell division, at sub-lytic doses (reviewed in Morgan, 1989).

As C7 will cooperate with other complement components to form the MAC as an immune response, I wanted to know if expression of other genes that encode proteins which are involved in the initiation and formation of the MAC would also be induced in the retina after MeHg exposure. I wanted to examine this question by whole mount ISH. However, as the complement systems in zebrafish have not yet been well characterised, I performed a database search to obtain the information of other complement components for making RNA probes (Cates, 2006). From the database, I could identify all the zebrafish MAC forming genes, the MAC initiation gene and another *c7* homologue in zebrafish, *c7-2*. Based on the database information, I designed primers for amplifying the genes for making RNA probes and performed whole-mount ISH for the genes *c5-1* (BC139862), *c6* (NM_200638), *c7-2* (XM_685854) *c8a* (NM_001003496), *c8b* (NM_001332783) and *c8g* (BC062865) and *c9* (NM_001024435) (Fig. 3.26). However, none of the genes examined showed any ectopic expression in the retina of MeHg-treated embryos.

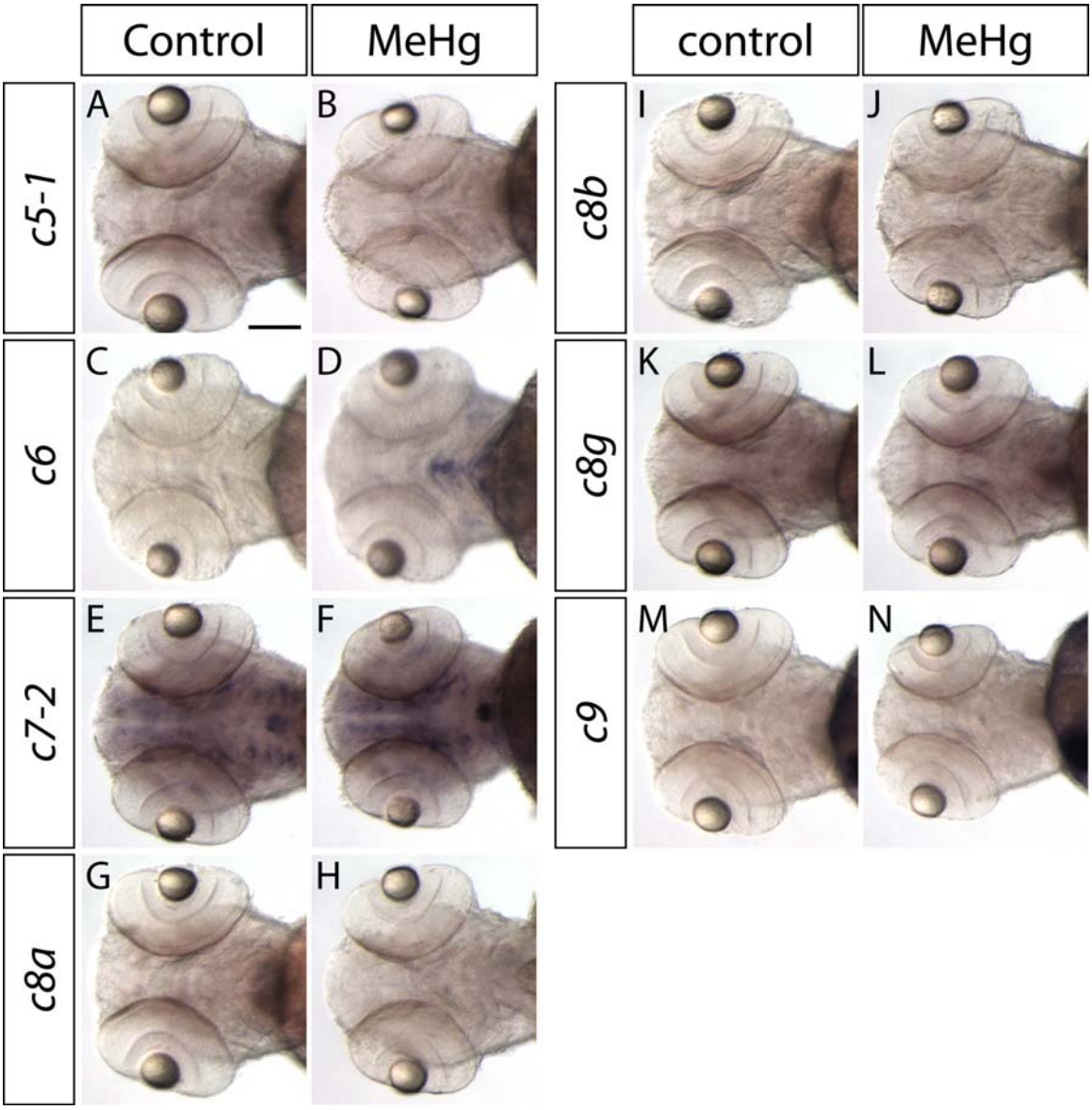

Fig. 3.26 No ectopic expression of other membrane attack complex complement components in the retina of embryos exposed to MeHg.

In situ hybridisation was performed using antisense RNA probes complementary to other membrane attack complex complement components including *c5-1* (A, B), *c6* (C, D), *c7-2* (E, F), *c8a* (G, H), *c8b* (I, J), *c8g* (K, L) and *c9* (M, N). Dorsal views of the head regions of control (A, C, E, G, I, K, M) and MeHg-treated (B, D, F, H, J, L, N) embryos at 72 hpf are shown. (B, D, F, H, J, L, M) Ectopic expression of other complement components involved in the initiation or formation of MAC was not observed in the retina of embryos treated with MeHg. Scale bar, 75 μm.

3.5.3 Expression of *c7-1* in scattered cells in the hindbrain, midline, trunk and tail during embryonic development

In order to have a better understanding of zebrafish *c7-1*, a study of the expression pattern of *c7-1* during development was performed by whole-mount ISH (Fig. 3.27). Results of ISH showed that *c7-1* expression was detected in the yolk and yolk sac extension of the embryo at 24 hpf. At 48 hpf, the expression pattern became more restricted and it was expressed in discrete cells in the ventral hindbrain close to the midline. At 72 hpf, *c7*-expressing cells were detected in the hind- and midbrain in a rather symmetrical manner. The transcripts were also detected in two rows of cells in the trunk and tail with one immediately above the notochord and another one more dorsally located.

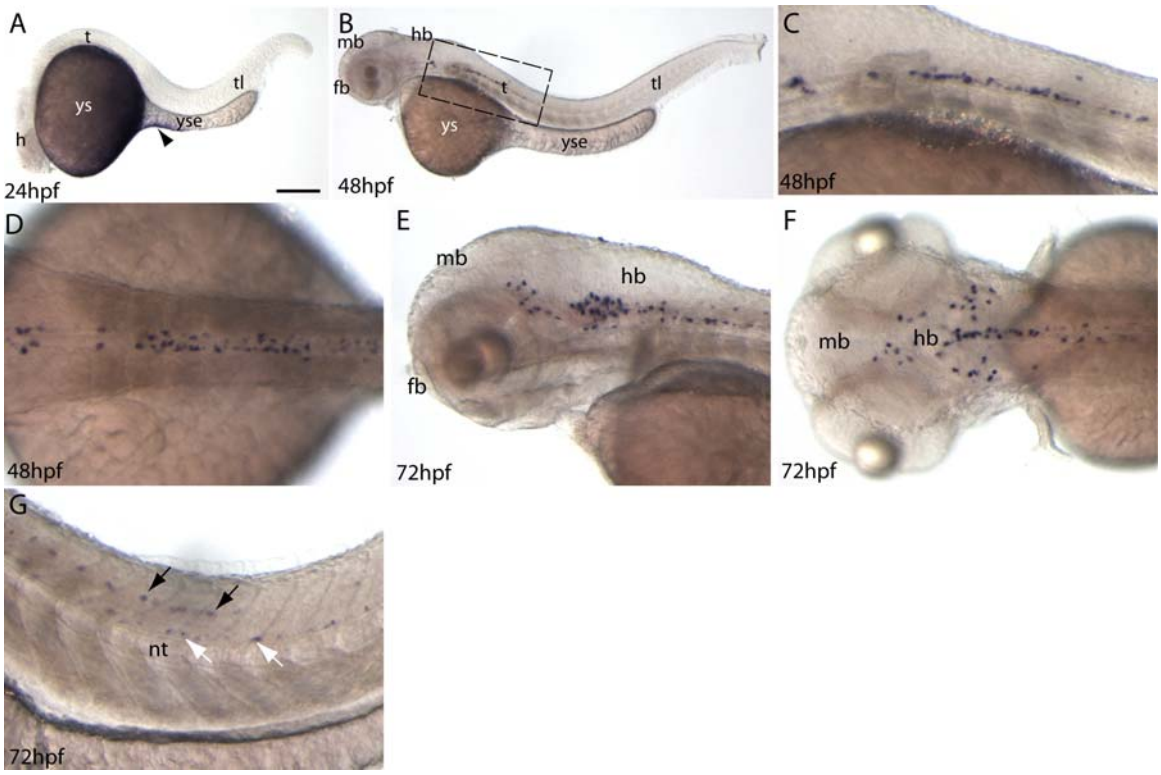

Fig. 3.27 Expression patterns of *c7-1* during development.

Lateral views (A, B, C, E, G, H) and dorsal views (D, F) of embryos stained by *in situ* hybridisation with *c7-1* probe. (C, D) Magnified images of the region boxed in (B). (A) 24 hpf; (B, C, D) 48 hpf; (E-H) 72-hpf-old zebrafish embryos. (A) The expression of *c7-1* could be detected at 24 hpf in the yolk and yolk sac extension (arrowhead). (B) The expression of *c7-1* faded out in the yolk but became localised to the ventral hindbrain at 48 hpf. (C, D) The transcripts were noted in discrete cells that reside in the ventral hindbrain close to the midline (asterisk). (E, F) By 72 hpf, *c7*-expressing cells were detected in the hind- and mid-brain in a rather symmetrical manner. The transcripts were also detected

in two rows of cells in the trunk (G) and tail (H) with one immediately above the notochord (white arrows) and another one more dorsally located (black arrows). Abbreviations, h, head; hb, hindbrain; mb, midbrain; nt, notochord; t, trunk; tl, tail; ys, yolk sac; yse, yolk sac extension. Scale bar, A, B, 200 μm, C-H, 80 μm.

3.5.4 No ectopic expression of myelin marker genes in the retina after MeHg exposure

Interestingly, the developmental expression pattern of *c7-1* resembles those of genes which encode proteins forming the major structural components of myelin sheath, such as *myelin basic protein* (*mbp*), *myelin protein zero* (*mpz*), *myelin associated glycoprotein* (*mag*) and *proteolipid protein 1b* (*plp1b*) (Brösamle and Halpern, 2002; Lyons *et al.*, 2005; Thisse *et al.*, 2008). Myelin sheath is a layer of dielectric material wrapping around the axons of many neurons. It helps to increase the speed of electric impulses propagation along the myelinated fiber and is essential for proper functioning of the nervous system. In the CNS, axons are wrapped by the membrane of cells called oligodendrocytes to form myelin sheaths while in the peripheral nervous system (PNS), axons are myelinated by specialised glial cells called Schwann cells (Arroyo and Scherer, 2000). Disruption of myelin sheaths affects conduction and health of myelinated CNS and PNS axons, and has been reported to cause neurological disorders in human, including multiple sclerosis (MS) and Charcot-Marie-Tooth diseases (CMT) (Bjartmar *et al.*, 1999; Zhou and Griffin, 2003).

The similar developmental expression patterns of these genes drove us to examine if the myelin proteins would also show an ectopic expression in the retina after MeHg exposure and try to get some clues whether the ectopic *c7-1* expression of in the retina of MeHg-treated embryos is due to ectopic formation of myelin in the retina. I addressed this question by performing whole mount ISH using probes complementary to the two myelin marker genes, *mpz* (NM_194361) and *plp1b* (NM_001005586), on MeHg-exposed embryos. However, no such an ectopic expression in the retina was induced in any of the myelin marker genes examined (Fig. 3.28).

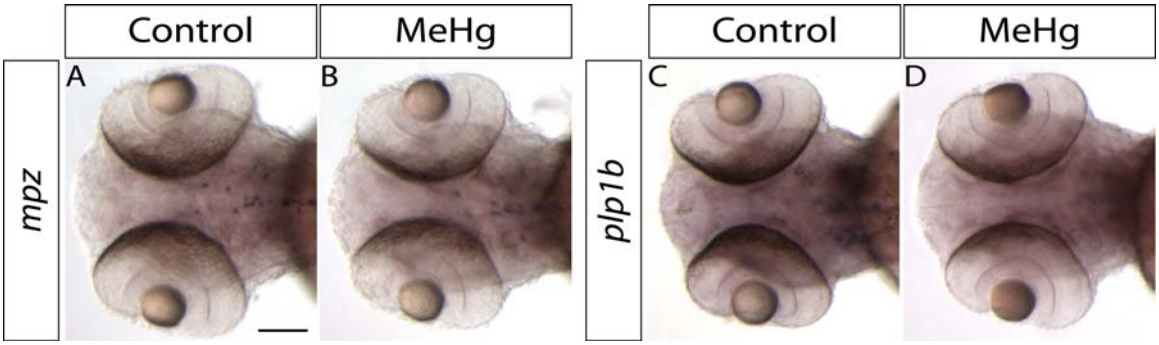

Fig. 3.28 No ectopic expression of *mpz* and *plp1b* in the eyes of embryos exposed to MeHg.
Whole mount ISH was performed using antisense probes complementary to *mpz* (A, B) and *plp1b* (C, D). Dorsal views of the head regions of control (A, C) and MeHg-treated (B, D) embryos at 72 hpf are shown. (B, D) No ectopic expression of the two myelin genes was detected in the retina of MeHg-treated embryos. Scale bar, 65 μm.

3.5.5 Functional study of *c7-1*

Both *in vitro* and *in vivo* data indicated that the C5b-C9 complex could have dual role on causing neuroinflammation and neuroprotection (Morgan *et al.*, 1997; Rus *et al.*, 2005, 2006; van Beek *et al.*, 2003). On one hand, it can induce demyelination, a process of destructive removal of the myelin sheaths from neurons, and complement is believed to cause multiple sclerosis (MS), an autoimmune nervous system disease in which the myelin producing oligodendrocytes are damaged due to abnormal immune response of the body as deposition of complement was found in MS lesions (Storch *et al.*, 1998; Compston *et al.*, 1989). However, genome screens in MS indicated that there is no evidence for the association of C7 with MS (Chataway *et al.*, 1999). On the other hand, the C5b-C9 complex has also been shown to help axon preservation or repair, limitation of glial scarring, remyelination, and protection from cell death within the CNS (Cudrici *et al.*, 2006; Tegla *et al.*, 2009). In human, Complement C7 deficiency (C7D) is frequently associated with the life-threatening meningococcal disease caused by the bacterium Neisseria meningitides infection (Barroso *et al.*, 2010; Kang *et al.*, 2006; O'Hara *et al.*, 1998; Rameix-Welti *et al.*, 2007).

Due to the specific induction of *c7-1* by MeHg exposure, I wanted to know what the function of *c7-1* is during development and under MeHg exposure, and why only *c7-1,* but not other complement components, is ectopically expressed in the retina of

MeHg-exposed embryos. I tried to gain some insights in answering these questions by knocking down *c7-1* in zebrafish embryos with a splice blocking MO, which blocks mRNA processing and thus the gene function by disrupting pre-mRNA splicing (Draper *et al.*, 2001).

To verify the effectiveness of MO-c7-1, mRNA was extracted form the *c7-1* morphants and PCR using primers targeting the exons flanking the splicing site was performed. MO-c7-1 was predicted to cause a deletion of the proximal exon (Morcos, 2007) and would result in the formation of a shorter mRNA. A PCR fragment with smaller size was observed in the MO-c7-1 but not in MO-control samples, indicating that the MO-c7-1 can block the splicing of the gene effectively (Fig. 3.29).

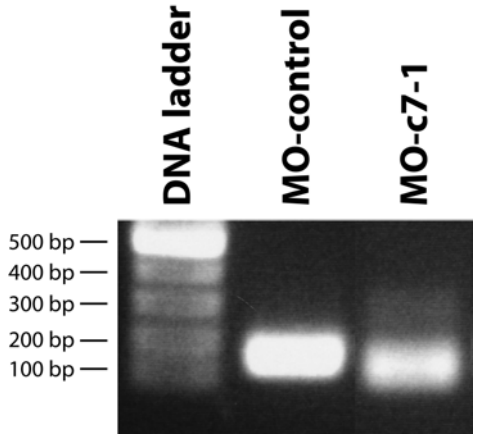

Fig. 3.29 Effective blocking of *c7-1* by morpholino MO-c7-1.
Gene rule DNA ladder mix (lane 1) was used as a marker to indicate the size of the PCR fragments. PCR fragments from MO-control (lane 2) and MO-c7-1 (lane 3) samples. A smaller DNA fragment was observed in the MO-c7-1 sample compared to the MO-control, indicating the *c7-1* splicing defects.

To examine if *c7-1* performs any function during development, MO-c7-1 and MO-control were microinjected into zebrafish embryos at zero- to two-cell stages and any malformation in the embryos were monitored during development. However, no observable difference was noticed in the *c7-1* morphants and control embryos (Fig. 3.30 A, B). I speculated that *c7-1* would show its function only under MeHg exposure. Thus, I subjected the MO-injected embryos to MeHg treatment. Again, the *c7-1* morphants and control embryos did not show any obvious morphological difference (Fig. 3.30 C, D).

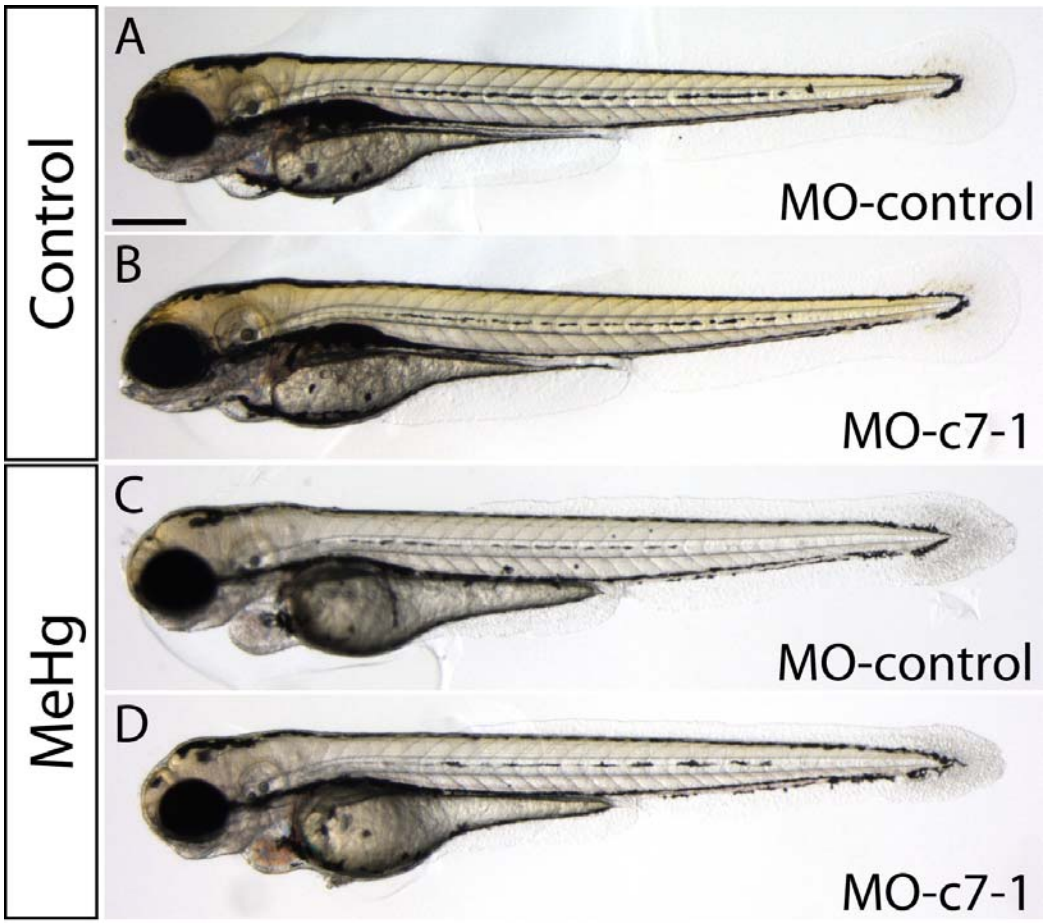

Fig. 3.30 No observable morphological difference in *c7-1* morphants.

Lateral views of zebrafish embryos at 4 dpf (A, B) and 72 hpf (C, D). (A, C) Injection control embryos; (B, D) *c7-1* morphants. (A, B) Control embryos exposed to embryos control medium (medium without MeHg); (C, D) embryos exposed to 60 µg/l MeHg. No obvious difference was observed in *c7-1* morphants (B, D) compared to injection control embryos (A, C) no matter the embryos were exposed to control medium (A, B) or to MeHg (C, D). Scale bar, 200 µm.

3.5.6 Summary

Specific induction of *c7-1* expression in the zebrafish retina was observed after MeHg treatment. Although *c7-1* is well-known to cooperate with several other complement components to form the MAC, such an ectopic induction in the retina was not observed in other MAC-forming complement components. The expression patterns of *c7-1* which are very similar to those of myelin genes during development, while no ectopic expression of any of the myelin genes examined were observed in MeHg-treated embryos. The type(s) of cells expressing *c7-1* and the function of *c7-1* in zebrafish embryos have yet to be determined.

4 Discussion

4.1 Malformations in fish caused by MeHg exposure

In consistence with the study performed by Samson and Shenker (2000), caudal fin fold abnormality and posterior tail flexures were observed in embryos exposed to MeHg. Very interestingly, I also observed the disruption of the melanophore gap, which marks the tail growth zone, by MeHg. This malformation has not been reported in any of the pervious studies. Besides the tail fin malformation, I also observed pericardial edema, smaller head and eye, stunted body and trunk flexure in the embryos treated with MeHg. Comparable malformations were observed in other MeHg-exposed fish embryos. Fathead minnow embryos with acute exposure to 20, 40, 80, 160, 320 μg/l MeHg showed flexures of the embryonic axis, pericardiac edema, irregularly-shaped heart tube, irregular heartbeat, shortened and disorganised tissue of the medial fin fold, smaller lower jaw or smaller eyes and stunted body (Devlin, 2006). Those embryos also exhibited abnormal behaviours with decreased swimming activity and erratic and twitching movements. Medaka embryos exposed to 15 μg/l Hg showed hemorrhaging, blood vessel deterioration, and loss of circulating blood cells and a decreased hatching rate (Heisinger and Green, 1975). Mummichog embryos exposed to 30 to 40 μg/l MeHg exhibited cardiovascular, skeletal and hatching defects (Weis and Weis, 1997; 1982). Cyclopia or intermediate conditions leading to cyclopia were also observed in the MeHg-exposed mummichog embryos. However, the occurrence of cyclopia was not observed in other fish species in response to MeHg.

4.2 Toxicogenomic screen of MeHg-responsive genes

The interactions with sulfhydryl groups, the induction of oxidative stress and the disruption of calcium ion homeostasis are believed to be the three major and critical mechanisms of MeHg toxicity. MeHg exposure will result in various cellular changes such as lipid peroxidation, DNA damage, membrane structure alternation, mitochondrial dysfunction, cell cycle alternation, apoptosis and necrosis.

In recent years, a few studies have been conducted to investigate the global genomic effects of acute or sub-acute MeHg or Hg exposure on individual organs of adult fish. Klaper *et al.* (2008) examined the gene expression changes in the liver and gonad of fathead minnow in response to MeHg exposure. Adult fathead minnows received a single intraperitoneal injection of MeHg of 2.0 μg/g body mass and after 96 hours, the minnows were scarified for a 15 k-gene microarray analysis. A total of 650 genes in the liver and 212 genes in the gonad were differentially regulated ($p > 0.05$ and $M > 1$ or < -1). The dysregulated genes were associated with protein folding, protein transport, fatty acid biosynthesis, tRNA processing, immune function, antigen presentation and apoptosis in the liver, and the GO categories of transcription from RNA polymerase II, rhythmic process, sterol biosynthesis, antigen presentation, amino acid metabolism and steroid biosynthesis in the gonad. Cambier *et al.* (2010) performed a serial analysis of gene expression (SAGE) on the skeletal muscle of adult male zebrafish fed with MeHg contaminated food (13.5 μg of Hg/g (dry weight)) for 25 days. They identified 60 up-regulated genes and 15 down-regulated genes ($p < 0.05$ and $M > 1$ or < -1) and observed the differential regulation of genes in the glycolysis pathways, oxidative pathways and mitochondria metabolism, detoxification, lipid metabolism, cell-cycle regulation, protein synthesis, structural compounds, muscle contraction, calcium ion homeostasis, reticulum endoplasmic apparatus, general metabolism, iron metabolism and transduction cascade. Ung *et al.* (2010) studied the Hg-induced effects in the liver of zebrafish using microarray spotted with 16,416 zebrafish oligo probes. Adult zebrafish were exposed to 200 μg/l $HgCl_2$ for 8, 24, 48 and 96 hours. Transcriptome analysis indicated that around 350 genes at 8 hours, 1000 genes at 24 hours, 1050 genes at 48 hours and 1650 genes were significantly regulated ($p < 0.05$) in response to $HgCl_2$ exposure. A sequential enrichments of GO categories of electron transport chain, mitochondrial fatty acid beta-oxidation, nuclear receptor signaling and apoptotic pathway, followed by complement system and proteasome pathway, and thereafter DNA damage, hypoxia, Wnt signaling, fatty acid synthesis, gluconeogenesis, cell cycle and motility were observed. Richter *et al.* (2011) investigated the gene expression changes in the zebrafish brain in response to MeHg exposure. Adult female zebrafish were intraperitoneally injected with 0.5μg/g MeHg and investigation was performed with 22K-probe microarray after 96 hours of exposure. Seventy-nine genes were up-regulated and 76 genes were down-regulated significantly in the MeHg-treated

samples ($p < 0.01$). Functional and pathway analysis indicated that MeHg exposure led to the deregulation of genes in steroid biosynthetic process, nucleotide binging, ATPase activity, cell differentiation, cell redox homeostasis, unfolded protein binding response to heat, serine esterase activity, ATP synthase activity, hydrolase activity and protein folding.

In this study, I provided a global transcriptome view of MeHg-induced acute toxicity in zebrafish embryo. The result of the microarray analysis was in consistent with a pervious toxicogenomic study performed by our group (Yang *et al.*, 2007). The finding here of having differentially expressed genes associated with oxidative stress, immune defence, DNA damage, apoptosis and cell death, and fatty acid peroxidation in response to MeHg exposure is in agreement with the current understanding on how MeHg induced its toxicity and with pervious genome-wise, acute MeHg or Hg exposure studies in fish. However, I could observe that quite a number of enriched GO categories and pathways were not consistent across studies. For examples, GO categories such as extracellular matrix organisation, blood circulation, response to hormone stimulus and MAP kinase phosphatase activity were detected in this study, but were not reported in the pervious studies; while GO categories such as electron transport chain, glycolysis/ gluconeogenesis and hypoxia induced pathway, which were enriched in the previous studies, were absent from this study. The discrepancies among studies could be attributed to the fact that this study determined the overall gene changes in whole embryo in response to MeHg, instead of the response in individual organs in the previous studies. Besides, pervious studies were carried out on adult fish while ours was on embryos. The concentrations of MeHg or Hg for exposure and different analytical methods and parameters used in the studies might also contribute to the differences.

I further investigating the change in the expression pattern of 88 MeHg-responsive genes by ISH. These genes are involved in various biological processes and molecular functions including regulation of transcription, antioxidant defence, immune response, enzymatic activity and transmembrane transport. Ectopic expressions of the genes were noted in various organs including the brain, eyes, olfactory bulb, branchial arches, heart, liver, intestine or gut, pronephos, somites, lateral lines, pectoral fins, caudal fin fold, blood vessels, dermal epithelium, and YSL. This study showed a 68%

positive correlation between ISH and microarray analyses. The consistent results of microarray analyses and ISH reinforced that toxicogenomics is a useful tool for examining the responses of an organism in the molecular level towards changes of the environment.

Besides the brain, lateral line and caudal fin fold, ectopic expression of genes also frequently observed in the eye, liver, blood vessels, pectoral fin and dermal epithelium and, this, probably, suggested that these structures are also sites of MeHg action. A study concerning the visual system in adult zebrafish showed that MeHg could pass through the blood-retina barrier and accumulated in various regions of the retina, especially in the photoreceptor layer and in the inner and outer nuclear layer (Mela *et al.*, 2010). Another study performed in larval axolotls showed that mercury exposure caused impaired rod photoreceptor morphology (Tessier-Lavigne *et al.*, 1985). Thus, it is likely that there was high level of MeHg accumulation in the retina of embryos exposed to MeHg, causing damage to the retinal cells and triggering changes in the expression of corresponding genes in the retina.

MeHg has been demonstrated to be hepatotoxic in adult zebrafish, rat and mummichog (Lin *et al*., 1996; Ung *et al.*, 2010; Weis *et al*., 1986). I speculate that hepatotoxicity also occurred in MeHg-exposed zebrafish embryos and the change in gene expressions in the liver was a response to hepatotoxicity. The increase in expression of antioxidant genes in the liver in MeHg-treated zebrafish embryos, such as *prx1*, *gclm* and *uricase*, indicated that the liver was under oxidative stress and this could be a cause of hepatocellular damage (Jaeschke *et al*., 2002; Liu *et al*., 2008). However, histological examination will be required to examine if there is any hepatoxic effects of MeHg on the embryos. On the other hand, the increased expression of some of the genes in the liver could also be due to the activation of innate immunity of the whole embryo for protecting the organism against the toxicity of MeHg as liver is an organ with predominant innate immunity (Gao *et al*., 2008; Racanelli and Rehermann, 2006). For example, *c3a*, *c4-2* and *cfb*, which were shown to be up-regulated in the liver in this study, are complement components and complement regulator proteins that are biosynthesised in the liver (Gao *et al*., 2008).

I observed the induction of 12 genes which are known for regulating blood circulation from the microarray analysis. I also detected increased expressions some of the genes in the blood vessels in embryos treated with MeHg. Fish embryos exposed to MeHg exhibited a variety of cardiovascular defects (Devlin, 2006; Heisinger and Gree, 1975, Weis and Weis, 1977). It was shown in a cell culture study that MeHg could cause oxidative-induced vascular endothelial dysfunction with increased permeability, depletion of glutathione and ATP, and inhibition of the activity of key thiol enzymes (Wolf and Baynes, 2007). I speculate that there was impaired blood vessel endothelial functions in MeHg-treated zebrafish embryos and the presence of pericardial edema in the MeHg-treated zebrafish embryos might possibly link to any endothelial dysfunction of the blood vessels. However, further studies on the vasculature are required to determine if there is any defect in the vasculature and the cause of pericardial edema in MeHg-treated embryos.

It is interesting to notice that there were genes expressed in both the pectoral and caudal fins (*apoeb, cxc46l, homez, junb, mmp9, mmp13a, noxo1, prdm1a, sqstm1, sgk1, txnl, zgc:56382, AW115990* and *BM101698)*, while there were also some expressed either in the pectoral fin (*c6, gclm, rrad, slc16a9a* and *BI474700*) or in the caudal fin (*copeb, mmp14a, sp9, p53, ucp1* and *AI397362*). The differences in the expression in these two structures might suggest that MeHg could induce some common mechanisms in both types of fins, but certain degree of divergence exists in these two structures in response to MeHg.

I further quantified the expression levels of 12 genes, which showed obvious changes in the expression level, in embryos exposed to 30 and 60 μg/l MeHg by real-time PCR. Eleven out of 12 was shown to be significantly regulated at 60 μg/l MeHg. The expression levels of 6 genes including *arfl, c4-2, c6, cbx7l, prdx1, txnl* and *zgc:101661* were significantly regulated even at 30 μg/l MeHg. The sensitivity of the change in the expression levels of these genes in response to MeHg suggested that they can serve as useful *in vivo* biosensors of waterborne MeHg.

4.3 The effects of MeHg on the nervous system of zebrafish embryos

In this study, although there were no obvious changes in expression patterns of the brain and neurotransmitter markers examined, I could detect changes of 24 other genes in the brain of zebrafish embryos exposed to MeHg. The genes detected in this study cover a wide range of biological processes including transcription regulation (*six3, atf3, homez, fos, agt, cbx7, cebpg* and *irf9*), response to oxidative stress (*gclm, fos* and *prdx1*), apoptosis (*agt* and *gclm*), immune response (*cebpg* and *prdx1*), protein dimerisation activity (*atf3, gclm, fos* and *cebpg*), cytokine production (*cebpg* and *irf9*) and blood vessel regulation (*agt* and *gclm*). The changes in the expression patterns of genes in the brain might suggest the induction of the behavioural changes reported by Samson *et al.* (2001) after MeHg treatment. Besides, it has been reported that the activity, but not the gene expression level, of acetylcholinesterase was altered in the zebrafish adult brain after exposure to heavy metals, including Hg (Richetti *et al.*, 2010). It will be interesting to examine if there are any alternation in the neurotransmitter activities in zebrafish embryos after MeHg exposure, even though I could not observe any manifest change in the expression patterns of the neurotransmitters.

In a pervious study carried out by Gonzalez *et al.* (2005), the effect of sub-chronic and chronic exposure to MeHg exposure on the brain of adult zebrafish was determined by dietary exposure of adult zebrafish to 5 and 13.5 μg/g MeHg for 7, 21 and 63 days. The changes in the expression levels of 13 genes known to be involved in anti-oxidative defenses, apoptosis, metal chelation, active efflux of organic compounds, mitochondrial metabolism were determined by real-time PCR. Although there were changes in the expression levels of some of the genes examined in the muscle and liver after MeHg exposure, no such changes were observed in the brain. In another study performed by Richter *et al.* (2011), the acute effect of MeHg exposure on adult zebrafish brain was investigated by intraperitoneal injection of 0.5 μg/g MeHg into female zebrafish and after 96 hours, the fish were scarified for the examination of the in the gene expression levels by a 22K-probe microarray. Seventy-nine genes were shown to be up-regulated and 76 genes were down-regulated ($p>0.01$) in response to

MeHg. In contrast to the study performed by Gonzalez *et al.*, they showed the regulations of anti-oxidative defenses and apoptosis genes in the brain after MeHg exposure. Consistent with Richter *et al.*, this study also showed the regulation of genes involved in oxidative stress and apoptosis. The differences between this and Richter *et al.*'s studies and Gonzalez *et al.*'s study may be attributed to the duration of exposure. Gonzalez *et al.* focused on the response of sub-chronic and chronic MeHg exposure while this and Richter *et al.*'s studies were on acute exposures. It has been reported that different pathways will be triggered at different time points in response to MeHg exposure (Klaper *et al.*, 2008; Ung *et al.*, 2010; Yang *et al.*, 2007). Besides, the coverage of genes studied by Gonzalez *et al.* and the concentrations of MeHg used in the studies might also contribute to the differences.

As the neuromasts of the lateral line are in direct contact with the environment and it has been reported that waterborne contaminants could lead to disruption of the neuromasts and death of hair cells. I also observed a decrease in the number of hair cells in embryos exposed to 60μg/l MeHg while there was no change in the location of the neuromasts in MeHg-treated embryos. Through the toxicogenomic screening, I identified 12 genes showing ectopic expression or decrease in expression in the lateral line of MeHg-treated embryos. These genes were expressed in different parts of the neuromasts and this may suggest their different functions in the neuromasts in response to MeHg. These genes may be involved in induction of hair cell or neuromast death, removal of dead cells, recovery or renewal of damaged lateral line, or protecting the lateral line from oxidative or other cellular stresses. It has been shown in other biological systems that the transcription factors *fos* and *maff* could activate oxidative stress genes through the regulation of the antioxidant response element (ARE) promoter (Itoh *et al.*, 1997; Jasiwal, 2004; Motohashi *et al.*, 1997). *gclm*, *prdx1* and *txnl* are genes of the glutathione and thioredoxin systems which are known to be implicated in antioxidative defence (Aracena *et al.*, 2006; Collet and Messens, 2010; Jones and Go, 2010; Neumann *e al.*, 2009). However, surprisingly, I also detected a decrease in the expression of another antioxidant gene *gpx4*, which can reduce hydrogen peroxide and phospholipid hydroperoxides to suppress lipid and other forms of peroxidation (Imai and Nakagawa, 2003; Savaskan *et al.*, 2007), in the lateral line. To remove dead cells for repairing, inflammatory cells are recruited to the site of injury by damage signals released form the site of inflammatory (Martin and

Leibovich, 2005; Redd *et al.*, 2004). Given that *cxc46l* is a member of the cxc chemokine family which functions as a chemoattractant and is one of the mediators of the inflammatory response (Zaja-Milatovic and Richmond, 2008), I speculated that *cxc46l* could recruit immune cells to the site of inflammation and remove dead hair cells from the neuromasts. Pervious studies on zebrafish hair cell regeneration suggested that support cells and hair cell progenitors may serve as the source of newly differentiated hair cells during regeneration of neuromast hair cells (Ghysen and Dambly-Chaudière, 2004; Hernandez *et al.*, 2007; Ma *et al.*, 2008; Wibowo *et al.*, 2011). MeHg-regulated genes expressed in the support cells or hair cell progenitors the may play a role in the hair cell regeneration. However, studies will be required to investigate which neuromast cell types express the MeHg-regulated genes.

4.4 The effects of MeHg on trunk pigmentation

Besides the tail phenotypes described by Samson and Shenker (2000), disruption of trunk pigmentation in the tail was also frequently and consistently detected in the MeHg-treated embryos. The effective time window of MeHg exposure for the disruption of the size of melanophore gap was restricted to 12 hpf and 48 hpf with the malformation rate increased with increasing duration of exposure. This effect appeared to be specific to MeHg, at least among the chemicals examined in this study.

Melanophores are derived from a population of trunk neural crest (TNC) cells. In zebrafish, TNC cells begin to migrate from the neural keel at around 15 hpf along stereotyped pathways to give rise to a diverse and well-defined set of cells types (Schilling and Kimmel, 1994; Vaglia and Hall, 2000). Under normal embryonic development, pigment cells flank both sides of the tail primordium and are absent from the tail primordium. I speculate that the change in melanophore gap size is due to the disruption of TNC migration to the region of the tail primordium and that genetic cues are generated from the tail primordium that keep the pigment cells away from this region. Disruption of the tail primordium takes the cues away and thus allows the intrusion of the pigment cells into the position where the fin primordium should normally be located. The observation that exposure to MeHg between 12 to 48 hpf disrupted the melanophore localisation is in agreement with this speculation.

However, I did not find impairment of neural crest differentiation and migration as inferred from the patterns of *crestin* expression in 24-hpf-old MeHg-treated embryos.

Various genes have been reported to be involved in the regulation of caudal fin development and *shh* is believed to be one of them (Hadzhiev *et al.*, 2007; Iovine, 2007). *Shh* is a key player of many fundamental processes in embryonic development including growth, patterning and morphogenesis through acting as a morphogen, which induces neighbouring cells to adopt distinct cell fates in a dose-dependent manner, as a mitogen, which regulates cell proliferation, or as an inducing factor, which controls the shape of a developing organ (Ingham and McMahon, 2001). Disruption of *shh* signalling genetically or chemically could affect the development of the caudal fin primordium and the tail fin in zebrafish embryos (Hadzhiev *et al.*, 2007). Interestingly, the phenotypes induced by MeHg were very similar to those resulted from the loss of *shh* expression in zebrafish embryos. Although a decrease in GFP expression in the caudal fin primordium of *Tg(-2.4shha-ABC:GFP)sb15* transgenic line was noted, it is rather not likely that MeHg affect the development of the caudal fin primordium through interacting with the *shh* signalling pathway since the time window that MeHg exerted its effects on tail fin development was restricted between 12 and 48 hpf while *shh* signaling seemed to be continuously required even at stages after 48 hpf (Hadzhiev *et al.*, 2007). Besides, other Shh-regulated developmental processes, such as somite development and motor neuron induction (Barresi *et al.*, 2000; Lewis and Eisen, 2001; Schauerte *et al.*, 1998), were not affected by MeHg exposure.

4.5 Study on the effects of MeHg on the caudal fin fold

It was shown here that there was a mild increase in the expression of the apoptosis-induced gene *p53* and a slight increase in the number of apoptotic cells in the caudal fin fold. However, inhibition of *p53*-mediated apoptosis by knockdown of *p53* could not rescue the caudal fin fold phenotype. Taken together, I concluded that MeHg treatment caused a slight induction of apoptosis in the caudal fin fold, but it did not seem to be a major cause of the caudal fin fold abnormality.

Besides *p53*, I identified 19 other genes which showed ectopic expression pattern in the caudal fin fold after MeHg treatment. These genes may play a role in the toxicological mechanism in inducing the caudal fin fold tissue disruption or may involve in the repair of the fin fold damage as some of these MeHg-regulated genes have also been shown to be implicated in fin regeneration (Yoshinari *et al.*, 2009). I further examined the role which *mmp9* and *mmp13a* play in the caudal fin tissue phenotype due to their strong and restricted expressions in the caudal fin fold in MeHg-treated embryos and their ability to degrade the collagenous ECM which is one of the structural components of the caudal fin fold.

I first tested the specificity of the induction of *mmp9* and *mmp13a*. Interestingly, although up-regulation of *mmp13*a was observed in scattered cells in embryos exposed with Pb, As and Cd, no ectopic expression of *mmp9* or *mmp13a* was induced in the caudal fin fold of these chemical-treated embryos which did not show any caudal fin defects. Besides the increased in transcript levels, I also showed that there was an increase in the collagenase activity.

Both *mmp9* and *mmp13a* have been reported to be expressed in various cell types, including myeloid cells. I also investigated if the ectopic expression of *mmp9* and *mmp13a* in the caudal fin fold was due to an inflammatory response by comparing the expression patterns of the macrophage and neutrophil markers with those of *mmp9* and *mmp13a*. However, I did not detect any up-regulation of these myeloid cell markers, suggesting that the *mmp9* and *mmp13a* expression are not the reflection of an inflammatory response.

Functional study on *mmp9* and *mmp13a* was performed to investigate their roles in caudal fin fold development. I adopted a pharmacological approach in which I co-treated embryos with a general Mmp inhibitor or a Mmp9 and Mmp13 specific inhibitor together with MeHg. The result showed that co-treatment with the general Mmp inhibitor could increase the fin fold area by 18% and application of Mmp9 and Mmp13 specific inhibitor could even increase the fin fold area by 25%. However, it was also noted that the inhibition of Mmp activity by this approach could not rescue the phenotype fully. This may be due to the incomplete inhibition of Mmp9 and

Mmp13 activities in this study. It was also possible that other genes were also involved in causing the phenotype. As mentioned earlier in the discussion, we could observe the induction of ectopic expression of genes other than *mmp9* and *mmp13a* in the caudal fin fold of MeHg-treated embryos.

4.6 Ectopic expression of c7-1 in the eye after MeHg exposure

In this study, *c7-1* was shown to be ectopically and specifically expressed in the retina, especially the INL, after MeHg exposure. *c7-1* is known to cooperate with several other complement components to form MAC involved in the lytic pathway of the complement system as a mean of immune defence. However, the result of this study showed that such an ectopic expression in the retina was unique to *c7-1* and was not induced in other MAC-forming complement components.

I also showed that during embryonic development *c7-1* was specifically expressed in the ventral hindbrain, close to the midline, and then spread rostrally to the midbrain and caudally to the region dorsal to the notochord. The localisation of *c7-1* transcripts was very similar to genes expressed in the myelin sheath during embryonic development. The similar developmental expression patterns of these genes drove us to examine if the myelin proteins would also show an ectopic expression in the retina after MeHg exposure in order to get some clues whether the ectopic *c7-1* expression of in the retina of MeHg-treated embryos is due to ectopic formation of myelin in the retina. I examined the expression of the myelin marker genes in MeHg-treated embryos. No ectopic expression in the retina was induced in any of the myelin marker genes examined, indicating that the ectopic *c7*-expressing cells were not because of the ectopic myelin formation in the retina after MeHg exposure.

The functions of the MAC in neuron survival are controversial as the complex has been shown to cause both neuroinflammation and neuroprotection. In human, Complement C7 deficiency (C7D) is frequently associated with the life-threatening meningococcal infection. Due to the specific induction of *c7-1* by MeHg exposure, I wanted to know what the functions of *c7-1* are during development and under MeHg

exposure, why only *c7-1*, but not other complement components, is ectopically expressed in the retina of MeHg-exposed embryos and what role does it play, and the effects on zebrafish embryos when *c7-1* does not function. I tried to gain some insights in answering these questions by knocking down *c7-1* in zebrafish embryos with splice-blocking MO. However, I could not observe differences in the *c7-1* morphants compared to the control during normal embryonic development or embryos subjected to MeHg. The lack of function may be due to the presence of gene duplication as through the database search, I found the existence of another *c7* homologue *c7-2* in zebrafish, despite that *c7-2* showed different expression pattern from *c7-1*.

5 Conclusion

A global view of gene expression changes in zebrafish embryos in response to acute MeHg exposure was generated in this study. Through the toxicogenomic screen, genes showing alternations in response to MeHg in the brain were identified. In addition, genes which showed specific expression in the neuromasts in the MeHg-treated embryos were reported and these genes could play a role in the impairment of neuromast in the presence of MeHg.

The present study showed that sub-lethal concentration of MeHg induced caudal fin fold tissue abnormality, disruption of trunk pigmentation strip gap and reduced hair cell number in the neuromast of the lateral line. MeHg induced fin fold tissue abnormality and disruption of trunk pigmentation strip gap specifically among all the heavy metal examined. As the *gfp* expression of the transgenic line *Tg(-2.4shha-ABC:GFP)sb15* was specially expressed in the melanophore strip gap and the signal was abolished significantly in the presence of MeHg as low as 6 μg/l, this transgenic line can serve as a highly sensitive readout system of waterborne MeHg. A set of genes which were specifically induced in the caudal fin fold of MeHg-exposed embryos were identified. Among those genes, *mmp9* and *mmp13a* have been revealed as two of the players of the caudal fin fold tissue disruption.

This study helped to gain insight into the mechanisms of the MeHg-induced toxicity and provide clues for further mechanism studies. The identification of MeHg-sensitive biomarkers could be used to develop *in vivo* biosensors to monitor waterborne MeHg or other toxicants that showed similar toxicological profile as MeHg. This study also underscored the usefulness of zebrafish as a model organism to access developmental toxicity.

References

Abbott N.J., Rönnbäck L., Hansson E. (2006). Astrocyte-endothelial interactions at the blood-brain barrier. *Nat Rev Neurosci*. 7, 41-53.

Abramoff M.D., Magelhaes P.J., Ram S.J. (2004). Image processing with ImageJ. *Biophotonics Int*. 11, 36-42.

Afshari C.A., Hamadeh H.K., Bushel P.R. (2010). The Evolution of Bioinformatics in Toxicology: Advancing Toxicogenomics. *Toxicol Sci*. 120 Suppl 1, S225-S237.

Ali S.F., LeBel C.P., Bondy S.C. (1992). Reactive oxygen species formation as a biomarker of methylmercury and trimethyltin neurotoxicity. *Neurotoxicology*. 13, 637-648.

Al-Shahristani H., Shihab K., Al-Haddad I.K. (1976). Mercury in hair as an indicator of total body burden. *Bull World Health Organ*. 53 Suppl, 105-112.

Andres R.H., Meyer M., Ducray A.D., Widmer H.R. (2008). Restorative neuroscience: concepts and perspectives. *Swiss Med Wkly*. 138,155-172.

Aracena P., Aguirre P., Muñoz P., Núñez M.T. (2006). Iron and glutathione at the crossroad of redox metabolism in neurons. *Biol Res*. 39, 157-165.

Arroyo E.J., Scherer S.S. (2000). On the molecular architecture of myelinated fibers. *Histochem Cell Biol*. 113, 1-18.

Aschner M., Syversen T., Souza D.O., Rocha J.B. (2006). Metallothioneins: mercury species-specific induction and their potential role in attenuating neurotoxicity. *Exp Biol Med (Maywood)*. 231, 1468-1473.

Ask K., Akesson A., Berglund M., Vahter M. (2002). Inorganic mercury and methylmercury in placentas of Swedish women. *Environ Health Perspect*. 110, 523-526.

Atchison W.D. (2003). Effects of toxic environmental contaminants on voltage-gated calcium channel function: from past to present. *J Bioenerg Biomembr*. 35, 507-532.

Bai S., Thummel R., Godwin A.R., Nagase H., Itoh Y., Li L., Evans R., McDermott J., Seiki M., Sarras M.P. Jr. (2005). Matrix metalloproteinase expression and function during fin regeneration in zebrafish: analysis of MT1-MMP, MMP2 and TIMP2. *Matrix Biol*. 24, 247-260.

Bakir F., Damluji S.F., Amin-Zaki L., Murtadha M., Khalidi A., al-Rawi N.Y., Tikriti S., Dahahir H.I., Clarkson T.W., Smith J.C., Doherty R.A. (1973). Methylmercury poisoning in Iraq. *Science*. 181, 230-241.

Ball L.K., Ball R., Pratt R.D. (2001). An assessment of thimerosal use in childhood vaccines. *Pediatrics*. 107, 1147-1154.

Baraldi M., Zanoli P., Tascedda F., Blom J.M.C., Brunello N. (2002). Cognitive deficits and changes in gene expression of NMDA receptors after prenatal methylmercury exposure. *Environ Health Perspect*. 110 Suppl 5, 855-858.

Barresi M.J., Stickney H.L., Devoto S.H. (2000). The zebrafish slow-muscle-omitted gene product is required for Hedgehog signal transduction and the development of slow muscle identity. *Development*. 127, 2189-2199.

Barroso S., López-Trascasa M., Merino D., Alvarez A.J., Núñez-Roldán A., Sánchez B. (2010). C7 deficiency and meningococcal infection susceptibility in two spanish families. *Scand J Immunol*. 72, 38-43.

Bartrons R., Caro J. (2007). Hypoxia, glucose metabolism and the Warburg's effect. *J Bioenerg Biomembr*. 39, 223-229.

Bayarsaihan D., Enkhmandakh B., Makeyev A., Greally J.M., Leckman J.F., Ruddle F.H. (2003). Homez, a homeobox leucine zipper gene specific to the vertebrate lineage. *Proc Natl Acad Sci U S A*. 100, 10358-10363.

Behra M., Cousin X., Bertrand C., Vonesch J.L., Biellmann D., Chatonnet A., Strähle U. (2002). Acetylcholinesterase is required for neuronal and muscular development in the zebrafish embryo. *Nat Neurosci*. 5, 111-118.

Bencko V. (1995). Use of human hair as a biomarker in the assessment of exposure to pollutants in occupational and environmental settings. *Toxicology*. 101, 29-39.

Benjamini Y., Hochberg Y. (1995). Controlling the false discovery rate: a practical and powerful approach to multiple testing. *J Roy Statist Soc Ser B*. 57, 289-300.

Bennett C.M., Kanki J.P., Rhodes J., Liu T.X., Paw B.H., Kieran M.W., Langenau D.M., Delahaye-Brown A., Zon L.I., Fleming M.D., Look A.T. (2001). Myelopoiesis in the zebrafish, Danio rerio. *Blood*. 98, 643-651.

Berglund A. (1990). Estimation by a 24-hour study of the daily dose of intra-oral mercury vapor inhaled after release from dental amalgam. *J Dent Res*. 69, 1646-1651.

Berglund M., Lind B., Björnberg K.A., Palm B., Einarsson O., Vahter M. (2005). Inter-individual variations of human mercury exposure biomarkers: a cross-sectional assessment. *Environ Health*. 4, 20.

Bernard D., Martinez-Leal J.F., Rizzo S., Martinez D., Hudson D., Visakorpi T., Peters G., Carnero A., Beach D., Gil J. (2005). CBX7 controls the growth of normal and tumor-derived prostate cells by repressing the Ink4a/Arf locus. *Oncogene*. 24, 5543-5551.

Bertrand C., Chatonnet A., Takke C., Yan Y.L., Postlethwait J., Toutant J.P., Cousin X. (2001). Zebrafish acetylcholinesterase is encoded by a single gene localized on linkage group 7. Gene structure and polymorphism; molecular forms and expression pattern during development. *J Biol Chem*. 276, 464-474.

Beyrouty P., Stamler C.J., Liu J.N., LouaK.M., Kubow S., Chan H.M. (2006). Effects of prenatal methylmercury exposure on brain monoamine oxidase activity and neurobehaviour of rats. *Neurotoxicol Teratol*. 28, 251-259.

Bi X., Corpina R.A., Goldberg J. (2002). Structure of the Sec23/24-Sar1 pre-budding complex of the COPII vesicle coat. *Nature*. 419, 271-277.

Bielli A., Haney C.J., Gabreski G., Watkins S.C., Bannykh S.I., Aridor M. (2005). Regulation of Sar1 NH2 terminus by GTP binding and hydrolysis promotes membrane deformation to control COPII vesicle fission. *J Cell Biol*. 171, 919-924.

Biol. 15, R213-28.

Bjartmar C., Yin X., Trapp BD. (1999). Axonal pathology in myelin disorders. *J Neurocytol*. 28, 383-395.

Björkman L., Sandborgh-Englund G., Ekstrand J. (1997). Mercury in saliva and feces after removal of amalgam fillings. *Toxicol Appl Pharmacol*. 144, 156-162.

Boshra H., Li J., Sunyer J.O. (2006). Recent advances on the complement system of teleost fish. *Fish Shellfish Immunol*. 20, 239-262.

Braunbeck T., Boettcher M., Hollert H., Kosmehl T., Lammer E., Leist E., Rudolf M., Seitz N. (2005). Towards an alternative for the acute fish LC(50) test in chemical assessment: the fish embryo toxicity test goes multi-species -- an update. *ALTEX*. 22, 87-102.

Brnjic S., Olofsson M.H., Havelka A.M., Linder S. (2010). Chemical biology suggests a role for calcium signaling in mediating sustained JNK activation during apoptosis. *Mol Biosyst*. 6, 767-774.

Brookes N. (1992). In vitro evidence for the role of glutamate in the CNS toxicity of mercury. *Toxicology*. 76, 245-256.

Brösamle C., Halpern M.E. (2002). Characterization of myelination in the developing zebrafish. *Glia*. 39, 47-57.

Burbacher T.M., Grant K.S., Mayfield D.B., Gilbert S.G., Rice D.C. (2005). Prenatal methylmercury exposure affects spatial vision in adult monkeys. *Toxicol Appl Pharmacol*. 208 (1), 21-28.

Burbacher T.M., Sackett G.P., Mottet N.K. (1990). Methylmercury effects on the social behavior of Macaca fascicularis infants. *Neurotoxicol Teratol*. 12, 65-71.

Cagiano R., De Salvia M.A., Renna G., Tortella E., Braghiroli D., Parenti C., Zanoli P., Baraldi M., Annau Z., Cuomo V. (1990). Evidence that exposure to methylmercury during gestation induces behavioral and neurochemical changes in offspring of rats. *Neurotoxicol Teratol*. 12, 23-28.

Cambier S., Gonzalez P., Durrieu G., Maury-Brachet R., Boudou A., Bourdineaud J.P. (2010). Serial analysis of gene expression in the skeletal muscles of zebrafish fed with a methylmercury-contaminated diet. *Environ Sci Technol*. 44, 469-475.

Capdevila J., Izpisúa Belmonte J.C. (2001). Patterning mechanisms controlling vertebrate limb development. *Annu Rev Cell Dev Biol*. 17, 87-132.

Carratù M.R., Borracci P., Coluccia A., Giustino A., Renna G., Tomasini M.C., Raisi E., Antonelli T., Cuomo V., Mazzoni E., Ferraro L. (2006). Acute exposure to methylmercury at two developmental windows: focus on neurobehavioral and neurochemical effects in rat offspring. *Neuroscience*. 141, 1619-1629.

Carvan M.J. 3rd., Solis W.A., Gedamu L., Nebert D.W. (2000). Activation of transcription factors in zebrafish cell cultures by environmental pollutants. *Arch Biochem Biophys*. 376, 320-327.

Castoldi A.F., Onishchenko N., Johansson C., Coccini T., Roda E., Vahter M., Ceccatelli S., Manzo L. (2008). Neurodevelopmental toxicity of methylmercury: Laboratory animal data and their contribution to human risk assessment. *Regul Toxicol Pharmacol*. 51, 215-229.

Cates S. (2006). NCBI: National Center for Biotechnology Information. Connexions, February 21, 2006. http://cnx.org/content/m11789/1.3/.

Celo V., Lean D.R., Scott S.L. (2006). Abiotic methylation of mercury in the aquatic environment. *Sci Total Environ*. 368, 126-137.

Centers for Disease Control and Prevention (CDC). (1999). Thimerosal in vaccines: a joint statement of the American Academy of Pediatrics and the Public Health Service. *MMWR Morb Mortal Wkly Rep*. 48, 563-565.

Cernichiari E., Myers G.J., Ballatori N., Zareba G., Vyas J., Clarkson T. (2007). The biological monitoring of prenatal exposure to methylmercury. *Neurotoxicology*. 28, 1015-1022.

Cernichiari E., Toribara T.Y., Liang L., Marsh D.O., Berlin M.W., Myers G.J., Cox C., Shamlaye C.F., Choisy O., Davidson P., Clarkson T.W. (1995). The biological monitoring of mercury in the Seychelles study. *Neurotoxicology*. 16, 613-628.

Chakraborti S., Mandal M., Das S., Mandal A., Chakraborti T. (2003). Regulation of matrix metalloproteinases: an overview. *Mol Cell Biochem*. 253, 269-285.

Chalmers A.T., Argue D.M., Gay D.A., Brigham M.E., Schmitt C.J., Lorenz D.L. (2011). Mercury trends in fish from rivers and lakes in the United States, 1969-2005. *Environ Monit Assess*. 175, 175-191.

Chan J., Huang Z., Merrifield M. E., Salgado M. T., Stillman M. J. (2002). Studies of metal binding reactions in metallothioneins by spectroscopic, molecular biology, and molecular modeling techniques. *Coord Chem Rev*. 233-234, 319-339.

Chandrasekhar A., Warren J.T. Jr., Takahashi K., Schauerte H.E., van Eeden F.J., Haffter P., Kuwada J.Y. (1998). Role of sonic hedgehog in branchiomotor neuron induction in zebrafish. *Mech Dev*. 76, 101-115.

Chang L.W., Reuhl K.R., Lee G.W. (1977a). Degenerative changes in the developing nervous system as a result of in utero exposure to methylmercury. *Environ Res*. 14, 414-423.

Chang L.W., Reuhl K.R., Spyker J.M. (1977b). Ultrastructural study of the latent effects of methyl mercury on the nervous system after prenatal exposure. *Environ Res*. 13, 171-185.

Chapleau R.R., Blomberg R., Ford P.C., Sagermann M. (2008). Design of a highly specific and noninvasive biosensor suitable for real-time in vivo imaging of mercury (II) uptake. *Protein Sci*. 17, 614-622.

Chapleau R.R., Sagermann M. (2009). Real-time in vivo imaging of mercury uptake in Caenorhabditis elegans through the foodchain. *Toxicology*. 261, 136-142.

Chataway J., Sawcer S., Sherman D., Hobart M., Fernie B., Coraddu F., Feakes R., Broadley S., Gray J., Jones H.B., Clayton D., Goodfellow P.N., Compston A. (1999).No evidence for association of multiple sclerosis with the complement factors C6 and C7. *J Neuroimmunol*. 99, 150-156.

Cheng J., Yang Y., Ma J., Wang W., Liu X., Sakamoto M., Qu Y., Shi W. (2009). Assessing noxious effects of dietary exposure to methylmercury, PCBs and Se coexisting in environmentally contaminated rice in male mice. *Environ Int*. 35, 619-625.

Cheng J.P., Wang W.H., Jia J.P., Hu W.X., Shi W., Lin X.Y. (2005). Effects of mercury contaminated rice from typical chemical plant area in China on nitric oxide changes and c-fos expression of rats brain. *J Environ Sci (China)*. 17, 177-180.

Clarkson T.W. (1993). Mercury: major issues in environmental health. *Environ Health Perspect*. 100, 31-38.

Clarkson T.W. (2002). The three modern faces of mercury. *Environ Health Perspect*. 110, Suppl 1, 11-23.

Clarkson T.W. Crawford B.D., Pilgrim D.B. (2005). Ontogeny and regulation of matrix metalloproteinase activity in the zebrafish embryo by in vitro and in vivo zymography. *Dev Biol*. 286, 405-414.

Clarkson T.W., Magos L. (2006). The toxicology of mercury and its chemical compounds. *Crit Rev Toxicol*. 36, 609-662.

Claudio L., Kwa W.C., Russell A.L., Wallinga D (2000). Testing methods for developmental neurotoxicity of environmental chemicals. *Toxicol Appl Pharmacol*. 164, 1-14.

Collet J.F., Messens J. (2010). Structure, function, and mechanism of thioredoxin proteins. *Antioxid Redox Signal*. 13, 1205-1216.

Commission of the European Communities. (1986). Council Directive of 24 November 1986 on the approximation of laws, regulations and administrative provisions of the Member States regarding the protection of animals used for experimental and other scientific purposes (86/609/EEC). *Official Journal of the European Communities*. L358, 1-28.

Compston D.A., Morgan B.P., Campbell A.K., Wilkins P., Cole G., Thomas N.D., Jasani B. (1989). Immunocytochemical localization of the terminal complement complex in multiple sclerosis. *Neuropathol Appl Neurobiol*. 15, 307-316.

Cooper A.J.L. (1983). Biochemistry of sulfur-containing amino acids. *Annu Rev Biochem*. 52, 187-222.

Corwin J.T., Cotanche D.A. (1988). Regeneration of sensory hair cells after acoustic trauma. *Science*. 240, 1772-1774.

Cotanche D.A., Lee K.H. (1994). Regeneration of hair cells in the vestibulocochlear system of birds and mammals. *Curr Opin Neurobiol*. 4, 509-514.

Coyle P., Philcox J.C., Carey L.C., Rofe A.M. (2002). Metallothionein: the multipurpose protein. *Cell Mol Life Sci*. 59, 627-647.

Crawford B.D., Pilgrim D.B. (2005). Ontogeny and regulation of matrix metalloproteinase activity in the zebrafish embryo by in vitro and in vivo zymography. *Dev Biol*. 286, 405-414.

Crow M.T., Stockdale F.E. (1986). The developmental program of fast myosin heavy chain expression in avian skeletal muscles. *Dev Biol*. 118, 333-342.

Crump K.S., Kjellström T., Shipp A.M., Silvers A., Stewart A. (1998). Influence of prenatal mercury exposure upon scholastic and psychological test performance: benchmark analysis of a New Zealand cohort. *Risk Anal*. 18, 701-713.

Cudrici C., Niculescu T., Niculescu F., Shin M.L., Rus H. (2006). Oligodendrocyte cell death in pathogenesis of multiple sclerosis: Protection of oligodendrocytes from apoptosis by complement. *J Rehabil Res Dev*. 43, 123-132.

Dambly-Chaudière C., Sapède D., Soubiran F., Decorde K., Gompel N., Ghysen A. (2003). The lateral line of zebrafish: a model system for the analysis of morphogenesis and neural development in vertebrates. *Biol Cell*. 95, 579-587.

Dane P.J., Tucker J.B. (1985). Modulation of epidermal cell shaping and extracellular matrix during caudal fin morphogenesis in the zebra fish Brachydanio rerio. *J Embryol Exp Morphol*. 87, 145-161.

Dave G., Xiu R.Q. (1991). Toxicity of mercury, copper, nickel, lead, and cobalt to embryos and larvae of zebrafish, Brachydanio rerio. *Arch Environ Contam Toxicol*. 21, 126-34.

Davidson P.W., Leste A., Benstrong E., Burns C.M., Valentin J., Sloane-Reeves J., Huang L.S., Miller W.A., Gunzler D., van Wijngaarden E., Watson G.E., Zareba G., Shamlaye C.F., Myers G.J. (2010). Fish consumption, mercury exposure, and their associations with scholastic achievement in the Seychelles Child Development Study. *Neurotoxicology*. 31, 439-447.

Davidson P.W., Myers G.J., Cox C., Axtell C., Shamlaye C., Sloane-Reeves J., Cernichiari E., Needham L., Choi A., Wang Y., Berlin M., Clarkson T.W. (1998). Effects of prenatal and postnatal methylmercury exposure from fish consumption on neurodevelopment: outcomes at 66 months of age in the Seychelles Child Development Study. *JAMA*. 280, 701-707.

Davidson P.W., Myers G.J., Weiss B., Shamlaye C.F., Cox C. (2006). Prenatal methyl mercury exposure from fish consumption and child development: a review of evidence and perspectives from the Seychelles Child Development Study. *Neurotoxicology*. 27, 1106-1109.

Davis S.R., Cousins R.J. (2000). Metallothionein expression in animals: a physiological perspective on function. *J Nutr*. 130, 1085-1088.

de Longueville F., Bertholet V., Remacle J. (2004). DNA microarrays as a tool in toxicogenomics. *Comb Chem High Throughput Screen*. 7, 207-211.

Devlin E., Mottel W. (1992). Embryotoxic action of methyl mercury on Coho salmon embryos. *Bull Environ Contam Toxicol*. 49, 449-454.

Devlin E.W. (2006). Acute toxicity, uptake and histopathology of aqueous methyl mercury to fathead minnow embryos. *Ecotoxicol*. 15, 97-110

Dial N.A. (1978). Methylmercury: some effects on embryogenesis in the Japanese Medaka, Oryzias latipes. *Teratology*. 17, 83-91.

DiPietro L.A. (1995). Wound healing: the role of the macrophage and other immune cells. *Shock*. 4, 233-240.

Donaldson J.G., Honda A. (2005). Localization and function of Arf family GTPases. *Biochem Soc Trans*. 33, 639-642.

Dooley, J. H. (1992) Natural Sources of Mercury in the Kirkwood-Cohansey Aquifer System of the New Jersey Coastal Plain. New Jersey Geological Survey Report 27.

Downes G.B., Granato, M. (2004). Acetylcholinesterase function is dispensable for sensory neurite growth but is critical for neuromuscular synapse stability. *Dev Biol*. 270, 232-245.

Draper B.W., Morcos P.A., Kimmel C.B. (2001). Inhibition of zebrafish fgf8 pre-mRNA splicing with morpholino oligos: a quantifiable method for gene knockdown. *Genesis*. 30, 154-156.

Driever W. (1995). Axis formation in zebrafish. *Curr Opin Genet Dev*. 5, 610-618.

D'Souza-Schorey C., Chavrier P. (2006). ARF proteins: roles in membrane traffic and beyond. *Nat Rev Mol Cell Biol*. 7, 347-358.

Duboc V., Logan M.P. (2009). Building limb morphology through integration of signalling modules. *Curr Opin Genet Dev*. 19, 497-503.

Duncan D.T., Prodduturi N., Zhang B. (2010). WebGestalt2: an updated and expanded version of the Web-based Gene Set Analysis Toolkit. *BMC Bioinformatics*. 11 Suppl 4, 10.

Durinck S., Moreau Y., Kasprzyk A., Davis S., De Moor B., Brazma A., Huber W. (2005). BioMart and Bioconductor: a powerful link between biological databases and microarray data analysis. *Bioinformatics*. 21, 3439-3440.

Eisler R. (1987) Mercury hazards to fish, wildlife, and invertebrates: A synoptic review. U.S. Fish and Wildlife Service. Biological Report 85. Report no. 10.

Ekino S., Susa M., Ninomiya T., Imamura K., Kitamura T. (2007). Minamata disease revisited: an update on the acute and chronic manifestations of methyl mercury poisoning. *J Neurol Sci*. 262, 131-144.

Ekker S.C., Larson, J.D. (2001). Morphant technology in model developmental system. *Genesis*. 30, 89-93.

Ekstrand J., Björkman L., Edlund C., Sandborgh-Englund G. (1998). Toxicological aspects on the release and systemic uptake of mercury from dental amalgam. *Eur J Oral Sci*. 106, 678-686.

Elhassani S.B. (1982). The many faces of methylmercury poisoning. *J Toxicol Clin Toxicol*. 19, 875-906.

Elia A.C., Galarini R., Taticchi M.I., Dörr A.J., Mantilacci L. (2003). Antioxidant responses and bioaccumulation in Ictalurus melas under mercury exposure. *Ecotoxicol Environ Saf*. 55, 162-167.

Elias C.F., Lee C.E., Kelly J.F., Ahima R.S., Kuhar M., Saper C.B., Elmquist J.K. (2001). Characterization of CART neurons in the rat and human hypothalamus. *J Comp Neurol*. 432, 1-19.

Elsner J., Hodel B., Suter K.E., Oelke D., Ulbrich B., Schreiner G., Cuomo V., Cagiano R., Rosengren L.E., Karlsson J.E., Haglid K.G. (1988). Detection limits of different approaches in behavioral teratology, and correlation of effects with neurochemical parameters. *Neurotoxicol Teratol*. 10, 155-167.

Escriva H., Safi R., Hänni C., Langlois M.C., Saumitou-Laprade P., Stehelin D., Capron A., Pierce R., Laudet V. (1997). Ligand binding was acquired during evolution of nuclear receptors. *Proc Natl Acad Sci U S A*. 94, 6803-6808.

Eskelinen E.L., Schmidt C.K., Neu S., Willenborg M., Fuertes G., Salvador N., Tanaka Y., Lüllmann-Rauch R., Hartmann D., Heeren J., von Figura K., Knecht E., Saftig P. (2004). Disturbed cholesterol traffic but normal proteolytic function in LAMP-1/LAMP-2 double-deficient fibroblasts. *Mol Biol Cell*. 15, 3132-3145.

Esser A.F. (1994). The membrane attack complex of complement. Assembly, structure and cytotoxic activity. *Toxicology*. 87, 229-247.

Eto K. (1997). Pathology of Minamata disease. *Toxicol Pathol*. 25, 614-623

Eto K., Marumoto M., Takeya M. (2010). The pathology of methylmercury poisoning (Minamata disease). *Neuropathology*. 30, 471-479.

Fekete D.M., Muthukumar S., Karagogeos D. (1998). Hair cells and supporting cells share a common progenitor in the avian inner ear. *J Neurosci*. 18, 7811-7821.

Filbin M.T., Walsh F.S., Trapp B.D., Pizzey J.A., Tennekoon G.I. (1990). Role of myelin P0 protein as a homophilic adhesion molecule. *Nature*. 344, 871-872.

Flicek P., Aken B.L., Ballester B., Beal K., Bragin E., Brent S., Chen Y., Clapham P., Coates G., Fairley S., Fitzgerald S., Fernandez-Banet J., Gordon L, Gräf S., Haider S., Hammond M., Howe K., Jenkinson A., Johnson N., Kähäri A., Keefe D., Keenan S., Kinsella R., Kokocinski F., Koscielny G., Kulesha E., Lawson D., Longden I., Massingham T., McLaren W., Megy K., Overduin B., Pritchard B., Rios D., Ruffier M., Schuster M., Slater G., Smedley D., Spudich G., Tang Y.A., Trevanion S., Vilella A., Vogel J., White S., Wilder S.P., Zadissa A., Birney E., Cunningham F., Dunham I., Durbin R., Fernández-Suarez X.M., Herrero J., Hubbard T.J., Parker A., Proctor G., Smith J., Searle S.M. (2010). Ensembl's 10th year. *Nucleic Acids Res*. 38, D557-562.

Follonier Castella L., Gabbiani G., McCulloch C.A., Hinz B. (2010). Regulation of myofibroblast activities: calcium pulls some strings behind the scene. *Exp Cell Res*. 316, 2390-2401.

Froehlicher M., Liedtke A., Groh K.J., Neuhauss S.C., Segner H., Eggen R.I. (2009). Zebrafish (Danio rerio) neuromast: promising biological endpoint linking developmental and toxicological studies. *Aquat Toxicol*. 95, 307-319.

Gao B., Jeong W.I., Tian Z. (2008). Liver: An organ with predominant innate immunity. *Hepatology*. 47, 729-736.

Gastl G., Huber C. (1988). The biology of interferon actions. *Blut*. 56, 193-199.

Gatzidou E.T., Zira A.N., Theocharis S.E. (2007). Toxicogenomics: a pivotal piece in the puzzle of toxicological research. *J Appl Toxicol*. 27, 302-309.

Geiben-Lynn R., Kursar M., Brown N.V., Addo M.M., Shau H., Lieberman J., Luster A.D., Walker B.D. (2003). HIV-1 antiviral activity of recombinant natural killer cell enhancing factors, NKEF-A and NKEF-B, members of the peroxiredoxin family. *J Biol Chem*. 278, 1569-1574.

Geier D.A., Sykes L.K., Geier M.R. (2007). A review of Thimerosal 6 (Merthiolate) and its ethylmercury breakdown product: specific historical considerations regarding safety and effectiveness. *J Toxicol Environ Health B Crit Rev*. 10, 575-596.

Geldmacher-Voss B., Reugels A.M., Pauls S., Campos-Ortega J.A. (2003). A 90 degrees rotation of the mitotic spindle changes the orientation of mitoses of zebrafish neuroepithelial cells. *Development*. 130, 3767-3780.

Ghysen A., Dambly-Chaudière C. (2004). Development of the zebrafish lateral line. *Curr Opin Neurobiol*. 14, 67-73.

Ghysen A., Dambly-Chaudière C. (2007). The lateral line microcosmos. *Genes Dev*. 21, 2118-2130.

Gilbert S.G., Rice D.C., Burbacher T.M. (1996). Fixed interval/fixed ratio performance in adult monkeys exposed in utero to methylmercury. *Neurotoxicol Teratol*. 18, 539-546.

Gillingham A.K., Munro S. (2007). The small G proteins of the Arf family and their regulators. *Annu Rev Cell Dev Biol*. 23, 579-611.

Goldman D., Hankin M-, Li Z., Dai X., Ding J. (2001). Transgenic zebrafish for studying nervous system development and regeneration. *Transgenic Res*. 10, 21-33.

Gomase V.S., Tagore S. (2008). Toxicogenomics. *Curr Drug Metab*. 9, 250-254.

Gompel N., Cubedo N., Thisse C., Thisse B., Dambly-Chaudière C., Ghysen A. (2001). Pattern formation in the lateral line of zebrafish. *Mech Dev*. 105, 69-77.

Gonzalez P., Dominique Y., Massabuau J.C., Boudou A., Bourdineaud J.P. (2005). Comparative effects of dietary methylmercury on gene expression in liver, skeletal muscle, and brain of the zebrafish (Danio rerio). *Environ Sci Technol*. 39, 3972-3980.

Grandjean P, Weihe P, White RF, Debes F., Araki S, Yokoyama K., Murata K., Sørensen N., Dahl R., Jørgensen P.J. (1997). Cognitive deficit in 7-year-old children with prenatal exposure to methylmercury. *Neurotoxicol Teratol*. 19, 417-428.

Grandjean P., Landrigan P.J. (2006). Developmental neurotoxicity of industrial chemicals. *Lancet*. 368, 2167-2178.

Grandjean P., Weihe P., Jørgensen P.J., Clarkson T., Cernichiari E., Viderø T. (1992). Impact of maternal seafood diet on fetal exposure to mercury, selenium, and lead. *Arch Environ Health*. 47, 185-195.

Greenwood M.R. (1985). Methylmercury poisoning in Iraq. An epidemiological study of the 1971-1972 outbreak. *J Appl Toxicol*. 5, 148-159.

Greigl R.A., Krzynowek J. (1979). Mercury Concentrations in Three Species of Tunas Collected from Various Oceanic Waters. *Bull. Environm. Contam. Toxicol*. 22,120-127

Gulati-Leekha A., Goldman D. (2006). A reporter-assisted mutagenesis screen using alpha 1-tubulin-GFP transgenic zebrafish uncovers missteps during neuronal development and axonogenesis. *Dev Biol*. 296, 29-47.

Hadzhiev Y, Lele Z, Schindler S, Wilson SW, Ahlberg P, Strähle U, Müller F. (2007). Hedgehog signaling patterns the outgrowth of unpaired skeletal appendages in zebrafish. *BMC Dev Biol*. 7, 75.

Hai T., Wolford C.C., Chang Y.S. (2010). ATF3, a hub of the cellular adaptive-response network, in the pathogenesis of diseases: is modulation of inflammation a unifying component? *Gene Expr*. 15, 1-11.

Halestrap A.P., Meredith D. (2004). The SLC16 gene family-from monocarboxylate transporters (MCTs) to aromatic amino acid transporters and beyond. *Pflugers Arch*. 447, 619-628.

Hamadeh H.K., Bushel P.R., Jayadev S., Martin K., DiSorbo O., Sieber S., Bennett L., Tennant R., Stoll R., Barrett J.C., Blanchard K., Paules R.S., Afshari C.A. (2002). Gene expression analysis reveals chemical-specific profiles. *Toxicol Sci*. 67, 219-231.

Harada M. (1995). Minamata disease: methylmercury poisoning in Japan caused by environmental pollution. *Crit Rev Toxicol*. 25, 1-24.

Hargreaves R.J., Evans J.G., Janota I., Magos L., Cavanagh J.B. (1988). Persistent mercury in nerve cells 16 years after metallic mercury poisoning. *Neuropathol Appl Neurobiol*. 14, 443-452.

Harr M.W., Distelhorst C.W. (2010). Apoptosis and autophagy: decoding calcium signals that mediate life or death. *Cold Spring Harb Perspect Biol*. 2, a005579.

Hassan S.A., Moussa E.A., Abbott L.C. (2011). The effect of methylmercury exposure on early central nervous system development in the zebrafish (Danio rerio) embryo. *J Appl Toxicol*. doi: 10.1002/jat.1675.

Heisinger J.F., Green W. (1975). Mercuric chloride uptake by eggs of the ricefish and resulting teratogenic effects. *Bull Environ Contam Toxicol*. 14, 665-673.

Hellou J., Fancey L.L. and Payne J.F. (1992). Concentrations of twenty-four elements in bluefin tuna, Thunnus thynnus from the Northwest Atlantic. *Chemosphere*. 24, 211-218,

Henkel G., Krebs B. (2004). Metallothioneins: zinc, cadmium, mercury, and copper thiolates and selenolates mimicking protein active site features--structural aspects and biological implications. *Chem Rev*. 104, 801-824.

Herbomel P., Thisse B., Thisse C. (1999). Ontogeny and behaviour of early macrophages in the zebrafish embryo. *Development*. 126, 3735-45.

Herdegen T., Waetzig V. (2001). AP-1 proteins in the adult brain: facts and fiction about effectors of neuroprotection and neurodegeneration. *Oncogene*. 20, 2424-2437.

Hernández P.P., Olivari F.A., Sarrazin A.F., Sandoval P.C., Allende M.L. (2007). Regeneration in zebrafish lateral line neuromasts: expression of the neural progenitor cell marker sox2 and proliferation-dependent and-independent mechanisms of hair cell renewal. *Dev Neurobiol*. 67, 637-654.

Hewitson L., Houser L.A., Stott C., Sackett G., Tomko J.L., Atwood D., Blue L., White E.R. (2010). Delayed acquisition of neonatal reflexes in newborn primates receiving a thimerosal-containing hepatitis B vaccine: influence of gestational age and birth weight. *J Toxicol Environ Health A*. 73, 1298-1313.

Hill A.J., Teraoka H., Heideman W., Peterson R.E. (2005). Zebrafish as a model vertebrate for investigating chemical toxicity. *Toxicol Sci*. 86, 6-19.

Hillegass J.M., Villano C.M., Cooper K.R., White L.A. (2007). Matrix metalloproteinase-13 is required for zebra fish (Danio rerio) development and is a target for glucocorticoids. *Toxicol Sci*. 100, 168-179.

Hillegass J.M., Villano C.M., Cooper K.R., White L.A. (2008). Glucocorticoids alter craniofacial development and increase expression and activity of matrix metalloproteinases in developing zebrafish (Danio rerio). *Toxicol Sci*. 102, 413-424.

Hinz S., Kempkensteffen C., Christoph F., Krause H., Schrader M., Schostak M., Miller K., Weikert S. (2008). Expression parameters of the polycomb group proteins BMI1, SUZ12, RING1 and CBX7 in urothelial carcinoma of the bladder and their prognostic relevance. *Tumour Biol*. 29, 323-39.

Ho C.Y. (2010). Hypertrophic cardiomyopathy. *Heart Fail Clin*. 6, 141-159.

Huang H., Wu Q. (2010). Cloning and comparative analyses of the zebrafish Ugt repertoire reveal its evolutionary diversity. *PLoS One*. 5, e9144.

Hunziker W., Simmen T., Höning S. (1996). Trafficking of lysosomal membrane proteins in polarized kidney cells. *Nephrologie*. 17, 347-350.

Imai H., Nakagawa Y. (2003). Biological significance of phospholipid hydroperoxide glutathione peroxidase (PHGPx, GPx4) in mammalian cells. *Free Radic Biol Med*. 34, 145-169.

Immenschuh S., Baumgart-Vogt E. (2005). Peroxiredoxins, oxidative stress, and cell proliferation. *Antioxid Redox Signal*. 7, 768-777.

Ingham P.W., McMahon A.P. (2001). Hedgehog signaling in animal development: paradigms and principles. *Genes Dev*. 15, 3059-3087.

Intebi A.D., Flaxman M.S., Ganong W.F., Deschepper C.F. (1990). Angiotensinogen production by rat astroglial cells in vitro and in vivo. *Neuroscience*. 34, 545-554.

Iovine M.K. (2007). Conserved mechanisms regulate outgrowth in zebrafish fins. *Nat Chem Biol*. 3, 613-618.

Ishii T., Yanagawa T. (2007) Stress-induced peroxiredoxins. *Subcell Biochem*. 44, 375-384.

Itoh K., Chiba T., Takahashi S., Ishii T., Igarashi K., Katoh Y., Oyake T., Hayashi N., Satoh K., Hatayama I., Yamamoto M., Nabeshima Y. (1997). An Nrf2/small Maf heterodimer mediates the induction of phase II detoxifying enzyme genes through antioxidant response elements. *Biochem Biophys Res Commun*. 236, 313-322.

Ivask A., Hakkila K., Virta M. (2001). Detection of organomercurials with sensor bacteria. *Anal Chem*. 73, 5168-5171.

Jaeschke H., Gores G.J., Cederbaum A.I., Hinson J.A., Pessayre D., Lemasters J.J. (2002). Mechanisms of hepatotoxicity. *Toxicol Sci*. 65, 166-176.

Jaiswal A.K. (2004). Nrf2 signaling in coordinated activation of antioxidant gene expression. *Free Radic Biol Med*. 36, 1199-1207.

Jalili M.A., Abbasi A.H. (1961). Poisoning by ethyl mercury toluene sulphonanilide. *Br J Ind Med*. 18, 303-308.

Jin M.H., Lee Y.H., Kim J.M., Sun H.N., Moon E.Y., Shong M.H., Kim S.U., Lee S.H., Lee T.H., Yu D.Y., Lee D.S. (2005). Characterization of neural cell types expressing peroxiredoxins in mouse brain. *Neurosci Lett*. 381, 252-257.

Johansson C., Castoldi A.F., Onishchenko N., Manzo L., Vahter M., Ceccatelli S., (2007). Neurobehavioural and molecular changes induced by methylmercury exposure during development. *Neurotoxicol Res*. 11, 241-260.

Johnson R.L., Riddle R.D., Laufer E., Tabin C. (1994). Sonic hedgehog: a key mediator of anterior-posterior patterning of the limb and dorso-ventral patterning of axial embryonic structures. *Biochem Soc Trans*. 22, 569-574.

Joint FAO/WHO Expert Committee on Food Additives. (2011). Evaluation of certain veterinary drug residues in food. Sixty-sixth report of the Joint FAO/WHO Expert Committee on Food Additives. *World Health Organ Tech Rep Ser*. 959, 55-56.

Jones D.P., Go Y.M. (2010). Redox compartmentalization and cellular stress. *Diabetes Obes Metab*. 12 Suppl 2, 116-125.

Julshamn K., Andersen A., Ringdal O., Mørkøre J. (1987). Trace elements intake in the Faroe Islands. I. Element levels in edible parts of pilot whales (Globicephalus meleanus). *Sci Total Environ*. 65, 53-62.

Kakita A., Wakabayashi K., Su M., Yoneoka Y., Sakamoto M., Ikuta F., Takahashi H. (2000b). Intrauterine methylmercury intoxication. Consequences of the inherent brain lesions and cognitive dysfunction in maturity. *Brain Res*. 877, 322-330.

Kakita A., Wakabayashi K., Su M., Yoneoka Y., Sakamoto, M., Ikuta, F. and Takahashi, H. (2000a). Distinct pattern of neuronal degeneration in the fetal rat brain induced by consecutive transplacental administration of methylmercury. *Brain Res*. 859, 233-239.

Kang H.J., Ki C.S., Kim Y.S., Hur M., Jang S.I., Min K.S. (2006). Two mutations of the C7 gene, c.1424G > A and c.281-1G > T, in two Korean families. *J Clin Immunol*. 26, 186-191.

Karamitopoulou E., Pallante P., Zlobec I., Tornillo L., Carafa V., Schaffner T., Borner M., Diamantis I., Esposito F., Brunner T., Zimmermann A., Federico A., Terracciano L., Fusco A. (2010). Loss of the CBX7 protein expression correlates with a more aggressive phenotype in pancreatic cancer. *Eur J Cancer*. 46, 1438-1444.

Kawakami K., Sato S., Ozaki H., Ikeda K. (2000). Six family genes--structure and function as transcription factors and their roles in development. *Bioessays*. 22, 616-626.

Kelsh R.N., Brand M., Jiang Y.J., Heisenberg C.P., Lin S., Haffter P., Odenthal J., Mullins M.C., van Eeden F.J., Furutani-Seiki M., Granato M., Hammerschmidt M., Kane D.A., Warga R.M., Beuchle D., Vogelsang L., Nüsslein-Volhard C. (1996). Zebrafish pigmentation mutations and the processes of neural crest development. *Development*. 123, 369-389.

Kenow K.P., Hoffman D.J., Hines R.K., Meyer M.W., Bickham J.W., Matson C.W., Stebbins K.R., Montagna P., Elfessi A. (2008). Effects of methylmercury exposure on glutathione metabolism, oxidative stress, and chromosomal damage in captive-reared common loon (Gavia immer) chicks. *Environ Pollut*. 156, 732-738.

Kidd P. (1997). Glutathione: Systemic protectant against oxidative and free radical damage. *Altern Med Rev*. 2, 155-176.

Kim S.U., Hwang C.N., Sun H.N., Jin M.H., Han Y.H., Lee H., Kim J.M., Kim S.K., Yu D.Y., Lee D.S., Lee S.H. (2008). Peroxiredoxin I is an indicator of microglia activation and protects against hydrogen peroxide-mediated microglial death. *Biol Pharm Bull*. 31, 820-825.

Kimmel C.B., Ballard W.W., Kimmel S.R., Ullmann B., Schilling T.F. (1995). Stages of embryonic development of the zebrafish. *Dev Dyn*. 203, 253-310.

King C.D., Rios G.R., Green M.D., Tephly T.R. (2000). UDP-glucuronosyltransferases. *Curr Drug Metab*. 1, 143-1461.

King J.K., Kostka J.E., Frischer M.E., Saunders F.M. (2000). Sulfate-reducing bacteria methylate mercury at variable rates in pure culture and in marine sediments. *Appl Environ Microbiol*. 66, 2430-2437.

Kjellstrom T., Kennedy P., Wallis S., Mantell C. (1986). Physical and Mental Development of Children with Prenatal Exposure to Mercury from Fish. Stage I: Preliminary Tests at Age 4. National Swedish Environmental Board, Solna. Report 3080.

Kjellstrom T., Kennedy P., Wallis S., Stewart A., Friberg L., Lind B., Wutherspoon T., Mantell C. (1989). Physical and Mental Development of Children with Prenatal Exposure to Mercury from Fish. Stage 2: Interviews and Psychological Tests at Age 6. National Swedish Environmental Board, Solna. Report 3642.

Klaassen C.D., Liu J., Choudhuri S. (1999). Metallothionein: an intracellular protein to protect against cadmium toxicity. *Annu Rev Pharmacol Toxicol*. 39, 267-294.

Klaper R., Carter B.J., Richter C.A., Drevnick P.E., Sandheinrich M.B., Tillitt D.E. (2008). Use of a 15 k gene microarray to determine gene expression changes in response to acute and chronic methylmercury exposure in the fathead minnow Pimephales promelas Rafinesque. *J Fish Biol.* 72, 2207-2280.

Kobal A.B., Horvat M., Prezelj M., Briski A.S., Krsnik M., Dizdarevic T., Mazej D., Falnoga I., Stibilj V., Arneric N., Kobal D., Osredkar J. (2004). The impact of long-term past exposure to elemental mercury on antioxidative capacity and lipid peroxidation in mercury miners. *J Trace Elem Med Biol*. 17, 261-274.

Kobayashi M., Toyama R., Takeda H., Dawid I.B., Kawakami K. (1998). Overexpression of the forebrain-specific homeobox gene six3 induces rostral forebrain enlargement in zebrafish. *Development*. 125, 2973-2982.

Koide S., Kugiyama K., Sugiyama S., Nakamura S., Fukushima H., Honda O., Yoshimura M., Ogawa H. (2003). Association of polymorphism in glutamate-cysteine ligase catalytic subunit gene with coronary vasomotor dysfunction and myocardial infarction. *J Am Coll Cardiol*. 41, 539-545.

Kojima E., Takeuchi A., Haneda M., Yagi A., Hasegawa T., Yamaki K., Takeda K., Akira S., Shimokata K., Isobe K. (2003). The function of GADD34 is a recovery from a shutoff of protein synthesis induced by ER stress: elucidation by GADD34-deficient mice. *FASEB J.* 17, 1573-1575.

Kondos S.C., Hatfaludi T., Voskoboinik I., Trapani J.A., Law R.H., Whisstock J.C., Dunstone M.A. (2010). The structure and function of mammalian membrane-attack complex/perforin-like proteins. *Tissue Antigens*. 76, 341-351

Korashy H.M., El-Kadi A.O. (2008). The role of redox-sensitive transcription factors NF-kappaB and AP-1 in the modulation of the Cyp1a1 gene by mercury, lead, and copper. *Free Radic Biol Med*. 44, 795-806

Korbas M., Blechinger S.R., Krone P.H., Pickering I.J., George G.N. (2008). Localizing organomercury uptake and accumulation in zebrafish larvae at the tissue and cellular level. *Proc Natl Acad Sci U S A*. 105, 12108-12112.

Korbas M., Krone P.H, Pickering I.J., George G.N.(2010). Dynamic accumulation and redistribution of methylmercury in the lens of developing zebrafish embryos and larvae. *J Biol Inorg Chem*. 15, 1137-1145.

Kozak S., Forsberg CW. (1979). Transformation of mercuric chloride and methylmercury by the rumen microflora. *Appl Environ Microbiol*. 38, 626-636.

Krauss S., Concordet J.P., Ingham P.W. (1993). A functionally conserved homolog of the Drosophila segment polarity gene hh is expressed in tissues with polarizing activity in zebrafish embryos. *Cell*. 75, 1431-1444.

Krauss S., Johansen T., Korzh V., Fjose A. (1991). Expression pattern of zebrafish pax genes suggests a role in early brain regionalization. *Nature*. 353, 267-270.

Kuhar M.J., Adams L.D., Hunter R.G., Vechia S.D., Smith Y. (2000). CART peptides. *Regul Pept*. 89, 1-6.

Kumari M.V., Hiramatsu M., Ebadi M. (1998). Free radical scavenging actions of metallothionein isoforms I and II. *Free Radic Res*. 29, 93-101.

Kumari M.V., Hiramatsu M., Ebadi M. (2000). Free radical scavenging actions of hippocampal metallothionein isoforms and of antimetallothioneins: an electron spin resonance spectroscopic study. *Cell Mol Biol (Noisy-le-grand)*. 46, 627-636.

Kusik B.W., Carvan M.J. 3rd, Udvadia A.J. (2008). Detection of mercury in aquatic environments using EPRE reporter zebrafish. *Mar Biotechnol (NY)*. 10, 750-757.

Laale H.W. (1977) The biology and use of zebrafish, Brachydanio rerio, in fisheries research. A literature review. *J Fish Biol*. 10, 121-173.

Lam C.S., Rastegar S., Strähle U. (2006). Distribution of cannabinoid receptor 1 in the CNS of zebrafish. *Neuroscience*. 138, 83-95.

Lavoie S., Chen Y., Dalton T.P., Gysin R., Cuénod M., Steullet P., Do K.Q. (2009). Curcumin, quercetin, and tBHQ modulate glutathione levels in astrocytes and neurons: importance of the glutamate cysteine ligase modifier subunit. *J Neurochem*. 108, 1410-1422.

Ledent V. (2002). Postembryonic development of the posterior lateral line in zebrafish. *Development*. 129, 597-604

Lee D., Michalak M. (2010). Membrane associated Ca2+ buffers in the heart. *BMB Rep*. 43, 151-157.

Legradi J. (2011). Microarray based transcriptomics and the search for biomarker genes in zebrafish. Unpublished dortoral dissertation. The Ruperto-Carola University of Heidelberg, Heidelberg, Germany.

Lemaître V., D'Armiento J. (2006). Matrix metalloproteinases in development and disease. *Birth Defects Res C Embryo Today*. 78, 1-10.

Lemke G., Axel R. (1985). Isolation and sequence of a cDNA encoding the major structural protein of peripheral myelin. *Cell*. 40, 501-508.

Letz R., Gerr F., Cragle D., Green R.C., Watkins J., Fidler A.T. (2000). Residual neurologic deficits 30 years after occupational exposure to elemental mercury. *Neurotoxicology*. 21, 459-474.

Lewis K.E., Eisen J.S. (2001). Hedgehog signaling is required for primary motoneuron induction in zebrafish. *Development*. 128, 3485-3495.

Liang G., Wolfgang C.D., Chen B.P., Chen T.H., Hai T. (1996). ATF3 gene. Genomic organization, promoter, and regulation. *J Biol Chem*. 271, 1695-1701.

Lin T.H., Huang Y.L., Huang S.F. (1996). Lipid peroxidation in liver of rats administrated with methyl mercuric chloride. *Biol Trace Elem Res*. 54, 33-41.

Liu Y., Wang J., Wei Y., Zhang H., Xu M., Dai J. (2008). Induction of time-dependent oxidative stress and related transcriptional effects of perfluorododecanoic acid in zebrafish liver. *Aquat Toxicol*. 89, 242-250.

Long K.R., Yamamoto Y., Baker A.L., Watkins S.C., Coyne C.B., Conway J.F., Aridor M. (2010). Sar1 assembly regulates membrane constriction and ER export. *J Cell Biol*. 190, 115-128.

Lowery L.A., Sive H. (2004). Strategies of vertebrate neurulation and a re-evaluation of teleost neural tube formation. *Mech Dev*. 121, 1189-1197.

Lu S.C. (2009). Regulation of glutathione synthesis. *Mol Aspects Med*. 30, 42-59.

Luo R., An M., Arduini B.L., Henion P.D. (2001). Specific pan-neural crest expression of zebrafish Crestin throughout embryonic development. *Dev Dyn*. 220, 169-174.

Lyons D.A., Pogoda H.M., Voas M.G., Woods I.G., Diamond B., Nix R., Arana N., Jacobs J., Talbot W.S. (2005). erbb3 and erbb2 are essential for schwann cell migration and myelination in zebrafish. *Curr Biol*. 15, 513-524.

Madenjian C.P., O'Connor D.V. (2008). Trophic transfer efficiency of mercury to lake whitefish Coregonus clupeaformis fro m its prey. *Bull Environ Contam Toxicol*. 81, 566-570.

Magos L., Brown A.W., Sparrow S., Bailey E., Snowden R.T., Skipp W.R. (1985). The comparative toxicology of ethyl- and methylmercury. *Arch Toxicol*. 57, 260-267.

Magos L., Clarkson T.W. (2006). Overview of the clinical toxicity of mercury. *Ann Clin Biochem*. 43, 257-268.

Mangrum W.I., Dowling J.E., Cohen E.D. (2002). A morphological classification of ganglion cells in the zebrafish retina. *Vis Neurosci*. 19, 767-779.

Markowski V.P., Flaugher C.B., Baggs R.B., Rawleigh R.C., Cox C., Weiss B. (1998). Prenatal and lactational exposure to methylmercury affects select parameters of mouse cerebellar development. *Neurotoxicology*. 19, 879-892.

Martin P., Leibovich S.J. (2005). Inflammatory cells during wound repair: the good, the bad and the ugly. *Trends Cell Biol*. 15, 599-607.

Mela M., Cambier S., Mesmer-Dudons N., Legeay A., Grötzner S.R., de Oliveira Ribeiro C.A., Ventura D.F., Massabuau J.C. (2010). Methylmercury localization in Danio rerio retina after trophic and subchronic exposure: a basis for neurotoxicology. *Neurotoxicology*. 31, 448-453.

Meredith D., Christian H.C. (2008). The SLC16 monocaboxylate transporter family. *Xenobiotica*. 38, 1072-1106.

Metcalfe W.K, Kimmel C.B, Schabtach E. (1985). Anatomy of the posterior lateral line system in young larvae of the zebrafish. *J Comp Neurol*. 233, 377-389.

Milde-Langosch K. (2005). The Fos family of transcription factors and their role in tumourigenesis. *Eur J Cancer*. 41, 2449-2461.

Minchenko O.H., Ochiai A., Opentanova I.L., Ogura T., Minchenko D.O., Caro J., Komisarenko S.V., Esumi H. (2005a). Overexpression of 6-phosphofructo-2-kinase/fructose-2,6-bisphosphatase-4 in the human breast and colon malignant tumors. *Biochimie*. 87, 1005-1010.

Minchenko O.H., Ogura T., Opentanova I.L., Minchenko D.O., Esumi H. (2005b). Splice isoform of 6-phosphofructo-2-kinase/fructose-2,6-bisphosphatase-4: expression and hypoxic regulation. *Mol Cell Biochem*. 280, 227-234.

Minchenko O.H., Opentanova I.L., Ogura T., Minchenko D.O., Komisarenko S.V., Caro J., Esumi H. (2005c). Expression and hypoxia-responsiveness of 6-phosphofructo-2-kinase/fructose-2,6-bisphosphatase 4 in mammary gland malignant cell lines. *Acta Biochim Pol*. 52, 881-888.

Miners J.O., McKinnon R.A., Mackenzie P.I. (2002). Genetic polymorphisms of UDP-glucuronosyltransferases and their functional significance. *Toxicology*. 181-182, 453-456.

Mitchell J.W., Kjellstrom T.E., Reeves R.L. (1982). Mercury in takeaway fish in New Zealand. *N Z Med J*. 95, 112-114.

Mizusawa H., Ishii T., Bannai S. (2000). Peroxiredoxin I (macrophage 23 kDa stress protein) is highly and widely expressed in the rat nervous system. *Neurosci Lett*. 283, 57-60.

Morcos P.A. (2007). Achieving targeted and quantifiable alteration of mRNA splicing with Morpholino oligos. *Biochem Biophys Res Commun*. 358, 521-527.

Morey L., Helin K. (2010). Polycomb group protein-mediated repression of transcription. *Trends Biochem Sci*. 35, 323-332

Morgan B.P., Gasque P., Singhrao S., Piddlesden S.J. (1997). The role of complement in disorders of the nervous system. *Immunopharmacology*. 38, 43-50.

Moszczyński P. (1997). Mercury compounds and the immune system: a review. *Int J Occup Med Environ Health*. 10, 247-258.

Motohashi H., Shavit J.A., Igarashi K., Yamamoto M., Engel J.D. (1997). The world according to Maf. *Nucleic Acids Res*. 25, 2953-2959.

Müller F., Albert S., Blader P., Fischer N., Hallonet M., Strähle U. (2000). Direct action of the nodal-related signal cyclops in induction of sonic hedgehog in the ventral midline of the CNS. *Development* 127, 3889-3897.

Müller F., Chang B., Albert S., Fischer N., Tora L., Strähle U. (1999). Intronic enhancers control expression of zebrafsih sonic hedgehog in floor plate and notochord. *Development* 126, 2103-2116.

Müller-Eberhard H.J. (1985). The killer molecule of complement. *J Invest Dermatol*. 85, 47s-52s.

Mullins D.N., Crawford E.L., Khuder S.A., Hernandez D.A., Yoon Y., Willey J.C. (2005). CEBPG transcription factor correlates with antioxidant and DNA repair genes in normal bronchial epithelial cells but not in individuals with bronchogenic carcinoma. *BMC Cancer*. 5, 141.

Myers G.J., Davidson P.W., Cox C., Shamlaye C.F., Palumbo D., Cernichiari E., Sloane-Reeves J., Wilding G.E., Kost J., Huang L.S., Clarkson T.W. (2003). Prenatal methylmercury exposure from ocean fish consumption in the Seychelles child development study. *Lancet*. 361, 1686-1692.

Myers G.J., Thurston S.W., Pearson A.T., Davidson P.W., Cox C., Shamlaye C.F., Cernichiari E., Clarkson T.W. (2009). Postnatal exposure to methyl mercury from fish consumption: a review and new data from the Seychelles Child Development Study. *Neurotoxicology*. 30, 338-349.

Nakamura S., Sugiyama S., Fujioka D., Kawabata K., Ogawa H., Kugiyama K. (2003). Polymorphism in glutamate-cysteine ligase modifier subunit gene is associated with impairment of nitric oxide-mediated coronary vasomotor function. *Circulation*. 108, 1425-1427.

Nakaso K., Kitayama M., Mizuta E., Fukuda H., Ishii T., Nakashima K., Yamada K. (2000). Co-induction of heme oxygenase-1 and peroxiredoxin I in astrocytes and microglia around hemorrhagic region in the rat brain. *Neurosci Lett*. 293, 49-52.

National Academy of Sciences (NAS). (2000). Toxicological Effects of Methylmercury. National Academy of Sciences, Washington, D.C. http://nap.edu/books/0309071402/html

Neumann C.A., Cao J., Manevich Y. (2009). Peroxiredoxin 1 and its role in cell signaling. *Cell Cycle*. 8, 4072-4078.

New Jersey Department of Environmental Protection and Energy (NJDEPE). (1993) Final Report on Municipal Solid Waste Incineration. Volume II: Environmental and Health Issues.

Nicholson D.W., Ali A., Thornberry N.A., Vaillancourt J.P., Ding C.K., Gallant M., Gareau Y., Griffin P.R., Labelle M., Lazebnik Y.A., Munday N.A., Raju S.M., Smulson M.E., Yamin T., Yu V.L., Miller D.K. (1995). Identification and inhibition of the ICE/CED-3 protease necessary for mammalian apoptosis. *Nature*. 376, 37-43.

Nickle B., Robinson P.R. (2007). The opsins of the vertebrate retina: insights from structural, biochemical, and evolutionary studies. *Cell Mol Life Sci*. 64, 2917-2932.

Novoa I., Zeng H., Harding H., Ron D. (2001). Feedback inhibition of the unfolded protein response by GADD34-mediated dephosphorylation of eIF2alpha. *J Cell Biol* 153, 1011-1022.

Novoa I., Zhang Y., Zeng H., Jungreis R., Harding H.P., Ron D. (2003) Stress-induced gene expression requires programmed recovery from translational repression. *EMBO J.* 22, 1180-1187.

Nuwaysir E.F., Bittner M., Trent J., Barrett J.C., Afshari C.A. (1999). Microarrays and toxicology: the advent of toxicogenomics. *Mol Carcinog*. 24, 153-159.

O'Hara A.M., Fernie B.A., Moran A.P., Williams Y.E., Connaughton J.J., Orren A., Hobart M.J. (1998). C7 deficiency in an Irish family: a deletion defect which is predominant in the Irish. *Clin Exp Immunol*. 114, 355-361.

Olsson S., Bergman M. (1992). Daily dose calculations from measurements of intra-oral mercury vapor. *J Dent Res*. 71, 414-423.

Opitz H., Schweinsberg F., Grossmann T., Wendt-Gallitelli M.F., Meyermann R. (1996). Demonstration of mercury in the human brain and other organs 17 years after metallic mercury exposure. *Clin Neuropathol*. 15, 139-144.

Ott M., Walz B.C., Paulsen U.J., Mack A.F., Wagner H.J. (2007). Retinotectal ganglion cells in the zebrafish, Danio rerio. *J Comp Neurol*. 501, 647-658.

Page-McCaw A., Ewald A.J., Werb Z. (2007). Matrix metalloproteinases and the regulation of tissue remodelling. *Nat Rev Mol Cell Biol*. 8, 221-233.

Pallante P., Federico A., Berlingieri M.T., Bianco M., Ferraro A., Forzati F., Iaccarino A., Russo M., Pierantoni G.M., Leone V., Sacchetti S., Troncone G., Santoro M., Fusco A. (2008). Loss of the CBX7 gene expression correlates with a highly malignant phenotype in thyroid cancer. *Cancer Res*. 68, 6770-6778.

Panzer J.A., Gibbs S.M., Dosch R., Wagner D., Mullins M.C., Granato M., Balice-Gordon R.J. (2005). Neuromuscular synaptogenesis in wild-type and mutant zebrafish. *Dev Biol*. 285, 340-357.

Park S.T., Lim K.T., Chung Y.T., Kim S.U. (1996). Methylmercury-induced neurotoxicity in cerebral neuron culture is blocked by antioxidants and NMDA receptor antagonists. *Neurotoxicology*. 17, 37-46.

Parng C., Roy N.M., Ton C., Lin Y., McGrath P. (2007). Neurotoxicity assessment using zebrafish. *J Pharmacol Toxicol Methods*. 55, 103-112.

Pennie W.D., Kimber I. (2002). Toxicogenomics; transcript profiling and potential application to chemical allergy. *Toxicol In Vitro*. 16, 319-326.

Pennie W.D., Woodyatt N.J., Aldridge T.C., Orphanides G. (2001). Application of genomics to the definition of the molecular basis for toxicity. *Toxicol Lett*. 120, 353-358.

Pestka S., Langer J.A., Zoon K.C., Samuel C.E. (1987). Interferons and their actions. *Annu Rev Biochem*. 56, 727-777.

Pilkis S.J., Claus T.H., Kurland I.J., Lange A.J. (1995). 6-Phosphofructo-2-kinase/fructose-2,6-bisphosphatase: a metabolic signaling enzyme. *Annu Rev Biochem*. 64, 799-835.

Piperno G., Fuller M.T. (1985). Monoclonal antibodies specific for an acetylated form of alpha-tubulin recognize the antigen in cilia and flagella from a variety of organisms. *J Cell Biol*. 101, 2085-2094.

Prabhakar N.R., Kumar G.K. (2004). Oxidative stress in the systemic and cellular responses to intermittent hypoxia. *Biol Chem*. 385, 217-221.

Price C.S., Thompson W.W., Goodson B., Weintraub E.S., Croen L.A., Hinrichsen V.L., Marcy M., Robertson A., Eriksen E., Lewis E., Bernal P., Shay D., Davis R.L., DeStefano F. (2010). Prenatal and infant exposure to thimerosal from vaccines and immunoglobulins and risk of autism. *Pediatrics*. 126, 656-664.

Qian F., Zhen F., Ong C., Jin S.W., Meng Soo H., Stainier D.Y., Lin S., Peng J., Wen Z. (2005). Microarray analysis of zebrafish cloche mutant using amplified cDNA and identification of potential downstream target genes. *Dev Dyn*. 233, 1163-1172.

Quig D. (1998). Cysteine metabolism and metal toxicity. *Altern Med Rev*. 3, 262-270.

Racanelli V., Rehermann B. (2006). The liver as an immunological organ. *Hepatology*. 43, S54-62.

Raible D.W, Kruse G.J. (2000). Organization of the lateral line system in embryonic zebrafish. *J Comp Neurol*. 421, 189-198.

Rameix-Welti M.A., Régnier C.H., Bienaimé F., Blouin J., Schifferli J., Fridman W.H., Sautès-Fridman C., Frémeaux-Bacchi V. (2007). Hereditary complement C7 deficiency in nine families: subtotal C7 deficiency revisited. *Eur J Immunol*. 37, 1377-1385.

Redd M.J., Cooper L., Wood W., Stramer B., Martin P. (2004). Wound healing and inflammation: embryos reveal the way to perfect repair. *Philos Trans R Soc Lond B Biol Sci*. 359, 777-784.

Rhee S.G., Chae H.Z., Kim K. (2005), Peroxiredoxins: a historical overview and speculative preview of novel mechanisms and emerging concepts in cell signaling. *Free Radic Biol Med*. 38, 1543-1552.

Rice D., Barone S. Jr. (2000). Critical periods of vulnerability for the developing nervous system: evidence from humans and animal models. *Environ Health Perspect*. 108 Suppl 3:511-33.

Rice D.C. (1998). Age-related increase in auditory impairment in monkeys exposed in utero plus postnatally to methylmercury. *Toxicol Sci*. 44, 191-196.

Rice D.C., Schoeny R., Mahaffey K. (2003). Methods and rationale for derivation of a reference dose for methylmercury by the U.S. EPA *Risk Anal*. 23, 107-115.

Richetti S.K., Rosemberg D.B., Ventura-Lima J., Monserrat J.M., Bogo M.R., Bonan C.D. (2010). Acetylcholinesterase activity and antioxidant capacity of zebrafish brain is altered by heavy metal exposure. *Neurotoxicology*. 32, 116-122.

Richter C.A., Garcia-Reyero N., Martyniuk C., Knoebl I., Pope M., Wright-Osment M.K., Denslow N.D., Tillitt D.E. (2011). Gene expression changes in female zebrafish (Danio rerio) brain in response to acute exposure to methylmercury. *Environ Toxicol Chem*. 30, 301-308.

Riddle R.D., Johnson R.L., Laufer E., Tabin C. (1993). Sonic hedgehog mediates the polarizing activity of the ZPA. *Cell*. 75, 1401-1416.

Roberson D.W., Alosi J.A., Cotanche D.A. (2004). Direct transdifferentiation gives rise to the earliest new hair cells in regenerating avian auditory epithelium. *J Neurosci Res*. 78, 461-471.

Robu M.E., Larson J.D., Nasevicius A., Beiraghi S., Brenner C., Farber S.A., Ekker S.C. (2007). p53 activation by knockdown technologies. *PLoS Genet*. 3, e78.

Rodier P.M. (1995). Developing brain as a target of toxicity. *Environ Health Perspect*. 103, 73-76.

Rodier P.M., Aschner M., Sager P.R. (1984). Mitotic arrest in the developing CNS after prenatal exposure to methylmercury. *Neurobehav Toxicol Teratol*. 6, 379-385.

Roesijadi G. (2000). Metal transfer as a mechanism for metallothionein-mediated metal detoxification. *Cell Mol Biol (Noisy-le-grand)*. 46, 393-405.

Rubinstein A.L., Lee D., Luo R., Henion P.D., Halpern M.E. (2000). Genes dependent on zebrafish cyclops function identified by AFLP differential gene expression screen. *Genesis*. 26, 86-97.

Rus H., Cudrici C., David S., Niculescu F. (2006). The complement system in central nervous system diseases. *Autoimmunity*. 39, 395-402.

Rus H., Cudrici C., Niculescu F. (2005). C5b-9 complement complex in autoimmune demyelination and multiple sclerosis: dual role in neuroinflammation and neuroprotection. *Ann Med*. 37, 97-104.

Russel S., Meadows L.A., Russell R.R. (2009). Microarry techonologies in practice, 3rd Edition. Elsevier B.V. Burlington, MA, USA.

Ryals B.M., Rubel E.W. (1988). Hair cell regeneration after acoustic trauma in adult Coturnix quail. *Science*. 240, 1774-1776.

Sager P.R., Aschner M., Rodier P.M. (1984). Persistent, differential alterations in developing cerebellar cortex of male and female mice after methylmercury exposure. *Brain Res*. 314, 1-11.

Saitoh T., Horsburgh K., Masliah E. (1993). Hyperactivation of signal transduction systems in Alzheimer's disease. *Ann N Y Acad Sci*. 695, 34-41.

Sakamoto M., Kakita A., Bezerra de Oliveira R., Pan H.S., Takahashi H. (2004). Dose-dependent effects of methylmercury administered during neonatal brain spurt in rats. *Dev Brain Res*. 152, 171-176.

Sakamoto M., Kakita A., Wakabayashi K., Takahashi H., Nakano A., Akagi H. (2002). Evaluation of changes in methylmercury accumulation in the developing rat brain and its effects: a study with consecutive and moderate dose exposure throughout gestation and lactation periods. *Brain Res*. 949, 51-59.

Sambrook J., Fritsch E.F., Maniatis, T. (1989). Molecular Cloning: A Laboratory Manual. Cold Spring Harbor Laboratory, Cold Spring Harbor, NY, USA.

Sams C.E. (2004). Methylmercury Contamination: Impacts on Aquatic Systems and Terrestrial Species, and Insights for Abatement. M Furniss, C Clifton, K Ronnenberg, eds., 2007. Advancing the Fundamental Sciences: Proceedings of the Forest Service National Earth Sciences Conference, San Diego, CA, 18-22 October 2004, PNWGTR-689, Portland, OR: U.S. Department of Agriculture, Forest Service, Pacific Northwest Research Station. 438-448.

Samson J.C., Goodridge R., Olobatuyi F., Weis J.S. (2001). Delayed effects of embryonic exposure of zebrafish (Danio rerio) to methylmercury (MeHg). *Aquat Toxicol*. 51, 369-376.

Samson J.C., Shenker J. (2000). The teratogenic effects of methylmercury on early development of the zebrafish, Danio rerio. *Aquat Toxicol*. 48, 343-354.

Sandborgh-Englund G., Elinder C.G., Langworth S., Schütz A., Ekstrand J. (1998). Mercury in biological fluids after amalgam removal. *J Dent Res*. 77, 615-624.

Sarafian T. A., Verity M. A., Vinters H. V., Shih C. C., Shi L., Ji X. D., Dong L., Shau H. (1999). Differential expression of peroxiredoxin subtypes in human brain cell types. *J Neurosci Res*. 56, 206-212.

Sarafian T.A. (1999). Methylmercury-induced generation of free radicals: biological implications. *Met Ions Biol Syst*. 36, 415-444.

Savaskan N.E., Ufer C., Kühn H., Borchert A. (2007). Molecular biology of glutathione peroxidase 4: from genomic structure to developmental expression and neural function. *Biol Chem*. 388, 1007-1017.

Schilling T.F., Kimmel C.B. (1994). Segment and cell type lineage restrictions during pharyngeal arch development in the zebrafish embryo. *Development*. 120, 483-494.

Schultz S.T. (2010). Does thimerosal or other mercury exposure increase the risk for autism? A review of current literature. *Acta Neurobiol Exp (Wars)*. 70, 187-195.

Schwartz Y.B., Pirrotta V. (2008). Polycomb complexes and epigenetic states. *Curr Opin Cell Biol*. 20, 266-273.

Scott C.L., Gil J., Hernando E., Teruya-Feldstein J., Narita M., Martínez D., Visakorpi T., Mu D., Cordon-Cardo C., Peters G., Beach D., Lowe S.W. (2007). Role of the chromobox protein CBX7 in lymphomagenesis. *Proc Natl Acad Sci U S A*. 104, 5389-5394.

Seigneur C., Vijayaraghavan K., Lohman K., Karamchandani P., Scott C. (2004). Global source attribution for mercury deposition in the United States. *Environ Sci Technol*. 38, 555-569.

Seo H.C., Drivenes O., Ellingsen S., Fjose A. (1998). Expression of two zebrafish homologues of the murine Six3 gene demarcates the initial eye primordia. *Mech Dev*. 73, 45-57.

Shafer T.J., Contreras M.L., Atchison W.D. (1990). Characterization of interactions of methylmercury with Ca2+ channels in synaptosomes and pheochromocytoma cells: radiotracer flux and binding studies. *Mol Pharmacol*. 38, 102-113.

Shanker G., Aschner J.L., Syversen T., Aschner M. (2004). Free radical formation in cerebral cortical astrocytes in culture induced by methylmercury. *Brain Res Mol Brain Res*. 128, 48-57.

Shanker G., Aschner M. (2003). Methylmercury-induced reactive oxygen species formation in neonatal cerebral astrocytic cultures is attenuated by antioxidants. *Brain Res Mol Brain Res*. 110, 85-91.

Shanker G., Syversen T., Aschner J.L., Aschner M. (2005). Modulatory effect of glutathione status and antioxidants on methylmercury-induced free radical formation in primary cultures of cerebral astrocytes. *Brain Res Mol Brain Res*. 137, 11-22.

Shau H., Gupta R.K., Golub S.H. (1993). Identification of a natural killer enhancing factor (NKEF) from human erythroid cells. *Cell Immunol*. 147, 1-11.

Silbergeld E.K., Silva I.A., Nyland J.F. (2005). Mercury and autoimmunity: implications for occupational and environmental health. *Toxicol. Appl. Pharmacol*. 207, 282–292.

Sirois J.E., Atchison W.D. (2000). Methylmercury affects multiple subtypes of calcium channels in rat cerebellar granule cells. *Toxicol Appl Pharmacol*. 167, 1-11.

Smith J.C., Farris F.F. (1996). Methyl mercury pharmacokinetics in man: a reevaluation. *Toxicol Appl Pharmacol*. 137, 245-252.

Solnica-Krezel L. 2005. Conserved patterns of cell movements during vertebrate gastrulation. *Curr*

Spiryda L.B. (1998). Myelin protein zero and membrane adhesion. *J Neurosci Res*. 54, 137-146.

Stamenkovic I. (2003). Extracellular matrix remodelling: the role of matrix metalloproteinases. *J Pathol*. 200, 448-464.

Stillman M.J., Thomas D., Trevithick C., Guo X., Siu M. (2000). Circular dichroism, kinetic and mass spectrometric studies of copper(I) and mercury(II) binding to metallothionein. *J Inorg Biochem*. 79, 11-19.

Stillmann M.J. (1995). Metallothioneins. *Coordination Chemistry Reviews*. 144, 461-511.

Stohs S.J., Bagchi D. (1995). Oxidative mechanisms in the toxicity of metal ions. *Free Radical Biol Med*. 18, 321-336.

Storch M.K., Piddlesden S., Haltia M., Iivanainen M., Morgan P., Lassmann H. (1998). Multiple sclerosis: in situ evidence for antibody- and complement-mediated demyelination. *Ann Neurol*. 43, 465-471.

Stornetta R.L., Hawelu-Johnson C.L., Guyenet P.G., Lynch K.R. (1998). Astrocytes synthesize angiotensinogen in brain. *Science*. 242, 1444-1446.

Sunyer J.O., Boshra H., Lorenzo G., Parra D., Freedman B., Bosch N. (2003). Evolution of complement as an effector system in innate and adaptive immunity. *Immunol Res*. 27, 549.

Suter L., Babiss L.E., Wheeldon E.B. (2004). Toxicogenomics in predictive toxicology in drug development. *Chem Biol*. 11, 161-171.

Sweet L.I., Zelikoff J.T. (2001). Toxicology and immunotoxicology of mercury: a comparative review in fish and humans. *J Toxicol Environ Health B Crit Rev*. 4, 161-205.

Szydlowska K., Tymianski M. (2010). Calcium, ischemia and excitotoxicity. *Cell Calcium*. 47, 122-129.

Takeuchi T. (1982). Pathology of Minamata disease. With special reference to its pathogenesis. *Acta Pathol Jpn*. 32 Suppl 1, 73-99.

Tamashiro H., Arakaki M., Akagi H., Futatsuka M., Roht LH. (1985). Mortality and survival for Minamata disease. *Int J Epidemiol*. 14, 582-588.

Tan M., Parkin J.E. (2000). Route of decomposition of thiomersal (thimerosal). *Int J Pharm*. 208, 23-34.

Taniguchi T., Ogasawara K., Takaoka A., Tanaka N. (2001). IRF family of transcription factors as regulators of host defense. *Annu Rev Immunol*. 19, 623-655.

Tegla C.A., Cudrici C., Rus V., Ito T., Vlaicu S., Singh A., Rus H. (2009). Neuroprotective effects of the complement terminal pathway during demyelination: implications for oligodendrocyte survival. *J Neuroimmunol*. 213, 3-11.

Templeton D.M., Cherian M.G. (1991). Toxicological significance of metallothionein. *Methods Enzymol*. 205, 11-24, 1991.

Tennant R.W. (2002). The National Center for Toxicogenomics: using new technologies to inform mechanistic toxicology. *Environ Health Perspect*. 110, A8-10.

Tessier-Lavigne M., Mobbs P., Attwell D. (1985). Lead and mercury toxicity and the rod light response. *Invest Ophthalmol Vis Sci*. 26, 1117-1123.

The *Danio rerio* Sequencing Project (http://www.sanger.ac.uk/Projects/D_rerio/). Wellcome Trust Sanger Institute. Accessed 26 August 2011.

Thisse B., Wright G.J., Thisse C. (2008). Embryonic and larval expression patterns from a large scale screening for novel low affinity extracellular protein interactions. ZFIN Direct Data Submission (http://zfin.org).

Thompson J.A., White C.C., Cox D.P., Chan J.Y., Kavanagh T.J., Fausto N., Franklin C.C. (2009). Distinct Nrf1/2-independent mechanisms mediate As 3+-induced glutamate-cysteine ligase subunit gene expression in murine hepatocytes. *Free Radic Biol Med*. 46, 1614-1625.

Thompson M.R., Xu D., Williams B.R. (2009). ATF3 transcription factor and its emerging roles in immunity and cancer. *J Mol Med*. 87, 1053-1060.

Ton C., Lin Y., Willett C. (2006). Zebrafish as a model for developmental neurotoxicity testing. *Birth Defects Res A Clin Mol Teratol*. 76, 553-567.

Tugwood J.D., Hollins L.E., Cockerill M.J. (2003). Genomics and the search for novel biomarkers in toxicology. *Biomarkers*. 8, 79-92.

U.S. Environmental Protection Agency (USEPA). (1995). National Primary Drinking Water Regulations, Contaminant Specific Fact Sheets, Inorganic Chemicals, Technical Version. EPA 811/F-95/002-T. Office of Water, U.S. Environmental Protection Agency, Washington, D.C., USA.

U.S. Environmental Protection Agency (USEPA). (1997). Mercury study report to congress. Volume III: fate and transport of mercury in the environment. EPA-452/R97-005. Office of Air Quality Planning & Standards and Office of Research and Development. U.S. Environmental Protection Agency. Washington, D.C., USA.

U.S. Environmental Protection Agency (USEPA). (2001). Water Quality Criterion for the Protection of Human Health: Methylmercury. EPA-823-R-01-001. Office of Science and Technology, Office of Water, U.S. Environmental Protection Agency, Washington, D.C., USA.

U.S. Environmental Protection Agency (USEPA). (2007). EPA Fact Sheet: 2005/2006 National listing of fish advisories. U.S. Environmental Protection Agency, Washington, DC, USA, EPA-823-F-07-003. http://www.epa.gov/waterscience/fish/advisories/2006/tech.pdf. Accessed 15 June 2011.

U.S. Food and Drug Administration (USFDA). (2010). http://www.fda.gov/BiologicsBloodVaccines/SafetyAvailability/VaccineSafety/UCM096228. Accessed 15 June 2011.

Ung C.Y., Lam S.H., Hlaing M.M., Winata C.L., Korzh S., Mathavan S., Gong Z. (2010). Mercury-induced hepatotoxicity in zebrafish: in vivo mechanistic insights from transcriptome analysis, phenotype anchoring and targeted gene expression validation. *BMC Genomics*. 11, 212.

Vaglia J.L., Hall B.K. (2000). Patterns of migration and regulation of trunk neural crest cells in zebrafish (Danio rerio). *Int J Dev Biol*. 44, 867-881.

Vahter M., Akesson A., Lind B., Björs U., Schütz A., Berglund M. (2000). Longitudinal study of methylmercury and inorganic mercury in blood and urine of pregnant and lactating women, as well as in umbilical cord blood. *Environ Res*. 84, 186-194.

Vallee B.L., Ulmer D.D. (1972). Biochemical effects of mercury, cadmium and lead. *Annu Rev Biochem*. 41, 91-128.

van Beek J., Elward K., Gasque P. (2003). Activation of complement in the central nervous system: roles in neurodegeneration and neuroprotection. *Ann N Y Acad Sci*. 992, 56-71.

van Eeden F.J., Granato M., Schach U., Brand M., Furutani-Seiki M., Haffter P., Hammerschmidt M., Heisenberg C.P., Jiang Y.J., Kane D.A., Kelsh R.N., Mullins M.C., Odenthal J,. Warga R.M., Nüsslein-Volhard C. (1996). Genetic analysis of fin formation in the zebrafish, Danio rerio. *Development*. 123, 255-262.

Vilagi I., Doczi J., Banczerowski-Pelyhe, I. (2000). Altered electrophysiological characteristics of developing rat cortical neurones after chronic methylmercury chloride treatment. *Int J Dev Neurosci*. 18, 493-499.

Villa P., Kaufmann S.H., Earnshaw W.C. (1997). Caspases and caspase inhibitors. *Trends Biochem Sci*. 22, 388-393.

Vu T.H., Werb Z. (2000). Matrix metalloproteinases: effectors of development and normal physiology. *Genes Dev*. 14, 2123-2133.

Wagner E.F., Eferl R. (2005). Fos/AP-1 proteins in bone and the immune system. *Immunol Rev*. 208, 126-140.

Wakabayashi K., Kakita A., Sakamoto M., Su M., Iwanaga K., Ikuta F. (1995). Variability of brain lesions in rats administered methylmercury at various postnatal developmental phases. *Brain Res*. 705, 267-272.

Wang Y., Takai R., Yoshioka H., Shirabe K. (2006). Characterization and expression of serotonin transporter genes in zebrafish. *Tohoku J Exp Med*. 208, 267-274.

Warfvinge K. (2000). Mercury distribution in the neonatal and adult cerebellum after mercury vapor exposure of pregnant squirrel monkeys. *Environ Res*. 83, 93-101.

Warfvinge K., Bruun A. (2000). Mercury distribution in the squirrel monkey retina after in Utero exposure to mercury vapor. *Environ Res*. 83, 102-109.

Warfvinge K., Hua J., Lögdberg B. (1994). Mercury distribution in cortical areas and fiber systems of the neonatal and maternal adult cerebrum after exposure of pregnant squirrel monkeys to mercury vapor. *Environ Res*. 67, 196-208.

Weis P., Bogden J.D., Enslee E.C. (1986). Hg- and Cu-induced hepatocellular changes in the mummichog, Fundulus heteroclitus. *Environ Health Perspect*. 65, 167-173.

Weis P., Weis J.S. (1977). Methylmercury teratogenesis in the killifish, Fundulus heteroclitus. *Teratology*. 16, 317-325.

Weis P., Weis J.S. (1982). Toxicity of methylmercury, mercuric chloride, and lead in killifish (Fundulus heteroclitus) from Southampton, New York. *Environ Res*. 28, 364-374.

Wennerberg K., Rossman K.L., Der C.J. (2005). The Ras superfamily at a glance. *J Cell Sci*. 118, 843-846.

Westerfield M. (2000). The zebrafish book. A guide for the laboratory use of zebrafish (Danio rerio). 4th ed., Univ. of Oregon Press, Eugene.

Wibowo I., Pinto-Teixeira F., Satou C., Higashijima S., López-Schier H. (2011). Compartmentalized Notch signaling sustains epithelial mirror symmetry. *Development*. 138, 1143-1152.

Wolf M.B., Baynes J.W. (2007). Cadmium and mercury cause an oxidative stress-induced endothelial dysfunction. *Biometals*. 20, 73-81.

Woo A.Y., Waye M.M., Tsui S.K., Yeung S.T., Cheng C.H. (2008). Andrographolide up-regulates cellular-reduced glutathione level and protects cardiomyocytes against hypoxia/reoxygenation injury. *J Pharmacol Exp Ther*. 325, 226-235.

Woods J.S., Ellis M.E. (1995). Up-regulation of glutathione synthesis in rat kidney by methyl mercury. Relationship to mercury-induced oxidative stress. *Biochem Pharmacol*. 50, 1719-1724

Wosik K., Cayrol R., Dodelet-Devillers A., Berthelet F., Bernard M., Moumdjian R., Bouthillier A., Reudelhuber T.L., Prat A. (2007). Angiotensin II controls occludin function and is required for blood brain barrier maintenance: relevance to multiple sclerosis. *J Neurosci*. 27, 9032-9042.

Wyatt R.A., Keow J.Y., Harris N.D., Haché C.A., Li D.H., Crawford BD. (2009). The zebrafish embryo: a powerful model system for investigating matrix remodeling. *Zebrafish*. 6, 347-354.

Yang L. (2007) Transcriptional profiling reveals barcode-like toxicogenomic responses in the zebrafish embryo. Dissertation. The Ruperto-Carola University of Heidelberg, Heidelberg, Germany.

Yang L., Ho N.Y., Alshut R., Legradi J., Weiss C., Reischl M., Mikut R., Liebel U., Müller F., Strähle U. (2009). Zebrafish embryos as models for embryotoxic and teratological effects of chemicals. *Reproductive Toxicology*. 28, 245-253.

Yang L., Kemadjou J.R., Zinsmeister C., Bauer M., Legradi J., Müller F., Pankratz M., Jäkel J., Strähle U. (2007). Transcriptional profiling reveals barcode-like toxicogenomic responses in the zebrafish embryo. *Genome Biol*. 8, R227.

Yoong S., O'Connell B., Soanes A., Crowhurst M.O., Lieschke G.J., Ward A.C. (2007). Characterization of the zebrafish matrix metalloproteinase 9 gene and its developmental expression pattern. *Gene Expr Patterns*. 7, 39-46.

Yoshida M., Watanabe C., Horie K., Satoh M., Sawada M., Shimada A. (2005). Neurobehavioral changes in metallothionein-null mice prenatally exposed to mercury vapor. *Toxicol Lett*. 155, 361-368.

Yoshida M., Watanabe C., Kishimoto M., Yasutake A., Satoh M., Sawada M., Akama Y. (2006). Behavioral changes in metallothionein-null mice after the cessation of long-term, low-level exposure to mercury vapor. *Toxicol Lett*. 161, 210-218.

Yoshinari N., Ishida T., Kudo A., Kawakami A. (2009). Gene expression and functional analysis of zebrafish larval fin fold regeneration. *Dev Biol*. 325, 71-81.

Zaja-Milatovic S., Richmond A. (2008). CXC chemokines and their receptors: a case for a significant biological role in cutaneous wound healing. *Histol Histopathol*. 23, 1399-1407.

Zanoli P., Truzzi C., Veneri C., Braghiroli D., Baraldi M. (1994). Methyl mercury during late gestation affects temporarily the development of cortical muscarinic receptors in rat offspring. *Pharmacol Toxicol*. 75, 261-264.

ZFIN Staff. (2002). Gene Ontology Annotation Through Association of InterPro Records with GO Terms. Automated Data Submission.

Zhang B., Kirov S.A., Snoddy J.R. (2005). WebGestalt: an integrated system for exploring gene sets in various biological contexts. *Nucleic Acids Res*, 33, W741-748.

Zhang X.W., Zhang L., Qin W., Yao X.H., Zheng L.Z., Liu X., Li J., Guo W.J. (2010). Oncogenic role of the chromobox protein CBX7 in gastric cancer. *J Exp Clin Cancer Res*. 29, 114.

Zhang Y., Bai X.T., Zhu K.Y., Jin Y., Deng M., Le H.Y., Fu Y.F., Chen Y., Zhu J., Look A.T., Kanki J., Chen Z., Chen S.J., Liu T.X. (2008). In vivo interstitial migration of primitive macrophages mediated by JNK-matrix metalloproteinase 13 signaling in response to acute injury. *J Immunol*. 181, 2155-2164.

Zhou L., Griffin J.W. (2003). Demyelinating neuropathies. *Curr Opin Neurol*. 16, 307-313.

Zhou T., Rademacher D.J., Steinpreis R.E., Weis J.S. (1999). Neurotransmitter levels in two populations of larval Fundulus heteroclitus after methylmercury exposure. *Comp Biochem Physiol C Pharmacol Toxicol Endocrinol.* 124, 287-294.

Zillioux E.J., Porcella D.B., Benoit J.M. (1993). Mercury cycling and effects in freshwater wetland ecosystems. *Environ Toxicol Chem*. 12, 2245-2264.

Appendix

Tab. A1 Stages of zebrafish embryonic development.

(This table is reproduced after Kimmel *et al.* (1995))

Stage	h	HB	Description
Zygote period			
1-cell	0	1,2	Cytoplasm streams toward animal pole to form the blastodisc
Cleavage period			
2-cell	¾	3	Partial cleavage
4-cell	1	4	2 × 2 array of blastomeres
8-cell	1¼	5	2 × 4 array of blastomeres
16-cell	1½	6	4 × 4 array of blastomeres
32-cell	1¾	7	2 regular tiers (horizontal rows) of blastomeres, sometimes in 4 × 8 array
64-cell	2	8	3 regular tiers of blastomeres
Blastula period			
128-cell	2¼	9	5 blastomere tiers; cleavage planes irregular
256-cell	2½		7 blastomere tiers
512-cell	2¾		9 tiers of blastomeres; NO: YSL forms
1k-cell	3	10	11 tiers of blastomeres; NO: single row of YSL nuclei; slight blastodisc cell cycle asynchrony
High	3⅓		>11 tiers of blastomeres; beginning of blastodisc flattening; NO: YSL nuclei in two rows; substantial division asynchrony
Oblong	3⅔	11	Flattening produces an elliptical shape; NO: multiple rows of YSL nuclei
Sphere	4	12	Spherical shape; flat border between blastodisc and yolk
Dome	4⅓	13	Shape remains spherical; yolk cell bulging (doming) toward animal pole as epiboly begins
30%-epiboly	4⅔	14	Blastoderm an inverted cup of uniform thickness; margin reaches 30% of distance between the animal and vegetal poles
Gastrula period			
50%-epiboly	5¼		Blastoderm remains uniform in thickness
Germ-ring	5⅔		Germ ring visible from animal pole; 50%-epiboly
Shield	6	15	Embryonic shield visible from animal pole, 50%-epiboly
75%-epiboly	8	16	Dorsal side distinctly thicker; epiblast, hypoblast, evacuation zone visible
90%-epiboly	9		Brain rudiment thickened; notochord rudiment distinct from segmental plate
Bud	10	17	Tail bud prominent; notochord rudiment distinct from neural keel; early polster; midsagittal groove in anterior neural keel; 100%-epiboly
Segmentation period			
1-somite	10⅓		First somite furrow
5-somite	11⅔	18	Polster prominent; optic vesicle, Kupffer's vesicle
14-somite	16	19	EL = 0.9 mm; otic placode; brain neuromeres, v-shaped trunk somites; YE barely forming; NO: pronephric duct
20-somite	19	20	EL = 1.4 mm; YE/YB > 0.5 and < 1; muscular twitches; lens, otic vesicle, rhombic flexure; hindbrain neuromeres prominent; tail well extended
26-somite	22		EL = 1.6 mm; HTA = 125°; side-to-side flexures; otoliths; Prim-3
Pharyngula period			
Prim-5	24		EL = 1.9 mm; HTA = 120°; OVL = 5; YE/YB = 1; early pigmentation in retina and skin; median fin fold; red blood cells on yolk, heartbeat
Prim-15	30		EL = 2.5 mm; HTA = 95°; OVL = 3; YE/YB > 1; YB/HD = 2; early touch reflex and reduced spontaneous movements; retina pigmented; dorsal stripe to somite 12; weak circulation; caudal artery halfway to end of tail; caudal vein braided; shallow pectoral fin buds; straight tail; NO: cellular degeneration at end of tail; circulation in aortic arch 1
Prim-25	36		EL = 2.7 mm; HTA = 75°; OVL = 1; PF(H/W) = ¾; early motility; tail pigmentation and ventral stripe filling out; strong circulation; single aortic arch pair; caudal artery is ¾ of the way to the end of tail; pericardium not swollen; NO: PF apical ectodermal ridge
High-pec	42		EL = 2.9 mm; HTA = 55°; OVL < 1 and > ½; YE/YB = 1.5; YB/HD < 1.3; PF(H/W) = 1; dechorionated embryos rest on side after swimming; YE remaining cylindrical; PF apical ridge prominent; early lateral stripe; complete dorsal stripe; xanthophores in head only; iridophores in retina only; pericardium prominent; NO: heart chambers; segmental blood vessels; mandibular and hyoid arches; foregut developments; olfactory cilia; thickened otic vesicle walls
Hatching period			
Long-pec	48		EL = 3.1 mm; HTA = 45°; OVL = ½; PF(H/W) = 2; resting dorsal up; YE beginning to taper; PF pointed; dorsal and ventral stripes meet at tail; ca. 6 melanophores in lateral stripe; iridophores plentiful on retina; distinct yellow cast to head; NO: circulation in 2–4 aortic arches and in segmental vessels; olfactory cilia beating; semicircular canals; neuromasts
Pec-fin	60		EL = 3.3 mm; HTA = 35°; movements too rapid to resolve; YB tapering into YE; up to 10 melanophores in lateral stripe; PF flattened into fin shape with prominent circulation; iridophore retinal ring fills out; iridophores in dorsal stripe; NO: PF cartilage and actinotrichia; gut tract; 2 chambers in otic vesicle; early jaw cartilages; circulation in 5–6 aortic arches; mouth remaining small and open at ventral location midway between eyes
Protruding-mouth	72		EL = 3.5 mm; HTA = 25°; wide open mouth protruding anterior to eye; iridophores in yolk stripe; eye half covered by iridophores; dorsal body as yellow as head; NO: gill slits and filament buds; cartilage in branchial arch 1 and 5; operculum covers the branchial arch 1 or 2; clerithrum

[a]EL, embryo length; PF, pectoral fin; h, hours of development at 28.5°C; HB, approximate stage no. in the Hisaoka and Battle (1958) zebrafish staging series (reasonably accurate through HB stage 20); HD, head diameter in dorsal view; NO, Nomarski optics; H/W, height/width; Prim, Prim stages refer to the no. of the myotome to which the leading end of the posterior lateral line *prim*ordium has advanced; YB, yolk ball; YE, yolk extension; YSL, yolk syncytial layer; HTA, head-trunk angle; OVL, otic vesicle length.

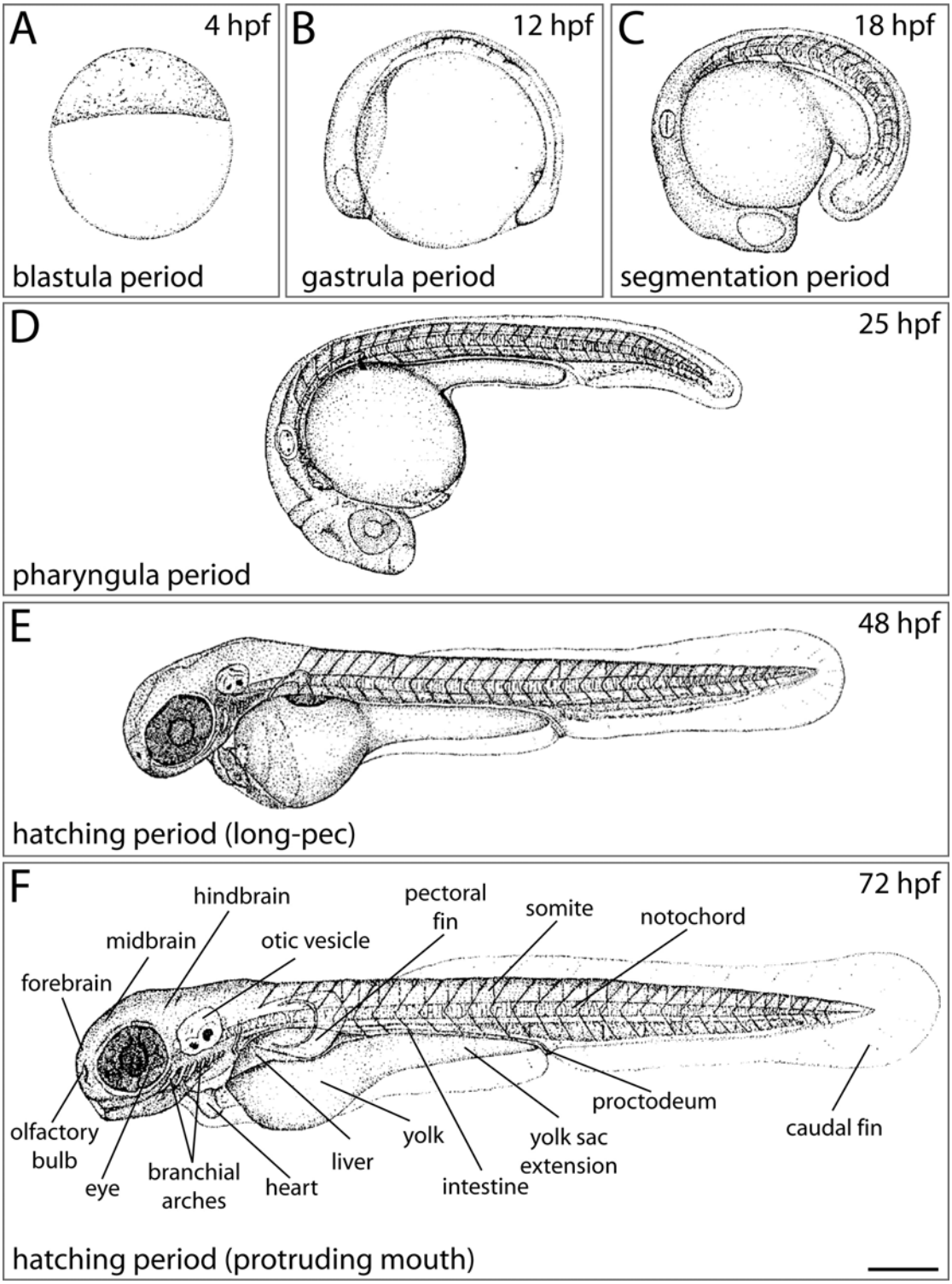

Fig. A1 Schematic drawing of zebrafish embryos at selected stages between 4 and 72 hpf. Zebrafish at 4 (A), 12 (B), 18 (C), 24 (D), 48 (E) and 72 (F) hpf are shown. The embryos are positioned with the animal pole to the top (A) or anterior to the left and dorsal side up (B-F). Pigmentation on the body is omitted for better illustration of the anatomical structures. Anatomical structures in the 72-hpf-old embryos are indicated. Scale bar, 250 μm. This figure is modified from Kimmel *et al.* (1995).

Tab. A2 MeHg-up-regulated genes determined by DNA-microarray with M > 1.30 and p < 0.05.

Gene Name (gene symbol)	GenBank accession number	M-value
matrix metalloproteinase 9 (mmp9)	NM_213123	11.66
matrix metalloproteinase 13a (mmp13a)	NM_201503	9.13
tissue inhibitor of metalloproteinase 2b (timp2b)	NM_213296	8.51
zgc:56537 (zgc:56537)	NM_199950	8.16
naa11e05.y1 Zebrafish whole eye. Unnormalized (naa) Danio rerio cDNA clone naa11e05	DN857240	7.69
complement component 7-1(c7-1)	BC100054	7.66
jun B proto-oncogene (junb)	NM_213556	7.40
zgc:101739 (zgc:101739)	NM_001004629	6.83
zgc:77038 (zgc:77038)	NM_213304	6.71
chemokine CXC-like protein (cxclpl)	XM_685640	6.64
zgc:63471 (zgc:63471)	NM_199798	6.46
FDR306-P00038-DEPE-F_A07 FDR306 Danio rerio cDNA clone FDR306-P00038-BR_A07	EH592105	6.44
hepcidin antimicrobial peptide 1 (hamp1)	NM_205583	6.16
zgc:103438 (zgc:103438)	NM_001006036	6.10
fibronectin 1b (fn1b)	NM_001013261	6.04
solute carrier family 16 (monocarboxylic acid transporters), member 9a (slc16a9a)	NM_200410	5.86
insulin-like growth factor binding protein 1 (igfbp1)	NM_173283	5.80
mesogenin 1 (msgn1)	NM_182882	5.33
complement factor B (cfb)	NM_131338	5.30
chromobox protein homolog 7-like (cbx7l); zgc:110152	NM_001017853	5.16
CCAAT/enhancer binding protein (C/EBP), beta (cebpb)	NM_131884	5.16
angiotensinogen (agt)	NM_198063	5.05
complement component 4-2 (c4-2)	XM_001334604	5.01
a disintegrin and metalloproteinase domain 8 (adam8)	NM_200637	4.89
zgc:92903 (zgc:92903)	NM_001002461	4.87
jun B proto-oncogene, like (junbl)	NM_212750	4.83
activating transcription factor 3 (atf3)	NM_200964	4.78
si:dkey-25e12.3 (si:dkey-25e12.3)	NM_001025555	4.75
zgc:154020 (zgc:154020)	NM_001077607	4.67
zgc:123218 (zgc:123218)	NM_001037117	4.59
v-fos FBJ murine osteosarcoma viral oncogene homolog (fos)	NM_205569	4.40
annexin A2a (anxa2a)	NM_181761	4.37
thioredoxin interacting protein a (txnipa)	NM_200087	4.32
Unknown	CK394874	4.14
putative transmembrane protein TA-2, like (ta2l)	XM_688653	4.14
zgc:73257 (zgc:73257)	NM_213397	4.08
Unknown	A_15_P118168	3.98
major vault protein (mvp)	NM_201325	3.93
wu:fl49b07(wu:fl49b07)	BC055392	3.90
hypothetical LOC565872 (LOC565872)	XM_689134	3.89
zgc:91912 (zgc:91912)	NM_001002176	3.87
glutathione S-transferase pi (gstp1)	NM_131734	3.85
bloodthirsty, like (btl)	XM_001345747	3.82
claudin c (cldnc)	NM_131764	3.77

Gene Name (gene symbol)	GenBank accession number	M-value
keratin 18 (krt18)	NM_178437	3.77
Unknown	A_15_P101617	3.75
zgc:110464 (zgc:110464)	BC095285	3.74
RAS-like, family 11, member B (rasl11b)	NM_200140	3.72
complement component 6 (c6l	XM_001332137	3.71
somatostatin 2 (sst2)	NM_131727	3.70
hypothetical LOC556467 (LOC556467)	XM_679283	3.67
zgc:85914 (zgc:85914)	NM_213190	3.58
cDNA clone IMAGE:7229274	CN013656	3.58
hypoxia induced gene 1 (hig1)	NM_200100	3.57
MAP kinase-interacting serine/threonine kinase 2 (mknk2)	TC303990	3.57
zgc:112234 (zgc:112234)	BC095697	3.54
Unknown	TC336408	3.52
zgc:92066 (zgc:92066)	TC355103	3.51
zgc:92034 (zgc:92034)	NM_001004605	14
zgc:110010 (zgc:110010)	NM_001020554	14
zgc:77806 (zgc:77806)	NM_205691	10
dual specificity phosphatase 5 (dusp5)	NM_212565	3.39
Unknown	A_15_P120379	3.35
clusterin (clu)	NM_200802	3.34
zgc:92097 (zgc:92097)	NM_205710	3.33
Q4RTG9_TETNG (Q4RTG9) Chromosome 1 SCAF14998, whole genome shotgun sequence	TC334607	3.30
complement component 3-2 (c3-2)	NM_001037236	3.28
zgc:111983 (zgc:111983)	NM_001017803	3.23
zgc:109934 (zgc:109934)	NM_001020531	3.20
zgc:92192 (zgc:92192)	NM_001002340	3.20
claudin b (cldnb)	NM_131763	3.12
hypothetical protein LOC796518 (LOC796518)	XM_001334489	3.11
Unknown	A_15_P101896	3.07
sequestosome 1 (sqstm1)	NM_213173	3.06
growth arrest and DNA-damage-inducible, beta b (gadd45bb)	NM_001012386	3.05
cadherin 1, epithelial (cdh1)	NM_131820	3.03
zgc:73310 (zgc:73310)	NM_200785	3.02
S100 calcium binding protein A1 (s100a1)	BC047833	3.00
zgc:76966 (zgc:76966)	NM_212869	2.93
hydroxysteroid (17-beta) dehydrogenase 12a (hsd17b12a)	NM_200881	2.92
elongation of very long chain fatty acids (FEN1/Elo2, SUR4/Elo3, yeast)-like 1 (elovl1)	NM_199778	2.92
zgc:109981 (zgc:109981)	NM_001002569	2.92
prostaglandin-endoperoxide synthase 2a (ptgs2a)	NM_153657	2.91
zgc:77906 (zgc:77906)	NM_205648	2.89
POU domain, class 5, transcription factor 1 (pou5f1)	NM_131112	2.89
zgc:91887 (zgc:91887)	NM_001004542	2.85
solute carrier family 7 (cationic amino acid transporter, y+ system), member 3 (slc7a3)	NM_001007329	2.85
guanine nucleotide binding protein (G protein), alpha transducing activity polypeptide 2 (gnat2)	NM_131869	2.82

Gene Name (gene symbol)	GenBank accession number	M-value
zgc:112226 (zgc:112226)	NM_001024409	2.81
zgc:91814 (zgc:91814)	NM_001003479	2.81
AL714172 Danio rerio embryonic inner ear subtracted cDNA Danio rerio cDNA clone BN0AA002ZF08	AL714172	2.77
claudin a (cldna)	NM_131762	2.76
zgc:153665 (zgc:153665)	NM_001077463	2.75
zgc:64051 (zgc:64051)	NM_200371	2.74
zgc:100919 (zgc:100919)	NM_001002748	2.73
thioredoxin interacting protein b (txnipb)	BC055213	2.72
zgc:92301 (zgc:92301)	NM_001007314	2.72
zgc:110380 (zgc:110380)	NM_001017660	2.72
zgc:109940 (zgc:109940)	NM_001020532	2.72
cDNA clone IMAGE:7403183	BC122156	2.69
FDR306-P00024-DEPE-F_P05 FDR306 Danio rerio cDNA clone FDR306-P00024-BR_P05	EH587241	2.68
FDR107-P00033-DEPE-F_C16 FDR107 Danio rerio cDNA clone FDR107-P00033-BR_C16	EH495313	2.67
zgc:101897 (zgc:101897)	NM_001007372	2.66
6-phosphofructo-2-kinase/fructose-2,6-biphosphatase 4-like (pfkfb4l)	NM_198816	2.66
zgc:77002 (zgc:77002)	NM_212910	2.65
claudin e (cldne)	NM_131765	2.64
serum/glucocorticoid regulated kinase (sgk)	NM_199212	2.62
cDNA clone IMAGE:7225372	CN017556	2.62
hypothetical protein LOC553515 (LOC553515)	BC081659	2.61
cDNA clone IMAGE:7923762	BC122366	2.60
protein phosphatase 1, regulatory (inhibitor) subunit 3B (ppp1r3b)	NM_212709	2.59
zgc:92069 (zgc:92069)	NM_001002376	2.58
Unknown	A_15_P113862	2.58
Ictalurus punctatus 18S small subunit ribosomal RNA gene	TC331454	2.57
myeloid cell leukemia sequence 1b (mcl1b)	NM_194394	2.57
growth arrest and DNA-damage-inducible, alpha like (gadd45al)	NM_200576	2.54
PDZ and LIM domain 7 (pdlim7)	NM_200840	2.53
claudin 7 (cldn7)	NM_131637	2.53
growth arrest and DNA-damage-inducible, beta a (gadd45ba)	NM_213031	2.52
cDNA clone IMAGE:7235342	CN014934	2.51
zgc:100868 (zgc:100868)	NM_001003526	2.51
claudin i (cldni)	XM_692448	2.49
zgc:92252 (zgc:92252)	NM_001002622	2.48
zgc:153827 (zgc:153827)	NM_001030120	2.47
Unknown	A_15_P116930	2.47
cDNA clone IMAGE:7247997	BC122137	2.47
pim-1 oncogene (pim1)	NM_131539	2.45
Q4S8G5_TETNG (Q4S8G5) Chromosome 2 SCAF14705, whole genome shotgun sequence	TC342277	2.45
zgc:136830 (zgc:136830)	NM_001040243	2.45
prostaglandin-endoperoxide synthase 1 (ptgs1)	NM_153656	2.43
stanniocalcin 1 (stc1)	NM_200539	2.43
cDNA clone IMAGE:7228979	BC086730	2.43

Gene Name (gene symbol)	GenBank accession number	M-value
prostaglandin I2 (prostacyclin) synthase like (ptgisl)	BC124454	2.43
hypothetical protein LOC792442 (LOC792442)	XM_001331916	2.42
transaldolase 1 (taldo1)	NM_199687	2.42
zgc:56136 (zgc:56136)	NM_200198	2.41
stathmin-like 4, like (stmn4l)	TC327874	2.40
Cd63 antigen (cd63)	NM_199543	2.36
cDNA clone IMAGE:7049914	BC117642	2.36
zgc:56585 (zgc:56585)	BC066622	2.35
zgc:56706 (zgc:56706)	NM_200274	2.35
aldehyde dehydrogenase 3 family, member D1 (aldh3d1)	NM_173221	2.35
fatty acid binding protein 3, muscle and heart (fabp3)	TC336225	2.33
retinol dehydrogenase 12, like (rdh12l)	NM_001009912	2.33
zgc:136956 (zgc:136956)	NM_001080029	2.32
Q4S373_TETNG (Q4S373) Chromosome 4 SCAF14752, whole genome shotgun sequence	TC305067	2.31
zgc:110304 (zgc:110304)	NM_001017593	2.31
Unknown	TC325806	2.31
zgc:63514 (zgc:63514)	NM_200013	2.31
hypothetical LOC559958 (LOC559958)	XM_683353	2.31
smoothelin, like (smtnl)	NM_212805	2.29
im:7144703 (im:7144703)	XM_686956	2.29
thiazide sensitine NaCl cotransporter (ncct)	NM_001045080	2.29
pyrophosphatase (inorganic) (pp)	NM_200733	2.29
cDNA clone IMAGE:7120309	CK400158	2.28
CT669859 ZF_mu Danio rerio cDNA clone ZF_mu_177e08	CT669859	2.28
tumor-associated calcium signal transducer (tacstd)	NM_213175	2.26
Q4SMY3_TETNG (Q4SMY3) Chromosome 6 SCAF14544, whole genome shotgun sequence	TC355382	2.25
zgc:112009 (zgc:112009)	NM_001017683	2.25
zgc:91909 (zgc:91909)	NM_001002178	2.25
basic leucine zipper and W2 domains 1, like (bzw1l)	NM_213092	2.25
Unknown	A_15_P116719	2.25
chromosome 20 open reading frame 149, like (c20orf149l)	NM_200008	2.23
legumain (lgmn)	NM_214759	2.23
zgc:100900 (zgc:100900)	NM_001003521	2.23
Unknown	A_15_P100589	2.22
Unknown	TC341137	2.21
claudin i (cldni)	NM_131768	2.21
H1 histone family, member X (h1fx)	NM_199276	2.20
zgc:158528 (zgc:158528)	BC095757	2.20
chloride intracellular channel a (clica)	NM_199524	2.20
Unknown	A_15_P113957	2.19
cDNA clone IMAGE:7425015	CO926454	2.19
Janus kinase 1 (jak1)	NM_131073	2.18
pleckstrin homology-like domain, family A, member 3 (phlda3)	NM_001002455	2.18
zgc:77882 (zgc:77882)	NM_199649	2.17
LIM domain kinase 2 (limk2)	NM_001002651	2.16
cfb protein, like (cfb)	XR_028904	2.15

Gene Name (gene symbol)	GenBank accession number	M-value
solute carrier family 1 (glutamate/neutral amino acid transporter), member 4 (slc1a4)	BC076285	2.14
ubquitin-like protein 1 (ubqlp1)	XM_682249	2.13
noggin 2 (nog2)	BC067541	2.11
Unknown	A_15_P118821	2.11
zgc:56330 (zgc:56330)	NM_199683	2.10
cDNA clone IMAGE:8744566	EE322470	2.08
hypothetical LOC560869 (LOC560869)	XM_684268	2.07
cDNA clone IMAGE:7401354	CO796229	2.07
zgc:100859 (zgc:100859)	NM_001003533	2.06
testis derived transcript (3 LIM domains) (tes)	NM_205720	2.06
Unknown	A_15_P110843	2.06
sphingolipid delta 4 desaturase/C-4 hydroxylase 2 (des2)	BC045962	2.06
Unknown	TC351463	2.05
dual specificity phosphatase 1 (dusp1)	NM_213067	2.05
transketolase (tkt)	NM_198070	2.05
fibrinogen, B beta polypeptide (fgb)	NM_212774	2.04
solute carrier family 16 (monocarboxylic acid transporters), member 3 (slc16a3)	NM_212708	2.04
fibrinogen, gamma polypeptide (fgg)	NM_213054	2.03
zgc:110267 (zgc:110267)	NM_001017613	2.03
spleen focus forming virus (SFFV) proviral integration oncogene (spi1)	AY293624	2.02
early growth response 2a (egr2a)	NM_183341	2.02
zgc:91870 (zgc:91870)	NM_001002190	2.00
cDNA clone IMAGE:8729487	EE310093	1.99
si:dkey-193b15.6 (si:dkey-193b15.6)	XM_689000	1.99
Unknown	TC319678	1.99
influenza virus NS1A binding protein b (ivns1abpb)	NM_201483	1.99
zgc:56011 (zgc:56011)	NM_212726	1.99
Unknown	A_15_P120377	1.98
coagulation factor V (f5)	NM_001007208	1.98
cathepsin L1, a (ctsl1a)	NM_212584	1.98
DnaJ (Hsp40) homolog, subfamily B, member 1 (dnajb1)	TC339980	1.97
zgc:101811 (zgc:101811)	NM_001006049	1.97
eukaryotic translation initiation factor 4E binding protein 3, like (elf4ebp3l)	CF269291	1.96
complement component 9 (c9)	TC320619	1.96
chemokine (C-X-C motif) ligand 12a (stromal cell-derived factor 1) (cxcl12a)	NM_178307	1.95
zgc:91976 (zgc:91976)	NM_001007325	1.95
empty spiracles homeobox 3 (emx3)	NM_131279	1.94
zgc:103456 (zgc:103456)	NM_001006032	1.93
zgc:66409 (zgc:66409)	NM_212737	1.93
bicaudal-C (LOC402785)	NM_203420	1.93
Unknown	TC343234	1.92
phosphogluconate hydrogenase (pgd)	NM_213453	1.92
prostaglandin E synthase (ptges)	NM_001014828	1.92
hypothetical protein LOC100002476 (LOC100002476)	XM_001337565	1.91
carbonyl reductase 1-like (cbr1l)	NM_194379	1.91
CD9 antigen, like (cd9l)	NM_213428	1.91

Gene Name (gene symbol)	GenBank accession number	M-value
Unknown	A_15_P116010	1.90
cDNA clone IMAGE:7434007	BC133168	1.90
zgc:110443 (zgc:110443)	BC066727	1.90
zgc:103604 (zgc:103604)	NM_001005973	1.89
caspase a (caspa)	TC306290	1.89
phosphoinositide-3-kinase, regulatory subunit, polypeptide 3 (p55, gamma) (pik3r3)	NM_201143	1.89
zgc:110340 (zgc:110340)	BC091458	1.89
Unknown	A_15_P100772	1.89
B-cell translocation gene 2 (btg2)	NM_130922	1.89
v-maf musculoaponeurotic fibrosarcoma oncogene homolog f (avian) (maff)	NM_200336	1.88
Carbamoyl-phosphate synthetase 2, aspartate transcarbamylase, and dihydroorotase	TC308952	1.88
zgc:112315 (zgc:112315)	NM_001020678	1.88
Unknown	A_15_P102259	1.88
Unknown	A_15_P114954	1.88
cytochrome b-245, alpha polypeptide (cyba)	NM_200579	1.87
PR domain containing 1, with ZNF domain (prdm1)	NM_199515	1.86
annexin A1a (anxa1a)	NM_181758	1.86
zgc:77868 (zgc:77868)	NM_199999	1.84
plexin D1 (plxnd1)	NM_205697	1.84
uncoupling protein 2 (ucp2)	NM_131176	1.84
retinal homeobox gene 1 (rx1)	NM_131225	1.83
transgelin 2 (tagln2)	NM_201576	1.83
v-maf musculoaponeurotic fibrosarcoma oncogene family, protein B (avian) (mafb)	NM_131015	1.82
arrestin domain containing 1 (arrdc1)	NM_001004561	1.82
zgc:152839 (zgc:152839)	BC124148	1.82
zgc:92762 (zgc:92762)	NM_001002561	1.81
Unknown	A_15_P119382	1.81
MGC84748 protein	TC335803	1.80
O55566_NPVLS (O55566) P12	TC327743	1.79
novel protein containing a ChaC-like protein domain (LOC563855)	NM_001045032	1.79
somatostatin 1 (sst1)	NM_183070	1.79
kelch-like ECH-associated protein 1 (keap1)	NM_182864	1.78
cDNA clone IMAGE:7998528	BC124510	1.78
zgc:91992 (zgc:91992)	NM_001002650	1.78
zgc:101791 (zgc:101791)	NM_001008623	1.78
tissue inhibitor of metalloproteinase 2 (timp2)	NM_182874	1.78
helicase MOV-10-like (mov10l)	TC345203	1.77
zgc:91905 (zgc:91905)	NM_001003459	1.77
Unknown	A_15_P114743	1.77
dual specificity phosphatase 6 (dusp6)	NM_194380	1.77
coronin, actin binding protein, 1A (coro1a)	NM_201114	1.77
zgc:77286 (zgc:77286)	NM_207062	1.76
prosaposin (psap)	NM_131883	1.76
zgc:55423 (zgc:55423)	NM_201171	1.76
zgc:158387 (zgc:158387)	NM_001080034	1.76

Gene Name (gene symbol)	GenBank accession number	M-value
zgc:92266 (zgc:92266)	NM_001002617	1.73
ubiquitin-conjugating enzyme E2H (UBC8 homolog, yeast) (ube2h)	NM_201489	1.73
Unknown	A_15_P109596	1.72
bcl2-like (bcl2l)	NM_131807	1.72
zgc:92198 (zgc:92198)	NM_001002642	1.71
tight junction protein 3 (tjp3)	NM_201494	1.71
popeye domain containing 3 (popdc3)	NM_001001848	1.71
retinol binding protein 4, like (rbp4l)	NM_199965	1.70
Unknown	TC348736	1.70
coxsackie virus and adenovirus receptor (cxadr)	BC045286	1.70
SAM domain, SH3 domain and nuclear localisation signals, 1 (samsn1)	BC083438	1.70
wu:fc21h08 (wu:fc21h08)	NM_001001815	1.70
vascular endothelial growth factor A (vegfa)	NM_131408	1.69
cDNA clone 2690585	EB788158	1.69
cytochrome c oxidase subunit III (cox3)	TC322630	1.69
glucosaminyl (N-acetyl) transferase 4, core 2 (gcnt4)	NM_201583	1.69
hypothetical LOC562892 (LOC562892)	XM_701076	1.69
methyl-CpG binding domain protein 2 (mbd2)	NM_212768	1.68
mitogen-activated protein kinase 3 (mapk3)	NM_201507	1.68
nephrosin (npsn)	NM_205756	1.68
potassium channel tetramerisation domain containing 12.2 (kctd12.2)	NM_001034019	1.68
Wiskott-Aldrich syndrome (eczema-thrombocytopenia) (was)	NM_199938	1.67
zgc:63645 (zgc:63645)	BC056794	1.67
serine protease inhibitor, Kunitz type 1-like (spint1l)	NM_213152	1.67
Unknown	A_15_P116135	1.67
MGC81751 protein	TC313771	1.67
Anguilla rostrata 28S ribosomal RNA gene	TC319492	1.66
retinol dehydrogenase 10 (rdh10)	NM_201331	1.66
Hydrolagus colliei internal transcribed spacer 1; 5.8S ribosomal RNA gene and internal transcribed spacer 2; and 28S ribosomal RNA gene	TC357777	1.66
sprouty (Drosophila) homolog 4 (spry4)	NM_131826	1.66
ral guanine nucleotide dissociation stimulator-like 1 (rgl1)	NM_205637	1.65
Unknown	A_15_P113515	1.65
Unknown	TC341913	1.64
Unknown	A_15_P100273	1.64
fibrinogen alpha chain (fga)	NM_001002039	1.64
hypothetical LOC554458 (LOC554458)	XM_696332	1.64
zinc finger, AN1-type domain 5a (zfand5a)	NM_213039	1.63
cathepsin D (ctsd)	NM_131710	1.63
sperm associated antigen 6 (spag6)	NM_001002210	1.63
zgc:112054 (zgc:112054)	NM_001017664	1.63
v-jun sarcoma virus 17 oncogene homolog (avian) (jun)	NM_199987	1.63
cDNA clone IMAGE:5072672	BI839216	1.62
cadherin 17, LI cadherin (liver-intestine) (cdh17)	NM_194422	1.62
solute carrier family 25 (mitochondrial carrier; phosphate carrier), member 25 (slc25a25)	NM_213257	1.61
Pax-family transcription factor 6.2 (pax6.2)	TC308490	1.61
zgc:77455 (zgc:77455)	NM_199754	1.61

Gene Name (gene symbol)	GenBank accession number	M-value
Unknown	A_15_P104204	1.61
enhancer of polycomb homolog 2 (Drosophila) (epc2)	NM_201075	1.61
zgc:65794 (zgc:65794)	NM_213349	1.61
bridging integrator 2, like (bin2l)	NM_199796	1.60
zgc:76933 (zgc:76933)	NM_207081	1.60
vang-like 2 (van gogh, Drosophila) (vangl2)	BC065983	1.60
B lymphoma Mo-MLV insertion region 1 (bmi1)	NM_194366	1.60
LOC495986 protein, like (LOC558475)	XM_681691	1.60
hypothetical LOC563193 (LOC563193)	XM_686554	1.59
caspase 8 (casp8)	NM_131510	1.59
nuclear lamin A (lmna)	TC304394	1.59
homogentisate 1,2-dioxygenase (hgd)	NM_152966	1.59
cDNA clone IMAGE:3717298	AI545183	1.59
adenosine deaminase (ada)	NM_001002646	1.58
zgc:103463 (zgc:103463)	NM_001007351	1.58
glutamate-cysteine ligase, catalytic subunit (gclc)	NM_199277	1.58
zgc:110333 (zgc:110333)	NM_001017799	1.57
cDNA clone IMAGE:7418695	CO927351	1.57
zgc:101776 (zgc:101776)	NM_001007404	1.57
zgc:92505 (zgc:92505)	NM_001004550	1.57
Unknown	A_15_P100047	1.56
zgc:63593 (zgc:63593)	BC058869	1.56
hematopoietically expressed homeobox (hhex)	NM_130934	1.56
gonadotropin-releasing hormone 2 (gnrh2)	NM_181439	1.56
HIV-1 Tat interactive protein 2 (htatip2)	NM_131681	1.56
ft64a05.y1 Gong zebrafish ovary Danio rerio cDNA clone IMAGE:5157801	BI867800	1.56
zgc:77123 (zgc:77123)	NM_001001825	1.56
Thy-1 cell surface antigen (thy1)	NM_198065	1.56
zgc:91996 (zgc:91996)	TC343798	1.56
zgc:77358 (zgc:77358)	NM_205632	1.56
zgc:92476 (zgc:92476)	NM_001002643	1.55
glutamate-ammonia ligase (glutamine synthase) b (glulb)	NM_182866	1.54
parathyroid hormone 1 (pth1)	NM_212950	1.53
zgc:103407 (zgc:103407)	NM_001004014	1.52
cDNA clone IMAGE:7116694	CK399020	1.52
zgc:153291 (zgc:153291)	NM_001045360	1.52
cathepsin B, a (ctsba)	NM_213336	1.52
notch-regulated ankyrin repeat protein a (nrarpa)	NM_181495	1.52
orthodenticle homolog 1 (otx1)	NM_131250	1.52
Unknown	CV113602	1.52
glutamate-ammonia ligase (glutamine synthase) a (glula)	NM_181559	1.52
zgc:101676 (zgc:101676)	NM_001004635	1.52
potassium channel, subfamily K, member 5 (kcnk5)	NM_200633	1.52
peptide YY (pyy)	NM_131016	1.52
cDNA clone IMAGE:7140684	BC090456	1.52
zic family member 2 (odd-paired homolog, Drosophila) b (zic2b)	NM_001001820	1.51
14781156 ZF35 Danio rerio cDNA clone 3426448sequence	EB959676	1.51

Gene Name (gene symbol)	GenBank accession number	M-value
activating transcription factor 4, like (atf4l)	XM_701690	1.51
pleckstrin homology domain containing, family F (with FYVE domain) member 2 (plekhf2)	NM_200244	1.51
Unknown	TC340992	1.50
Tax1 (human T-cell leukemia virus type I) binding protein 3 (tax1bp3)	NM_213470	1.50
zgc:64085 (zgc:64085)	NM_200408	1.50
zgc:153034 (zgc:153034)	NM_001076637	1.50
cDNA clone IMAGE:7012610	BC085676	1.49
zgc:153860 (zgc:153860)	NM_001077248	1.49
zgc:85680 (zgc:85680)	NM_212929	1.48
zgc:92897 (zgc:92897)	NM_001003430	1.48
myeloid cell leukemia sequence 1a (mcl1a)	NM_131599	1.48
zgc:56116 (zgc:56116)	NM_200196	1.48
zgc:123105 (zgc:123105)	NM_001039994	1.48
spermine oxidase (smox)	BC066413	1.48
cDNA clone IMAGE:7053031	BC075971	1.48
cDNA clone IMAGE:7012947	CF550131	1.47
zgc:63950 (zgc:63950)	NM_200111	1.47
LIM domain only 4 (lmo4)	NM_177984	1.47
cDNA clone IMAGE:6795541	CA474484	1.47
core promoter element binding protein (copeb)	NM_201461	1.47
ornithine decarboxylase 1 (odc1)	NM_131801	1.47
Unknown	A_15_P119625	1.46
zgc:111821 (zgc:111821)	NM_001002308	1.46
zgc:110779 (zgc:110779)	NM_001013318	1.46
Unknown	A_15_P114228	1.46
cDNA clone IMAGE:8109385	BC122381	1.46
PR domain containing 8 (prdm8)	NM_213410	1.46
renin binding protein (renbp)	NM_001008610	1.46
aminolevulinate, delta-, synthetase 1 (alas1)	NM_201287	1.45
Q4SC04_TETNG (Q4SC04) Chromosome 14 SCAF14660, whole genome shotgun sequence	TC357468	1.45
zgc:73201 (zgc:73201)	NM_199668	1.45
leucine rich repeat containing 6 (lrrc6)	TC349542	1.45
Q4SU80_TETNG (Q4SU80) Chromosome 5 SCAF13976, whole genome shotgun sequence	TC315445	1.45
connector enhancer of kinase suppressor of Ras 1 (cnksr1)	NM_205659	1.44
zgc:55316 (zgc:55316)	NM_199601	1.44
zgc:101711 (zgc:101711)	NM_001007426	1.44
zgc:64161 (zgc:64161)	NM_213126	1.44
zgc:113058 (zgc:113058)	NM_001014320	1.43
forkhead box B1.2 (foxb1.2)	NM_131285	1.43
zgc:153258 (zgc:153258)	NM_001076579	1.43
Unknown	TC323161	1.43
zgc:92512 (zgc:92512)	NM_001002364	1.42
Sp8 transcription factor a (sp8a)	TC324262	1.42
CCAAT/enhancer binding protein (C/EBP), gamma (cebpg)	NM_131886	1.42
zgc:100897 (zgc:100897)	NM_001003753	1.42

Gene Name (gene symbol)	GenBank accession number	M-value
nudix (nucleoside diphosphate linked moiety X)-type motif 4 (nudt4)	NM_200110	1.42
cDNA clone IMAGE:8154077	DV586283	1.41
zgc:123339 (zgc:123339)	NM_001037695	1.41
nocA related zinc finger 1 (nlz1)	NM_131822	1.40
bromodomain-containing 2, transcript variant 8 (brd2)	XM_704349	1.40
catenin (cadherin-associated protein)	NM_131456	1.40
ETS-related factor1 (ef1)	NM_131159	1.40
TC338066	TC338066	1.39
zgc:153437 (zgc:153437)	NM_001045127	1.39
Unknown	A_15_P112857	1.39
FDR103-P00038-DEPE-F_J23 FDR103 Danio rerio cDNA clone FDR103-P00038-BR_J23 5'	EH445291	1.39
Hspa8 protein (Heat shock protein 8)	TC308414	1.38
ft22a01.y1 Zebrafish neuronal Danio rerio cDNA clone IMAGE:5082121 5'	BI865577	1.38
zgc:77112 (zgc:77112)	NM_213180	1.38
Unknown	A_15_P106131	1.38
prostaglandin-endoperoxide synthase 2b (ptgs2b)	NM_001025504	1.38
zgc:55456 (zgc:55456)	NM_197942	1.38
trh3 protein (trh3)	NM_153671	1.38
cDNA clone IMAGE:7086778	BC083533	1.37
mitogen-activated protein kinase kinase 1 (map2k1)	NM_213419	1.37
zgc:114089 (zgc:114089)	NM_001025472	1.37
ADP-ribosylation factor-like 4, like (arl4l)	NM_200318	1.37
zgc:77836 (zgc:77836)	NM_213196	1.37
zgc:85866 (zgc:85866)	NM_001001826	1.36
hypothetical protein LOC407664 (LOC407664)	BC066705	1.36
purkinje cell protein 4-like 1 (pcp4l1)	TC341327	1.36
zgc:92339 (zgc:92339)	NM_001002452	1.36
zgc:77671 (zgc:77671)	NM_200063	1.36
mitogen-activated protein kinase-activated protein kinase 2 (mapkapk2)	NM_201303	1.35
zgc:101788 (zgc:101788)	NM_001013535	1.35
sp8 transcription factor (sp8)	NM_213241	1.34
zgc:85790 (zgc:85790)	NM_213299	1.34
zgc:112165 (zgc:112165)	NM_001020656	1.34
geranylgeranyl diphosphate synthase 1 (ggps1)	NM_200035	1.33
tumor protein p53 (tp53)	NM_131327	1.33
dynein, axonemal, light intermediate polypeptide 1 (dnali1)	XM_001333070	1.33
myelocytomatosis oncogene a (myca)	NM_131412	1.33
hypothetical protein LOC798347 (LOC798347)	XM_001335762	1.32
syndecan binding protein (syntenin) (sdcbp)	NM_212691	1.32
zgc:92926 (zgc:92926)	NM_001002524	1.32
homeo box D13a (hoxd13a)	NM_131169	1.32
hydroxyacylglutathione hydrolase (hagh)	NM_200043	1.32
insulin-like growth factor 1b receptor (igf1rb)	NM_152969	1.32
nuclear factor of kappa light polypeptide gene enhancer in B-cells 2, p49/p100 (nfkb2)	NM_001001840	1.32
cDNA clone IMAGE:8779532	EE719009	1.32
zgc:101688 (zgc:101688)	NM_001008652	1.32

Gene Name (gene symbol)	GenBank accession number	M-value
ER degradation enhancer, mannosidase alpha-like 1 (edem1)	NM_201189	1.32
Unknown	A_15_P108457	1.31
sine oculis homeobox homolog 3b (six3b)	NM_131363	1.31
sine oculis homeobox homolog 3a (six3a)	NM_131362	1.31
wu:fc23f06 (wu:fc23f06)	NM_194372	1.31
heterogeneous nuclear ribonucleoprotein K (hnrpk)	NM_212994	1.31
zgc:92465 (zgc:92465)	NM_001003496	1.31
hypothetical protein LOC798783 (LOC798783)	XM_001339180	1.30
sp9 transcription factor (sp9)	NM_212960	1.30
zgc:100997 (zgc:100997)	NM_001003605	1.30
ephrin A1 (efna1)	NM_200783	1.30

Tab. A3 MeHg-down-regulated genes determined by DNA-microarray with M < -1.30 and p < 0.05.

Gene Name (gene symbol)	GenBank accession number	M-value
cDNA clone IMAGE:8008341	BC124740	-5.62
zgc:136930 (zgc:136930)	NM_001039819	-3.72
glutathione peroxidase 1 (gpx1)	NM_001007281	-3.54
cDNA clone IMAGE:7075880	BC076207	-18
FabG (beta-ketoacyl-acyl-carrier-protein] reductase, E. coli) like (fabgl)	NM_001005292	-3.38
selenoprotein P, plasma, 1a (sepp1a)	TC356400	-3.20
cDNA clone IMAGE:6525439	BC067158	-3.13
zgc:92263 (zgc:92263)	NM_001002618	-3.05
zgc:109898 (zgc:109898)	NM_001020726	-3.02
zgc:73311 (zgc:73311)	NM_200036	-2.90
Unknown	A_15_P105535	-2.83
zinc finger, CCHC domain containing 17 (zcchc17)	NM_200544	-2.71
si:ch211-240l14.3 (si:ch211-240l14.3)	NM_001020525	-2.69
lactate dehydrogenase D (ldhd)	NM_199873	-2.64
zgc:112527 (zgc:112527)	NM_001017751	-2.63
secernin 3 (scrn3)	NM_199738	-2.62
hypothetical protein LOC553371 (LOC553371)	BC116529	-2.61
deiodinase, iodothyronine, type I (dio1)	NM_001007283	-2.60
Unknown	CO804345	-2.58
zgc:92643 (zgc:92643)	NM_001002436	-2.51
zgc:101035 (zgc:101035)	TC327561	-2.49
amyloid beta precursor protein binding protein 1 (appbp1)	NM_200499	-2.46
NudC domain containing 2 (nudcd2)	NM_001003539	-2.45
zehn2354.seq.F Zebrafish Embryonic Heart cDNA Library Danio rerio cDNA	AI618852	-2.42
zgc:85626 (zgc:85626)	NM_213321	-2.42
acyl-Coenzyme A dehydrogenase family, member 8 (acad8)	NM_201155	-2.42
zgc:77065 (zgc:77065)	NM_212884	-2.39
pyridoxine 5'-phosphate oxidase (pnpo)	BC057246	-2.39
Unknown	A_15_P104050	-2.38
Unknown	A_15_P115112	-2.38
Chromosome 18 SCAF14712, whole genome shotgun sequence	TC342108	-2.37
zgc:110030 (zgc:110030)	NM_001029968	-2.36
cDNA clone IMAGE:7143041	BC090532	-2.33
CHMP (charged multivesicular body) family, member 7 (chmp7)	NM_200781	-2.33
zgc:85611 (zgc:85611)	NM_213095	-2.31
Unknown	A_15_P109775	-2.30

Gene Name (gene symbol)	GenBank accession number	M-value
zgc:91969 (zgc:91969)	NM_001002661	-2.30
zgc:77144 (zgc:77144)	NM_205656	-2.30
zgc:92496 (zgc:92496)	TC338522	-2.28
SEC22 vesicle trafficking protein homolog A (S. cerevisiae) (sec22a)	NM_199698	-2.27
zgc:103574 (zgc:103574)	NM_001005980	-2.26
zgc:63986 (zgc:63986)	NM_213332	-2.25
zgc:56429 (zgc:56429)	NM_200277	-2.24
zgc:85882 (zgc:85882)	NM_212942	-2.21
ARP6 actin-related protein 6 homolog (yeast) (actr6)	NM_199696	-2.18
zinc finger protein zfp113 (zfp113)	TC323584	-2.16
zgc:103490 (zgc:103490)	NM_001004613	-2.15
cDNA clone IMAGE:7259207	CN320754	-2.14
zgc:55652 (zgc:55652)	NM_199775	-2.13
zgc:92822 (zgc:92822)	NM_001004567	-2.12
zinc finger protein zfp108 (zfp108)	TC316500	-2.12
si:dkey-218n20.4 (si:dkey-218n20.4)	NM_001080803	-2.11
zgc:136363 (zgc:136363)	NM_001045267	-2.10
zinc finger protein zfp235 (zfp235)	TC352505	-2.07
zgc:56466 (zgc:56466)	NM_200264	-2.07
zgc:91853 (zgc:91853)	NM_001002196	-2.06
selenoprotein M (sepm)	NM_178286	-2.06
kaptin (actin binding protein) (kptn)	NM_001003642	-2.05
cDNA clone IMAGE:8105683	BC122256	-2.04
meiotic recombination 11 homolog A (S. cerevisiae) (mre11a)	NM_001001407	-2.04
zgc:112000 (zgc:112000)	NM_001017690	-2.03
zgc:109720 (zgc:109720)	NM_205611	-2.02
zgc:63468 (zgc:63468)	NM_199785	-2.01
RNA (guanine-9-) methyltransferase domain containing 2, like (rg9mtd2l)	XM_683615	-2.01
FDR202-P00033-DEPE-F_K16 FDR202 Danio rerio cDNA clone FDR202-P00033-BR_K16	EH548059	-2.01
zgc:101710 (zgc:101710)	NM_001006068	-2.01
zgc:56476 (zgc:56476)	NM_199930	-2.01
zgc:101627 (zgc:101627)	NM_001007447	-2.01
zgc:110366 (zgc:110366)	NM_001017779	-2.01
zgc:56388 (zgc:56388)	NM_200262	-2.00
coenzyme Q3 homolog, methyltransferase (yeast) (coq3)	NM_001002620	-1.99
zgc:92067 (zgc:92067)	NM_001002377	-1.99
hypothetical protein LOC402865 (LOC402865)	BC056692	-1.97

Gene Name (gene symbol)	GenBank accession number	M-value
hypothetical protein MGC10433-like (H. sapiens) (mgc10433l)	NM_001003850	-1.96
zgc:91813 (zgc:91813)	NM_001002209	-1.96
zgc:101066 (zgc:101066)	NM_001003572	-1.96
polyglutamine binding protein 1-like (pqbp1l)	NM_001002435	-1.95
zgc:136869 (zgc:136869)	NM_001040304	-1.95
hypothetical protein LOC553323 (LOC553323)	BC090516	-1.95
zgc:112432 (zgc:112432)	NM_001017780	-1.94
hypothetical protein LOC100003154 (LOC100003154)	XM_001342741	-1.94
DNA-binding protein (dbp)	TC317091	-1.94
Unknown	TC351278	-1.93
WW domain containing oxidoreductase (wwox)	NM_200913	-1.93
zgc:92656 (zgc:92656)	NM_001002427	-1.93
acyl-Coenzyme A dehydrogenase, long chain (acadl)	NM_201181	-1.93
zgc:55781 (zgc:55781)	NM_214694	-1.92
zgc:92633 (zgc:92633)	NM_001002442	-1.91
hypothetical LOC568461 (LOC568461)	XM_691792	-1.91
zgc:110741 (zgc:110741)	TC336566	-1.89
macrophage migration inhibitory factor (mif)	NM_001043321	-1.89
zgc:136330 (zgc:136330)	NM_001045327	-1.89
hydroxysteroid (17-beta) dehydrogenase 4 (hsd17b4)	NM_200136	-1.89
parkinson disease (autosomal recessive, early onset) 7 (park7)	NM_001005938	-1.88
OTU domain, ubiquitin aldehyde binding 1 (otub1)	NM_001002500	-1.88
reticulocalbin 3, EF-hand calcium binding domain (rcn3)	NM_001002158	-1.88
zgc:153376 (zgc:153376)	NM_001076739	-1.86
Unknown	A_15_P116555	-1.86
zgc:92030 (zgc:92030)	NM_001002645	-1.85
traf and tnf receptor associated protein, like (ttrapl)	NM_001079703	-1.85
zgc:77071 (zgc:77071)	NM_212685	-1.85
cDNA clone IMAGE:7435998	BC122194	-1.84
zgc:158612 (zgc:158612)	BC133134	-1.84
zgc:101720 (zgc:101720)	NM_001006065	-1.83
keratin 5 (krt5)	BC063955	-1.82
zgc:111984 (zgc:111984)	NM_001017796	-1.82
zgc:153031 (zgc:153031)	NM_001044830	-1.82
zgc:92915 (zgc:92915)	NM_001007052	-1.82
SUMO1 activating enzyme subunit 1 (sae1)	NM_001002058	-1.82
3-hydroxyisobutyryl-Coenzyme A hydrolase (hibch)	NM_001014316	-1.81

Gene Name (gene symbol)	GenBank accession number	M-value
SUB1 homolog (S. cerevisiae) (sub1)	NM_001002505	-1.81
zgc:101723 (zgc:101723)	NM_001005600	-1.81
Bardet-Biedl syndrome 2 (bbs2)	NM_152887	-1.81
zgc:110008 (zgc:110008)	NM_001020553	-1.81
zgc:56036 (zgc:56036)	NM_213052	-1.81
cDNA clone IMAGE:7214146	CK871898	-1.80
Unknown	A_15_P120745	-1.80
heterogeneous nuclear ribonucleoprotein D-like (hnrpdl)	NM_213392	-1.80
serine hydrolase-like (serhl)	NM_199615	-1.80
l(3)mbt-like 2 (Drosophila) (l3mbtl2)	NM_200032	-1.79
zgc:101896 (zgc:101896)	NM_001007373	-1.79
zgc:77531 (zgc:77531)	NM_212607	-1.79
Unknown	A_15_P102844	-1.78
mesoderm specific transcript (mest)	NM_131043	-1.78
SET domain containing 6 (setd6)	NM_199600	-1.78
zgc:55479 (zgc:55479)	NM_200158	-1.78
zeh0124.seq.F Zebrafish Embryonic Heart cDNA Library Danio rerio cDNA	AI353170	-1.78
zgc:63568 (zgc:63568)	NM_200455	-1.78
RAB28, member RAS oncogene family (rab28)	NM_199752	-1.78
Unknown	A_15_P120334	-1.78
zgc:100998 (zgc:100998)	NM_001003604	-1.77
novel IBR domain containing protein (LOC573901)	NM_001045231	-1.77
acyl-Coenzyme A dehydrogenase, C-4 to C-12 straight chain (acadm)	NM_213010	-1.76
Homo sapiens chromosome 6 open reading frame 203, like (HSPC230l)	XM_688914	-1.75
zgc:63722 (zgc:63722)	NM_201300	-1.75
zgc:76871 (zgc:76871)	NM_213103	-1.75
Meiotic recombination 11 homolog A (mre11a)	TC339226	-1.75
tubulin, beta 5 (tubb5)	NM_198818	-1.74
type I cytokeratin (cyt1)	AI958753	-1.74
COX15 homolog, cytochrome c oxidase assembly protein (yeast) (cox15)	BC066452	-1.74
zgc:55317 (zgc:55317)	NM_200126	-1.74
ubiquitin-activating enzyme E1-domain containing 1 (ube1dc1)	BC046031	-1.73
LOC496071 protein (LOC496071)	TC324268	-1.73
si:busm1-265n4.4 (si:busm1-265n4.4)	NM_001030184	-1.73
Unknown	A_15_P118106	-1.72
peroxisomal biogenesis factor 3 (pex3)	NM_200228	-1.71
zgc:112518 (zgc:112518)	NM_001017758	-1.71

Gene Name (gene symbol)	GenBank accession number	M-value
zgc:77366 (zgc:77366)	NM_212645	-1.71
neural precursor cell expressed, developmentally down-regulated 8 (nedd8)	NM_201321	-1.71
MGC83215 protein, like (LOC100000478)	XM_001335434	-1.71
dipeptidylpeptidase 3 (dpp3)	NM_001002683	-1.71
zgc:85777 (zgc:85777)	NM_212935	-1.71
zgc:63632 (zgc:63632)	NM_200469	-1.70
v-ral simian leukemia viral oncogene homolog A (ras related) (rala)	NM_201018	-1.70
swelling dependent chloride channel (icln)	NM_131424	-1.70
AB002389 Start codon is not identified (Homo sapiens) (AB002389)	TC336593	-1.69
anaphase promoting complex subunit 5 (anapc5)	NM_199622	-1.69
keratin 4 (krt4)	BC066728	-1.69
catenin, beta like 1 (ctnnbl1)	NM_200866	-1.69
zgc:100795 (zgc:100795)	NM_001004011	-1.68
zgc:77346 (zgc:77346)	NM_212901	-1.68
NADPH dependent diflavin oxidoreductase 1 (ndor1)	NM_200648	-1.68
zgc:112404 (zgc:112404)	NM_001017609	-1.68
cDNA clone IMAGE:8756495	EG572643	-1.68
zgc:111967 (zgc:111967)	NM_001020758	-1.67
hypothetical LOC558108 (LOC558108)	XM_679819	-1.67
zgc:92496 (zgc:92496)	NM_001002375	-1.67
si:rp71-1o1.6 (si:rp71-1o1.6)	NM_001030131	-1.67
MAK10 homolog, amino-acid N-acetyltransferase subunit (S. cerevisiae) (mak10)	NM_199550	-1.67
FDR103-P00027-DEPE-F_B20 FDR103 Danio rerio cDNA clone FDR103-P00027-BR_B20	EH441106	-1.66
si:ch211-20b12.1 (si:ch211-20b12.1)	NM_001001836	-1.65
cDNA clone IMAGE:8132070	BC122393	-1.65
zgc:92773 (zgc:92773)	NM_001002554	-1.65
peptidylprolyl isomerase (cyclophilin)-like 4 (ppil4)	NM_199890	-1.65
zgc:100930 (zgc:100930)	NM_001003630	-1.65
Unknown	CN327020	-1.64
coiled-coil domain containing 124 (ccdc124)	NM_200565	-1.64
zgc:109897 (zgc:109897)	NM_001020523	-1.64
zgc:123194 (zgc:123194)	NM_001037410	-1.64
PRP31 pre-mRNA processing factor 31 homolog (yeast) (prpf31)	NM_200504	-1.64
tubulin, alpha 8 like 3 (tuba8l3)	NM_001003558	-1.63
zgc:92784 (zgc:92784)	NM_001002548	-1.63
zgc:92033 (zgc:92033)	NM_001003490	-1.63
thioredoxin domain containing 5 (txndc5)	NM_213016	-1.63

Gene Name (gene symbol)	GenBank accession number	M-value
zgc:110332 (zgc:110332)	NM_001013473	-1.63
excision repair protein/xeroderma pigmentosum D (errc2/xpd)	TC326821	-1.63
retinoblastoma binding protein 5 (rbbp5)	NM_200245	-1.62
mitochondrial trans-2-enoyl-CoA reductase (mecr)	NM_001017852	-1.62
hypothetical LOC563453 (LOC563453)	XM_686813	-1.62
cDNA clone IMAGE:7054660	CK026881	-1.62
thyroid autoantigen (Ku antigen) (g22p1)	NM_199904	-1.62
kinesin family member 5B, like (kif5bl)	XM_680141	-1.61
zgc:110323 (zgc:110323)	NM_001017809	-1.61
Q4RTY0_TETNG (Q4RTY0) Chromosome 12 SCAF14996, whole genome shotgun sequence	TC350990	-1.61
zgc:103522 (zgc:103522)	NM_001005993	-1.61
methylcrotonoyl-Coenzyme A carboxylase 1 (alpha), like (mccc1l)	NM_001044915	-1.61
zgc:136962 (zgc:136962)	NM_001040051	-1.60
cDNA clone IMAGE:8810392	EE710623	-1.60
yippee-like 5 (ypel5)	NM_200477	-1.60
mitochondrial ribosome recycling factor (mrrf)	NM_001002174	-1.59
zgc:77526 (zgc:77526)	NM_207068	-1.59
zgc:136566 (zgc:136566)	NM_001045240	-1.58
processing of precursor 7, ribonuclease P family (pop7)	NM_001006004	-1.58
zgc:66371 (zgc:66371)	NM_200689	-1.58
zgc:103591 (zgc:103591)	NM_001004681	-1.58
zgc:55794 (zgc:55794)	NM_199834	-1.58
zgc:63674 (zgc:63674)	NM_200616	-1.58
hypothetical protein LOC100002391 (LOC100002391)	XM_001337620	-1.58
zgc:77093 (zgc:77093)	NM_212780	-1.58
RAB interacting factor (rabif)	NM_001002511	-1.57
intraflagellar transport protein 52 (ift52)	NM_001001834	-1.57
zgc:65774 (zgc:65774)	NM_199924	-1.56
zgc:101792 (zgc:101792)	NM_001008622	-1.56
polymerase (RNA) II (DNA directed) polypeptide G-like (polr2gl)	NM_199669	-1.56
NIMA (never in mitosis gene a)-related kinase 4 (nek4)	NM_201012	-1.56
zgc:77852 (zgc:77852)	NM_205658	-1.55
zgc:66396 (zgc:66396)	NM_200057	-1.55
zgc:91935 (zgc:91935)	NM_001003511	-1.55
O-sialoglycoprotein endopeptidase-like 1 (osgepl1)	NM_001005301	-1.55
cDNA clone IMAGE:7267460	CN513453	-1.54
zgc:153434 (zgc:153434)	BC122292	-1.54

Gene Name (gene symbol)	GenBank accession number	M-value
zgc:92356 (zgc:92356)	NM_001002444	-1.53
zgc:153243 (zgc:153243)	NM_001080753	-1.53
hypothetical protein LOC794682 (LOC794682)	XM_001332661	-1.53
l-isoaspartyl protein carboxyl methyltransferase, like (pcmtl)	NM_200768	-1.53
cDNA clone IMAGE:8808742	EE698006	-1.53
Chromosome 7 SCAF14601, whole genome shotgun sequence	TC325349	-1.53
zgc:77056 (zgc:77056)	NM_212698	-1.53
zgc:91944 (zgc:91944)	NM_001002668	-1.53
zgc:91844 (zgc:91844)	NM_001003473	-1.52
Unknown	A_15_P112500	-1.52
zgc:65873 (zgc:65873)	NM_200542	-1.51
zgc:103767 (zgc:103767)	NM_001006006	-1.51
reticulon 4 interacting protein 1 (rtn4ip1)	NM_200352	-1.51
zgc:77086 (zgc:77086)	NM_212905	-1.51
ring finger protein 13 (rnf13)	NM_201044	-1.51
COP9 constitutive photomorphogenic homolog subunit 5 (cops5)	NM_200725	-1.5
zgc:91931 (zgc:91931)	NM_001002672	-1.5
zgc:153240 (zgc:153240)	NM_001045389	-1.5
upstream transcription factor 2, c-fos interacting (usf2)	NM_213194	-1.5
tenascin-W (tnw)	AJ001423	-1.5
acyl-Coenzyme A dehydrogenase, C-2 to C-3 short chain (acads)	TC337290	-1.5
2-hydroxyacyl-CoA lyase 1 (hacl1)	NM_213085	-1.5
si:ch211-153c20.2 (si:ch211-153c20.2)	NM_001030218	-1.5
zgc:55392 (zgc:55392)	NM_199849	-1.5
fatty acid desaturase 2 (fads2)	NM_131645	-1.49
zgc:101649 (zgc:101649)	NM_001013537	-1.49
cDNA clone IMAGE:7159603	BC096816	-1.49
ATP-binding cassette, sub-family G (WHITE), member 2c (abcg2c)	NM_001039639	-1.49
cDNA clone IMAGE:4468666	BG799470	-1.49
hypothetical LOC567256 (LOC567256)	XM_690548	-1.49
hypothetical LOC570857 (LOC570857)	XM_694382	-1.49
protein C14orf159, mitochondrial precursor, like, transcript variant 1 (C14orf159l)	XM_678640	-1.49
zinc finger, CCCH-type with G patch domain (zgpat)	TC305183	-1.48
inositol(myo)-1(or 4)-monophosphatase 1 (impa1)	NM_001002745	-1.48
si:dkey-110c1.6 (si:dkey-110c1.6)	NM_001020551	-1.48
O-6-methylguanine-DNA methyltransferase, like (mgmtl)	XM_691575	-1.48
mitochondrial ribosomal protein S33 (mrps33)	NM_001002306	-1.48

Gene Name (gene symbol)	GenBank accession number	M-value
hypothetical protein LOC553234 (LOC553234)	BC077125	-1.47
zgc:101581 (zgc:101581)	NM_001007777	-1.47
zgc:101872 (zgc:101872)	NM_001008589	-1.47
Unknown	A_15_P105168	-1.47
zgc:92714 (zgc:92714)	NM_001002393	-1.47
RNA polymerase II transcriptional coactivator (tcp4)	TC311082	-1.47
zgc:103539 (zgc:103539)	NM_001005988	-1.47
WD repeat domain 24 (wdr24)	NM_213063	-1.47
zgc:66327 (zgc:66327)	NM_200663	-1.47
zgc:56106 (zgc:56106)	NM_200194	-1.46
zgc:92683 (zgc:92683)	NM_001002412	-1.46
general transcription factor IIH, polypeptide 4 (gtf2h4)	NM_199927	-1.46
zgc:92863 (zgc:92863)	NM_001002484	-1.46
cDNA clone IMAGE:7243331	CN172869	-1.46
pyrophosphatase (ppa)	TC306400	-1.46
glycine receptor, alpha 4a (glra4a)	NM_131782	-1.45
Q6AZ98_BRARE (Q6AZ98) SEC23B	TC339823	-1.45
zgc:101826 (zgc:101826)	NM_001004677	-1.45
zgc:92052 (zgc:92052)	NM_001002385	-1.45
zgc:91802 (zgc:91802)	NM_001005584	-1.45
intraflagellar transport 172 (ift172)	NM_001002312	-1.44
general transcription factor IIF, polypeptide 1 (gtf2f1)	NM_199729	-1.44
zgc:101658 (zgc:101658)	NM_001006085	-1.44
zgc:153348 (zgc:153348)	NM_001077575	-1.44
serum amyloid A-like 1 (saal1)	NM_200135	-1.43
choroideremia (chm)	NM_203461	-1.43
zgc:64174 (zgc:64174)	NM_200389	-1.43
FDR107-P00032-DEPE-F_N07 FDR107 Danio rerio cDNA clone FDR107-P00032-BR_N07	EH495195	-1.43
zgc:100927 (zgc:100927)	NM_001003633	-1.41
solute carrier family 30 (zinc transporter), member 9 (slc30a9)	NM_001008575	-1.41
zgc:63563 (zgc:63563)	NM_200044	-1.41
zgc:56702 (zgc:56702)	NM_201103	-1.41
Unknown	A_15_P103095	-1.41
phosphatidylinositol glycan, class F (pigf)	NM_205645	-1.41
peroxisomal biogenesis factor 19 (pex19)	BC056815	-1.41
debranching enzyme homolog 1 (S. cerevisiae) (dbr1)	NM_199653	-1.41
mediator of RNA polymerase II transcription, subunit 18 homolog (yeast) (med18)	NM_200335	-1.41

Gene Name (gene symbol)	GenBank accession number	M-value
catalase (cat)	NM_130912	-1.4
tetratricopeptide repeat domain 35 (ttc35)	NM_213544	-1.4
zgc:153530 (zgc:153530)	NM_001045394	-1.40
zgc:110776 (zgc:110776)	NM_001024375	-1.40
dynein light chain 2, like (dnl2l)	NM_001030000	-1.40
zgc:103414 (zgc:103414)	NM_001007394	-1.39
zgc:114128 (zgc:114128)	NM_001030103	-1.39
steroid 5 alpha-reductase 2-like (srd5a2l)	NM_001044939	-1.39
zgc:63669 (zgc:63669)	NM_201162	-1.39
cDNA clone IMAGE:7922729	BC124310	-1.39
synembryn-like (synbl)	NM_001005293	-1.39
zgc:55944 (zgc:55944)	NM_200153	-1.39
zgc:154012 (zgc:154012)	NM_001077270	-1.39
Unknown	ENSDART00000091324	-1.39
zgc:77713 (zgc:77713)	NM_205602	-1.39
cDNA clone IMAGE:7001673	CF347661	-1.39
selenoprotein T, 1b (selt1b)	NM_178292	-1.38
zgc:77617 (zgc:77617)	NM_213253	-1.38
hypothetical LOC569291 (LOC569291)	XM_692669	-1.38
zgc:112378 (zgc:112378)	NM_001029953	-1.38
zgc:91896 (zgc:91896)	NM_001003460	-1.38
zgc:85676 (zgc:85676)	NM_212919	-1.38
ceroid-lipofuscinosis, neuronal 6 (cln6)	NM_001005982	-1.38
FDR103-P00004-DEPE-F_F22 FDR103 Danio rerio cDNA clone FDR103-P00004-BR_F22 5'	EH432967	-1.38
intraflagellar transport 88 homolog (ift88)	NM_001001725	-1.38
cleavage and polyadenylation specific factor 2 (cpsf2)	NM_001002384	-1.38
zgc:109963 (zgc:109963)	NM_001024405	-1.37
G elongation factor, mitochondrial 2 (gfm2)	NM_001077545	-1.37
zgc:91951 (zgc:91951)	NM_001007764	-1.37
si:ch211-258l4.3 (si:ch211-258l4.3)	NM_001080197	-1.37
CDKN1A interacting zinc finger protein 1 (ciz1)	NM_213525	-1.37
bisphosphate nucleotidase 1 (bpnt1)	NM_001002354	-1.36
zgc:92286 (zgc:92286)	NM_001002607	-1.36
coiled-coil domain containing 12 (ccdc12)	NM_001003589	-1.36
zgc:66407 (zgc:66407)	NM_200430	-1.36
aldehyde dehydrogenase 9 family, member A1 (aldh9a1)	NM_201508	-1.36
	A_15_P107865	-1.36

Gene Name (gene symbol)	GenBank accession number	M-value
hypothetical protein LOC100005714 (LOC100005714)	XM_001342210	-1.36
leucine zipper transcription factor-like 1 (lztfl1)	NM_199587	-1.36
solute carrier family 39 (zinc transporter), member 7 (slc39a7)	NM_130931	-1.36
zgc:103579 (zgc:103579)	NM_001007391	-1.36
zgc:64138 (zgc:64138)	NM_213129	-1.36
zgc:92785 (zgc:92785)	NM_001002547	-1.35
zgc:92702 (zgc:92702)	NM_001002401	-1.35
FDR103-P00052-DEPE-F_N17 FDR103 Danio rerio cDNA clone FDR103-P00052-BR_N17 5'	EH450455	-1.35
zgc:153688 (zgc:153688)	NM_001076561	-1.35
selenophosphate synthetase 1 (sephs1)	NM_199701	-1.35
si:dkey-72l14.8 (si:dkey-72l14.8)	NM_001044811	-1.34
zgc:109972 (zgc:109972)	NM_001020499	-1.34
delta-5/delta-6 fatty acid desaturase (fads)	CN171115	-1.34
zgc:86602 (zgc:86602)	NM_001002161	-1.34
family with sequence similarity 86, member A (fam86a)	NM_001006058	-1.34
hypothetical LOC568246 (LOC568246)	XM_691567	-1.34
zinc finger protein 330 (znf330)	NM_213373	-1.34
nuclear distribution gene C homolog (nudc)	NM_200919	-1.34
IK cytokine (ik)	NM_199589	-1.34
WD repeat domain 48 (wdr48)	NM_214709	-1.33
zinc finger protein ZFP235 (zfp235)	TC337765	-1.33
capsid protein VP2 (vp2)	TC324106	-1.33
Q4SNU0_TETNG (Q4SNU0) Chromosome 15 SCAF14542, whole genome shotgun sequence	TC319378	-1.33
Unknown	A_15_P103019	-1.33
hypothetical LOC566872, transcript variant 1 (LOC566872)	XM_685201	-1.33
zgc:103741 (zgc:103741)	NM_001007458	-1.33
heat shock factor binding protein 1, transcript variant 1 (hsbp1)	XM_679029	-1.33
zgc:110684 (zgc:110684)	NM_001020623	-1.33
zgc:100909 (zgc:100909)	NM_001003752	-1.33
zgc:136926 (zgc:136926)	NM_001039932	-1.32
zgc:92802 (zgc:92802)	NM_001002523	-1.32
SEC22 vesicle trafficking protein homolog B (S. cerevisiae), b (sec22bb)	NM_201302	-1.32
zgc:103655 (zgc:103655)	NM_001005949	-1.32
breast cancer metastasis-suppressor 1 (brms1)	NM_200097	-1.32
zgc:103632 (zgc:103632)	NM_001005953	-1.32
zgc:110219 (zgc:110219)	NM_001017645	-1.32
similar to DEAD box (84.8 kD) (3G940) (LOC562123)	NM_001044978	-1.32

Gene Name (gene symbol)	GenBank accession number	M-value
nucleoside diphosphate kinase-Z4 (ndpkz4)	NM_130929	-1.32
hypothetical LOC558808 (LOC558808)	XM_682074	-1.32
zgc:153664 (zgc:153664)	NM_001045358	-1.32
zgc:110742 (zgc:110742)	NM_001013344	-1.31
type I cytokeratin, enveloping layer (cyt1)	TC346768	-1.31
zgc:86807 (zgc:86807)	NM_001002120	-1.31
zgc:103525 (zgc:103525)	NM_001007338	-1.31
zgc:77396 (zgc:77396)	NM_205665	-1.30
zgc:86625 (zgc:86625)	NM_001002054	-1.30
intraflagellar transport 80 homolog (Chlamydomonas) (ift80)	NM_001008625	-1.30

Tab. A4 Gene ontology of MeHg-responsive genes selected for *in situ* hybridisation analysis.

Gene name (gene symbol)	GenBack accession number	Molecular function, biological process and cellular component
a disintegrin and metalloproteinase domain 8 (adam8)	NM_200637	Metalloendopeptidase activity; zinc ion binding; integrin-mediated signaling pathway; proteolysis
activating transcription factor 3 (atf3)	NM_200964	DNA binding; protein dimerisation activity; sequence-specific DNA binding; sequence-specific DNA binding transcription factor activity; response to virus; regulation of transcription, DNA-dependent; protein dimerisation activity; nucleus; nucleolus; intracellular
ADP-ribosylation factor-like (arfl); Zgc:112199	AI477644	GTP binding, nucleotide binding, small GTPase mediated signal transduction; intracellular
angiotensinogen (agt)	BG727310	Regulation of gene expression; ranscription factor activity; regulation of NAD(P)H oxidase activity; serine-type endopeptidase inhibitor activity; response to cold; cytokine production; positive regulation of muscle hypertrophy; type 2 angiotensin receptor binding; acetyltransferase activator activity; soluble fraction; cell fraction; intracellular
apolipoprotein eb (apoeb)	NM_131098	Lipid binding; Lipid transport; lipoprotein metabolic process; transport; extracellular region
CCAAT/enhancer binding protein (C/EBP), gamma (cebpg)	NM_131886	DNA binding; protein dimerisation activity; sequence-specific DNA binding; sequence-specific DNA binding transcription factor activity; regulation of transcription, DNA-dependent; natural killer cell mediated cytotoxicity; cytokine metabolic process; protein heterodimerisation activity; protein dimerisation activity; nucleus; nucleolus; intracellular
chromobox protein homolog 7-like (cbx7l); zgc:110152	NM_001017853	Chromatin binding; chromatin assembly or disassembly; chromatin; nucleus; intracellular
cocaine and amphetamine regulated transcript protein type I-like (cartII)	DN857240	Brain development; regulated by testosterone; response to stress
complement component 3-like (c3l); si:dkey-76b14.4	AF047413	Endopeptidase inhibitor activity; extracellular region; extracellular space
complement component 4-2-like (c4-2l)	BI672168	Complement activation; component of the classical pathway
complement component 6 (c6)	BI474371	Complement activation; complement cascade for immune response; component of the membrane attack complex of complement
complement component 7 (c7)	BC100054	Complement activation; component of the membrane attack complex of complement; induction of apoptosis
complement factor b (cfb)	AW019018	Catalytic activity; serine-type endopeptidase activity; response to bacterium; complement activation; proteolysis; extracellular region
core promoter element binding protein (copeb)	NM_201461	Nucleic acid binding; zinc ion binding; digestive tract development; liver development; organ growth; pancreas development; intracellular
CXC chemokine 46-like (cxc46l)	BI845861	Inducing directed chemotaxis
ubiquitin carboxyl-terminal hydrolase CYLD-like (cyldl)	BE016427	Unknown

Gene name (gene symbol)	GenBack accession number	Molecular function, biological process and cellular component
E74-like factor 3 (ets domain transcription factor, epithelial-specific) (elf3)	AI385059	DNA binding
fibronectin 1b (fn1b)	NM_001013261	Somitogenesis; Cell adhesion and migration processes including embryogenesis, wound healing, blood coagulation, host defense, and metastasis; extracellular region
forkhead box B1.2 (foxb1.2)	NM_131285	DNA binding; sequence-specific DNA binding; sequence-specific DNA binding transcription factor activity; regulation of transcription; regulation of transcription, DNA-dependent; transcription; nucleus
glutamate-cysteine ligase modifier subunit (gclm)	BG304082	Ligase activity; oxidoreductase activity; oxidation-reduction process; response to nitrosative stress; glutamate-cysteine ligase catalytic subunit binding; protein heterodimerisation activity; protein dimerisation activity; glutamate-cysteine ligase activity; glutamate-cysteine ligase complex; soluble fraction; cell fraction; intracellular
glutathione peroxidase 1a (gpx1a)	AW232474	Glutathione peroxidase activity; oxidoreductase activity; peroxidase activity; oxidation-reduction process; response to oxidative stress
glutathione peroxidase 4a (gpx4a)	BI896246	Glutathione peroxidase activity; oxidoreductase activity; peroxidase activity; oxidation-reduction process; response to oxidative stress
glycine dehydrogenase (decarboxylating) (gldc)	BM777961	Glycine dehydrogenase (decarboxylating) activity, glycine metabolic process; oxidation-reduction process
hematopoietically expressed homeobox (hhex)	NM_130934	DNA binding; sequence-specific DNA binding; sequence-specific DNA binding transcription factor activity; transcription regulator activity; multicellular organismal development; regulation of transcription; regulation of transcription, DNA-dependent; transcription; heart development; positive regulation of endothelial cell differentiation; regulation of organ growth; thyroid gland development; nucleus
homeodomain leucine zipper gene (homez)	NM_001007120	DNA binding; sequence-specific DNA binding; sequence-specific DNA binding transcription factor activity; regulation of transcription; regulation of transcription, DNA-dependent; nucleus; intracellular
interferon regulatory factor (irf9)	NM_205710	Sequence-specific DNA binding transcription factor activity; regulation of transcription; regulation of transcription, DNA-dependent; transcription; cytokine metabolic process; nucleus; intracellular
jun B proto-oncogene (junb)	NM_213556	DNA binding; protein dimerisation activity; sequence-specific DNA binding; sequence-specific DNA binding transcription factor activity; regulation of transcription; regulation of transcription, DNA-dependent; heart contraction; nucleus
kruppel-like factor 10-like (klf10l)	AI641738	DNA binding; TGFbeta-mediated signaling cascades; regulation of pancreatic epithelial cell growth
kruppel-like factor 11b (klf11b)	NM_001077604	Zinc ion binding; intracellular
lysosome-associated membrane glycoprotein 1l (lamp1l); zgc:64072	AI793516	Membrane
matrix metalloproteinase 9 (mmp9)	AW174507	Hydrolase activity; metal ion binding; metalloendopeptidase activity; metallopeptidase activity; peptidase activity; zinc ion binding; response to bacterium; metabolic process; proteolysis; positive regulation of granuloma formation; extracellular matrix
matrix metalloproteinase 13a (mmp13a)	AW305943	Calcium ion binding; hydrolase activity; metal ion binding; metalloendopeptidase activity; metallopeptidase activity; peptidase activity; zinc ion binding; metabolic process; proteolysis; embryo development; macrophage chemotaxis; extracellular matrix

Gene name (gene symbol)	GenBack accession number	Molecular function, biological process and cellular component
matrix metalloproteinase 14a (mmp14a)	NM_194416	Calcium ion binding; hydrolase activity; metal ion binding; metalloendopeptidase activity; metallopeptidase activity; peptidase activity; zinc ion binding;response to hypoxia; metabolic process; proteolysis; cell migration involved in gastrulation; convergent extension; convergent extension involved in gastrulation; establishment of cell polarity; anterior/posterior axis specification; cartilage development; embryonic cranial skeleton morphogenesis; extracellular matrix
NADPH oxidase organizer 1 (noxo1)	BI878214	Hosphoinositide binding; cell communication
opsin 1 (cone pigments), long-wave-sensitive, 1 (opn1lw1)	AF109371	G-protein coupled receptor activity; photoreceptor activity; receptor activity; signal transducer activity; red or far-red light photoreceptor activity; photoperiodism; response to light stimulus; G-protein coupled receptor protein signaling pathway; phototransduction; protein-chromophore linkage; response to stimulus; signal transduction; visual perception; integral to membrane; membrane
opsin 1 (cone pigments), medium-wave-sensitive, 1 (opn1mw1)	AF109369	G-protein coupled receptor activity; photoreceptor activity; receptor activity; signal transducer activity; photoreceptor activity; G-protein coupled receptor protein signaling pathway; phototransduction; protein-chromophore linkage; response to stimulus; signal transduction; visual perception; photoreceptor outer segment; integral to membrane; membrane
opsin 1 (cone pigments), short-wave-sensitive 1 (opn1sw1)	AF109373	G-protein coupled receptor activity; photoreceptor activity; receptor activity; signal transducer activity; G-protein coupled receptor protein signaling pathway; phototransduction; protein-chromophore linkage; response to stimulus; signal transduction; visual perception; integral to membrane; membrane
paired box gene 2a (pax2a)	NM_131184	DNA binding; cell differentiation; multicellular organismal development; nervous system development; regulation of transcription; transcription; anterior/posterior pattern formation; cell fate specification; embryonic camera-type eye morphogenesis; midbrain development; otic placode formation; cerebellum development; embryonic pattern specification; hindbrain development; kidney development; midbrain-hindbrain boundary development; peripheral nervous system development; pronephros development; thyroid gland development; nucleus
paired box gene 6a (pax6a)	NM_131304	Transcription activator activity; DNA binding; sequence-specific DNA binding; sequence-specific DNA binding transcription factor activity; transcription regulator activity; multicellular organismal development; regulation of transcription;regulation of transcription, DNA-dependent; transcription; forebrain development; anterior/posterior pattern formation; hindbrain development; nucleus
peroxiredoxin1 (prdx1); zgc:110343	BI980610	Antioxidant activity; oxidoreductase activity; peroxiredoxin activity; cell redox homeostasis; natural killer cell mediated cytotoxicity; cellular response to oxidative stress; pigment granule; nucleus; melanosome; intracellular
phosphoenolpyruvate carboxykinase 1 (pck1)	BG727092	GTP binding; kinase activity; phosphoenolpyruvate carboxykinase activity; purine nucleotide binding; response to glucose stimulus; gluconeogenesis
6-phosphofructo-2-kinase/fructose-2,6-biphosphatase 4-like (pfkfb4l)	BI888564	6-phosphofructo-2-kinase activity; ATP binding; catalytic activity; kinase activity; fructose 2,6-bisphosphate metabolic process; fructose metabolic process; metabolic process; intracellular
PLAC8-like protein 1-like (plac8l1l)	BE557057	Unknown
POU domain, class 5, transcription factor 1 (pou5f1)	NM_131112	DNA binding; sequence-specific DNA binding; sequence-specific DNA binding transcription factor activity; transcription regulator activity; multicellular organismal development; regulation of transcription; regulation of transcription, DNA-dependent; transcription; positive regulation of transcription, DNA-dependent; anatomical structure morphogenesis; brain development; brain segmentation; dorsal/ventral pattern formation; ectoderm development; embryonic pattern specification; endoderm formation; epiboly involved in gastrulation with mouth forming second; hindbrain development; mesoderm development; morphogenesis of

Gene name (gene symbol)	GenBack accession number	Molecular function, biological process and cellular component
		embryonic epithelium; nucleus
PR domain containing 1a, with ZNF domain (prdm1a)	NM_199515	Transcription repressor activity; nucleic acid binding; zinc ion binding; embryonic axis specification; embryonic pectoral fin morphogenesis; fin development; muscle cell fate determination; pectoral fin morphogenesis; positive regulation of neuron differentiation; intracellular
protein phosphatase 1 regulatory subunit 15A (ppp1r15a)	BI889255	regulation of gene expression; intracellular
Ras-related associated with diabetes (rrad)	NM_199798	GTP-binding; GTPase activity; nucleotide binding; signal transduction; small GTPase mediated signal transduction; membrane
retinal homeobox gene 1 (rx1)	NM_131225	DNA binding; sequence-specific DNA binding; sequence-specific DNA binding transcription factor activity; transcription regulator activity; multicellular organismal development; regulation of transcription; regulation of transcription, DNA-dependent; transcription; camera-type eye photoreceptor cell differentiation; neural retina development; retina layer formation; nucleus
S100 calcium binding protein Z (s100z)	BC095285	Calcium ion binding
secretion-associated and Ras-related gene homolog 2 (sar2)	BM102635	GTP binding; intracellular
selenoprotein W, 1 (sepw1)	AW128247	Selenium binding, cell redox homeostasis; cytoplasm
sequestosome 1 (sqstm1)	AW343560	Zinc ion binding
serum/glucocorticoid regulated kinase 1 (sgk1)	BI673466	ATP-binding; kinase activity; nucleotide binding; protein kinase activity; protein serine/threonine kinase activity; transferase activity; apoptosis; protein phosphorylation; response to stress, cytoplasm, endoplasmic reticulum, nucleus
si:ch211-106h4.4	BG302634	Membrane
si:ch1073-126c3.2	AI974163	Unknown
sine oculis homeobox homolog 3a (six3a)	NM_131362	DNA binding; sequence-specific DNA binding; sequence-specific DNA binding transcription factor activity; regulation of transcription; regulation of transcription, DNA-dependent; brain development; nucleus
sine oculis homeobox homolog 3b (six3b)	NM_131363	DNA binding; sequence-specific DNA binding; sequence-specific DNA binding transcription factor activity; regulation of transcription; regulation of transcription, DNA-dependent; embryonic camera-type eye morphogenesis; brain development; nucleus
solute carrier family 16 (monocarboxylic acid transporters), member 9a (slc16a9a)	AW421040	Transmembrane transport
solute carrier family 16 (monocarboxylic acid transporters), member 9b (slc16a9b)	BE016639	Transmembrane transport
sp9 transcription factor (sp9)	NM_212960	DNA binding; metal ion binding; nucleic acid binding; zinc ion binding; regulation of transcription; transcription; embryonic pectoral fin morphogenesis; positive regulation of fibroblast growth factor receptor signaling pathway; intracellular; nucleus

Gene name (gene symbol)	GenBack accession number	Molecular function, biological process and cellular component
spleen focus forming virus (SFFV) proviral integration oncogene spi1 (spi1)	AY293624	DNA binding; sequence-specific DNA binding; sequence-specific DNA binding transcription factor activity; regulation of transcription, DNA-dependent; regulation of myeloid leukocyte differentiation; nucleus
SRY-box containing gene 7 (sox7)	NM_001080750	DNA binding; vasculogenesis; nucleus
Sulfide quinone reductase-like (sqrdl)	BI882244	Oxidoreductase activity; oxidation-reduction process
suppressor of cytokine signaling 3a (sosc3a)	BI878700	Intracellular signal transduction
suppressor of cytokine signaling 3b (sosc3b)	BG727181	Intracellular signaling pathway
thioredoxin-like (txnl); zgc:92903	BI864190	Cell redox homeostasis
thioredoxin-like 4A (txnl4a)	BI886657	Mitosis ; spliceosomal complex
tumor protein p53 (p53)	NM_131327	Transcription activator activity; DNA binding; metal ion binding; sequence-specific DNA binding transcription factor activity; zinc ion binding; transcription regulator activity; protein binding; positive regulation of transcription, DNA-dependent; response to methylmercury; apoptosis; cell cycle; negative regulation of cell growth; regulation of transcription; regulation of transcription, DNA-dependent; response to tumor cell; transcription; DNA damage response, signal transduction by p53 class mediator resulting in induction of apoptosis; positive regulation of apoptosis; positive regulation of neuron apoptosis; DNA damage checkpoint; DNA damage response, signal transduction by p53 class mediator resulting in transcription of p21 class mediator; induction of apoptosis; negative regulation of cell cycle; negative regulation of cell division; positive regulation of apoptosis; positive regulation of caspase activity; positive regulation of cell cycle; response to UV; response to X-ray; cytoplasm; nucleus
UDP glucuronosyltransferase 5 family, polypeptide A2 (ugt5a2)	AW127886	Transferase activity; transferase activity, transferring glycosyl groups; transferase activity, transferring hexosyl groups; metabolic process
uncoupling protein 1 (ucp1)	AW420321	Binding; response to chemical stimulus; mitochondrial transport; transmembrane transport; transport; integral to membrane; membrane; mitochondrion
urate oxidase (uox)	AW019321	Oxidoreductase activity; urate oxidase activity; oxidation-reduction process; purine base metabolic process
v-fos FBJ murine osteosarcoma viral oncogene homolog (fos)	NM_205569	Double-stranded DNA binding; DNA binding; protein dimerisation activity; sequence-specific DNA binding; sequence-specific DNA binding transcription factor activity; regulation of transcription; regulation of transcription, DNA-dependent; cellular response to oxidative stress; protein heterodimerisation activity; protein dimerisation activity; nucleus; synaptosome; cell fraction; intracellular
v-maf musculoaponeurotic fibrosarcoma oncogene family, protein B (avian) (mafba)	NM_131015	DNA binding; sequence-specific DNA binding; sequence-specific DNA binding transcription factor activity; regulation of transcription; regulation of transcription, DNA-dependent; transcription; anterior/posterior pattern formation; embryonic pattern specification; nucleus
v-maf musculoaponeurotic fibrosarcoma oncogene homolog f (avian) (maff)	NM_200336	DNA binding; sequence-specific DNA binding; sequence-specific DNA binding transcription factor activity; protein heterodimerisation activity; regulation of transcription; regulation of transcription, DNA-dependent; positive regulation of transcription, DNA-dependent; transcription factor complex; nucleus

Gene name (gene symbol)	GenBack accession number	Molecular function, biological process and cellular component
zgc:56382	BM101640	Unknown
zgc:92254	AW019036	Glutathione transferase activity; cytoplasm
zgc:101661	AI657551	Unknown
AI397362	AI397362	Unknown
AI544649	AI544649	Unknown
AI793818	AI793818	Unknown
AW115990	AW115990	Unknown
BE016163	BE016163	Unknown
BG727211	BG727211	Unknown
BG891932	BG891932	Unknown
BI474700	BI474700	Unknown
BI883993	BI883993	Unknown
BI892110	BI892110	Unknown
BI983579	BI983579	Unknown
BM036361	BM036361	Unknown
BM101698	BM101698	Unknown

Publications related to the dissertation

Yang L.*, **Ho N.Y.***, Müller F., Strähle U. (2010). Methyl mercury suppresses the formation of the tail primordium in developing zebrafish embryos. Toxicological Sciences. 115, 379-390. (* equal contribution)

Yang L., **Ho N.Y.**, Alshut R., Legradi J., Weiss C., Reischl M., Mikut R., Liebel U., Müller F., Strähle U. (2009). Zebrafish embryos as models for embryotoxic and teratological effects of chemicals. Reproductive Toxicology. 28, 245-253.

Declarations

I, hereby, declare that I have written the submitted dissertation myself and, in this process, have used no other sources or materials than those expressly indicated.

Karlsruhe, 21st July 2011 Nga Yu Ho